



**Fluid Power Vehicle Challenge  
The Incompressibles  
Final Design Report  
2018-2019**

June 12, 2019

Russell Posin  
rposin@calpoly.edu

David Vitt  
dvitt@calpoly.edu

Nicholas Gholdoian  
ngholdoi@calpoly.edu

Julian Rodkiewicz  
jrodkiew@calpoly.edu

Alex Knickerbocker  
knickerb@calpoly.edu

Kyle Franck  
kfranck@calpoly.edu



*“Comfortable Under Pressure”*

**Instructor:**  
John Fabijanac

**Sponsor:**  
Dr. James Widmann

**Industry Mentor:**  
Mark Decklar (Hydraforce)

Mechanical Engineering Department  
California Polytechnic State University - San Luis Obispo

# TABLE OF CONTENTS

<b>TABLE OF CONTENTS .....</b>	<b>1</b>
<b>LIST OF FIGURES .....</b>	<b>8</b>
<b>LIST OF TABLES .....</b>	<b>15</b>
<b>EXECUTIVE SUMMARY .....</b>	<b>16</b>
<b>1 INTRODUCTION.....</b>	<b>17</b>
<b>1.1 Problem Statement.....</b>	<b>17</b>
<b>2 BACKGROUND .....</b>	<b>18</b>
<b>2.1 Customers .....</b>	<b>19</b>
<b>2.2 Existing Designs: Competition Winners 2017-18.....</b>	<b>19</b>
2.2.1 Overall Winner: .....	19
2.2.2 Second Overall:.....	20
2.2.3 Third Overall: .....	21
<b>2.3 Component Research .....</b>	<b>22</b>
2.3.1 Pumps and motors (driving and driven).....	22
2.3.2 Hydraulic circuits.....	24
2.3.3 Electronics/Mechatronics.....	24
2.3.4 Accumulator.....	24
2.3.5 Brakes .....	25
2.3.6 Custom bike frame .....	26
<b>3 OBJECTIVES .....</b>	<b>27</b>
<b>4 CONCEPT DESIGN.....</b>	<b>29</b>
<b>4.1 Frame.....</b>	<b>29</b>
4.1.1 Frame Type Selection .....	29
5.1.1.1 Standard Bike .....	30
5.1.1.2 Recumbent Bike .....	31
5.1.1.3 Prone Bike .....	31
5.1.1.4 Velomobile.....	32
4.1.2 Preliminary Frame Design .....	33
4.1.3 Further Development .....	33
<b>4.2 Drivetrain.....</b>	<b>34</b>
4.2.1 Current Design .....	34
5.2.1.1 Front Drivetrain.....	34

5.2.1.2 Rear Drivetrain .....	36
4.2.2 New Design.....	37
5.2.2.1 Front Drivetrain.....	37
5.2.2.2 Rear Drivetrain .....	38
4.2.3 Further Development .....	39
<b>4.3 Hydraulics .....</b>	<b>39</b>
4.3.1.1 Direct Drive Mode.....	39
4.3.1.2 Discharge Mode .....	40
4.3.1.3 Regenerative Braking Mode.....	41
4.3.1.4 PIT Mode.....	41
4.3.2 Accumulator Selection.....	42
4.3.3 Pump and Motor .....	43
4.3.3.1 Bent-Axis Pump/Motor .....	44
4.3.3.2 Gear Pump.....	45
4.3.3.3 Gerotor Pump/Motor .....	45
4.3.4 Valve Selection .....	46
4.3.4.1 Spool-Type Solenoids .....	46
4.3.4.2 Poppet-Type Solenoids.....	46
4.3.5 Further Development .....	47
<b>4.4 Mechatronics.....</b>	<b>47</b>
4.4.1 Past Design .....	47
4.4.2 New Hardware Design.....	49
4.4.3 Software Design.....	53
4.4.4 Further Development .....	54
<b>4.5 Power Decoupling.....</b>	<b>54</b>
4.5.1 Friction Disc Clutch .....	55
4.5.2 Fluid Circulation Line.....	56
4.5.3 Dog Tooth Clutch .....	56
4.5.4 Further Development .....	57
<b>4.6 Modeling.....</b>	<b>57</b>
4.6.1 Accumulator Discharge Model - Current Design .....	57
4.6.2 Accumulator Discharge Model - Future Development .....	61
4.6.3 Patterson Control Model.....	61
4.6.4 Patterson Control Model – Future Development .....	64
4.6.5 Losses and User Requirements – Current Design.....	64
4.6.6 Losses and User Requirements – Future Development.....	66

4.6.7 Direct Drive Model – Current Design.....	66
4.6.8 Direct Drive Model – Future Development .....	66
<b>5 FINAL DESIGN.....</b>	<b>68</b>
<b>5.1 Frame.....</b>	<b>70</b>
5.1.1 Frame Geometry .....	70
5.1.2 Frame Tube Material Selection .....	77
5.1.3 Patterson Control Model .....	80
5.1.4 Structural Analysis.....	84
<b>5.2 Hydraulics .....</b>	<b>85</b>
5.2.1 Hydraulic Circuit .....	85
5.2.1.1 Direct Drive Mode.....	85
5.2.1.2 Discharge Mode .....	86
5.2.1.3 Regenerative Braking Mode .....	87
5.2.1.4 Coast Mode .....	88
5.2.2 Solenoids.....	91
5.2.3 Manifold.....	93
5.2.4 Accumulator.....	95
5.2.5 Pump/Motor.....	97
5.2.6 Reservoir.....	97
<b>5.3 Front Drivetrain .....</b>	<b>98</b>
5.3.1 Chain and Sprockets .....	99
5.3.2 Planetary Gearbox.....	102
5.3.3 Mounting.....	104
<b>5.4 Rear Drivetrain .....</b>	<b>105</b>
5.4.1 Mounting.....	106
5.4.2 Sprockets.....	106
5.4.3 Analysis .....	107
5.4.3.1 Drivetrain Ratio.....	107
5.4.3.2 Stress analysis .....	108
<b>5.5 Mechatronics.....</b>	<b>110</b>
5.5.1 Functionality .....	110
5.5.2 Platform .....	111
5.5.3 Components .....	111
5.5.3.1 Display .....	111
5.5.3.2 Buttons .....	112

5.5.3.3 Pressure Transducer.....	112
5.5.3.4 Speed Sensor .....	113
5.5.3.5 Solenoid Driver .....	113
5.5.3.6 Battery .....	114
5.5.4 Packaging .....	114
5.5.4.1 Button Enclosure .....	114
5.5.4.2 Display Enclosure.....	115
5.5.4.3 Packaging Proof of Concept.....	115
5.5.5 Current Design Progress .....	116
5.5.5.1 Circuit.....	116
5.5.5.2 Software .....	116
5.5.5.3 Display Functionality .....	117
5.5.6 Final Design Plan .....	117
5.5.6.1 Hardware .....	117
5.5.6.2 Software .....	118
5.5.7 Final Design Prototype .....	118
5.5.7.1 Solenoid Driver .....	118
5.5.7.2 Microcontroller.....	118
5.5.7.3 Packaging .....	119
5.5.7.2 Software .....	119
5.5.8 Actual Final Design .....	119
5.5.8.1 Solenoid Driver .....	119
5.5.8.2 Microcontroller.....	119
5.5.8.3 Printed Circuit Board.....	120
<b>5.7 Modeling.....</b>	<b>120</b>
5.7.1 Direct Drive Model.....	120
5.7.2 Accumulator Discharge Model .....	124
5.7.3 Accumulator Recharge/Regen Model .....	126
5.7.4 Loss and User Requirements.....	127
<b>6 MANUFACTURING.....</b>	<b>129</b>
<b>6.1 Procurement .....</b>	<b>129</b>
6.1.1 Frame .....	129
6.1.1.1 Frame Tubes .....	129
6.1.1.2 Frame Auxiliaries .....	129
6.1.2 Hydraulics .....	130
6.1.2.1 Solenoids .....	130
6.1.2.2 Reservoir .....	130

6.1.2.3 Accumulator .....	130
6.1.2.4 Lines/Fittings.....	130
6.1.2 Front Drivetrain .....	130
6.1.2.1 Front Crank .....	130
6.1.2.1 Planetary Gear Set .....	130
6.1.3 Rear Drivetrain.....	130
6.1.4 Mechatronics.....	131
<b>6.2 Manufacturing.....</b>	<b>131</b>
6.2.2 Frame .....	131
6.2.2 Frame Tube Machining .....	131
6.2.2 Hydraulics .....	139
6.2.2.1 Solenoids .....	139
6.2.2.2 Reservoir .....	139
6.2.3 Front Drivetrain .....	140
6.2.3.1 Planetary and Pump Mount .....	140
6.2.3.2 Chain Tensioner Mount.....	142
6.2.3 Rear Drivetrain .....	142
6.2.4 Mechatronics.....	145
<b>6.3 Assembly .....</b>	<b>146</b>
6.3.1 Frame .....	146
6.3.2 Hydraulics .....	148
6.3.2.1 Solenoids .....	148
6.3.2.2 Reservoir .....	148
6.3.2.3 Fittings.....	148
6.3.3 Front Drivetrain .....	148
6.3.3.1 Planetary and Pump.....	148
6.3.3.2 Chain and Sprocket Assembly.....	149
6.3.4 Rear Drivetrain.....	150
6.3.5 Mechatronics.....	151
<b>6.4 Outsources.....</b>	<b>152</b>
6.4.1 Frame .....	152
6.4.2 Manifold.....	152
6.4.3 Waterjet.....	152
<b>7 DESIGN VERIFICATION .....</b>	<b>153</b>
<b>7.1 Initial Bike Performance Testing.....</b>	<b>154</b>
7.1.1 Mock Dynamic Bike Challenges .....	154

7.1.1.2 Mock Endurance Challenge.....	154
7.1.1.2 Mock Efficiency Challenge .....	154
7.1.1.3 Mock Sprint Challenge.....	155
<b>7.2 Competition Bike Performance Testing.....</b>	<b>156</b>
7.2.1 Dynamic Bike Challenges.....	156
7.2.1.1 Sprint Challenge .....	156
7.2.1.2 Efficiency Challenge .....	156
7.2.1.3 Endurance Challenge.....	157
<b>7.3 Drivetrain.....</b>	<b>158</b>
7.3.1 Front Drivetrain .....	158
<b>7.4 Hydraulics .....</b>	<b>159</b>
7.4.1 Solenoids.....	159
<b>7.5 Mechatronics.....</b>	<b>160</b>
<b>7.6 Modeling.....</b>	<b>160</b>
<b>8 PROJECT MANAGEMENT.....</b>	<b>161</b>
<b>8.1 Roles and Responsibilities .....</b>	<b>161</b>
<b>8.2 Project Timeline .....</b>	<b>161</b>
<b>8.3 Project Management Recommendations .....</b>	<b>162</b>
<b>9 RECOMMENDATIONS.....</b>	<b>164</b>
<b>9.1 Design Recommendations.....</b>	<b>164</b>
9.1.1 Frame .....	164
9.1.2 Front Drivetrain .....	164
9.1.3 Modeling.....	164
9.1.4 Hydraulics .....	165
9.1.5 Mechatronics.....	165
<b>9.2 Manufacturing Recommendations .....</b>	<b>165</b>
9.2.1 Frame .....	165
9.2.2 Hydraulics .....	165
<b>9.3 Testing Recommendations.....</b>	<b>165</b>
<b>10 CONCLUSION .....</b>	<b>167</b>
<b>REFERENCES.....</b>	<b>168</b>
<b>APPENDIX.....</b>	<b>169</b>
<b>Attachment 1: Summary of Customer Needs.....</b>	<b>169</b>

<b>Attachment 2: Quality Function Deployment - House of Quality .....</b>	<b>170</b>
<b>Attachment 3: Comprehensive Gantt Chart .....</b>	<b>171</b>
<b>Attachment 4: Decision Matrices.....</b>	<b>172</b>
Weighted design matrix for different types of bikes.....	172
Weighted design matrix for drivetrain connections .....	172
Weighted decision matrix for mechatronics controller selection .....	173
Weighted design matrix for power decoupling mechanism .....	173
<b>Attachment 5: Concept Drawing .....</b>	<b>174</b>
<b>Attachment 6: Mechatronics Code .....</b>	<b>175</b>
<b>Attachment 7: Safety Hazard Checklist.....</b>	<b>186</b>
<b>Attachment 8: Drawings.....</b>	<b>188</b>
<b>Attachment 9: Specification Sheets .....</b>	<b>198</b>
<b>Attachment 10: Bill of Materials.....</b>	<b>199</b>
<b>Attachment 11: MATLAB Simscape Script .....</b>	<b>201</b>
<b>Attachment 12: Simscape Models.....</b>	<b>205</b>
<b>Attachment 13: Printed Circuit Board.....</b>	<b>206</b>
Schematics .....	206
Board Layout .....	207
<b>Attachment 14: 2019 FPVC Competition Results.....</b>	<b>208</b>



## LIST OF FIGURES

Figure 1. Murray State University final recumbent vehicle design .....	20
Figure 2. Cleveland State University final vehicle design.....	21
Figure 3. Milwaukee School of Engineering final vehicle design.....	21
Figure 4. Cal Poly 2017-2018 fluid power standard bike .....	30
Figure 5. Touring bike handles to adjust rider position. ....	30
Figure 6. Example of a recumbent bike .....	31
Figure 7. Example of a prone bike.....	32
Figure 8. Recumbent tricycle velomobile design .....	32
Figure 9. Conceptual bike layout .....	33
Figure 10. Bottom welded plates used for mounting the bevel gear set and planetary coupling .	35
Figure 11. Bevel gear and mounting.....	35
Figure 12. Pictures of the current drivetrain and drivetrain mounting .....	36
Figure 13. Last year’s rear drivetrain assembly.....	37
Figure 14. Conceptual design front drivetrain .....	38
Figure 15. Conceptual CAD of new rear drivetrain.....	39
Figure 16. Direct Drive mode hydraulic diagram.....	40
Figure 17. Discharge mode hydraulic diagram.....	40
Figure 18. Regenerative braking mode hydraulic diagram.....	41
Figure 19. PIT mode hydraulic diagram .....	42
Figure 20. 2018 Competition Results .....	42
Figure 21. Micromax Accumulator Specifications from SteelHead Composites.....	43
Figure 22: Bent Axis Pump.....	44
Figure 23: Parker Hannifin F11 Efficiency Curves .....	44
Figure 24: Gear Pump/Motor .....	45
Figure 25: Gerotor Pump/Motor .....	45
Figure 26: Spool-Type Solenoid Valve .....	46
Figure 27: Poppet-Type Solenoid Valve.....	47
Figure 28. 805 Hubmaster’s full mechatronics enclosure with 3-way toggle switch.....	48

Figure 29. Example of crimp connections made for mechatronics wiring .....	48
Figure 30. Example photo of Arduino Uno microcontroller .....	49
Figure 31. Pros and cons comparison of the Raspberry Pi 3 and Arduino Uno Rev3 platforms .	50
Figure 32. Preliminary mechatronics layout including sensors, buttons and solenoid drivers.....	52
Figure 33. LCD display and drive mode button layout on front bike handlebar .....	53
Figure 34. Task diagram for mechatronics .....	53
Figure 35. User interface State Diagram.....	54
Figure 36. Honda CBR600 on the 805 Hubmaster's Bike.....	55
Figure 37. Dog Tooth Clutch Preliminary Design.....	56
Figure 38. Equivalent Mathworks' models of a mass-spring-damper system using Simulink and Simscape .....	58
Figure 39. Plot of bike displacement over time using the 805 Hubmaster's MATLAB accumulator discharge model (0.29 gallon accumulator volume with 900 psi precharge) .....	58
Figure 40. Simscape derived accumulator discharge model.....	59
Figure 41. Plot of bike translational displacement over time using the Simscape accumulator discharge model (0.29 gallon accumulator volume with 900 psi precharge). Estimated efficiency score of 14.5.....	60
Figure 42. Plot of bike translational displacement over time using the Simscape accumulator discharge model (0.98 gal accumulator volume with 900 psi precharge). Estimated efficiency score of 15.7.....	61
Figure 43. Patterson model bicycle geometry.....	62
Figure 44. Patterson model front wheel coordinate system .....	62
Figure 45. Steering spring rate vs. velocity .....	63
Figure 46. Control authority characteristics of a short wheelbase and a long wheelbase bike.....	64
Figure 47. Estimated power losses of current bike using the following parameters: road friction coefficient set to 0.005, road at 1% grade, drag coefficient set to 0.75 with frontal area of 5 ft <sup>2</sup> , and hydraulic circuit efficiency estimated to be 50%.....	64
Figure 48. Input power and required user torque for given bike speed and user cadence. The model will take a particular given input power and find the user torque and cadence at steady state operation considering all of the previous mentioned bike parameters. ....	65
Figure 49. (a) Torque curve with a rear gear ratio of 1:6. (b) Torque curve with a rear gear ratio of 1:2. ....	65
Figure 50. Simscape derived model for direct drive mode.....	66

Figure 51: Overview of final bike.....	69
Figure 52: Another view of final bike.....	69
Figure 53. Image of Trek FX Sport 4 .....	70
Figure 54. Dimensions of the large size Trek FX Sport 4 Frame .....	71
Figure 55. Image of revised BikeCAD frame geometry .....	72
Figure 56. Final frame geometry in Solidworks sketch (all dims. in mm) .....	73
Figure 57. Solidworks model of final frame geometry.....	74
Figure 58. Image of the accumulator mounted on the frame rear upper support tubes .....	74
Figure 59. Image of rear motor attachment to rear vertical support tubes and seat stays with tube bends indicated with red circles .....	75
Figure 60. Image of front drivetrain attachment to frame chainstays.....	76
Figure 61. Example of chainstay bridged welded between tubes for lateral rigidity .....	76
Figure 62. Picture showing the differences between straight tubing and butted tubing.....	77
Figure 63. Model of final frame with tube numbers referencing to Table 11. ....	79
Figure 64. Variation of control spring with velocity for control bike and proposed design.....	83
Figure 65. Variation of control sensitivity with velocity for control bike and proposed design. .	83
Figure 66. Mass of the bike and location of CG with 180lb rider .....	84
Figure 67. Truss analysis of bike frame.....	84
Figure 68. Direct Drive Mode Hydraulic Diagram.....	86
Figure 69. Discharge Mode Hydraulic Diagram.....	87
Figure 70. Regenerative Braking Mode Hydraulic Diagram.....	88
Figure 71. PIT Mode Hydraulic Diagram.....	89
Figure 72: Testing Hydraulic Coast Mode.....	89
Figure 73: Coast Test Track.....	90
Figure 74: Eaton SBV1-10-C Solenoid Pressure Loss .....	91
Figure 75: SBV1-10-C Acceptable Line Block Options .....	92
Figure 76: Hydraulic Mounting Position .....	92
Figure 77: Solenoid Mounting Solution .....	93
Figure 78. Representative wire frame of hydraulic manifold design showing internal features. .	94
Figure 79. Line configuration of hydraulic manifold .....	94

Figure 80. Hydraulic anifold mounting bracket.....	95
Figure 81. Mounting configuration of hydraulic accumulator.....	95
Figure 82. Pulsing discharge compared to complete discharge of the accumulator.....	96
Figure 83. Distance traveled based on discharge technique. ....	97
Figure 84. Bosh bent axis pump .....	97
Figure 85: Reservoir .....	98
Figure 86. Front drivetrain assembly.....	99
Figure 87. Single mile time sweep over different gear ratios for front drivetrain.....	100
Figure 88. Shimano Acera FC-M3000-B2 crankset & BB-UN26 square taper bottom bracket.	100
Figure 89. Simple chain tensioner mounted on right chainstay.....	101
Figure 90. Dual jockey wheel chain tensioner to update previous single jockey wheel version	102
Figure 91. Freewheel to Axle Adapter with Right Hand Threads for 5/8" Axle from electricscooterparts.com.....	102
Figure 92. Planetary gearbox and pump orientation on bicycle .....	103
Figure 93. Comparison of previous and current planetary gearbox models. ....	103
Figure 94. KF060-004-S2 planetary gearbox from Apex Dynamics.....	104
Figure 95. Front drivetrain mounting bracket.....	105
Figure 96. Rear drivetrain assembly .....	105
Figure 97. Rear drivetrain mounted to the back of the bike .....	106
Figure 98. Rear Drivetrain with frame hidden.....	107
Figure 99. Single mile time sweep over different gear ratios for rear drive train.....	107
Figure 100. Driving force on rear drive train sprockets.....	108
Figure 101. Rear drivetrain mount with loads applied .....	109
Figure 102. Solidworks FEA for rear drivetrain mount.....	110
Figure 103. Mechatronics Circuit Layout.....	111
Figure 104. 2.8" LCD Screen .....	112
Figure 105. Momentary Button.....	112
Figure 106. 3000psi Pressure Transducer .....	113
Figure 107. Hall Effect Sensor.....	113
Figure 108. Solenoid Driver IC .....	114

Figure 109. 12V/10000mAh Battery .....	114
Figure 110. Button Enclosure .....	115
Figure 111. Display Enclosure.....	115
Figure 112. Mechatronics Mounted on Test Bike .....	116
Figure 113. Breadboard Prototype Circuit.....	116
Figure 114. Display Functionality .....	117
Figure 115. Arduino Pro Micro .....	117
Figure 116. Example of a Finished Perfboard .....	118
Figure 117. Final Design Prototype on Perf-Board .....	119
Figure 118. Printed Circuit Board Layout .....	120
Figure 119. Overview of Simscape direct drive model .....	120
Figure 120. First portion of direct drive model showing cyclic pedal force conversion .....	121
Figure 121. Close up view of motor to pump portion of direct drive model.....	121
Figure 122. Close up view of vehicle body block and outputs to workspace of direct drive model .....	122
Figure 123. Bike speed and distance traveled comparison between the 2018 Simscape and 2017 Simulink direct drive models .....	122
Figure 124. Horizontal distance traveled from stop with a 300W input, 10.3:1 front GR, 1:3 rear GR using Simscape direct drive model.....	123
Figure 125. Horizontal distance traveled from stop with a 300W input, 6.3:1 front GR, 1:3 rear GR using Simscape direct drive model.....	124
Figure 126. Simscape accumulator discharge model.....	125
Figure 127. FPVC efficiency challenge score .....	125
Figure 128. Graph of various accumulator sweeps and effect on efficiency challenge score with and without PWM-like pulsing.....	126
Figure 129. Simscape model of accumulator recharge/regen.....	126
Figure 130. Plot of accumulator pressure over time for a 1.06 gal accumulator .....	127
Figure 131. Power losses at steady state operation for various speeds.....	127
Figure 132. Power losses when traveling up a 2% grade. ....	128
Figure 133. Unmachined tubes with miter templates taped on each end.....	131
Figure 134. Anvil Universal Mitering Jig attached to a rotary vice on a mill .....	132

Figure 135. Russell showing how mitering is done .....	132
Figure 136. Close up of hole saw miter in tube .....	133
Figure 137. Another Anvil fixture used for the tubes attached to the bottom bracket .....	133
Figure 138. Another Anvil fixture used for tubes attached to the seat tube .....	134
Figure 139. Anvil tube bender .....	134
Figure 140. Anvil Bikeworks Type 3.1 Journeyman bicycle frame fixture .....	135
Figure 141. Dimensions needed to setup Anvil Journeyman fixture.....	135
Figure 142. Example of the bottom bracket purge hole process.....	136
Figure 143. We had to move the rear portion of the Anvil fixture holding the rear dummy axle backwards past the normal limits of the fixture to weld the bike. We held the fixture piece to the assembly with a c-clamp.....	136
Figure 144. Image of rear brake boss brazing fixture attached to the rear dropouts .....	137
Figure 145. Final version of the frame with paint .....	137
Figure 146. Facing the bottom bracket and chasing the threads.....	138
Figure 147. Reaming the seat tube.....	138
Figure 148. Facing and reaming the head tube .....	139
Figure 149. Final reservoir getting welded .....	140
Figure 150. Front drivetrain mounting bracket flat pattern and mounting tab .....	140
Figure 151. Bending the front drivetrain mounting bracket on the sheet metal brake .....	141
Figure 152. Machining additional slots into the front drivetrain mounting bracket using the mill in Mustang 60 .....	141
Figure 153. Fixture to locate the front drivetrain mounting plate.....	142
Figure 154. Rear drivetrain mount welded in place.....	143
Figure 155. Fixie sprocket with teeth machined down.....	143
Figure 156. Rear fixie sprocket components welded together.....	144
Figure 157. Final rear wheel and sprocket.....	144
Figure 158. Broached keyway on McMaster sproket .....	145
Figure 159. Completed bike assembly.....	146
Figure 160. Fork, handlebar and stem installation.....	147
Figure 161. Frame with all bike auxiliaries installed.....	147

Figure 162. Planetary gearbox mounted to pump.....	149
Figure 163. Planetary gearbox and pump attached to mounting bracket.....	149
Figure 164. Front drivetrain assembly in motion.....	150
Figure 165. Rear drivetrain assembled and chain being sized.....	151
Figure 166. Rear drivetrain assembled and chain being sized 2.....	151
Figure 167. Mock endurance course in the H1 parking lot on campus .....	154
Figure 168. Mock sprint course adjacent to H1 parking lot on campus .....	155
Figure 169. 2019 competition sprint challenge top 5 results .....	156
Figure 170. 2019 competition efficiency challenge top 5 results .....	157
Figure 171. 2019 competition endurance challenge top 5 results.....	157
Figure 172. Demsontration of lack of chain wrap and chain tension in front driveetrian .....	158
Figure 173. Schematic of hydraulic circuit with the specific solenoid in question circled in red .....	159
Figure 174. Gantt Chart Excerpt.....	162

## LIST OF TABLES

Table 1. 2017 NFPA Competition Awards.....	18
Table 2. A summary table of the 2017-2018 competition pump and motor selection.....	22
Table 3. Pros vs. Cons for different braking systems .....	25
Table 4. Design Parameter Targets with their associated tolerances, risks and notes .....	27
Table 5. Weighted design matrix for different types of bikes .....	29
Table 6. Weighted design matrix for drivetrain connections.....	37
Table 7. Weighted decision matrix for mechatronics controller selection .....	51
Table 8. Weighted design matrix for power decoupling mechanism .....	57
Table 9: Mass Properties for 2018-2019 Bicycle .....	68
Table 10. Final 2D bike frame parameters from Solidworks guide sketch .....	73
Table 11. Summary of frame tube diameters and wall thicknesses (See Figure 63 for corresponding tube numbers).....	79
Table 12. Input Parameters for Patterson Control Model .....	82
Table 13. Tube Factor of safety based on truss analysis.....	85
Table 14: Coast Mode Test Results .....	88
Table 15: Hydraulic Mode Losses (@ top speed).....	90
Table 16. Rear drivetrain loads into mounting plate.....	108
Table 17. Summary table of above analysis with major inputs and outputs with Simscape direct drive model .....	123
Table 18. Summary table of above analysis with major inputs and outputs with Simscape direct drive model .....	124
Table 19: 2018-2019 Hydraulic Bicycle Budget .....	129
Table 20. Design specifications table with predicted performance with current design .....	153
Table 21. Mock efficiency challenge results .....	155
Table 22. Mock sprint challenge results .....	155
Table 23. Individual Roles and Responsibilities.....	161



## **EXECUTIVE SUMMARY**

This report provides a comprehensive description of the research, analysis and design work that The Incompressibles have completed thus far in the senior project process. This document includes all the work that The Incompressibles have completed for the team's Preliminary Design Review (PDR), Critical Design Review (CDR), the work leading up to the 2019 FPVC competition and the competition results. This report includes the initial research that the team completed for the fluid power competition, first iterations of designs, final iterations of designs, manufacturing results and processes, and finally testing and results from competition. With a new design for the bike frame, drivetrain, mechatronics, power decoupling and hydraulics, The Incompressibles dramatically changed Cal Poly's fluid power bike platform in the Fluid Power Vehicle Challenge. This bike was built with the direct intention of getting first place at this year's fluid powered bike challenge competition.

# 1 INTRODUCTION

The goal of this project is to build a human powered vehicle that uses hydraulic fluid as a means of power transfer between the rider and the wheels and compete in the National Fluid Power Association Competition. The intent of the competition is to foster an understanding of fluid mechanics through its utilization in an unconventional and unsuitable application. The association hopes to challenge students and promote original thinking in a competitive setting. Human powered vehicles are recognized as extremely efficient but using fluid power at low speeds poses challenges. Combining the unlikely pair together creates an environment that encourages uncommon connections and developments. This project will give teams hands on experience in working as a team, meeting schedules and deadlines, simulating, designing, manufacturing, and testing. From this program, participants will be more prepared to enter the fast-paced fluid power industry environment and other engineering fields.

## Team members:

1. Nicholas Gholdoian: *Sponsor Contact, Editor*
2. Julian Rodkiewicz: *Testing Facilitator*
3. David Vitt: *Vendor Contact, Manufacturing Coordinator*
4. Kyle Franck: *Secretary, Editor*
5. Russell Posin: *Project Planner*
6. Alex Knickerbocker: *Treasurer, Manufacturing Coordinator*

## 1.1 Problem Statement

The Incompressibles will strive to design a vehicle which will achieve the top overall winner at the 2019 Fluid Power Challenge in Colorado. The team will be undertaking a comprehensive redesign based upon the feedback from the previous team and competition results. With this goal in mind, this year's team is going to focus on reliability, overall weight reduction, mechanical decoupling and circuit improvements for both the electronics and the hydraulic systems. Testing time from the previous team was neglected, therefore The Incompressibles are planning on having a fully testable vehicle 5 weeks before the start of competition.

## 2 BACKGROUND

The Fluid Power Vehicle Challenge, originally named The Chainless Challenge by Parker Hannifin Corporation in 2005 but renamed in 2017 by the National Fluid Power Association, was founded to challenge young engineers through the design of a pneumatic or hydraulic powered vehicle to compete in a series of specified trials. The three primary challenges used to judge each team's vehicle are sprint, efficiency, and endurance. Additional awards are given in a number of other categories, including design, presentation, teamwork, workmanship, and reliability & safety (See Table 1 for award specifications). Each vehicle is assessed on-site by a team of industry judges and event safety is monitored by a team of marshals during each trial, and time is kept by the designated timekeepers when applicable.

Table 1. 2017 NFPA Competition Awards

<b>Award</b>	<b>Prize</b>
Overall Champion	\$3,000
Best Presentation	\$2,000
Fastest Sprint Race	\$1,000
Highest Efficiency Challenge	\$1,000
Best Reliability / Durability Challenge	\$1,000
Best Design	\$500
Best Reliability and Safety	\$500
Best Manufacturability	\$500
Best Teamwork	\$500

There are several technical requirements as specified by the NFPA that each team's vehicle must adhere to qualify under their safety and usability standards. These requirements have formed the absolute base level specifications for The Incompressibles vehicle design. The specifications include:

- The implementation of a fluid link within the power transmission system between the rider's input and the final propulsion of the vehicle
- The use of an energy storage device
- A fluid power circuit that can transmit power in both a direct drive mode and a regenerative braking mode

- Environmentally friendly fluid used in the hydraulic system
- Vehicle must be operated completely by a single rider with no help to enter or exit
- Weight limited to 210 lbs if being shipped, otherwise no weight requirement
- Vehicle must have brakes that are able to hold the vehicle at a stop under full accumulator charge
- There must be no discernable leakage from the system

If a team fails to meet any of these requirements, they will not be able to participate in the competition. However, with the goal of outperforming the competition, it necessary to specify further design requirements regarding vehicle performance. To establish a baseline of technical specifications from which the vehicle will be designed, extensive background research on previous year's vehicle entries was conducted, both those from Cal Poly and those from competing schools.

## **2.1 Customers**

The customers for this project are The Incompressibles, Dr. James Widmann, and the competition judges. The most important of these customers is us as we have the most exposure to the many stages of the bike's development. Dr. Widmann is the advisor and financial supporter for the project and his greatest requirement concerns are the weight, cost, and safety of the vehicle. The competition judges are concerned with the weight, speed, efficiency and safety of the vehicle. These customer specific requirements were recognized and accounted for during the project specification development. The team will be responsible for designing, manufacturing, testing and competing with the vehicle. Furthermore, because our project is a competition, the customer needs can be instead interpreted as both design goals necessary to win the events, as well as compliance with the regulations of the organization. The Appendix includes a summarized list of the project needs that have been deemed most important.

## **2.2 Existing Designs: Competition Winners 2017-18**

The most pertinent sources of information on existing products include all designs from past competitions, focusing primarily on Cal Poly's 2018 team design and the 2018 competition winners. Although useful information has been gained from older designs, our analysis is driven primarily by the senior project reports of Cal Poly and the top placing teams from this year. The most detailed and accessible data is from the previous Cal Poly teams, and this information has been compared with the highlighting features of winning teams to gain an understanding of beneficial design choices.

### ***2.2.1 Overall Winner:***

Murray State University designed a recumbent three wheeled vehicle which used the driver's hands to pump fluid using linear actuators to drive bent axis pumps, and utilized a leg steering system, seen in Figure 1. The unit contained three accumulators totaling 2.21 gallons of hydraulic fluid with two reservoirs totaling 3.67 gallons. The largest accumulator, made from carbon fiber, weighed only 14 pounds making it relatively light for its high volume of 2.5 gallons. The hydraulic circuit operated at a maximum pressure of 3000 psi, which was common for the competition. The Murray State team also attempted to implement an electric clutch to address motor drag which

they indicated caused noticeable losses during coasting. However, the team was unable to utilize the clutch and cited that the design was too complex to complete in time. The hydraulic circuit consisted of only two modes, propulsion and regenerative braking, which was atypical considering most teams had at least one more direct drive mode. The Murray State team had no way to modulate the accumulator discharge.



Figure 1. Murray State University final recumbent vehicle design

### ***2.2.2 Second Overall:***

Cleveland State University designed a standard position bicycle with one pump, one motor and a single accumulator, seen in Figure 2. The pump was turned by a conventional crank-pedal design that sends its power through a gear set consisting of 6 gears, 2 jack shafts, 2 sprockets, and a chain. The motor design was simpler, consisting of only 1 set of sprockets and a chain to send power to the rear wheel. Cleveland's hydraulic system offered 4 drive modes, including direct drive, regenerative braking, accumulator discharge, and emergency discharge, all achievable through a single 2-in-2-out solenoid. The first three modes were common amongst fluid power challenge teams, however the 4th mode was unique. Emergency discharge allowed Cleveland to release all accumulator pressure into their reservoir without travelling through the pump or motor, and therefore not moving the pedals or bike in the process. Cleveland's vehicle was similar to Cal Poly's in weight at 105 pounds and offered 3 operating speeds by changing the sprocket size on their motor.



Figure 2. Cleveland State University final vehicle design.

### ***2.2.3 Third Overall:***

Milwaukee School of Engineering designed a standard position road bike with a custom aluminum manifold meant to improve the packaging of their hydraulic circuit, which is evident in their clean looking design in Figure 3. The use of this manifold allowed for a minimal amount of external hydraulic piping to be used, ultimately reducing clutter and energy losses. The team selected a 1L gas piston accumulator with 4000 psi capacity, and manufactured a custom aluminum reservoir. Power was delivered to the pump via a chain and sprocket driven by the crank-pedal. The motor, which was located just above the rear hub, also transmitted power via chain and sprocket to the rear wheel. Because of their custom manufactured parts and use of chains and sprockets instead of gears, Milwaukee succeeded in having a lightweight, aesthetic design.



Figure 3. Milwaukee School of Engineering final vehicle design.

## 2.3 Component Research

Due to the specific application of a hydraulic powered vehicle, component research will be focused on previous competition teams. An emphasis will be placed on Cal Poly's "805 HubMasters" because The Incompressibles have direct access to a large amount of their analysis and are in contact with their members.

### 2.3.1 Pumps and motors (driving and driven)

Last year Cal Poly utilized a Bosch fixed axial piston pump for both the pump and the motor, whereas other teams used the more common Parker F-11 pump/motor. Both are fixed axial "bent axis" pumps but the Bosch pump is made from aluminum while the Parker F-11 is cast iron giving the Bosch a 6.5 lb weight advantage (12 lb vs. 5.5 lb) over the Parker unit. The internal structure of a bent axis pump is made up of several small pistons attached to an angled disc rotated by the driving force or providing the driving force. Small displacements of fluid are pushed continuously through the unit, giving a smooth flow and even pressure with relatively high efficiency.

Table 2. A summary table of the 2017-2018 competition pump and motor selection

Team	Pump Type	Motor Type
Cal Poly SLO	Bent-Axis	Bent-Axis
Murray State	Piston	Bent-Axis
Iowa State	Gear	Gear
Purdue	Piston, Gear	Bent-Axis
Milwaukee State	N/A	N/A
Cleveland	N/A	N/A
Akron	Gear	Bent-Axis
West Virginia	Gear	N/A

Looking at

Table 2, amongst teams that used piston pumps, only Murray State used them as their main driving pump, while many other teams used them simply to charge their accumulator. Murray State did not utilize a conventional style pedal crank mechanism, instead they used levers in a rowing motion. Every other team with a conventional pedal style system used either gear or bent-axis pumps.

When speaking to a member of the 805 HubMasters senior project group about using a gear pump as opposed to a bent-axis pump, he advocated for the bent-axis, stating the gear pump was choppy.





### ***2.3.2 Hydraulic circuits***

There is a large amount of flexibility with hydraulic circuit design due to the variety of pumps, motors, solenoids, and their expansive placement. Some teams such as Cal Poly SLO and Purdue used computer controlled solenoids for their expeditious control. However, the 805 HubMasters' bike does have internal leakage through the solenoids reducing the effectiveness of accumulator storage.

Valve selection plays a huge role in determining the performance of a hydraulic system. A balance between the cost, weight, and efficiency must be determined when designing a hydraulic system. The driving factor determining our valve selection will be finding solenoids that have little or no internal leakage, which proved to be a major issue in the previous team's bike.

### ***2.3.3 Electronics/Mechatronics***

Electronics and Mechatronics integration varied in complexity from team to team during the 2018 competition. Milwaukee University developed a data acquisition system to record their velocity data using an Arduino and storing the data on a SD card. This was purely for validating vehicle speed. Purdue University designed an electric circuit that monitored the vehicle's speed, gps position, and drive mode via a phone app.

Cal Poly integrated electronics into their bike starting in 2016. A display was placed in front of the rider's view to show accumulator pressure, pedal cadence and speed in real-time. An Arduino Uno microcontroller grabbed data from two Hall Effect sensors, a pressure transducer and a user operated switch. Based on the drive mode selection, two solenoids were electrically activated to control the flow of hydraulic fluid. This system allows the user to quickly change drives modes during competition versus a traditional mechanical lever system used by previous Cal Poly teams. The 2018 team, The 805 HubMasters, revised on the previous mechatronics system, utilizing an LCD with adjustable contrast, switches to select drive modes, and sensors to monitor accumulator pressure and rider cadence.

Riding the current bike highlighted the ergonomics issue of operating a mechanical lever quickly while concentrating on controlling the bike. Using simple buttons to actuate the different drive modes would be easier and simpler to operate versus switches. An electronics system also opens new avenues in terms of variable pressure control either via solenoid operation or accumulator discharge. This function could be beneficial at improving the overall efficiency score. A robust and easy to operate mechatronics system could be invaluable in a competition environment.

### ***2.3.4 Accumulator***

Looking at the teams from the competition last year, teams utilized a variety of accumulator sizes. Teams such as Cal Poly and Milwaukee University opted for smaller accumulator sizes around one liter or one quart, whereas teams like Murray State opted for a significantly larger accumulator at 3.5 gallons of storage. The design constraints to consider when looking at accumulator size are the pressure of the hydraulic system, the overall weight of the bike, and the rate at which we want to discharge the accumulator to obtain the maximum amount of points at the different races. In

general, the more capacity that you can store, the more the bike will weigh. This can be seen with Murray’s overall weight being roughly twice that of Cal Poly (105 lb vs 200 lb). Still, when sizing up accumulators, volume increases at a higher rate than weight, so purchasing a larger accumulator may be worthwhile.

There were two major categories of accumulators used for the competition, bladder accumulators and piston accumulators. Bladder accumulators typically have faster responses to changes in system pressure whereas piston accumulators provide higher flow rates. Installation also tends to be more complicated for the bladder accumulators.

### 2.3.5 Brakes

In regard to braking components, there are two main things to consider: the brake actuation method and the brake clamping method. The two most common types of actuating brakes for bicycles are hydraulics and cable. Clamping methods include rim/V-brakes or disc brakes. Although there are more common pairings of power transfer and clamping methods such as hydraulic disc brakes vs cable pulled V-brakes, it is possible to change the combinations. Both cable pulled disc brakes and hydraulic V brakes can be purchased or built but are less common. Table 3 contains a list of advantages and disadvantages for different braking systems.

Table 3. Pros vs. Cons for different braking systems

Type	Pro	Con
Cable Driven	Simple, reliable, cheap, easy to replace	Smaller potential mechanical leverage
Hydraulics	Larger potential mechanical leverage	High complexity, Cost, difficulty to replace, potential leaks
V-Brake	Simple, cheap, minimal components, easy to replace	Less modulation, quicker wear
Disc	Longer wear time, more modulation	More complex, expensive, smaller torque radius

With the progression of biking technology and ease of implementation, any of the proposed styles of brakes above should be relatively easy to implement. While cable driven V-brakes might be the most simple, the difference in implementation time is relatively small considering the overall scope of the hydraulic bike.

Due to the nature of the races at competition, high braking deceleration as a result of clamping brakes is not expected around the course and should actually be avoided as much as possible. Regenerative braking instead of clamping brakes allows us to store energy back into the accumulator instead of losing it as heat. For these reasons, the main criteria for the brake system on the bike is to fulfill the requirements that the rear tire can remain locked under full accumulator discharge, and that the brakes can bring the bike to a stop safely if regen were to not be functioning.

### ***2.3.6 Custom bike frame***

Traditionally, teams from Cal Poly have built custom frames to accommodate the numerous components that must be used in this challenge which are uncommon for a bicycle. Regarding the style of bicycle used, Cal Poly has always opted for the standard seating position bicycle. Some teams in the past decided to simply improve the previous year's bike, however we feel that we have the manpower and resources to take on the design of an entirely new frame. After comparing Cal Poly's current bike with the competitors' from this year, we have decided that there is considerable room for improvement with a reimagined frame design, not only regarding weight, but also with locating and attaching components. Moreover, with our intention to potentially reduce the number of gears in the system and instead use chains and sprockets, a frame design would be helpful. Considering the frame was not originally the most pertinent area of focus, we did not want to take on this task unless it was clear that it could be done in addition to our more important design considerations. After our meeting with the Bike Builders club, we agreed that designing and manufacturing a new frame was within the boundaries of this project, so long as we stick to well-known bike frame geometry.

### 3 OBJECTIVES

The team began developing the specification for this year's bike by completing a standard Quality Function Deployment (QFD). The specifications listed below in Table 4 were pulled directly from the QFD document. Risks and tolerances were then generated based upon the goals of the competition. This list of specifications from the QFD gave the team a clear direction to go to accomplish our big picture goals.

Table 4. Design Parameter Targets with their associated tolerances, risks and notes

Spec #	Parameter Description	Requirement or Target	Tolerance	Risk	Compliance	Notes
1	Endurance Time (1 mile)	4 minutes	Max	H	A,T,S	See Note 1 Below
2	Efficiency Score	20 points	Min	H	A,T,S	
3	Sprint Time (600 ft)	24 seconds	Min	H	A,T	
5	Top Speed	40 mph	Max	M	A,T	Rules Requirement
7	Time to Assemble Completely	1 hour	Max	M	S	See Note 2 Below
8	Time to charge accumulator	5 minutes	Max	L	A,T	See Note 3 Below
9	Drive mode selection latency	1 second	Max	M	T,S	See Note 4 Below
11	System Lifespan	2 year	Min	M	T	See Note 5 Below
12	Number of Machined Components	8 parts	±2	H	I	See Note 6 Below
13	Internal Leakage	2 psi/s	Max	H	A,T	See Note 7 Below
14	Braking Torque	Max. torque of accumulator discharge	Min	H	A,T	Rules Requirement
15	Weight	85 lbs	Max	H	A,T	See Note 1 Below
17	External Leakage	0 drips	Max	H	T	Rules Requirement

Note 1.

While operating under the assumption that each team increases their performance by ~15% from the previous year, these requirements give us a good probability of placing in top 3 in the next competition.

Note 2.

Time to assemble from bare frame to working bicycle. This is for the possibility of a critical part on the bike breaking and the time it would take to fully assemble the bike.

Note 3.

Teams are given 10 minutes between competition events to make changes to their bikes. A charging time of 5 minutes gives ample time to recharge the accumulator.

Note 4.

Time it takes for the driver to select a certain drive mode and for the bike to completely switch to the selected drive mode. This includes mechatronics and hydraulics latencies.

Note 5.

A 2 year lifespan allows for testing and refinement of the vehicle for the next team in future years.

Note 6.

Low experience and CNC availability limits our ability to produce complex/time intensive parts. 8 parts will provide a reasonable limit to allow for design flexibility but limit designs from becoming difficult to manufacture (subject to change as manufacturing schedule develops).

Note 7.

The previous year's team had significant internal solenoid leakage, the amount of leakage was such that the driver could visibly see the pressure gauge drop over time.

As far as the development of the bike in relationship to the goals described in Table 4, it is clear that no single item or part of the bike exists "in a vacuum". There are inherent and important relationships among many of the parameters listed. For example, the maximum torque delivered by the motor depends on the maximum weight of the bike. Another example is the maximum speed of the bike depends on drag/friction on the bike, maximum torque output, gear ratio, accumulator volume, motor efficiency and driver wattage output. The more friction and drag in the system, the more power the driver will have to put out to achieve the same speed, however the maximum power from the driver makes little difference if the bike is not in the efficiency range.

## 4 CONCEPT DESIGN

### 4.1 Frame

One of the larger goals for the Incompressibles this year is to redesign the vehicle frame with the intention of making significant weight reduction and allowing more freedom to package components efficiently.

#### 4.1.1 Frame Type Selection

The overall design principle that the Incompressibles are using to approach the vehicle is to design the frame last. This means that we want to size all other components (accumulator, pump, drivetrain, etc.) to gain the maximum number of points and only then size the frame such that it can hold all the components. There are some obvious limits regarding a frame geometry that can hold the rider and components and still be stable; the main idea is to select components first and design the frame second.

As of now, The Incompressibles have selected a standard bike frame design for our vehicle type. This decision was made after considering five different types of possible frames for this year's competition. The Incompressibles considered the following frames types: standard upright bike, recumbent bike, monowheel, prone bike, and velomobile. The strengths and weaknesses of each of the five types of frames were weighed in relation to the overall goals for the team this year. The Incompressibles decided the important criteria for frame design were reliability, weight, manufacturability, packaging flexibility, and cost, while aerodynamics and driver comfort were decided to be less important. The frame weighted decision matrix is shown in Table 5.

Table 5. Weighted design matrix for different types of bikes

Criteria	Weight (0-5)	Frame Concept				
		Upright Standard	Recumbent	MonoWheel	Prone Bike	Velomobile
Weight	4	Datum	-4	-4	0	0
Cost	3		-3	-3	-3	-3
Reliability	5		0	0	0	0
Handling	3		-3	-3	-3	-3
Manufacturability	3		-3	-3	-3	-3
Packaging Flexibility	3		3	-3	0	-3
Driver Comfort	2		0	-2	-2	0
Aero Dynamics	2		2	-2	2	2
<b>Total</b>				-8	-20	-9

### 5.1.1.1 Standard Bike

The standard bike is the most common vehicle layout for this competition and is also what all previous Cal Poly teams have used. The advantages of this type of bike include the ease of manufacturing and the familiarity of the rider with its handling. Additionally, the Cal Poly Bike Builders club agreed to help the Incompressibles through the manufacturing of our bike. Their club already has a number of jigs for a standard bike frame, which would help improve our manufacturing time. The previous year's team's bike can be seen in Figure 4.



Figure 4. Cal Poly 2017-2018 fluid power standard bike

When compared to the other frame types we analyzed, the standard bike frame is less aerodynamic due to the large cross sectional area. However, the aerodynamic drag effects can be mitigated by using touring handlebars that change the sitting position of the rider, seen in Figure 5, making the rider more streamline. The touring handlebars were proposed by the previous year's team, thus they have already been purchased and can be easily implemented this year. It is important to keep in mind that aerodynamic drag becomes substantial at speeds higher than those reached in this competition, therefore drag reduction efforts would not likely make a massive difference.



Figure 5. Touring bike handles to adjust rider position.

### 5.1.1.2 Recumbent Bike

The recumbent bike/trike, shown in Figure 6, was another viable vehicle design for competition. One of the greatest advantages of this style is the packaging freedom that it would provide. Last year's competition overall winner, Murray State, used a recumbent tricycle design. Murray State approached the competition with a different design philosophy than the other teams, as they used 2.5 gallons of accumulator storage, nearly ten times the storage capacity of the 805 Hubmasters. They were only successful in having this large amount of storage because of their larger recumbent frame. The three large accumulators were mounted on the rear end of the tricycle.

A considerable drawback to this vehicle style in comparison to the standard bike frame is the difficulty of manufacturing. While the Incompressibles do have access to fixtures and manufacturing experience in making a standard bike frame, the same resources are not available for the recumbent style bike/trike.



Figure 6. Example of a recumbent bike

### 5.1.1.3 Prone Bike

The prone bike, shown in Figure 7, was a third consideration for the Incompressibles' vehicle frame type. The most appealing characteristic of this vehicle design was the decrease in aerodynamic drag that it would provide. Research showed a substantial difference in drag effects when lying in prone position compared to the upright position since frontal area is greatly decreased, and the rider's body is positioned along the streamlines. On the other hand, the speed at which riders travel during this competition is usually not high enough to warrant the heavy consideration of aerodynamic drag effects.

The drawbacks of the prone bike were ultimately too great to proceed with this design option. As with the recumbent vehicle frame, the prone vehicle posed obstacles in manufacturability since it is a less established design. The resources to successfully design and manufacture a prone bike are not as readily available as those for the standard bike frame design. Additionally, the unfamiliar position for the rider on the prone bike would likely make pedaling and steering somewhat difficult.





Figure 7. Example of a prone bike

#### 5.1.1.4 Velomobile

The Incompressibles also considered implementing a velomobile as our vehicle design. The velomobile, seen in Figure 8, was similar to the recumbent bike/trike except that it included a fairing, which served to greatly decrease aerodynamic drag and protect the rider from outside weather conditions. The coefficient of drag associated with a velomobile was significantly smaller than that of any other of our potential frame designs. However once again, aerodynamics was not a high priority criterion for the vehicle design.

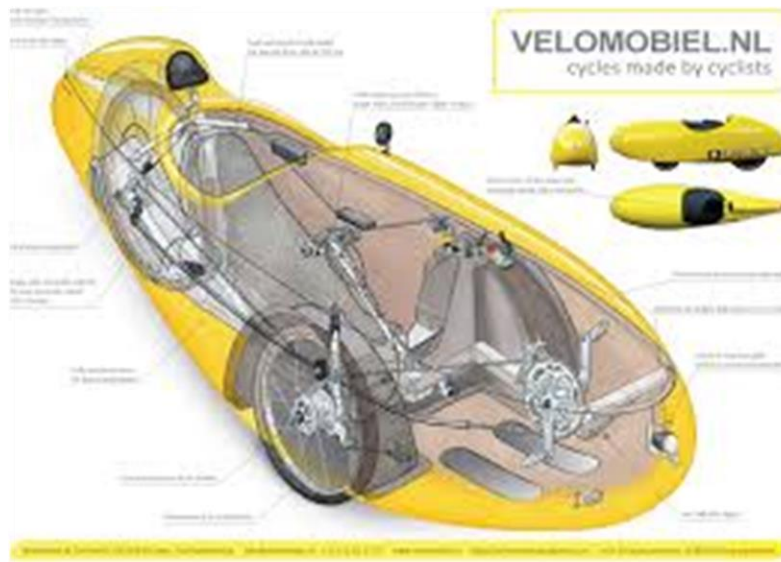


Figure 8. Recumbent tricycle velomobile design

Overall, the velomobile also had a number of drawbacks outweighing its strengths. First, having a similar frame design to the recumbent vehicle, the velomobile would pose difficulties in manufacturing because of the general unfamiliarity with its design. More importantly, the fairing, which is the essential component of the velomobile, would likely be constructed out of a composite fiber material, adding one more degree of complexity and drastically increasing the overall cost of

the vehicle. Lastly, the enclosed fairing would limit the amount of space available for component fittings.

#### ***4.1.2 Preliminary Frame Design***

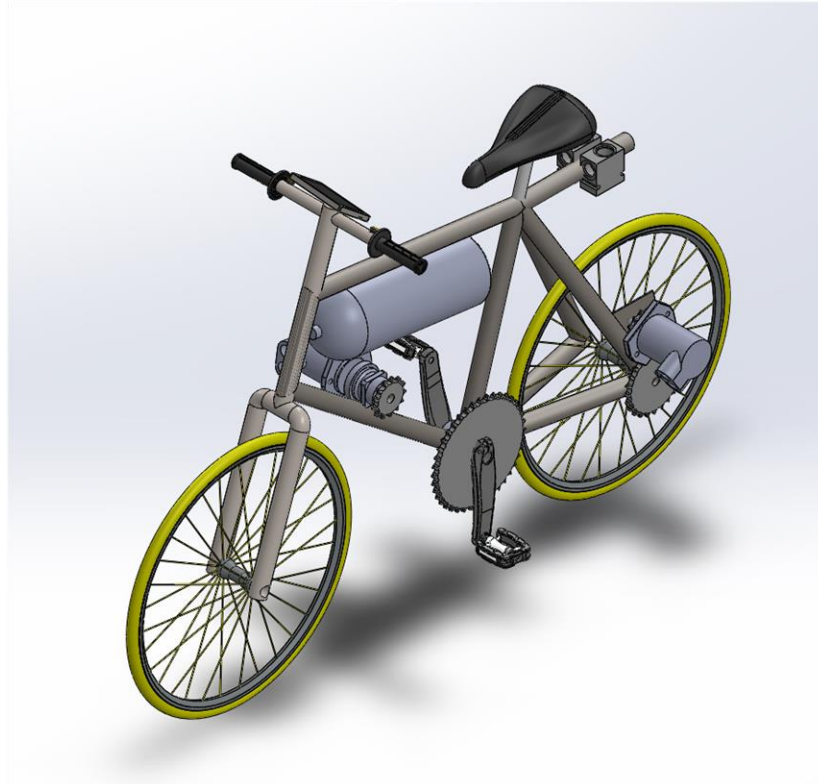


Figure 9. Conceptual bike layout

Figure 9 shows the basic conceptual layout of the bike for next year. One of the biggest changes to the design over the previous years is the movement of the accumulator to the front of the bike and change from bevel gears to chain driven. The Solidworks model used to create this idea was made such that it could be easily adjusted for different changes in components. The layout shown above is just a conceptual layout and it is believed that adjustments will be made before the final design.

#### ***4.1.3 Further Development***

The overall layout of the frame is similar to what we believe the final product will look like. Further layout and geometry adjustments might be made as we look more into how comfortable the component placement is for the rider and what the stability and handling characteristics of the bike are. Preliminary top-level analysis has demonstrated that it may be beneficial to design the bike with a long wheel base, which would improve packaging flexibility, stability, and rider comfort. The next steps in frame design include implementing and tweaking the Patterson Control Model with the finalized component placement and communicating with frame builders to ensure the proposed design is manufacturable and rideable.

## 4.2 Drivetrain

One of the larger changes the Incompressibles are making next year is a comprehensive redesign of the drivetrain. For the past few years, Cal Poly has used bevel gears and a planetary gearbox to transfer torque from the pedals to the pump. This drivetrain was designed when the fluid power challenge was still run by Parker. With Parker in charge of the competition, competitors were not allowed to use any chains for intermediate power transfer. However, when the competition changed hands and intermediate chains were allowed again, Cal Poly continued to reuse the same drivetrain with no chains. Moving forward next year, the Incompressibles believe that the weight of the bike can be reduced significantly and packaging flexibility can be increased by utilizing chains in both the front and the rear drivetrain.

One of the main factors to consider in making a successful drivetrain for this competition is to successfully adjust the pedaling speed of the rider to a reasonable input speed of the pump. A typical pedaling cadence for a standard bike rider is about 90 rpm, while the optimal pump operating efficiency is about 1500 rpm. This difference leads us to a gear reduction of 15:1, which is the same as the old drivetrain. However, this year we hope to reduce the weight and packaging size of the drivetrain by both replacing the coupling mechanism between motor and planetary set and implementing a chain and sprocket gear reduction. The current drivetrain design is very heavy and unnecessarily beefy as a result of using gears for torque reduction. The competition guidelines stipulate that chains can be used to connect intermediate components in the vehicle as long as the motor and pump are not mechanically linked. The use of sprockets and chains will allow the new bike to have the same gear reduction, but with a decrease in weight. In addition to being significantly lighter, the chain and sprocket drivetrain allows for increased flexibility in the placement of components and introduces the possibility of variable gear ratios.

### 4.2.1 Current Design

#### 5.2.1.1 Front Drivetrain

As mentioned before, the front drivetrain for the bike included a set of bevel gears and a planetary gearbox. The planetary gearbox and its shaft coupling were mounted vertically from the pedal cranks. This design requires a different type of mounting than the standard bicycle mounting. Two flat .25" plates were welded to the frame and used to mount the bevel gears along with their housing. These plates for mounting can be seen in Figure 10.



Figure 10. Bottom welded plates used for mounting the bevel gear set and planetary coupling

The bevel gears provide a 1:3 torque reduction from the crank to the drive shaft, and the planetary gearbox then has 1:5 gear reduction. This leads to a total of 1:15 torque reduction from the driven pedals to the pump. Figure 11 shows the bevel gear assembly while mounted on the frame.

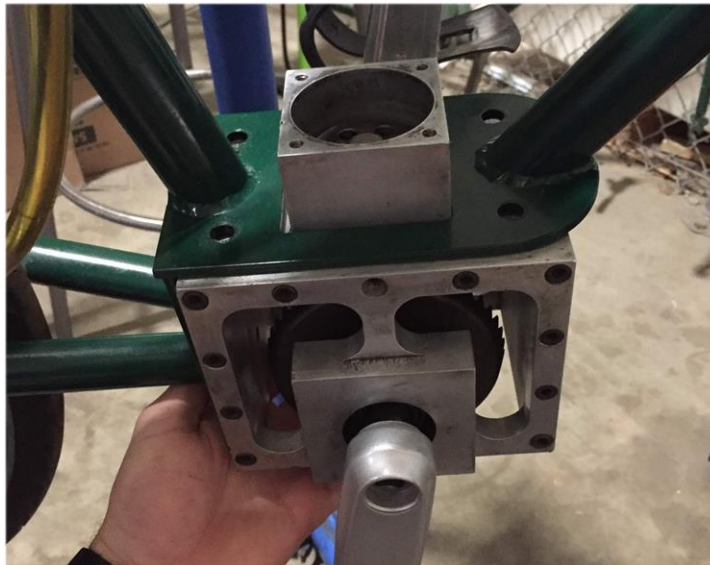


Figure 11. Bevel gear and mounting

This drivetrain seen in Figure 12 has been used by Cal Poly for several years, and the system has seen a decent amount wear. The shaft coupling out of the planetary gearbox used a shaft collar. Last year before the team left for competition, the shaft started to slip in the collar and to quickly repair the system, the slot on the collar was cut a slightly larger such that the collar could clamp down with more force on the shaft. Even with this modification, the shaft continued to slip relative to the collar. Moving forward, this year's team does not have the option to reuse the system from last year. Some redesign is required solely due to the wear on the system.

In addition to the wear the drivetrain has seen, there are a notable number of disadvantages in the way in which this system was designed, in particular the size and weight of the shaft coupling from the planetary gearbox. A large steel shaft with an aluminum insert was used to connect to the shaft key on the pump. Then, a large flanged aluminum housing was placed over the mechanism for safety. A large amount of weight and space can be saved by simply changing the coupling between the shafts. Also, because of the gear reductions used on the front and the back of the bike, the required torque to pedal was very high, meaning that the rider could only get a cadence around 30 rpm, about one third the target speed of 90 rpm.

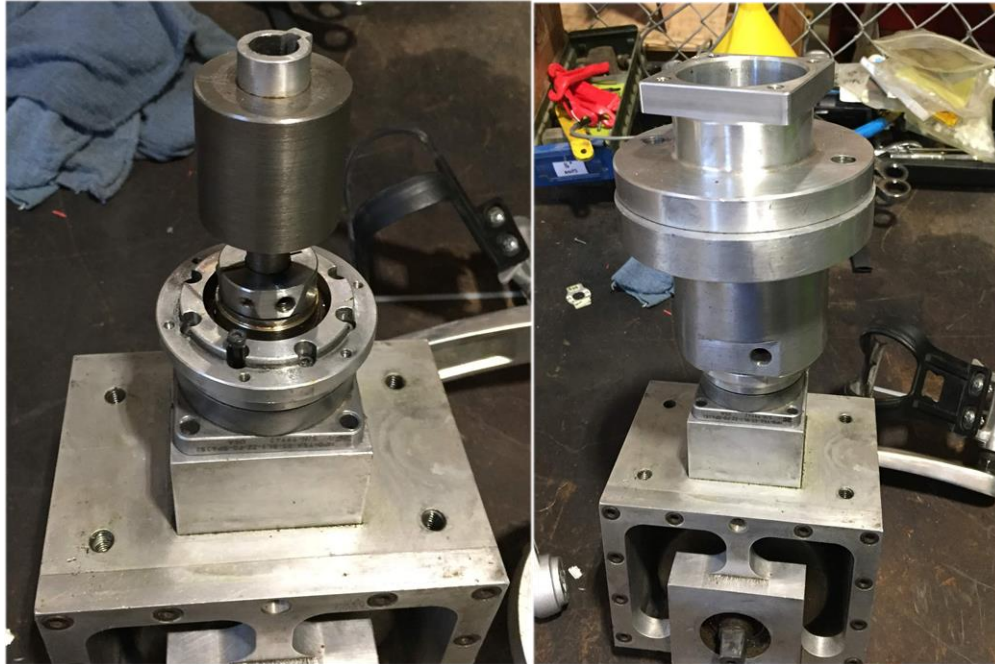


Figure 12. Pictures of the current drivetrain and drivetrain mounting

#### 5.2.1.2 Rear Drivetrain

The rear drivetrain of the bike from last year, seen in Figure 13, used a set of gears in order to transfer torque from the motor to the rear wheel. A friction clutch was added so that the rear wheel could disconnect from the motor, allowing the rear wheel to spin freely. The gear on the outside of the clutch was used as a step-down gear. The overall gear reduction was 3:1 in the rear, with the motor shaft spinning 3 times the speed of the rear wheel.

Overall, the design of the rear drivetrain was compact and practical. The biggest problem with the system was the friction clutch on the rear. Due to a lack of time last year, the clutch was never fully implemented and could not actually disengage—it added unnecessary weight without performing any function.

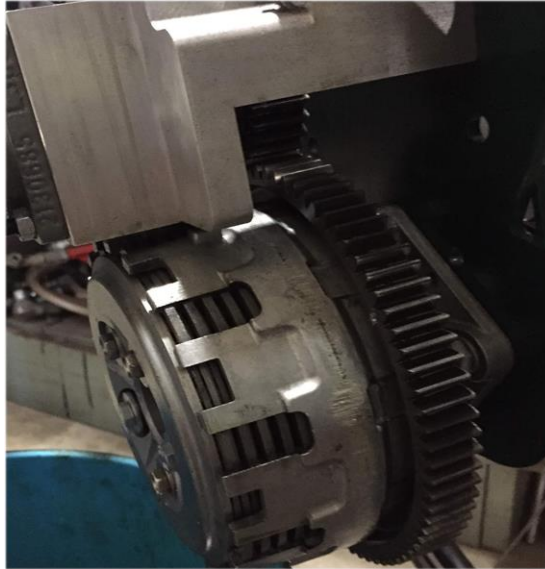


Figure 13. Last year's rear drivetrain assembly

#### 4.2.2 New Design

##### 5.2.2.1 Front Drivetrain

Moving forward this year, the Incompressibles are planning on redesigning the front drivetrain by using a sprocket and chain instead of a bevel gear set or a gear train. The sprocket and chain design has a number of advantages over the bevel gear design. First of all, the bike frame would no longer include the large flat plates in order to mount the bevel gear housing. Instead of the plates, the bike can use a standard bottom bracket to mount the cranks, which could be purchased off the shelf rather than custom manufacturing. Additionally, the overall weight of the bike would be significantly reduced. The sprocket driven drivetrain should weigh roughly 2 pounds using the chain and sprocket assembly, whereas last year's bevel gears and housing weighed about 7 pounds. The table below, Table 6, contains the weighted design matrix for power transmission.

Criteria	Weight (0-5)	Power Transmission		
		Planetary Gearbox	Sprocket & Chain	Gear Train
Weight	3	Datum	0	-3
Size/packaging	4		-4	-4
Cost	3		3	0
Reliability	5		0	0
Efficiency	5		0	0
<b>Total</b>				-1

Table 6. Weighted design matrix for drivetrain connections

A preliminary layout of the front drive train can be seen in Figure 14. The conceptual layout has the driven pump located in front of the pedal cranks, meaning that the bottom of the chain will be the tension side and the top will be the slack side. This has the potential to have derailment issues, however this could be avoided with enough chain tension. Depending on the severity of this issue, an intermediate roller could be used to keep tension. Additionally, with this set up, some additional machining will have to be made to the sprockets so that they can properly couple with our components, in particular the shaft key out of the pump.

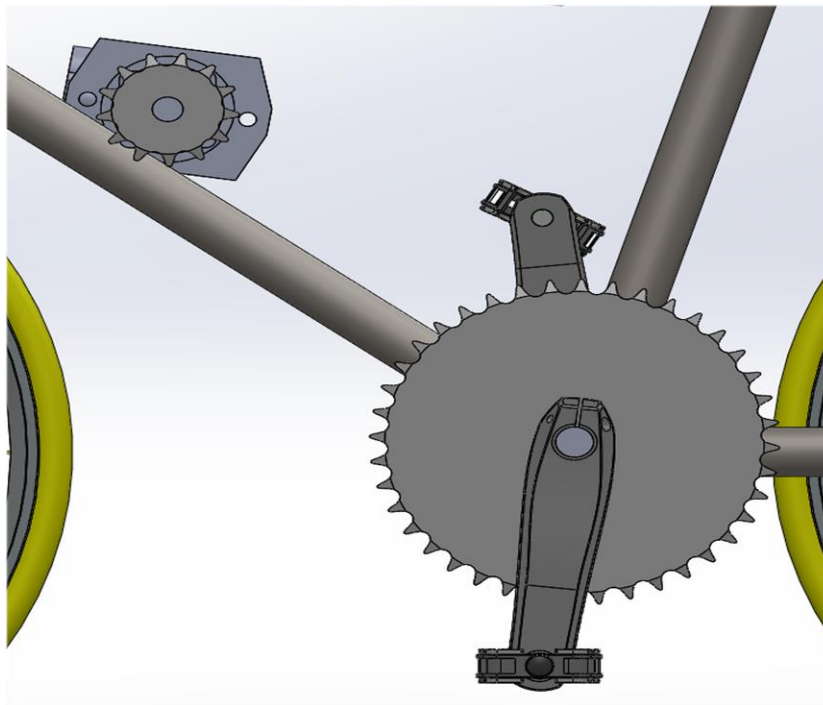


Figure 14. Conceptual design front drivetrain

As an addendum to the preliminary front drivetrain design, the driven pump was moved behind the crankset, mounted just in front of the rear wheel. However, to improve packaging, it was decided to implement a right-angle planetary gearbox instead of last year's straight planetary gearbox. Furthermore, this packaging configuration would keep the bicycle weight more balanced.

#### 5.2.2.2 Rear Drivetrain

For the rear drivetrain, the Incompressibles are planning on implementing a sprocket and chain, similar to the proposed idea for the front drivetrain. The motor would be mounted to a welded plate on the lower rear left side of the frame, as shown in Figure 15. This rear drivetrain will have the same reduction from the back wheel to the motor as the previous year's design but will be significantly lighter as it will not use the same large gears or friction plate clutch. Instead of a friction plate clutch, the Incompressibles are considering implementing a dog tooth clutch. More details about this may be seen in section 5.5 of the report.

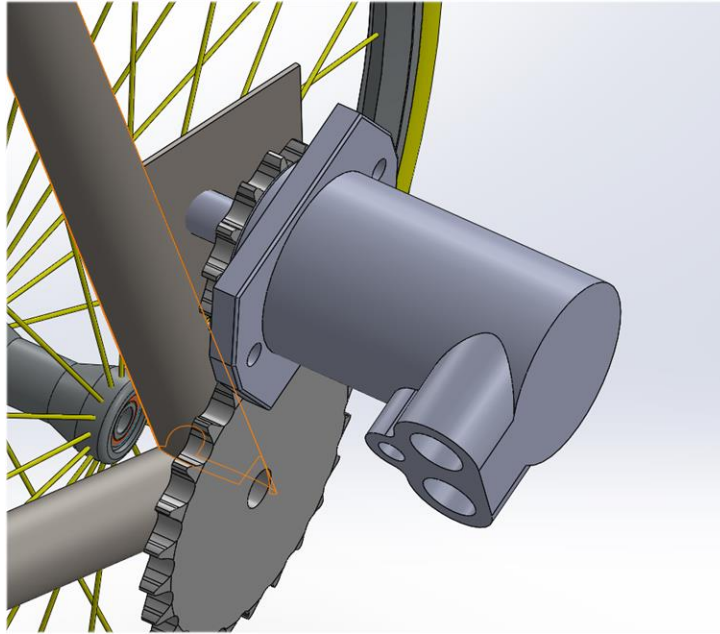


Figure 15. Conceptual CAD of new rear drivetrain.

### ***4.2.3 Further Development***

The majority of the remaining design for the drivetrain involves the detailed design and analysis of the components. This would include how the parts mount to the frame, how to ensure the sprockets are aligned, where to include intermediate roller slots for chain tension, and if the components can take the various load cases experienced while riding. Additionally, as designs are developed for other sections, the drivetrain architecture may have to be tweaked such that all components can mesh properly.

## **4.3 Hydraulics**

The Incompressibles' goal is to design and implement a hydraulic circuit that is efficient, reliable, and meets all the drive mode requirements. Added emphasis will be placed on the reliability of the hydraulic circuit, specifically in minimizing internal leakage.

### ***4.3.1 Hydraulic Circuit Design***

Four drive modes must be implemented in the hydraulic circuit to meet both the competitions and the team's personal requirements: direct drive, accumulator discharge, accumulator regenerative braking, and PIT mode.

#### **4.3.1.1 Direct Drive Mode**

Direct drive mode connects the pump and the motor via the reservoir and two valves as shown in Figure 16. This mode allows for pressure generated from the rider through the pump to be utilized directly by the motor. In this mode, fluid flows from the pump through two valves before reaching the reservoir; each valve has a pressure drop associated with it that has a direct relationship with flowrate. The pump not only needs to be connected to the motor but



also must have the suction side directly connected to the reservoir to pull fluid and avoid cavitation effects.

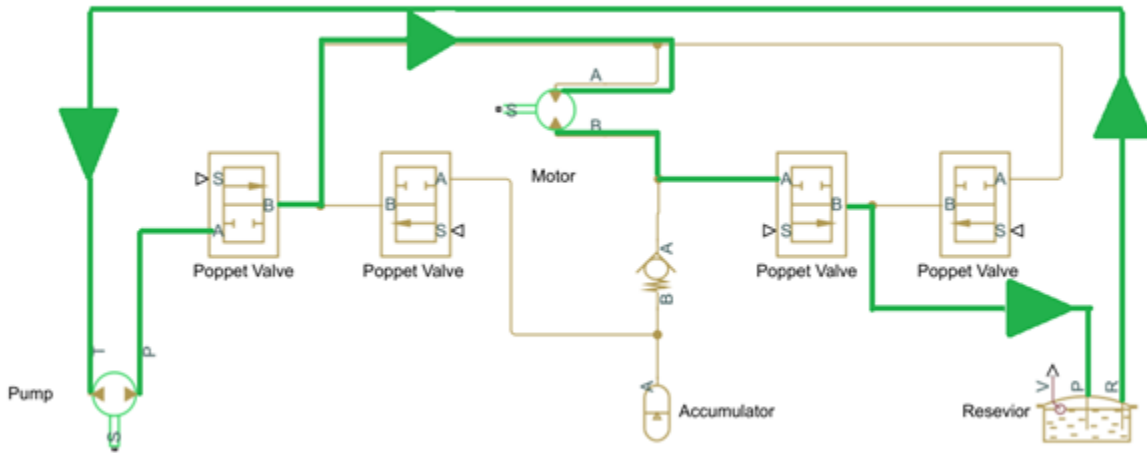


Figure 16. Direct Drive mode hydraulic diagram

#### 4.3.1.2 Discharge Mode

Discharge mode allows for the pressurized fluid stored in the accumulator to discharge through the motor to propel the bicycle forward. Fluid travels from the accumulator through one valve to the motor, then through a second valve to the reservoir, as seen in Figure 17. Because of the high pressures associated with the discharge mode and a flow rate dictated by the speed of the bicycle, the pressure drop across the valves in discharge mode is not as considerable as in direct drive mode.

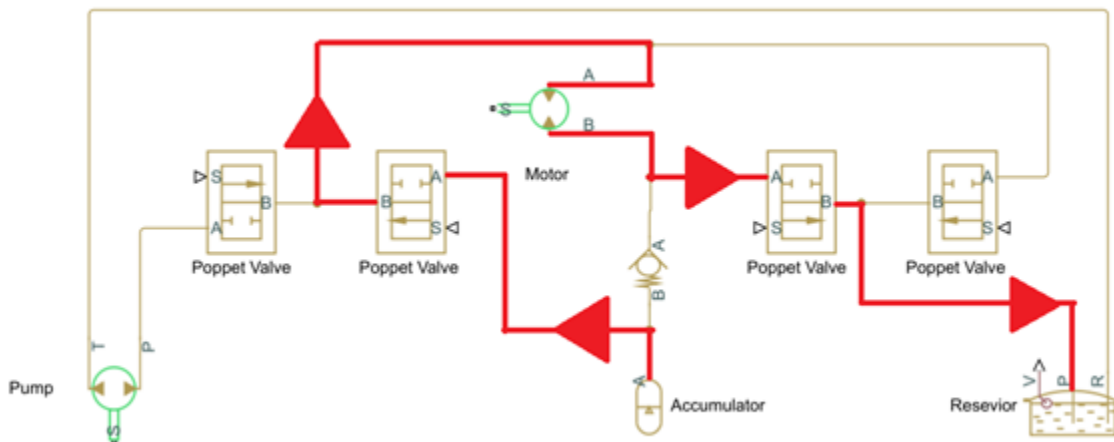


Figure 17. Discharge mode hydraulic diagram

#### 4.3.1.3 Regenerative Braking Mode

Regenerative braking mode utilizes the energy associated with the motion of the bike to build pressure in the accumulator. When this mode is engaged, the motor at the rear wheel acts as a pump, increasing the pressure and volume of the accumulator. Fluid flows from the motor through a one-way valve into the accumulator; this one-way valve prevents the accumulator pressure from discharging back into the motor and causing the wheel to spin the opposite direction. The motor pulls fluid from the reservoir, as seen in Figure 18.

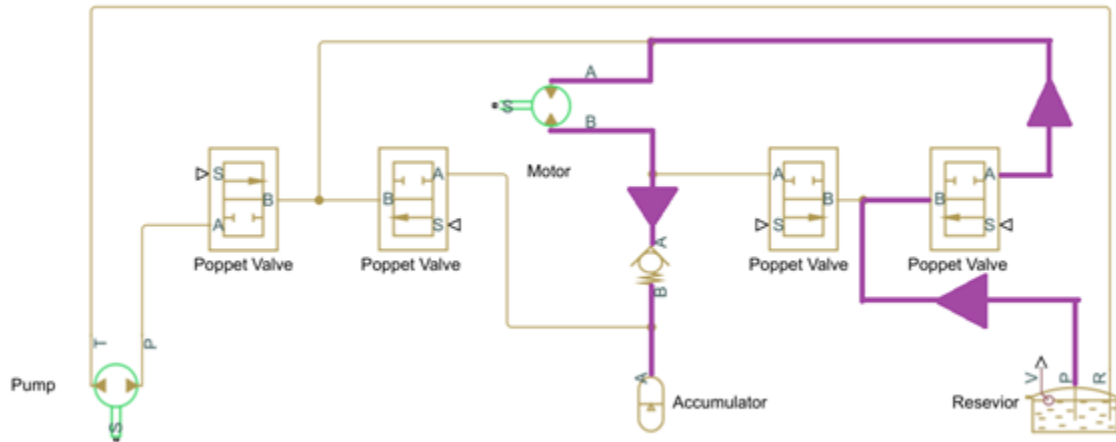


Figure 18. Regenerative braking mode hydraulic diagram

#### 4.3.1.4 PIT Mode

Last year's circuit design caused difficulties in moving the bike around in the PITs, as the de-energized state of the solenoids prevented fluid from moving freely through the system and thus prevented the rear wheel from turning forward. The Incompressibles' circuit design incorporates PIT mode, which is nominally closed, letting fluid circulate freely through the rear motor without generating pressure, shown in Figure 19. PIT mode ultimately allows the bike to move around the PIT's with ease.

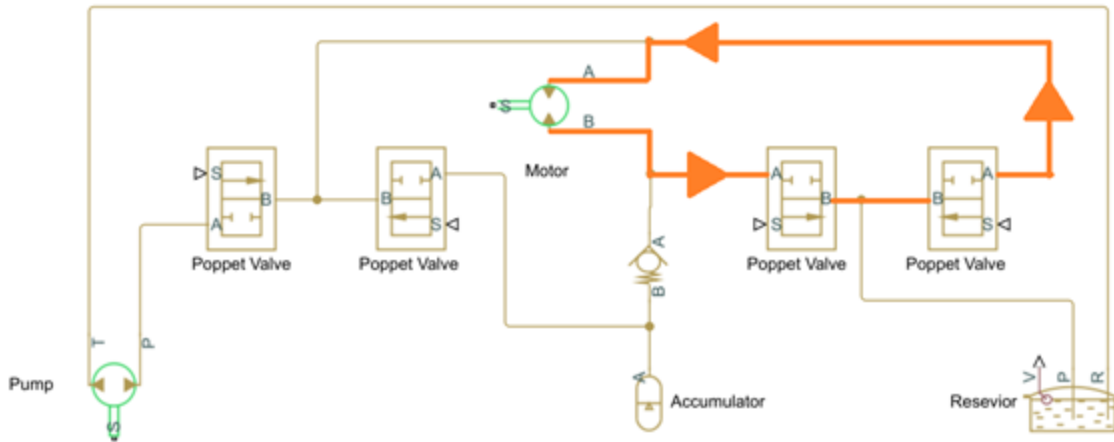


Figure 19. PIT mode hydraulic diagram

#### 4.3.2 Accumulator Selection

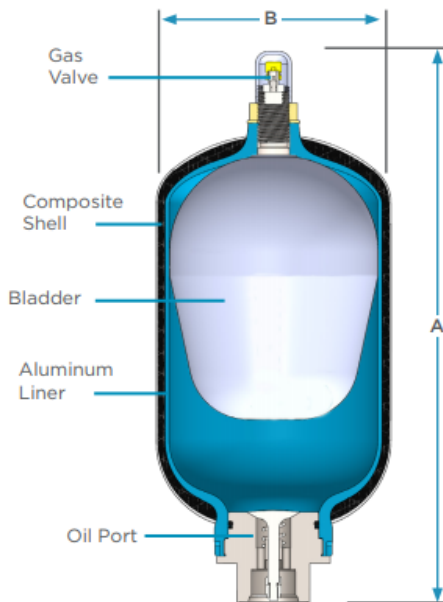
The 805 Hub Masters proved to do well in the endurance competition, placing second, but in competitions relying on accumulator discharge they were not competitive. Analyzing the sprint and efficiency competition results, shown in Figure 20, indicates there is a clear advantage in having a large sized accumulator. Murray State, the only team to have accumulator capacity more than one gallon, took first place in these two events by a significant margin.

Efficiency Challenge	Calculated	Distance	Sprint Race	
	Score			Time (sec)
Murray State U	25.15124434	3330.00	Murray State U	16.90
Cleveland State U	5.108346963	1034.00	Cleveland State U	36.39
Purdue	2.729029344	1026.00	Purdue	43.46
CalPoly	1.776667746	338.00	MSOE	69.68

Figure 20. 2018 Competition Results

The conclusion reached from analyzing last year's competition results was that the addition of a larger accumulator would be an advantageous design choice for this year's vehicle. The current Hydac 1L bladder accumulator, weighing 10 pounds, is particularly heavy for its small volume. Similar 1-gallon accumulators weigh upwards of 30 pounds and would be detrimental to the team's weight reduction goal. Therefore, to increase the efficiency score and reduce sprint time, the accumulator volume will need to be increased without a significant weight increase. Upon further research into alternative accumulator designs, the team found a composite manufacturer, Steelhead Composites, which produces a 1-gallon composite accumulator weighing approximately 10 pounds. The technical specifications of selected models can be seen below in Figure 21. The additional fluid volume would add approximately 5 pounds to the overall vehicle weight, which is acceptable. Murray State utilized a carbon fiber accumulator, further validating the Incompressibles' decision to steer towards a composite material.

# MICROMAX SERIES BLADDER ACCUMULATOR



Steelhead Composites Micromax series lightweight 3,000 psi (207 bar) to 5,000 psi (345 bar) bladder accumulators come in 1.0 gallon (4 liter) and 1.3 gallons (5 liter) capacities. These small and lightweight composite accumulators are a superior alternative to steel accumulators for any weight-restricted uses, mobile and industrial applications where access is remote, elevated or limited.

## SPECIFICATIONS

- Type 3 Pressure Vessel
- Operating Pressure: 3000 psi (206 bar)-5,000 psi (345 bar)
- Minimum Burst Pressure: 3x Max Operating Pressure
- Fluid Connection: Industry standard port options available
- Operating Temperature Range: -4° to 160° F (-20° to 71° C)
- Liner: Impermeable 6061-T6 Aluminum
- Structural: Carbon fiber and epoxy composite
- Bladder: Buna-Nitrile (other materials available)

NOMINAL VOLUME GAL (L)	OPERATING PRESSURE PSI (BAR)**	DIMENSION A IN (MM)	DIMENSION B IN (MM)	WEIGHT LBS (KGS)
1 (4)	3,000 (206)	15.7 (399)	6.5 (165)	10.8 (5)
1.3 (5)	3,000 (206)	19.4 (493)	6.5 (165)	12.8 (6)
2.5 (10)	3,000 (206)	28.7 (729)	6.5 (165)	17.7 (8)

Figure 21. Micromax Accumulator Specifications from SteelHead Composites

A bladder-style accumulator was decided to be the optimal type of accumulator for our application due to the low relative weight and fast response time compared to piston and diaphragm styles. The ideal accumulator volume has yet to be determined and will be dependent upon simulation results that are still under development. The intention is to choose an accumulator size that will allow the bike to be optimally competitive in all three events.

### 4.3.3 Pump and Motor

Three types of pumps and/or motors are common amongst Fluid Power Challenge vehicles: bent-axis, gear pump, and gerotor pump. Because the vehicles in this challenge are human powered, it is difficult to achieve a high shaft speed to match nominal operating speeds of most pumps and/or motors. Given this limitation, it was necessary to select a pump based on highest efficiency when operating at low speeds. After evaluating the efficiency curves for each of the potential pumps, it was found that the bent-axis pump was the only pump that maintained efficiency values above 80% for speeds below 1000 rpm and still had comparable efficiency with the two other pumps at higher speeds.

### 4.3.3.1 Bent-Axis Pump/Motor



Figure 22: Bent Axis Pump

Bent-axis pumps use a series of reciprocating pistons mounted to a single rotating plate that provide steady flow in a range of operating speeds. The characteristic steady flow gives a large advantage to rideability over the other pump styles that are known to produce uneven flow at lower speeds.

The previous Fluid power Challenge Bike utilized a Bosch bent-axis pump that has an aluminum housing instead of iron. This housing limits the operating pressure to 3000 psi, however the weight benefits overcome the increased performance realized in a higher-pressure system. An efficiency curve for the Bosch bent-axis pump was not able to be obtained from Bosch, but the internal structure of the Bosch pump is similar to that of the Parker F-11 bent-axis pump. The efficiency curve for the Parker F-11 bent-axis pump will be used for analysis when designing the bike; this curve can be seen below in Figure 23.

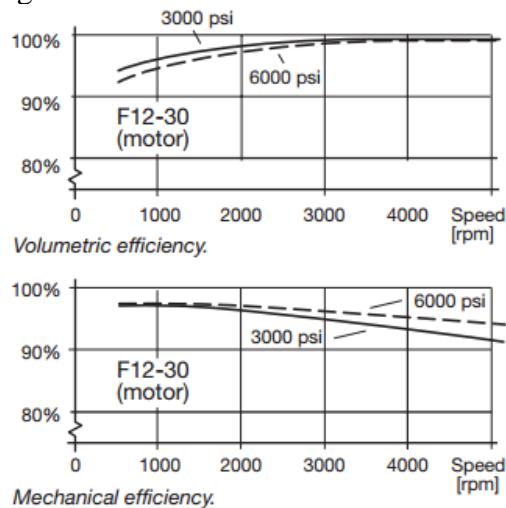


Figure 23: Parker Hannifin F11 Efficiency Curves

### 4.3.3.2 Gear Pump

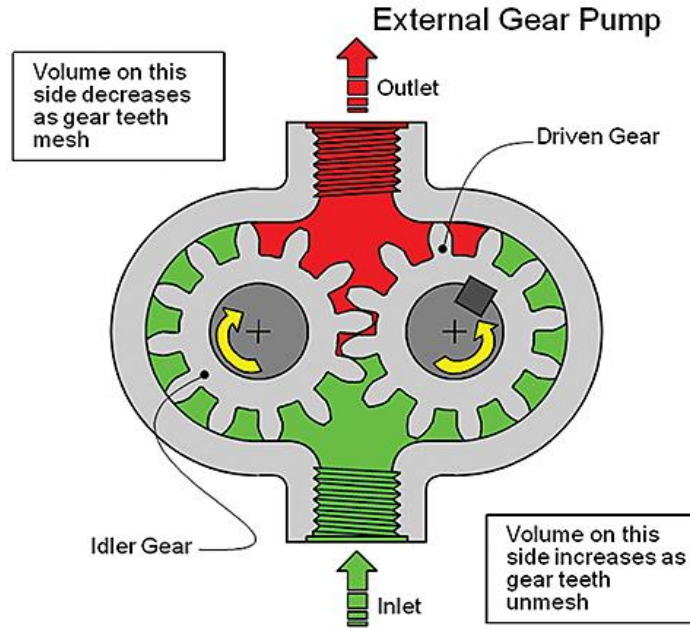


Figure 24: Gear Pump/Motor

Gear pumps are another fixed displacement style pump that utilize a driven gear and an idler gear to pump high viscosity oil. The fluid path in a gear pump circles around the outside of the gears and the meshing of the gears forces the fluid out of the pump. The flow path in this pump is characterized by numerous bends, resulting in inherent inefficiencies. These inefficiencies coupled with the uneven flow at low speeds make this pump an undesirable option.

### 4.3.3.3 Gerotor Pump/Motor

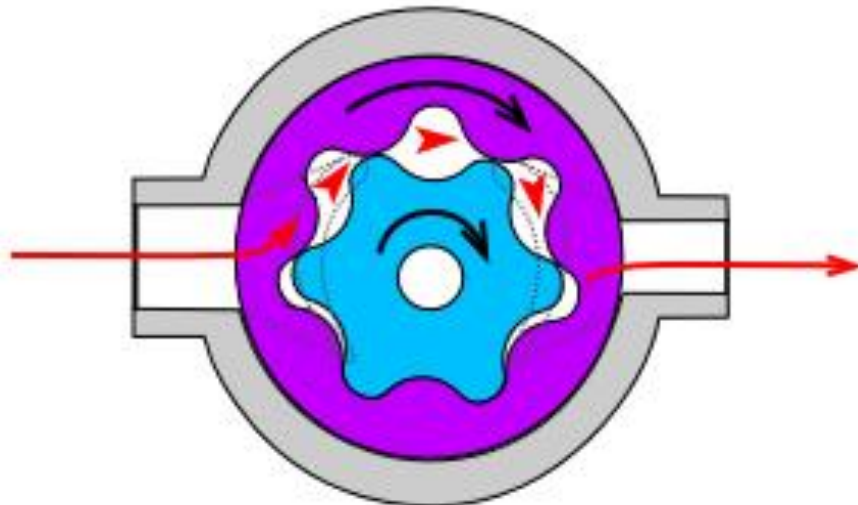


Figure 25: Gerotor Pump/Motor

Gerotor pumps operate by using 2 offset meshing rotors to pump fluid, as seen in Figure 25. These pumps are efficient for hot, low pressure fluids, and efficiency decreases greatly below 1000 rpm. The strengths of this pump are not beneficial to our application and therefore it will not be the correct choice.

#### 4.3.4 Valve Selection

Previous year's teams utilized spool-type solenoids to control flow and pressure of the hydraulic fluid between components. High amounts of internal leakage through the spool solenoid crippled the previous year's team in competition by allowing 1000 psi to prematurely discharge in the span of only 15 seconds. Because of the previous severity of leakage, avoiding this will be the number one focus when selecting solenoids for the upcoming year.

##### 4.3.4.1 Spool-Type Solenoids

Spool-type solenoids offer much freedom when choosing the number of inputs/outputs and the corresponding modes. This characteristic allows for one solenoid to perform tasks that would typically take 3 or 4 on-off solenoids to accomplish, which also lowers weight and packaging space. Spool-type solenoids seal on a piston-cylinder style interface that can be seen in Figure 26, circled in red; this seal design results in 166cc/min of leakage at 3000 psi.

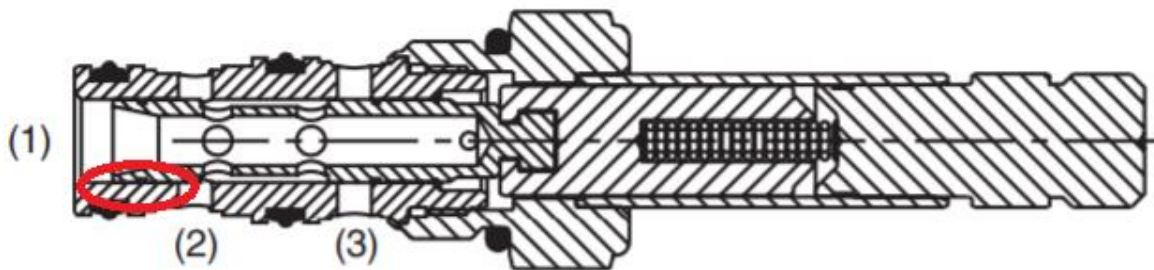


Figure 26: Spool-Type Solenoid Valve

##### 4.3.4.2 Poppet-Type Solenoids

Poppet-Type solenoids utilize a plunger that seals on a tapered surface similar to an AN-style fitting as shown in Figure 27, outlined in red. This seal type allows each solenoid to only be either on or off, thus requiring four poppet-type solenoids to accomplish all drive modes. This quantity of valves may increase weight, cost, and packaging area. This sealing surface also only experiences 0.33 cc/min of leakage at 5000 psi, a miniscule value compared to the 166 cc/min of the spool type. The leakage benefit means the poppet-type is the correct choice for the upcoming bike despite its other drawbacks.

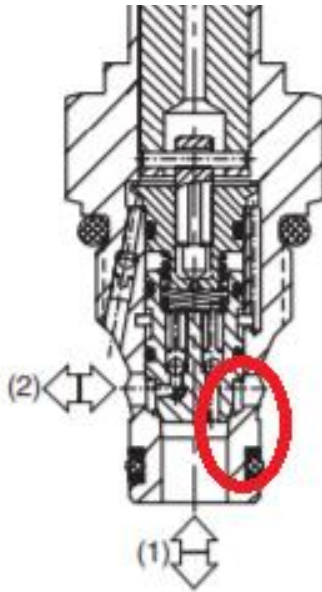


Figure 27: Poppet-Type Solenoid Valve

#### ***4.3.5 Further Development***

The next step in developing the bike's hydraulic circuit is characterizing the head loss through each of the solenoids for different operating modes. Parker offers graphs for all their solenoids that illustrate the pressure drop and opening time compared to flow rate. We can determine the flowrate through the system using the speed of the bike and motor speed, then use this to determine what the head loss through each of the solenoid size is. Comparing the weight, head loss, and power requirements will allow us to make the best choice for what size of poppet-style solenoids to use.

Each hydraulic component must be accompanied by a manifold, which can be made from either iron with a 5000 psi limit or aluminum with a 3000 psi limit. The weight benefit of using aluminum outweighs the increased pressure limit of using iron, therefore the pressure limit of 3000 psi will drive the selection of hoses and fittings. Determination of hose type, either soft or hard, is pending weight and packaging studies that will be completed later as more detailed analysis is performed.

### **4.4 Mechatronics**

#### ***4.4.1 Past Design***

The intent for this year's design is the successful implementation of a simple yet practical mechatronics system. Last year's team, the 805 Hubmasters, had a significant focus on mechatronics integration with their bike, however they were unable to successfully implement every objective. The 805 Hub Masters attempted to follow the ME 507 Fall course schedule in order to design and manufacture a custom board for their vehicle, which provided a great educational experience, but was incredibly time-consuming due to the large amount of time spent debugging code, fixing hardware, and designing a custom microcontroller board. Purchasing



prefabricated hardware would alleviate most of problems associated with board design and board debugging and allow for more development time for sensor integration, user interface development, and reliable wiring. The team ended up not being able to optimize their design to the desired level and concluded that too much time was spent on a mechatronics system that provided little benefit compared to the work invested. An image of their final product is shown in Figure 28.

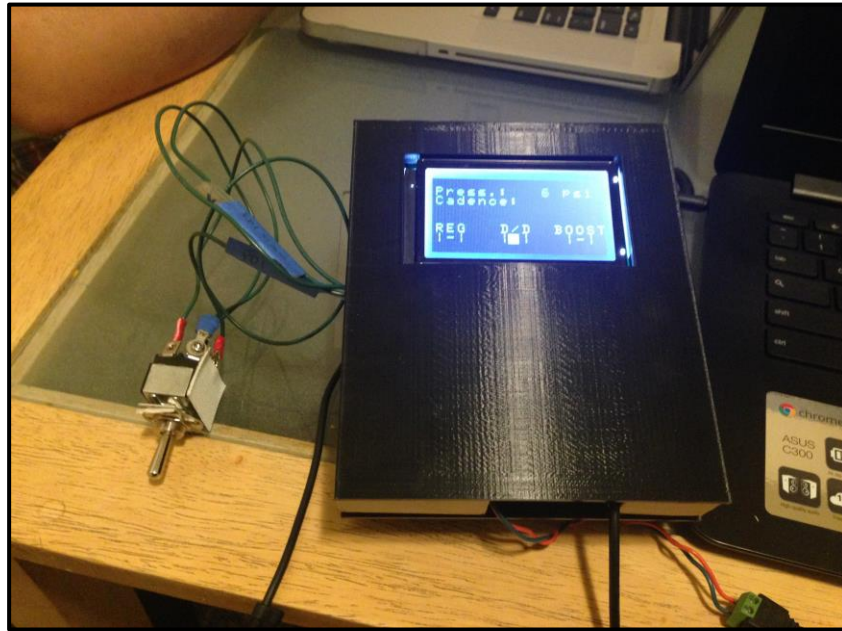


Figure 28. 805 Hubmaster's full mechatronics enclosure with 3-way toggle switch

Another improvement to the 805 Hubmaster's mechatronics design is reliable wiring, as poor connections caused poor reliability. Although crimp connections, shown in Figure 29, were made in order to accomplish a sturdier circuit, vibrations near the board compromised the connections that proved to be unreliable at competition. Reducing vibrations near the board and using physical plug connectors will mitigate this issue.

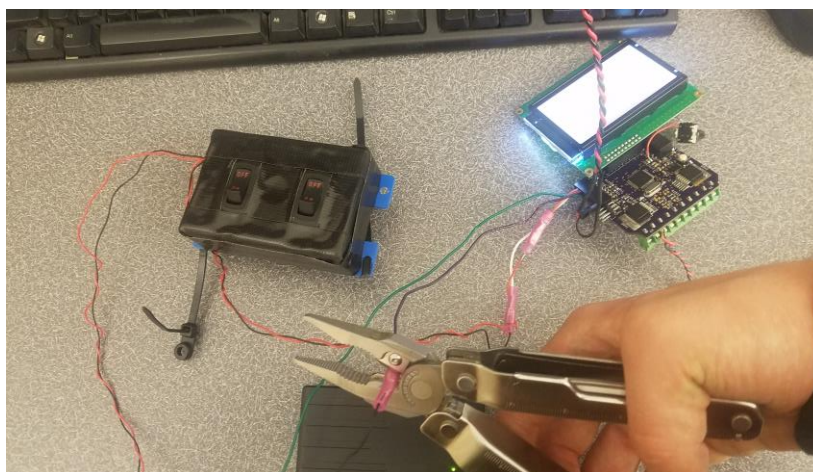


Figure 29. Example of crimp connections made for mechatronics wiring

#### 4.4.2 New Hardware Design

The plan for this year is to design a mechatronics system utilizing as many prefabricated components as possible within our budgetary limitations. A specific interest is being placed on the Arduino microcontroller platform. Arduino is an open source hardware and software ecosystem that features support for a multitude of microcontrollers and peripherals. An example photo of an Arduino Uno microcontroller is shown in Figure 30.



Figure 30. Example photo of Arduino Uno microcontroller

The versatility and simplicity of this platform allows it to be used for many different applications without intensive hardware redesign. Documentation and tutorials already exists for solenoid driver circuits, sensor data collection circuits, and switch circuits, therefore, a comprehensive and robust mechatronics system can easily be developed using existing off-the-shelf components with minimal time. The time-consuming process of designing and manufacturing an in-house developed mechatronics board costed the previous year's team valuable testing and debugging time. Going with an industry proven controller will reduce the hardware debugging and board design time. Another possible candidate for a microcontroller is the Raspberry Pi. The Raspberry Pi is a full-fledged computer based off of a Linux operating system versus the Arduino which is solely a microcontroller programmed in C++. However, it will not be necessary to have the complexity and comprehensive capability of the Raspberry Pi for our system because of the simple and small number of controller tasks. Figure 31 outlines the advantages and disadvantages between the Raspberry Pi 3 and Arduino Uno Rev3 platforms.



	Raspberry Pi 3	Arduino Uno Rev3
		
<b>Advantages</b>	<ul style="list-style-type: none"> <li>• Stronger and quicker processor, multitasking available</li> <li>• Built in Ethernet port, Wi-Fi and Bluetooth capability</li> <li>• OS can be switched easily</li> <li>• Audio output, Camera port, USB ports, HDMI output all included</li> <li>• Great to start learning to code with its helpful learning programs already installed</li> <li>• Great for projects that need to connect online and have multiple activities going on at the same time</li> </ul>	<ul style="list-style-type: none"> <li>• Easier to connect to analog sensors, motors and other electronic components</li> <li>• Variety of Shields that can add functionality</li> <li>• Long set-up not needed, just plug in and code will run</li> <li>• Price is cheaper (around \$20) and will not need much cables (standard A/B USB)</li> <li>• Great for projects that need to quickly get data from sensors and do one activity from that data</li> </ul>
<b>Disadvantages</b>	<ul style="list-style-type: none"> <li>• Long set up and will need extra components when first starting (HDMI cable, monitor, keyboard and mouse)</li> <li>• Might need to install programs to get simple actions going</li> <li>• Can be more expensive (around \$35, not including SD cards, cables, keyboards/mouse)</li> </ul>	<ul style="list-style-type: none"> <li>• Can run one code at a time, so can't multitask activities, slower speed</li> <li>• No Internet connectivity right out the box (can add with Shield)</li> <li>• Bigger learning curve since it's C/C++ language and will need to get outside sources to learn</li> </ul>

Figure 31. Pros and cons comparison of the Raspberry Pi 3 and Arduino Uno Rev3 platforms

The expedient implementation time, extensive amount of hardware support, and reliability of an Arduino platform outweighs the educational benefits of designing a custom board to fit our requirements. This will allow the Incompressibles to reliably utilize the advantages of a mechatronics integrated system at competition. A weighted decision matrix outlining the benefits of the Arduino platform over the previous in-house designed board and Raspberry Pi is shown in Table 7.

Table 7. Weighted decision matrix for mechatronics controller selection

Criteria	Weight (0-5)	Mechatronics Controller Board		
		Custom In-House	Arduino	Raspberry Pi
Cost	2	Datum	0	0
Implementation Time	5		5	5
Simplicity	3		3	0
Reliability	5		5	5
Support	3		3	3
Versatility/Robustness	4		4	4
<b>Total</b>				20

A tentative mechatronics layout is shown in Figure 32. The schematic details the components that constitute the mechatronics system and demonstrates their integration with the microcontroller. A preliminary component list is as follows:

- Four solenoid driver circuits to drive each solenoid for each drive mode selection
- Two pressure transducers to output hydraulic line pressure into the motor and output pressure from the accumulator
- Two hall effect sensors to measure input crank speed and rear wheel speed
- Four push buttons to select each drive mode (direct drive, accumulator discharge, regenerative braking, and clutch engagement)
- A lithium-ion polymer battery to supply constant power to the Arduino and solenoid drivers (+12Vdc & +5 Vdc)
- A digital voltmeter circuit to measure battery voltage
- An LCD/TFT display to output bike line pressure, speed, drive mode selection, and battery voltage

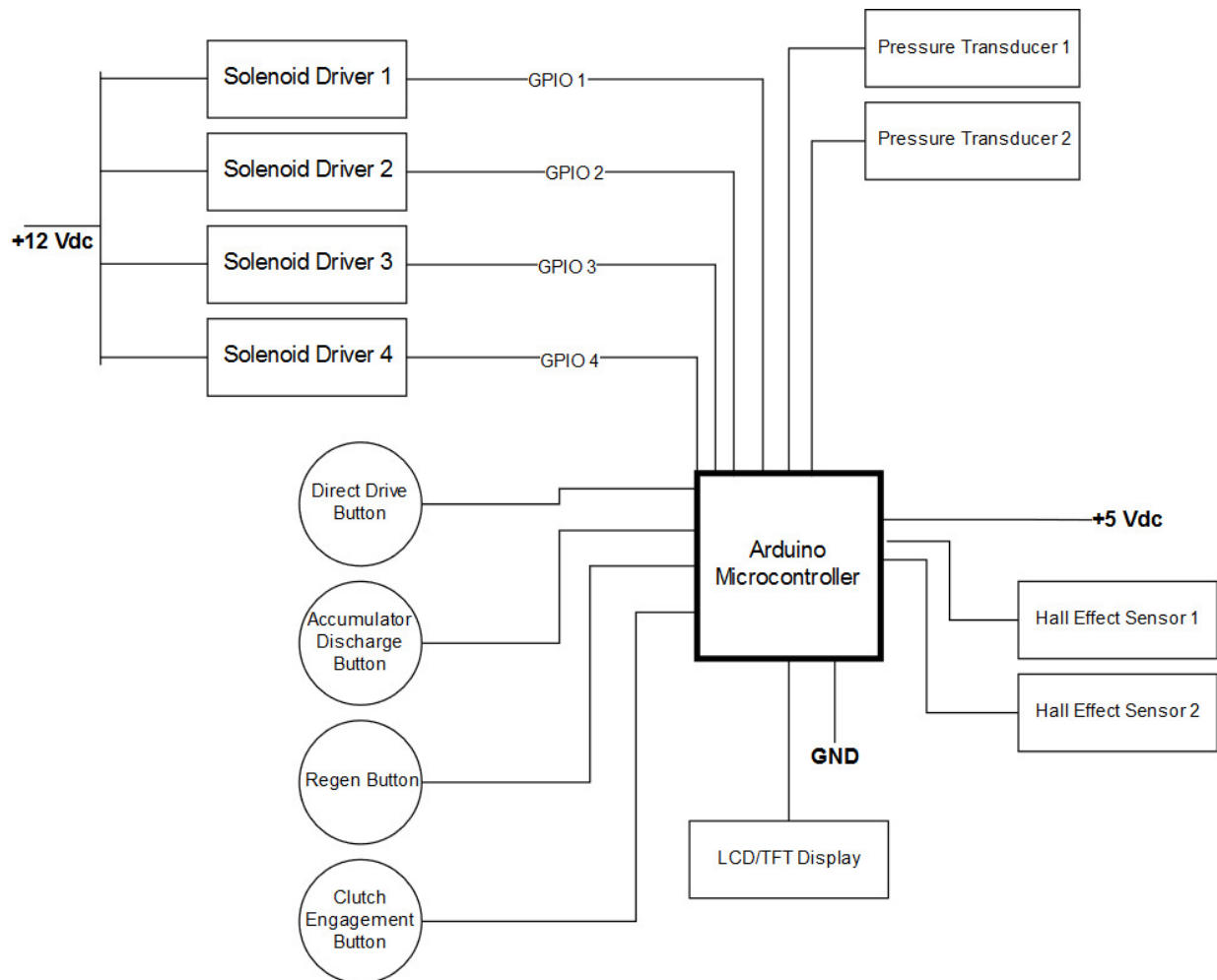


Figure 32. Preliminary mechatronics layout including sensors, buttons and solenoid drivers

The solenoid driver circuits are necessary as the Arduino will not be able to provide the large amount of current required and will utilize a +12Vdc power supply. The Arduino will actuate the solenoids through general purpose input/output pins. The two pressure transducers are used to measure hydraulic line pressure at the motor and accumulator pressure. During the accumulator discharge, the pressure sensor will output the accumulator pressure value to the rider via an LCD/TFT display. The Hall Effect sensors will allow the rider to see their cadence and the bike's velocity in real time. The four push buttons are used to select each drive mode repeatedly and reliably. Based off of rider experience, rocker switches and toggles will be difficult to actuate while the rider is controlling the bike. The push button switches allow the rider to select each drive mode rapidly without questioning if the switch is in the correct position. A digital voltmeter circuit will be used to monitor the battery voltage. The LCD/TFT display will output the basic bike performance metrics, for example, line & accumulator pressure, bike cadence, drive mode selection, and battery voltage. A lithium-ion polymer battery was selected as it has a high-power density for a compact and lightweight package. The competition is relatively short and will not require a large lead-acid battery used in modern day cars or an alternator to provide power. Further power requirement analysis will need to be performed to determine the proper battery size. Figure 33 shows the preliminary placement of the LCD/TFT display with the push buttons placed near the rider's hands for easy actuation.

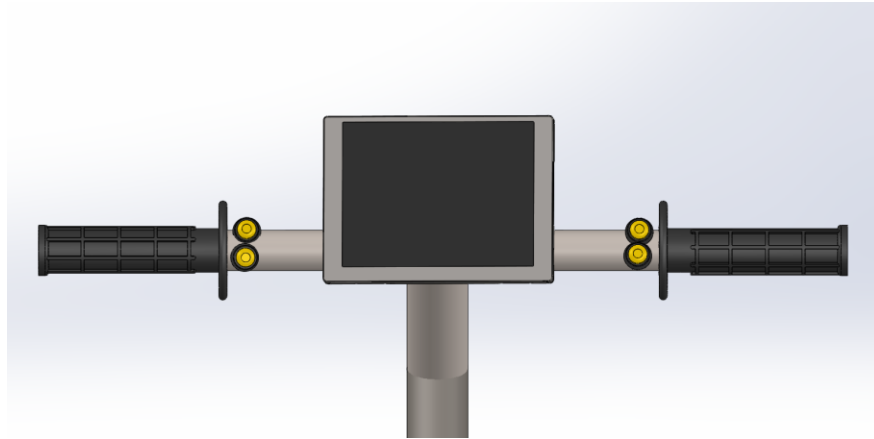


Figure 33. LCD display and drive mode button layout on front bike handlebar

#### 4.4.3 Software Design

The software for the microcontroller will be written using C++ or C. Using cooperative multitasking, we will be able to control multiple operations at once. Figure 34 shows the basic task diagram for the bike's microcontroller. The main tasks we will have to manage simultaneously are the user interface, sensor reader, and solenoid handler. The user interface will take in and manage all of the user inputs as well as update the LCD display for the driver. The sensor reader will constantly check the value of the sensors and send a signal to the user interface when the display needs to be updated. Finally, the solenoid handler will get the drive mode information from the user interface and will change the voltage head to the solenoid such that the solenoid is in the right position. This will most likely involve a little controller model.

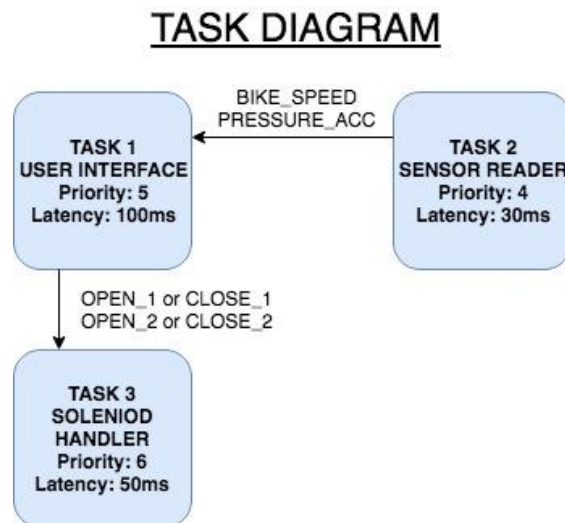


Figure 34. Task diagram for mechatronics

Figure 35 shows a preliminary state diagram for the user interface task. The user interface will most likely be the most complicated task since it will have to handle both button inputs that change the drive mode and updating the display for the drive mode and the live sensor data. The solenoid handle state will interpret the user inputs and change the drive mode if deemed necessary. Similar

state diagrams for the other tasks will be created, however, they will most likely be very simple as they will be predominantly “driven” by the UI task. This means that most of the logic will be handled by the UI tasks while other tasks will only be running continual data collection or solenoid position control until told to do otherwise by the user interface task.

## User Interface State Diagram

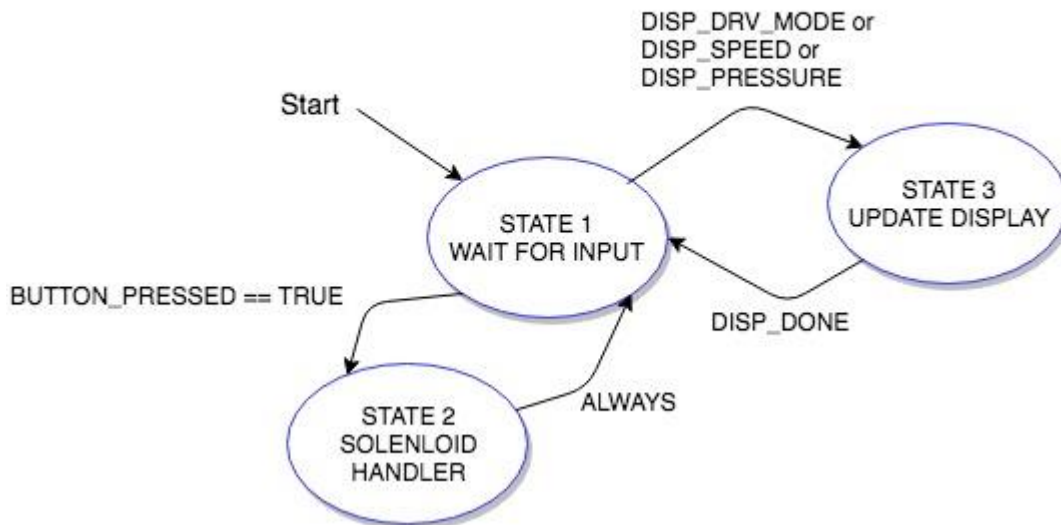


Figure 35. User interface State Diagram

### 4.4.4 Further Development

The next steps involved from now to the Critical Design Review deadline are to size the Arduino microcontroller, determine the required battery size, and finalize sensor mounting solutions on the bike. Totalling the amount of power required for each device in the mechatronics circuit will allow us to determine a proper battery size to last the entire competition. Proper mounting solutions for each sensor will need to be finalized so each sensor can read data reliably and output it to the display. The sensor readings will also provide data to validate the current bike models and determine their accuracy in predicting bike performance for future teams. Retrofitting the previous year’s bike with buttons and a display will be done to find convenient and ergonomic placements for each component. The latency or speed requirement for each component will need to be taken into consideration to find an adequate microcontroller speed. Finally, the amount of data displayed to the LCD will determine the overall size and type of screen.

### 4.5 Power Decoupling

A power decoupling system is not a required component in this competition, however it may significantly improve vehicle performance. In discussing power decoupling with the previous year’s team, it was noted that their model predicted a substantial increase in distance traveled with complete accumulator discharge while freewheeling. Therefore, the Incompressibles decided it would be beneficial to explore the implementation of a power decoupling system. The system would disengage the rear wheel from the motor, allowing the bike to coast with minimal losses in

energy. All drive modes require that the rear wheel be engaged, thus the rider would not be able to pedal, discharge, or regenerate when the system is disengaged.

The 805HubMasters attempted to implement a multi disc clutch system repurposed from a Honda CBR600, however they were ultimately unable to operate it correctly. Taking note of the difficulties associated with the previous clutch design, the Incompressibles weighed the use of several other power decoupling methods as well.

Power decoupling is not specified as a required vehicle component within the official competition rules, therefore the Incompressibles did not want to spend an excess amount of time theorizing and implementing this system. Additionally, the power decoupling system should have a simple method of operation and should not add an excessive amount of weight to the vehicle. The potential power decoupling methods included the previous disc clutch, a dog gear, a fluid bypass system, and an electromagnetic clutch.

#### ***4.5.1 Friction Disc Clutch***

The previous year's chosen method for power decoupling was a friction disc clutch, originally used on a Honda CBR600. The clutch can be seen mounted on the bike in Figure 36. The main reasoning behind the selection of the disc clutch was that it met requirements of torque capacity, reliability, and serviceability, however it was noted that its packaging was a drawback. This clutch was to be actuated by the rider via a cable system. Last year's team's calculations indicated that the stock springs and friction plates on the clutch would not be sufficiently strong to allow consistent torque transfer. The team decided to install new, stiffer springs that would not slip during operation. Although the clutch was effective while engaged, the team was unable to properly operate the clutch due to the high force required to disengage the springs. Thus, the clutch remained installed on the bike without being used for drive disengagement. In addition to not being operational, the clutch is unnecessarily large and heavy for the application.

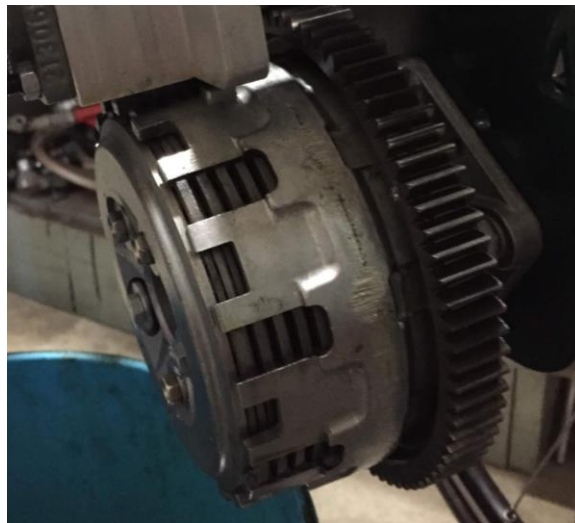


Figure 36. Honda CBR600 on the 805 Hubmaster's Bike



### ***4.5.2 Fluid Circulation Line***

A line connecting the input and output of the motor would allow for fluid to circulate through the unit when coasting. Theoretically, the pressure across the motor would be small and coasting would incur almost no losses due to the fluid. However, there would be non-negligible mechanical losses associated with the rear drive train and motor operation. Murray State, in their final presentation, noted that motor drag caused noticeable losses during coasting operation of their vehicle. This option of power decoupling would, however, be the simplest and cheapest to implement. The only requirement to accommodate the new drive mode is the inclusion of an additional valve in the hydraulic circuit.

### ***4.5.3 Dog Tooth Clutch***

The concept of a dog tooth clutch was explored as a simple and cost-effective solution to power decoupling. A typical dog clutch couples rotating components through interference between teeth on one half of the mechanism to a set of identical recesses on the other half. This method of operation allows high amounts of torque transfer with zero slip while keeping component weight low. A tentative design, shown in Figure 37, was developed in which a dog toothed coupler clutch would translate along the rear drive shaft and be able to lock into a freely rotating sprocket. The clutch would rest on either splines or a key and, once connected to the sprocket, translate the torque from the sprocket directly to the shaft. The rear wheel would have a splined hub attached to the shaft and the movement of the shaft would also rotate the wheel. The system could be actuated by a solenoid or through a simple hand-operated lever. The advantage of the dog clutch design is the very low weight and the complete disengagement of the rear wheel from the motor. The model was designed parametrically so that dimensions can easily be altered if future failure analysis deems it necessary.

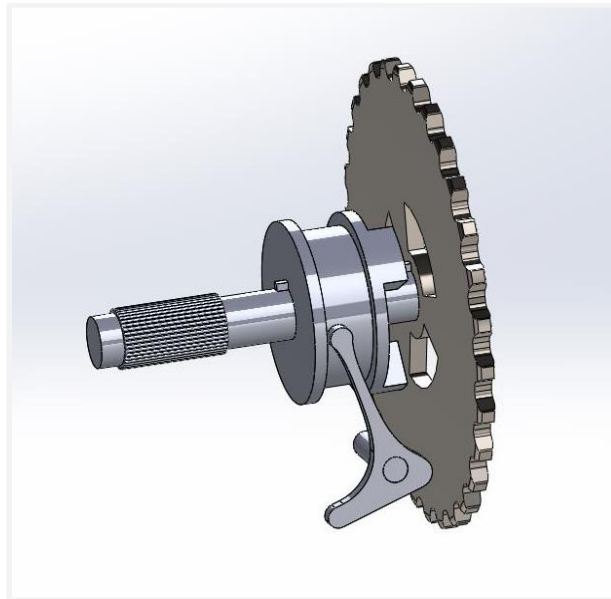


Figure 37. Dog Tooth Clutch Preliminary Design

#### 4.5.4 Further Development

A weighted decision matrix comparing the three different mechanisms is shown in Table 8. The dog tooth scores highest thanks to its large advantage in efficiency over the hydraulic system. Although the dog clutch appears to be the best option, the team is still considering the inclusion of an additional drive mode into the hydraulic circuit. Having a circuit bypass, even if as a backup system to another mechanism, is prudent due to the ease of implementation and minimal inconvenience. More testing must still be done in order to quantify the efficiency gain from the implementation of a clutch. After the 2018 Spring Quarter Senior Project Exposition, the team plans to manipulate the current hydraulic circuit to include a bypass mode and test the resistance while coasting in this configuration. As well as calculating losses associated with a hydraulic clutch, the team plans to implement clutch actuation into the Simscape model. This will allow for the simulation of coasting action after accumulator discharge and show the distance traveled when compared with the same run without clutch disengagement.

Table 8. Weighted design matrix for power decoupling mechanism

Criteria	Weight (0-5)	Power Transmission		
		Planetary Gearbox	Sprocket & Chain	Gear Train
Weight	3	Datum	0	-3
Size/packaging	4		-4	-4
Cost	3		3	0
Reliability	5		0	0
Efficiency	5		0	0
<b>Total</b>			-1	-7

## 4.6 Modeling

### 4.6.1 Accumulator Discharge Model - Current Design

Modeling the bike's performance through the accumulator discharge mode was accomplished through Mathworks' Simscape software. Simscape enables the creation of Simulink type models of physical systems through a schematic-design methodology. System models can range from the electric energy domain to the mechanical and fluid energy domain. Simscape also allows for multidomain model based on physical connections without the need to derive equations of motion or use a complex system dynamics approach to predict the performance of a multi-domain system. There are components or blocks that represent physical components, i.e. pumps, motors, resistors, etc., and one can input basic values found on a datasheet to define the characteristics of the component. Simscape can also accommodate changes to a model more easily compared to a Simulink model as it is not necessary to re-derive equations of motion and instead different blocks

can be connected together even if they are in different energy domains. Due to Simscape's simplicity and modularity, it was selected to model the accumulator discharge. Figure 38 shows the simplicity of a Simscape model compared to an analogous Simulink model of a mass-spring-damper system.

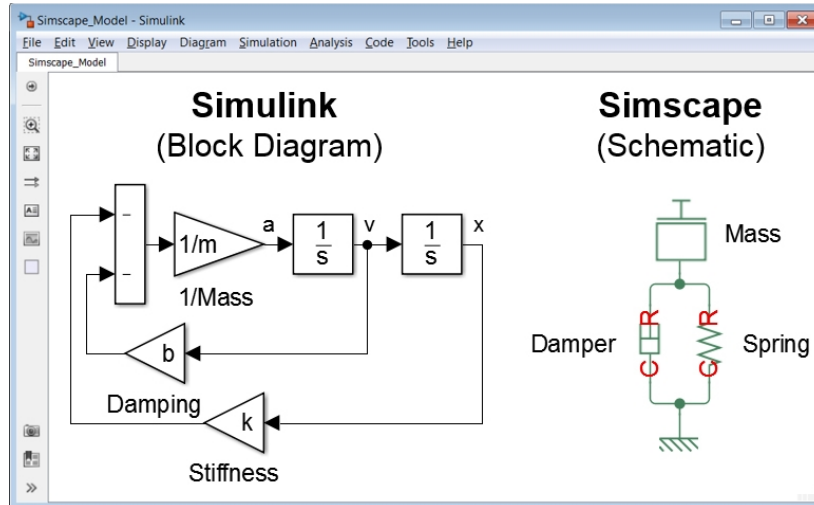


Figure 38. Equivalent Mathworks' models of a mass-spring-damper system using Simulink and Simscape

The previous team's accumulator discharge model outputted results that were questionable to how the physical system worked, which prompted the development of a new model. Figure 39 shows the horizontal distance traveled by the bike over time for a 0.29 gallon accumulator with a pre-charge pressure of 900 psi using the previous year's model. From the graph, the bike doesn't move until 45 seconds after the accumulator has discharged. This contradicts the actual accumulator discharge as it should push the bike initially and accelerate it until the accumulator volume reaches zero, only then coasting to a stop.

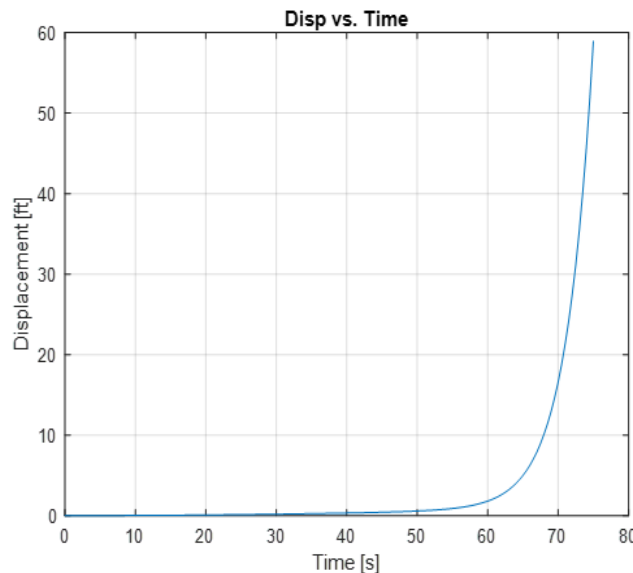


Figure 39. Plot of bike displacement over time using the 805 Hubmaster's MATLAB accumulator discharge model (0.29 gallon accumulator volume with 900 psi precharge)

The current Simscape model, shown in Figure 40, models the accumulator discharging from full charge into the rear motor which is connected to the rear tire. The accumulator initially starts with a specified fluid volume based on the maximum working pressure and nitrogen pre-charge pressure. It discharges through a check valve to the current Bosch A2FO-5 bent axis motor/pump and dumps into a fluid reservoir. The motor spins a shaft which goes through a rear gear ratio to the rear tire which transfer rotational motion into translation. The current model accounts for the equivalent fluid resistance of the pipes from the accumulator to the motor, the motor inertia, the fluid properties, the rolling resistance on the rear tire, and the total bike mass.

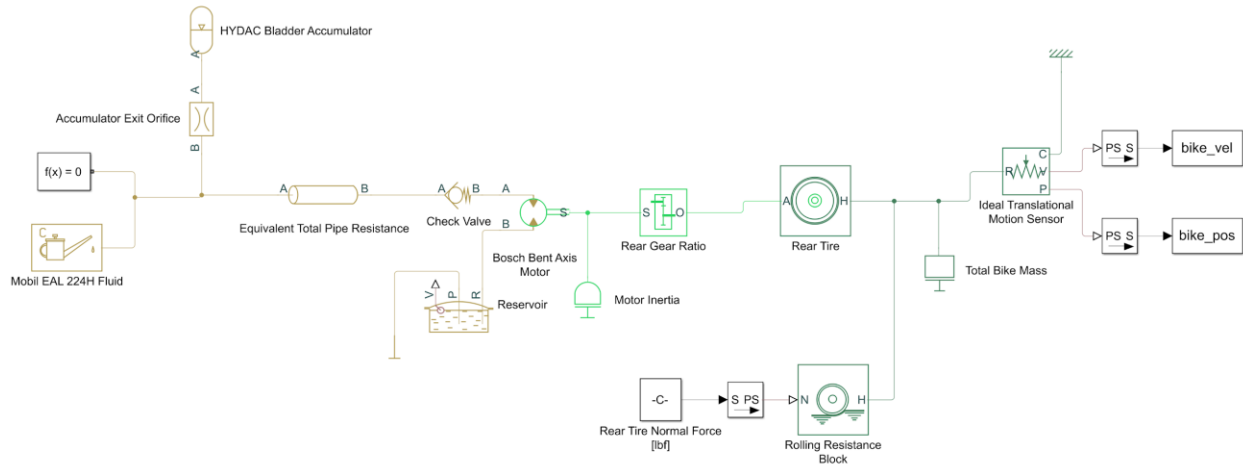


Figure 40. Simscape derived accumulator discharge model

A plot of bike translational distance over time is shown in Figure 41. The results use the same accumulator and mass parameters as last year's model, but the bike initially moves and increases velocity as the accumulator discharges. The discharge time is also greatly decreased ending around 15 seconds versus 75 seconds from last year's model which seems more realistic to the physical discharge.

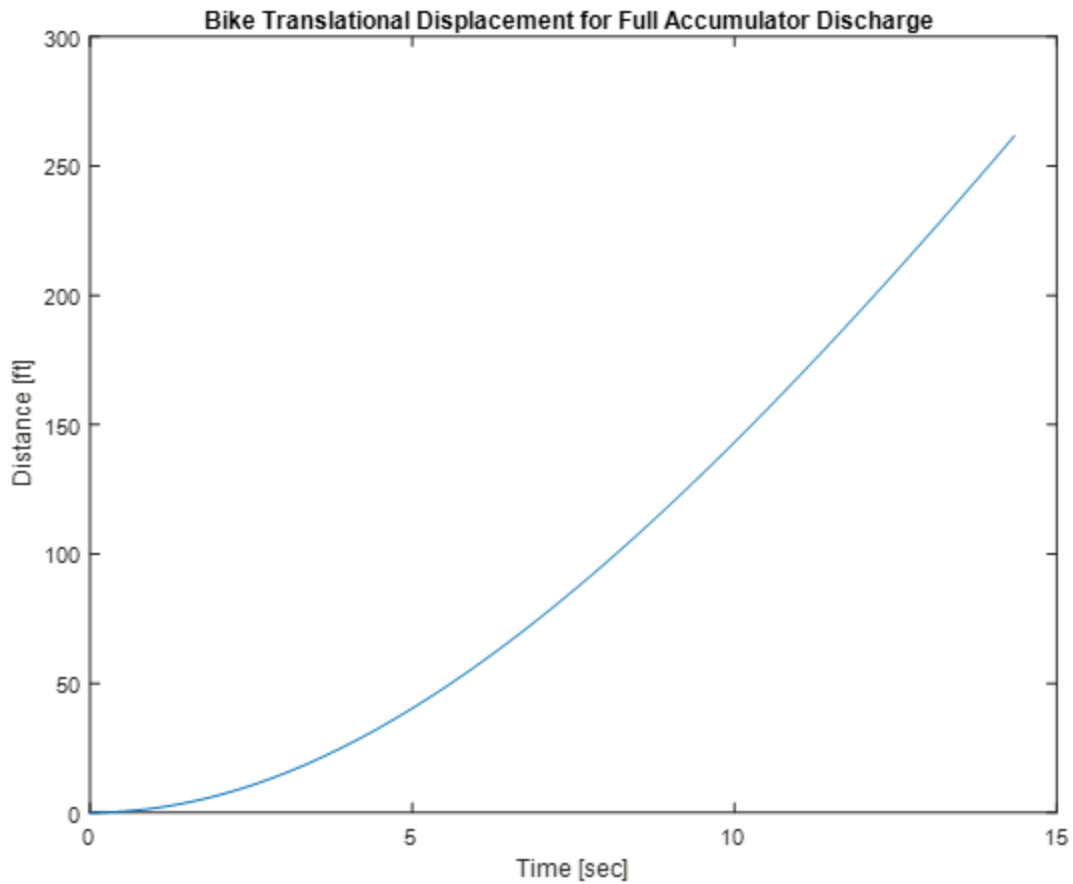


Figure 41. Plot of bike translational displacement over time using the Simscape accumulator discharge model (0.29 gallon accumulator volume with 900 psi precharge). Estimated efficiency score of 14.5

The purpose of the accumulator discharge model is to predict the performance of the bike while varying accumulator volume, accumulator precharge, and accumulator maximum pressure to determine which accumulator specifications maximize our bike’s efficiency score to meet our requirements. A plot of bike displacement over time using a 1 gallon accumulator with a 900 psi precharge pressure is shown in Figure 42. Compared to the 0.29 gallon accumulator, the efficiency score increased from 14.5 to 15.7 using a 1 gallon accumulator, predicting that a larger accumulator should lead to a higher efficiency score.

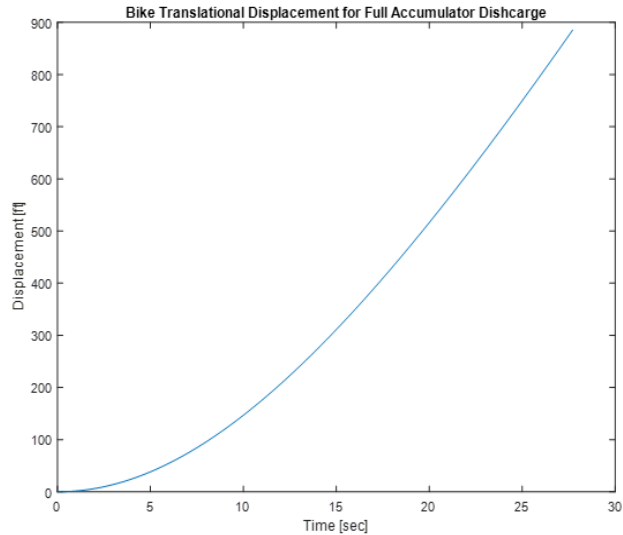


Figure 42. Plot of bike translational displacement over time using the Simscape accumulator discharge model (0.98 gal accumulator volume with 900 psi precharge). Estimated efficiency score of 15.7

#### ***4.6.2 Accumulator Discharge Model - Future Development***

Although the Simscape model predicts the performance of the bike during the accumulator discharge, the model doesn't predict the performance of the bike during coasting after all of the fluid energy is expended. The next model revision will require a state where the bike coasts down after the accumulator is fully discharged which should encompass the total distance traveled and more accurately reflect the efficiency score results. This can be accomplished by performing a piecewise-solution and combining results in MATLAB. Once that is complete, sweeps of different accumulator parameters should point to the proper accumulator size to maximize the bike's efficiency score. More additions such as aerodynamic drag, fluid inertance, and road slope will be added to further replicate the actual system.

#### ***4.6.3 Patterson Control Model***

Given that the Incompressibles have decided to design and manufacture a new vehicle frame, it is necessary to perform an analysis of the handling and stability characteristics of the selected vehicle type. The frame decision process led to the selection of the upright standard frame bicycle as the vehicle of choice, which already has a somewhat established handling model named the Patterson Control Model (PCM). This model accounts for a number of geometric parameters of the bicycle frame, as seen in Figure 43 and Figure 44, and ultimately expresses stability and handling as functions of velocity. With the unique nature of this vehicle in regard to its various components, it will be necessary to ensure the bike is stable at the proposed speeds.

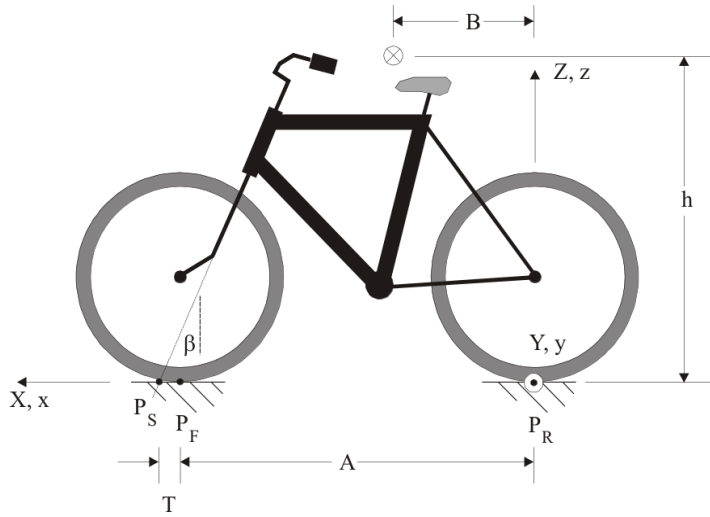


Figure 43. Patterson model bicycle geometry

The PCM will be used to extract several relationships describing vehicle handling characteristics. First are the relationships that describe vehicle motion, specifically roll and yaw, for a given steering angle, which are called roll and yaw authority. In order to determine if our proposed bicycle geometry provides a familiar riding experience, the roll and yaw authority of our bike will be compared to that of an existing bike with known handling characteristics. Another important relationship is control authority, which characterizes the feel of the bicycle by incorporating the distance of the handlebar grip points from the center of the roll axis, denoted  $R_h$ . This parameter will also be compared to that of an existing bike to ensure the desired control characteristics.

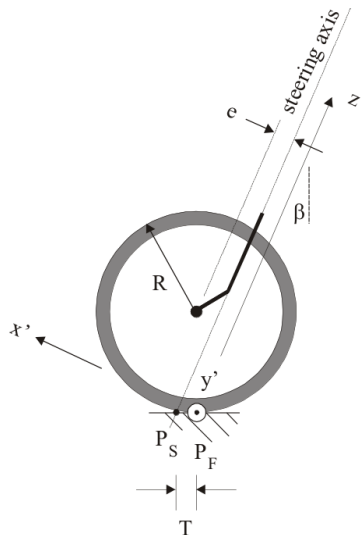


Figure 44. Patterson model front wheel coordinate system

The PCM also develops a relationship for the moment felt about the steering axis when the handlebars are turned through an angle,  $\delta$ . The torsional spring constant developed in this relationship,  $k_\delta$ , characterizes the resistance to rotation of the handlebars at a given velocity;

plotting  $k_\delta$  against velocity illustrates an important stability relationship. As seen in Figure 45,  $k_\delta$  begins positive at low velocities, meaning that for a turn of the handlebars in a certain direction, the bicycle will tend to roll in that same direction; this is an unstable situation. As velocity increases,  $k_\delta$  decreases parabolically and eventually becomes negative, at which point a turn of the handlebars in a certain direction will cause the bicycle to roll in the opposite direction. This is a stable situation; therefore, it is desirable to maintain a negative torsional spring constant across all velocities if possible.

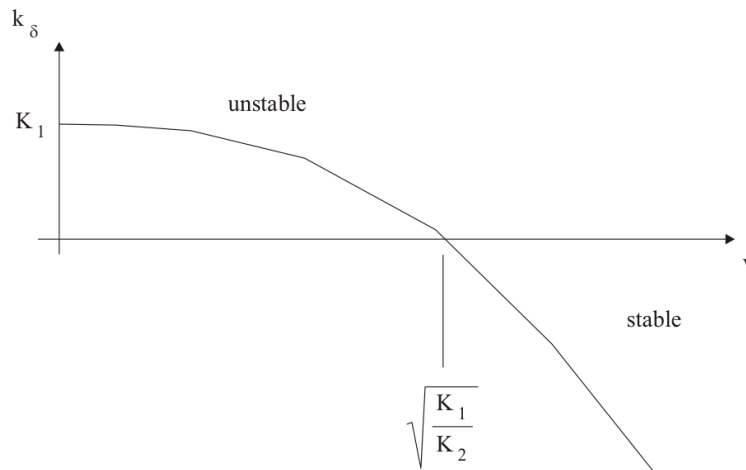


Figure 45. Steering spring rate vs. velocity

Another parameter developed in the PCM is called fork flop, which characterizes the force felt at the end of the handlebars due to a certain roll angle,  $\theta$ . Unlike the torsional spring constant, the fork flop spring constant does not depend on bicycle velocity, but solely on geometry. According to Patterson, the minimum value for the fork flop spring constant depends on the vertical location of the center of gravity of the bike and rider. Patterson deduced through empirical analysis that a typical safety bike has a minimum fork flop constant of about 50 N/rad, and the maximum allowable fork flop constant for any bike is about 225 N/rad.

The last relationship developed in the PCM is control sensitivity, which characterizes roll velocity per rider intention, where intention is defined as displacement of the handlebars plus force on the handlebars. Control sensitivity is also a function of bicycle velocity, as seen in Figure 46. High control sensitivity means the bike is over-controlled and thus responds too quickly to rider intention. Low control sensitivity means the bike is under-controlled and thus responds sluggishly to rider intention. An important relationship within the bike geometry affecting control sensitivity is  $B/A$ , or the percentage of the wheel base that the center of gravity is in front of the rear wheel contact point. This value will be compared to that of an existing bike to ensure stability.



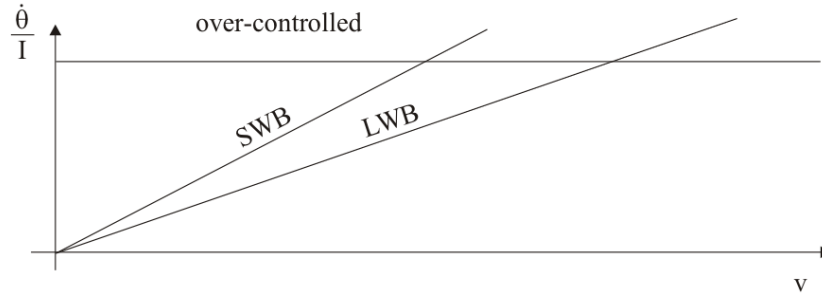


Figure 46. Control authority characteristics of a short wheelbase and a long wheelbase bike

#### 4.6.4 Patterson Control Model – Future Development

Since our bicycle design incorporates the addition of numerous components that are unusual to a bike frame, great care must be taken in arranging the components such that the center of gravity is in a desirable location. Cal Poly’s Fluid Power Challenge team from two years ago, 0-Chainz, also redesigned their bicycle frame and used the PCM to do so. The Incompressibles will use 0-Chainz’s version of the PCM as a preliminary tool to help design the new frame. 0-Chainz also developed an excel tool to determine the center of gravity of the bike based on the mass moment of inertia of each component, which the Incompressibles will use to find the center of gravity of our finalized bike design.

#### 4.6.5 Losses and User Requirements – Current Design

Losses and user input requirements as a function of steady state bike speed were quantified in order to design the drivetrain. This information, along with accumulator discharge and bike acceleration modeling, will determine final gearing ratios and the qualitative value of a shifting mechanism at the rear drive. The MATLAB model accounts for road roughness, road incline, drag, hydraulic circuit efficiency, and bike parameters such as weight and gearing ratios. See Figure 47 for losses at a given set of parameters. Note that aerodynamic drag is responsible for losses comparable to that of the hydraulic system when bike speed reaches around 15 mph and that road slope, even at 1-2% grade, accounts for significant losses due to high bike weight.

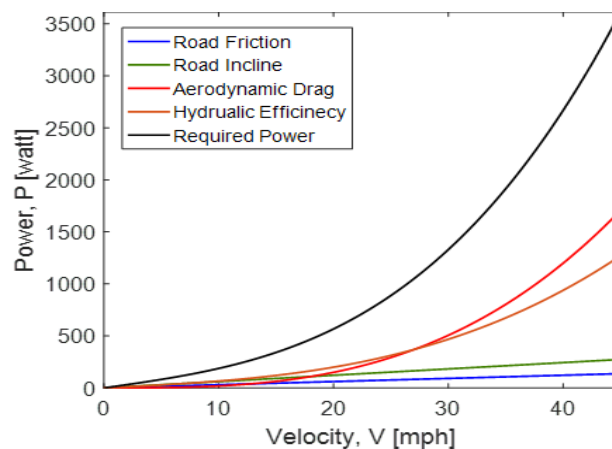


Figure 47. Estimated power losses of current bike using the following parameters: road friction coefficient set to 0.005, road at 1% grade, drag coefficient set to 0.75 with frontal area of 5 ft<sup>2</sup>, and hydraulic circuit efficiency estimated to be 50%.

The previous year's bike used a ratio of 1:15 from the pedals to the pump and 3:1 from the motor to the rear wheel. A rider was able to maintain the motor at a speed of approximately 450 rpm with a cadence of 30 rpm. These results confirm the model as they are predicted based on bike parameters. See Figure 48 for the model results.

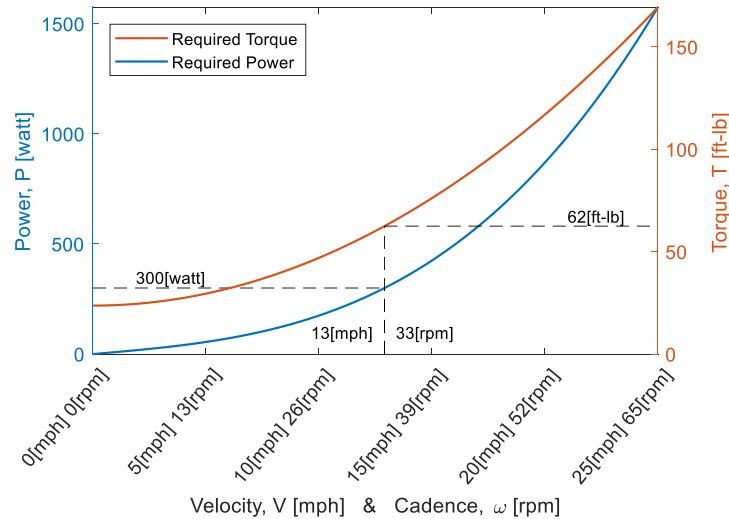


Figure 48. Input power and required user torque for given bike speed and user cadence. The model will take a particular given input power and find the user torque and cadence at steady state operation considering all of the previous mentioned bike parameters.

As expected based on testing of the current bike, at 300 [watts] of continuous power the cadence is around 30 [rpm] with a torque requirement of 62 [ft-lb]. At the moment the model does not account for changes in efficiency based on pump speed, motor speed, and user cadence. Thus, entering different rear gear ratios will only be seen in the torque curve. See Figure 49 for changes to the user torque based on rear gear ratio.

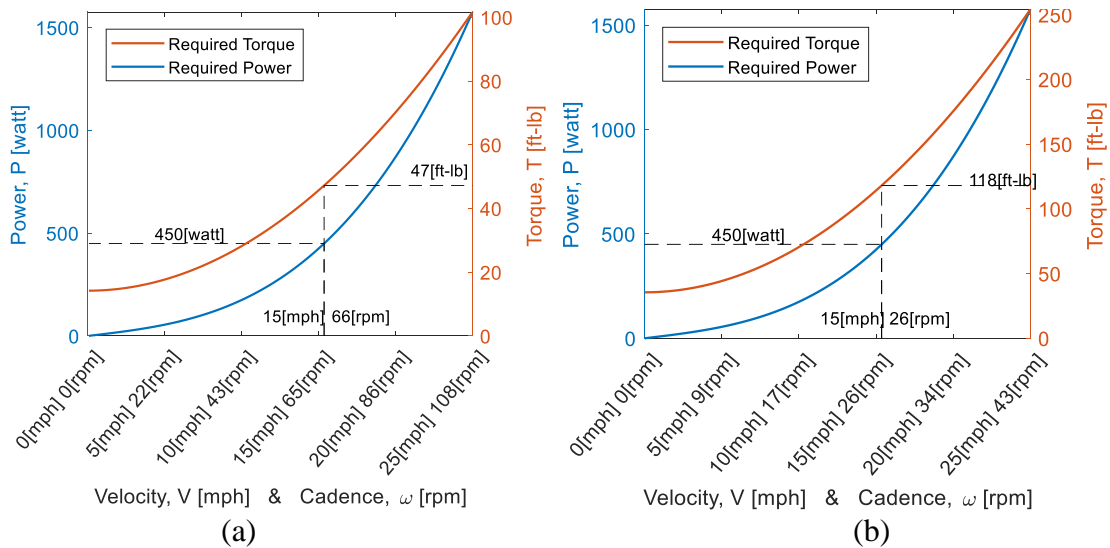


Figure 49. (a) Torque curve with a rear gear ratio of 1:6. (b) Torque curve with a rear gear ratio of 1:2.

#### 4.6.6 Losses and User Requirements – Future Development

At the moment the model is unable to predict transient behavior. Acceleration predictions will be needed in order to understand starting torque requirements and shifting times if a transmission is to be implemented. Also, pump, motor, and hydraulic circuit efficiency are not functions of speed, resulting in inaccurate power requirements. This information will be necessary to further validate any preliminary gearing choices and drive train design.

#### 4.6.7 Direct Drive Model – Current Design

Portions of the Simscape accumulator discharge model were used to develop a preliminary Simscape direct drive model of the bike. Figure 50 below shows the Simscape model layout.

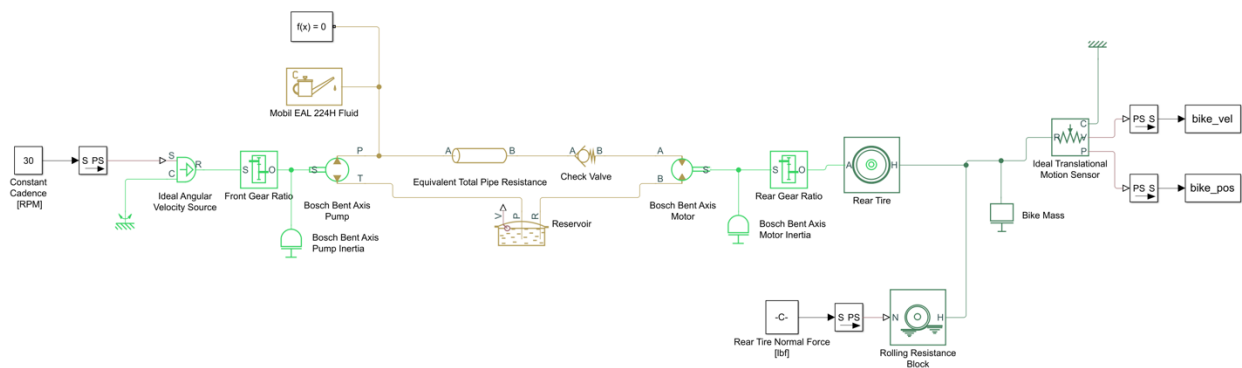


Figure 50. Simscape derived model for direct drive mode

The model currently predicts steady state characteristics of the bike at a certain rider cadence in RPM. The constant angular velocity source travels through a front gear ratio into the Bosch A2FO-5 bent axis pump and through another Bosch A2FO-5 bent axis motor which spins the rear wheel through a rear gear ratio. The current model accounts for the same parameters as the accumulator discharge model; equivalent fluid resistance of the pipes from the accumulator to the motor, the motor inertia, the fluid properties, the rolling resistance on the rear tire, and the total bike mass. The purpose of this model is to quantify hydraulic losses from the circuit to differentiate which configuration is most efficient and meets our leakage requirement. Simscape can also output forces as well as motion and the direct drive model will be useful to predict the initial pedaling torque experienced by the rider and the bike's top speed to drive gear ratio selection. Simscape's robustness will also allow us to recreate our intended hydraulic circuit for each drive mode to test its feasibility before implementing it on the actual bike.

#### 4.6.8 Direct Drive Model – Future Development

Currently the model starts from a steady state condition and has a constant velocity input. This doesn't account for the transient start from a standstill where the required torque will be the highest to get the bike moving. This will require the model to have a constant power input rather than a constant angular velocity or angular torque input. The torque exerted by the rider will decrease as angular velocity increase and vice versa. This change will allow the model to predict transient bike

behavior rather than only steady-state performance. Transient bike performance will be crucial to determine gear ratios that are achievable by human power.

## 5 FINAL DESIGN

The 2018-2019 bicycle utilized a hydraulic pump and motor as well as two chain driven drivetrain systems designed to maximize the power transfer from the rider to the rear wheel. The bike incorporated a modified steel bicycle frame with an extended wheel base for efficient component packaging. The hydraulic system included 4 drive modes regulated by electronic solenoids controlled by an Arduino Uno.

In order to design the bike, a coordinate system was made with its origin located at where the rear wheel contacts the ground plane below the rear wheel axle line with the X, Y, and Z directions of the bike facing forward, to the right, and down respectively, following the standard SAE J670 coordinates. The coordinate system is illustrated in Figure 51 and Figure 52 and the mass properties of the bicycle separated by system can be found in Table 9.

Table 9: Mass Properties for 2018-2019 Bicycle

<b>Sub-System</b>	<b>Weight (lbs.)</b>
Front Fork Assy.	8.5
Front Drivetrain	12.7
Rear Drivetrain	10.1
Mechatronics	2.2
Hydraulics	30.5 (includes fluid)
<b>Total (w/o 180 lb rider)</b>	<b>69.3</b>

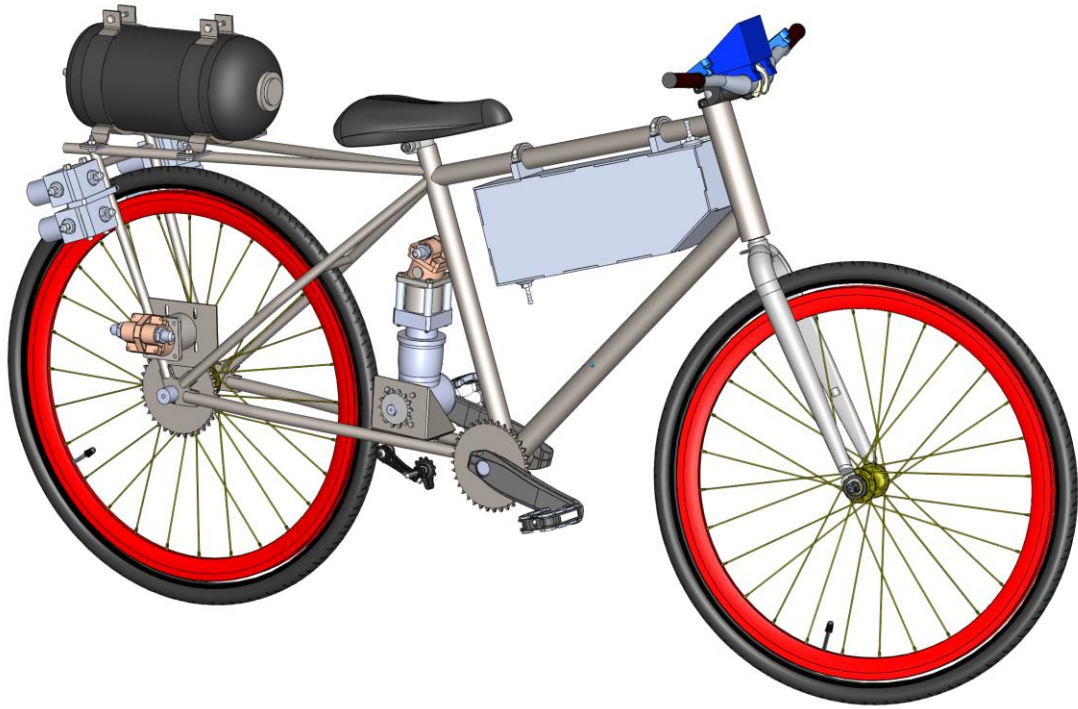


Figure 51: Overview of final bike



Figure 52: Another view of final bike

## 5.1 Frame

### 5.1.1 Frame Geometry

After PDR, the final geometry of the bike frame was initially modeled after the Trek FX Sport 4 bike, seen in Figure 53. This bike combines the comfort of a recreational bike with the sportiness of a road bike as Trek advertises this bike as a versatile hybrid bike. This design would be a happy medium between a road bike and a mountain bike to determine our base frame geometry.



Figure 53. Image of Trek FX Sport 4

The bike frame also needed to accommodate various rider heights therefore the “large” size frame was selected to model after. This allows riders from 5’8” to 6’2” to fit the bike. The dimensions of the large size Trek FX Sport 4 frame is shown below in Figure 54.

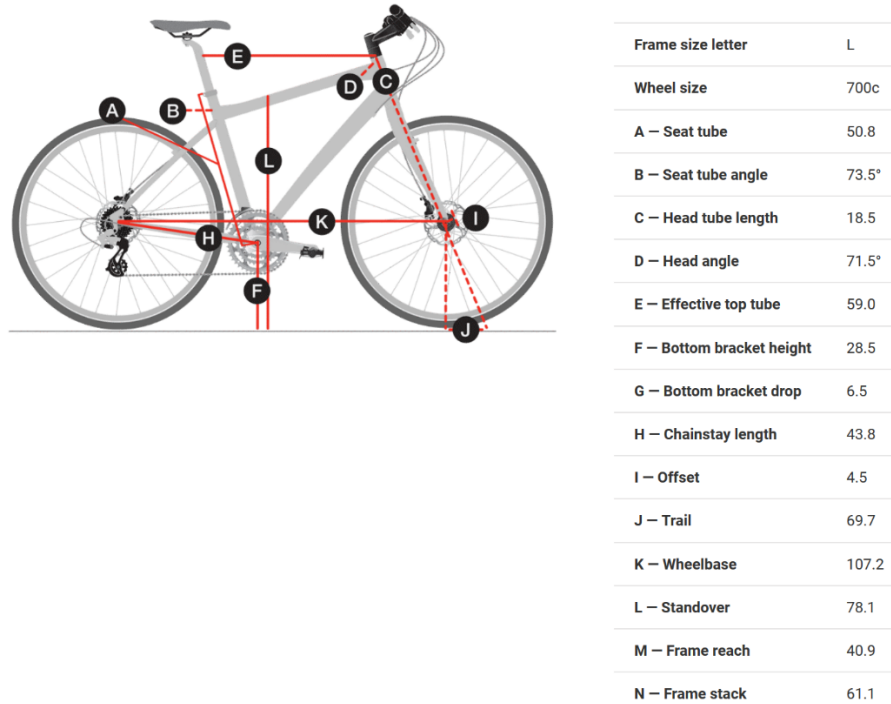


Figure 54. Dimensions of the large size Trek FX Sport 4 Frame

The Incompressibles utilized BikeCAD and Solidworks software to develop and model the frame. BikeCAD is a bicycle design software which allows the user to develop a custom frame based on common bike dimensions (i.e. stack, reach, head tube length, wheelbase, etc.). The front polygon of the final frame remained the same as the Trek FX Sport 4, but the wheelbase had to increase from 1072 mm to 1239 mm to allow for hydraulic component packaging. The inputs into the BikeCAD model from Figure 54 were:

1. Seat tube angle (Dim. B)
2. Seat tube length (Dim. A)
3. Bottom bracket height (Dim. F)
4. Chain stay length (Dim. H)
5. Head angle (Dim. D)
6. Reach (Dim. M)
7. Stack (Dim. N)

Figure 55 shows the inputted frame geometry using BikeCAD. There are two horizontal support tubes and two vertical support tubes going from the rear dropout in the final frame geometry not shown in the BikeCAD model, but are modeled in Solidworks. Due to the long wheelbase, the chainstay and seatstay increased in length from around 430 mm to 600 mm.



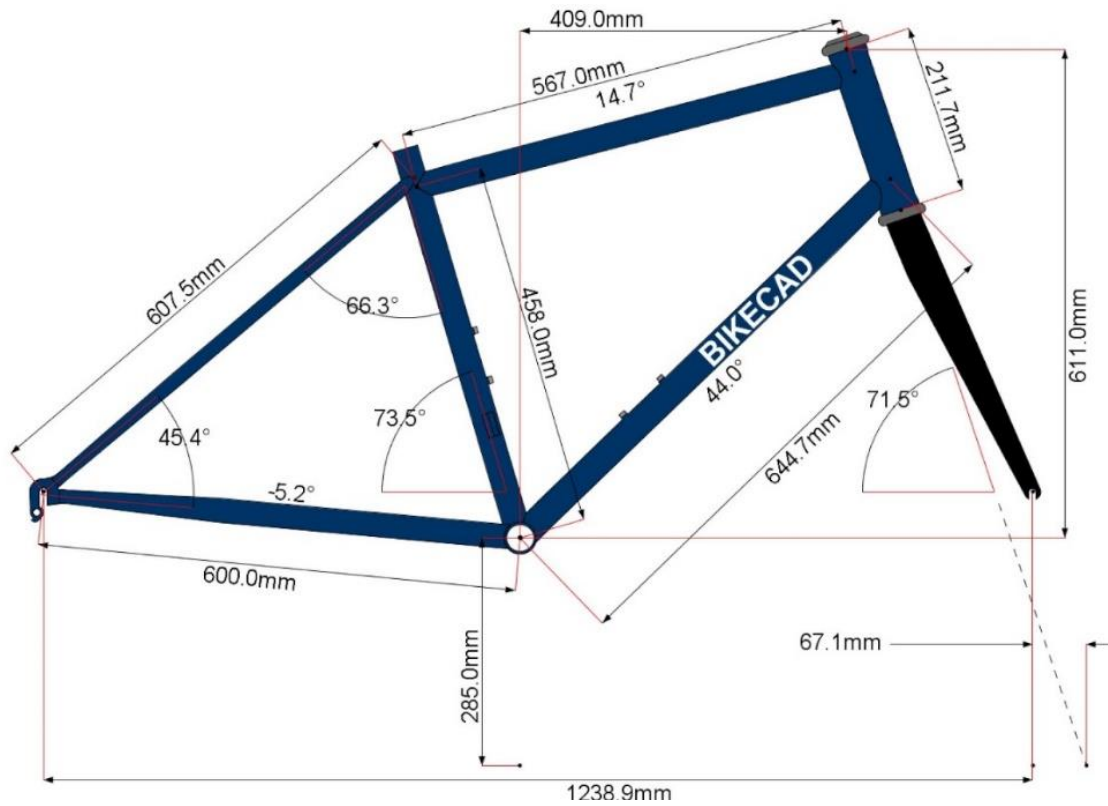


Figure 55. Image of revised BikeCAD frame geometry

The above bike dimensions were translated into a Solidworks sketch to model the final frame seen in Figure 56. Dimensions from the BikeCAD model vary slightly from the Solidworks geometry due to the necessary Solidworks mates to develop the frame geometry using the intersection of the ground plane and the rear wheel axle as the origin. The Solidworks sketch defines the final geometry for the frame. The final frame dimensions are outlined in Table 10.

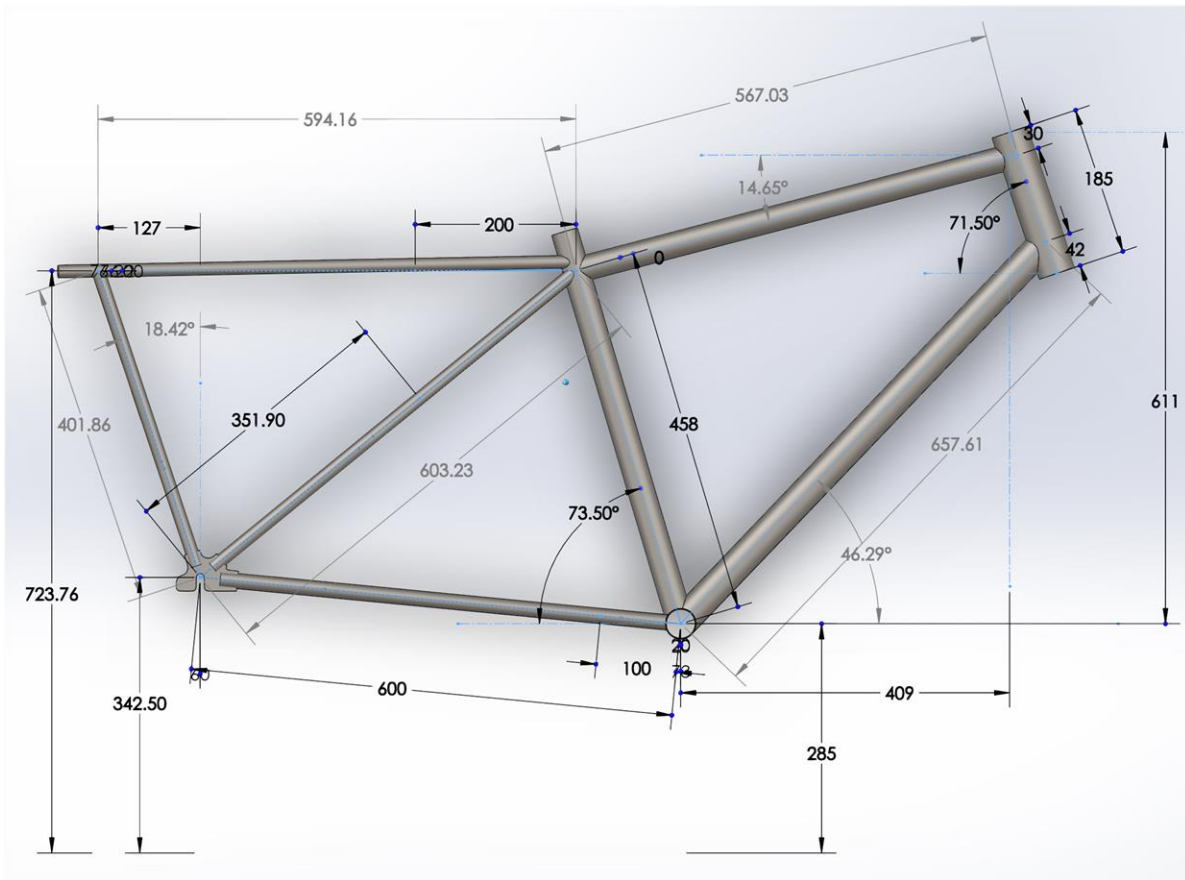


Figure 56. Final frame geometry in Solidworks sketch (all dims. in mm)

Table 10. Final 2D bike frame parameters from Solidworks guide sketch

Bike Frame Parameter	Length	Angle
Stack	409.0 mm	N/A
Reach	611.0 mm	N/A
Wheelbase	1238.9 mm	N/A
Head Tube (t-t)	185.0 mm	71.5 deg from horizontal
Top Tube (c-c)	567.0 mm	14.6 deg from horizontal
Down Tube (c-c)	657.6 mm	46.3 deg from horizontal
Seat Tube (c-c)	458.0 mm	73.5 deg from horizontal
Chainstay Tube (c-c)	600.0 mm	N/A
Seatstay Tube (c-c)	603.2 mm	N/A

Once the Solidworks master guide sketch for the frame was made, sweeps and lofts were used to generate frame tubes. Figure 57 below shows the final frame tube geometry with the rear support tubes to mount the accumulator and subsequent hydraulic components.

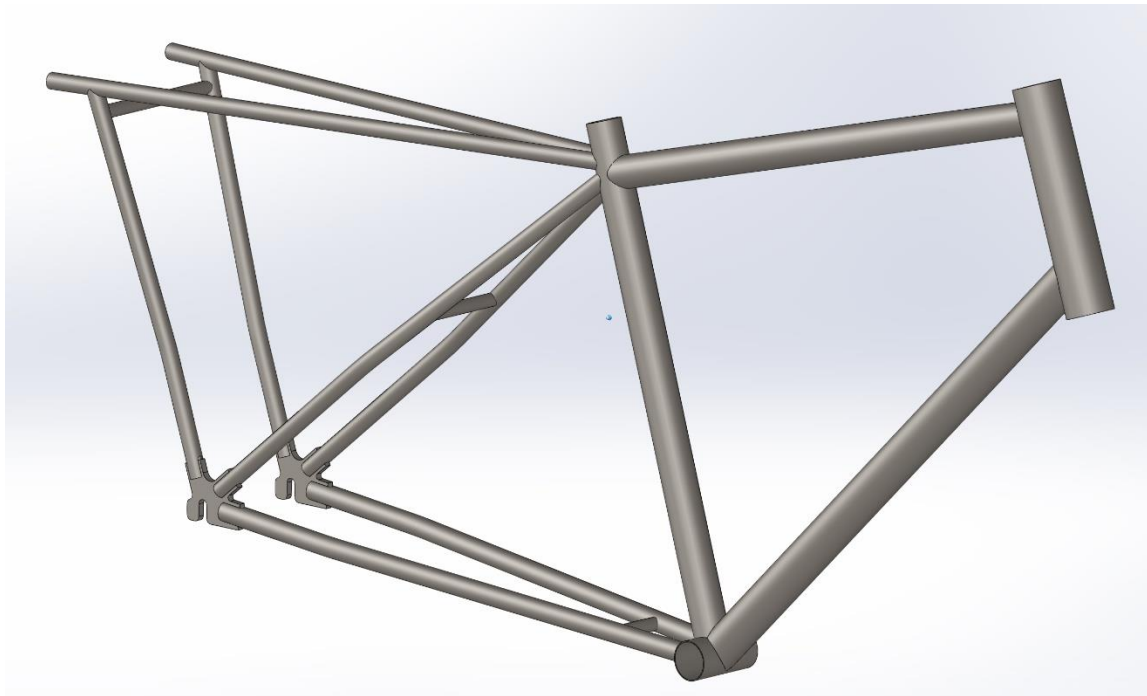


Figure 57. Solidworks model of final frame geometry

The front polygon was left untouched to not disrupt the handling of the bike, whereas the rear tubes behind the seat tube were modified in length and angle to accommodate the hydraulic components. The upper support tubes on the frame allowed the accumulator to attach horizontally, shown in Figure 58. Due to the accumulator's wide size, placing it underneath the rider's legs was not an option as it would have hit the rider while pedaling. Placing it behind the rider and on the centerline of the bike allows for much better packaging and easier routing for hydraulic lines while giving an even left to right weight distribution. The tubes are also angled slightly lower than horizontal allowing the accumulator to sit low without contacting the top of the rear wheel, aimed at lowering the CG height.

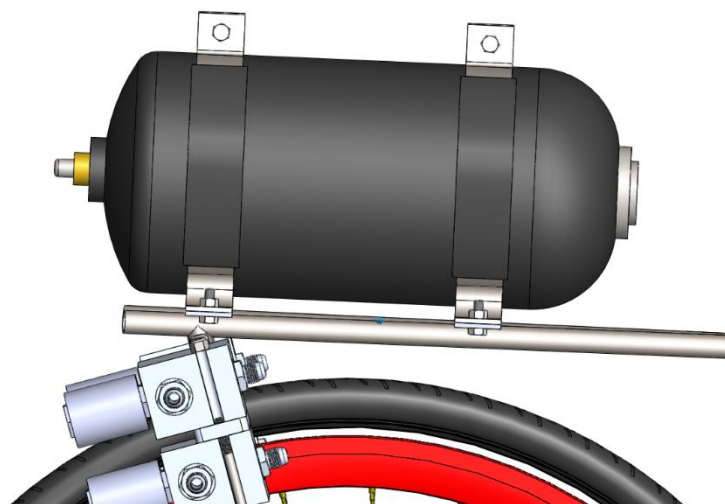


Figure 58. Image of the accumulator mounted on the frame rear upper support tubes

The vertical support tubes and the seatstays contain a single bend to allow proper attachment of the rear motor mount to the frame. The tubes bend to a vertical position before attaching to the rear dropout, so the motor can mount perpendicular to the ground on the right-hand side of the frame, seen in Figure 59. It is critical that the rear motor and rear sprocket have minimal misalignment for proper operation.

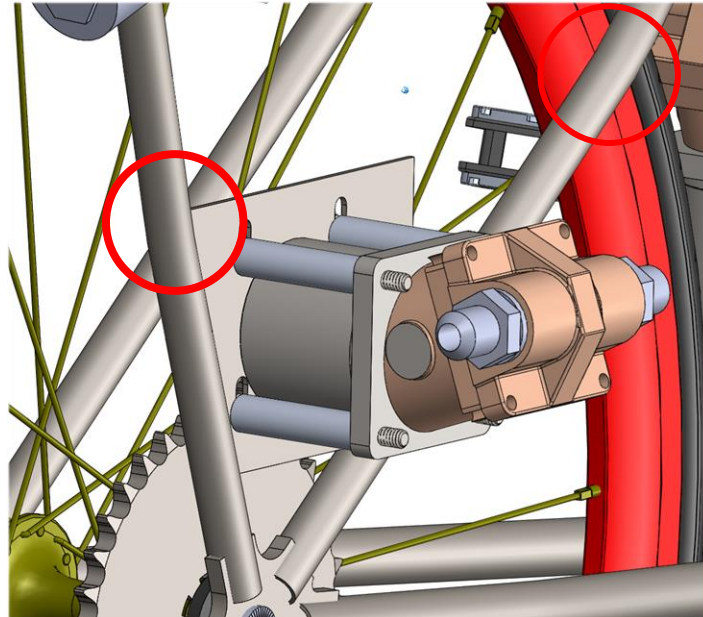


Figure 59. Image of rear motor attachment to rear vertical support tubes and seat stays with tube bends indicated with red circles

The front pump and chain tensioner are attached to the lower chainstays in front of the rear wheel behind the front crank, see Figure 60. The chainstay length was largely based on the packaging requirements for the front drivetrain. The front drivetrain had to be placed further back in order to allow clearance for the rider's feet and pedals.

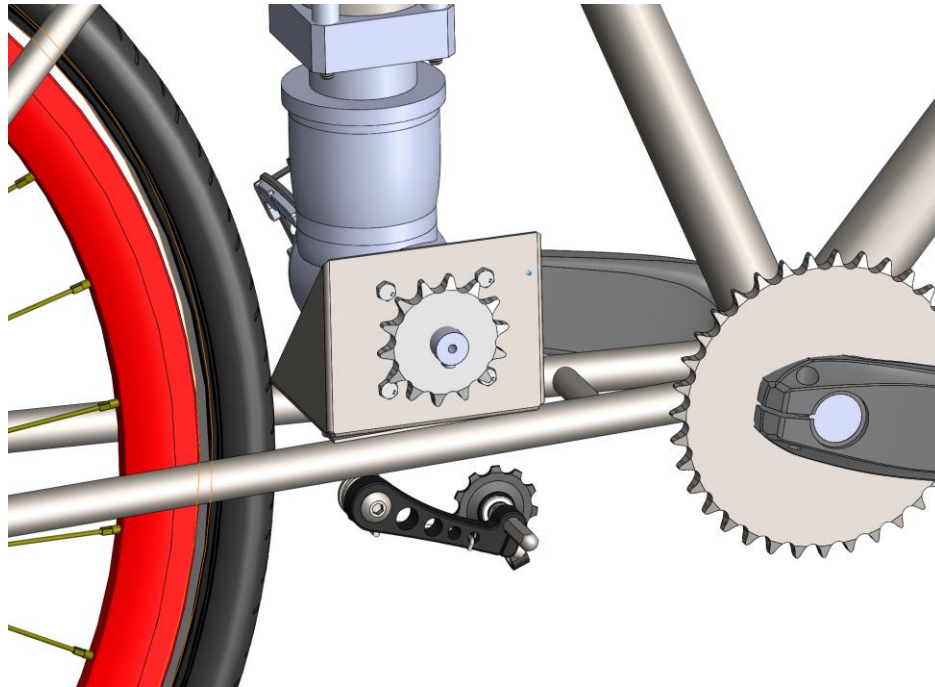


Figure 60. Image of front drivetrain attachment to frame chainstays

Bridges were welded to the chainstays, seatstays and upper support tubes, seen in Figure 61, for lateral rigidity.

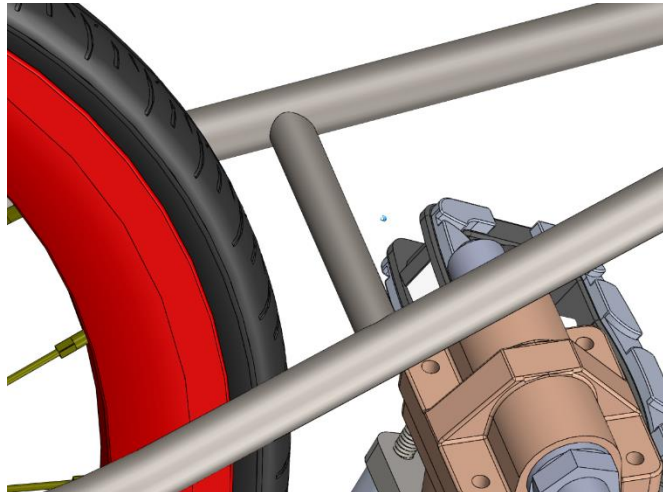


Figure 61. Example of chainstay bridged welded between tubes for lateral rigidity

To maintain a similar amount of mechanical trail to the Trek FX Sport 4 bicycle, 69.7 mm, a front fork with a 45 mm offset was chosen creating a mechanical trail of 67.1 mm for our final bike. The final frame geometry was a compromise of providing an efficient surface to package components onto while providing comparable handling characteristics to an existing off-the-shelf bike.

### 5.1.2 Frame Tube Material Selection

Material selection for the frame was focused between steel, aluminum, titanium and carbon fiber. Although the weight and stiffness benefits of a carbon fiber frame are better than the traditional metallic frames, unfortunately our limited composites manufacturing and analysis knowledge, coupled with the large amount of testing required for attachments to the carbon frame, made this choice out of our scope of work. This challenge could be tackled by future teams. Deciding between titanium, steel and aluminum came down to welding expertise and post-welding treatments. Few individuals at our school know how to weld titanium properly and outsourcing this would have been very expensive. If aluminum was chosen, we would have to heat treat the frame after welding to restore the entire frame to a T-6 temper. The post-heat treatment process will a fixture to restrain the frame. After annealing and re-aligning, the frames would then need to be artificially aged in an oven at 350 deg F to achieve a T-6 temper. The Bike Builders club have been able to achieve low weight, steel frame bikes that are easily weldable and as light as some aluminum frames. We decided to choose a 41XX Chromoly steel frame due to its easy weldability, no requirement of post-welding heat treatment and its low weight if designed properly. A large majority of bike tubes utilize butted internal structures where the inner portion of the tube has a smaller wall thickness compared to the ends, see Figure 62 for a pictorial showing the differences. This decreases tube weight and only contains thicker material near the welds. Based on the eccentric/non-standard loading on the frame and the increased weight from a standard bike due to the hydraulic components, the tubes were sized for an oversized mountain bike frame, but could be reduced if more frame analysis is done.

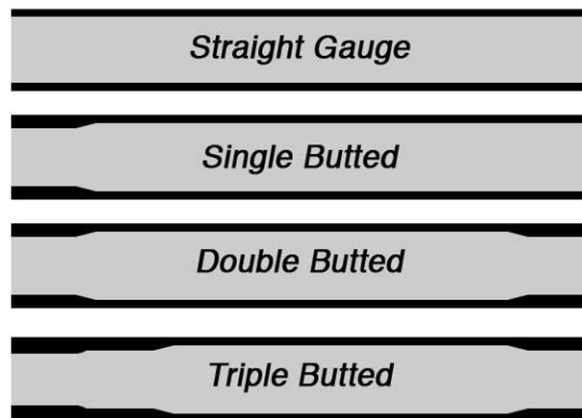


Figure 62. Picture showing the differences between straight tubing and butted tubing

After determining the final geometry of the bike, The Incompressibles investigated different OD and wall thickness tubes for an oversized MTB frame, mainly from [Nova Cycles Supply](#). This website was given as a recommended site to purchase frame tubes. The final dimensions for each tube on the frame are given in

Table 11.

Table 11. Summary of frame tube diameters and wall thicknesses (See Figure 63 for corresponding tube numbers)

Tube Name	Outer Diameter	Wall Thickness
Top Tube [1]	31.7 mm	0.8x0.5x0.8 mm
Head Tube [2]	46.4 mm	1.25 mm
Down Tube [3]	38.1 mm	0.9x0.6x0.9 mm
Seat Tube [4]	32.7 – 33.5 mm	0.9x0.5x0.95 mm
Chainstay Tube [5]	0.75 in	0.065 in
Seatstay Tube [6]	0.625 in	0.065 in
Vertical Support Tube [7]	0.625 in	0.065 in
Upper Support Tube [8]	0.625 in	0.065 in
Chainstay Bridge [9]	0.50 in	0.065 in
Seatstay Bridge [10]	0.50 in	0.065 in
Upper Support Bridge [11]	0.50 in	0.065 in

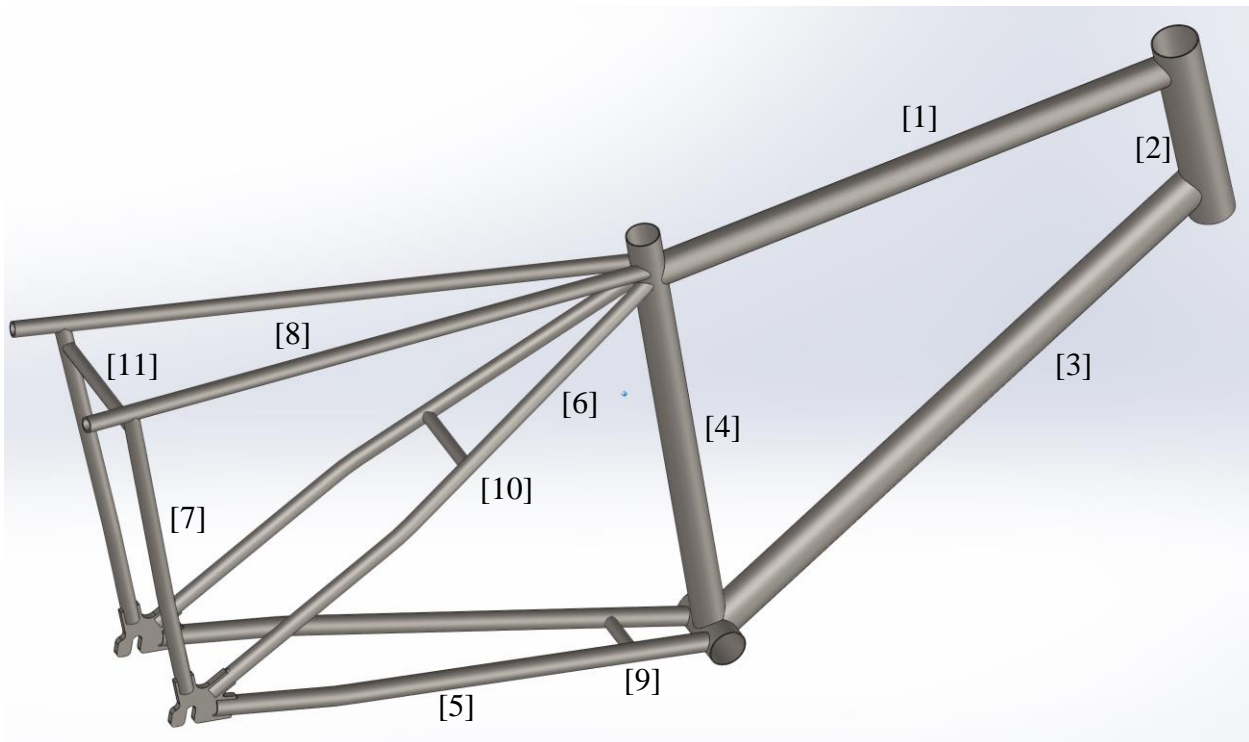


Figure 63. Model of final frame with tube numbers referencing to



Table 11.

### ***5.1.3 Patterson Control Model***

The Incompressibles used the Patterson Control Model (PCM) to verify stability and handling characteristics of the final bicycle frame. The Fluid Power Vehicle Challenge team from two years ago, 0-Chainz, provided their version of the PCM along with their results to use for comparison. After determining the geometry of the new frame, the parameters specified previously in section 4.6.3 were inputted into the model. The tabulated PCM input parameters are shown in

Table 12.

Table 12. Input Parameters for Patterson Control Model

Inputs		
A	1.25	m
h	0.89	m
Rh	0.66	m
$k_x$	0.317	m
m	116	kg
B	0.56	m
$\beta$	18.5	deg.
R	0.35	m
e	0.045	m
g	9.81	m/s <sup>2</sup>

All parameters for the PCM were derived from frame geometry except for the radius of gyration,  $k_x$ , and mass,  $m$ , which were estimated using the mass properties feature in SolidWorks. Once the bicycle is built, testing utilizing an inertia swing will determine the actual radius of gyration and mass of the bicycle and the results will be compared with the initial inputs. Also, the values for radius of gyration and mass here include all the components to be mounted on the bicycle. Since the bare frame design does not stray far from a typical frame, it was important to determine whether the additional components would drastically affect dynamic characteristics of the bike.

The results of the PCM allowed the comparison of handling and stability characteristics with a standard Trek bicycle. Figure 64 gives variation in control spring constant with velocity. As stated previously in section 4.6.3, the control spring constant characterizes the resistance to rotation of the handlebars at a given velocity. The trend lines labeled “gyro” refer to an updated version of the PCM that incorporates gyroscopic effects from the rotation of the wheels. The trends seen between the control bicycle and the proposed bicycle design strongly agree. A notable value in this graph is the point of intersection with the x-axis, which denotes the speed at which the bicycle becomes stable in handling. Both the gyro and non-gyro trend lines for the 2018 bicycle intersect the x-axis at lower speeds than the gyro and non-gyro trend lines for the Trek bike, meaning the proposed design will become stable at lower speeds than the control bike.

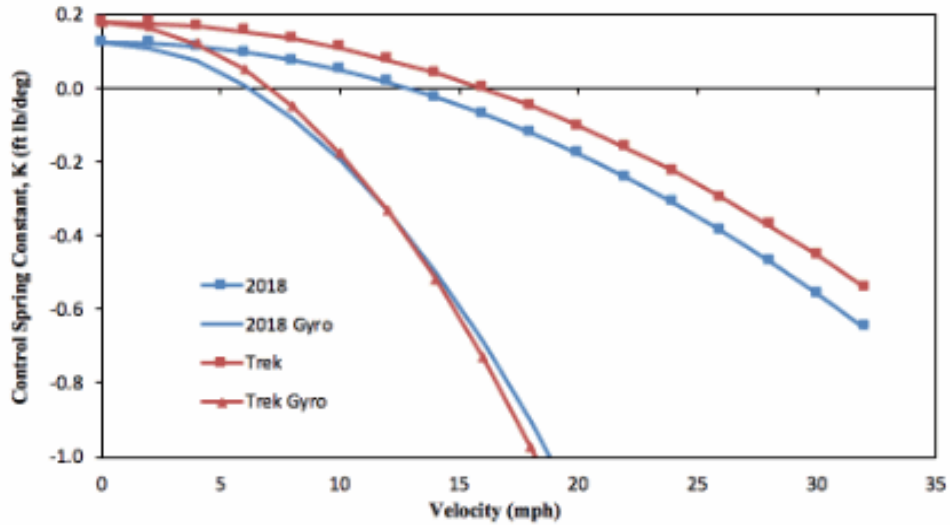


Figure 64. Variation of control spring with velocity for control bike and proposed design.

A second important handling characteristic considered was control sensitivity, which is a measure of roll rate for a given rider intention, with intention being displacement of the handlebars plus force on the handlebars. The trends between the control bike and the proposed design do not agree exactly. The control sensitivity for the 2018 design increases slowly with an increase in speed compared to the Trek bike, i.e., the 2018 bike would handle sluggishly in comparison to the Trek bike at speeds from approximately 10-15 mph. However, at high speeds, the control sensitivity of the 2018 bike and the Trek bike have very similar gyro trend lines. This suggests the proposed bicycle design would handle similar to a typical bicycle at speeds around 30 mph, which is just below the estimated top speed of 32 mph.

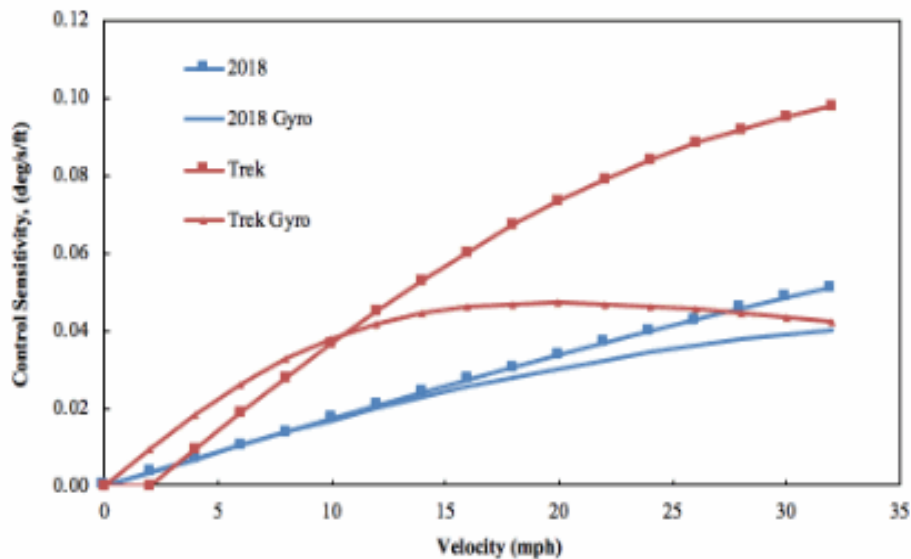


Figure 65. Variation of control sensitivity with velocity for control bike and proposed design.

### 5.1.4 Structural Analysis

Initial sizing of tubing for the bike frame was determined based upon the experience of the members of bike builders as well as the available tubing on Nova cycle. This size was then validated using simple truss analysis of the bike frame. It is notable that our bike compared to a standard is mostly the same for the front geometry but varied when it came to the length of the wheelbase, length of the chainstay and seat stay and the overall weight of the bike. Figure 66 shows the CG of the bike with all the components on it including the fluid weight of the hydraulics.

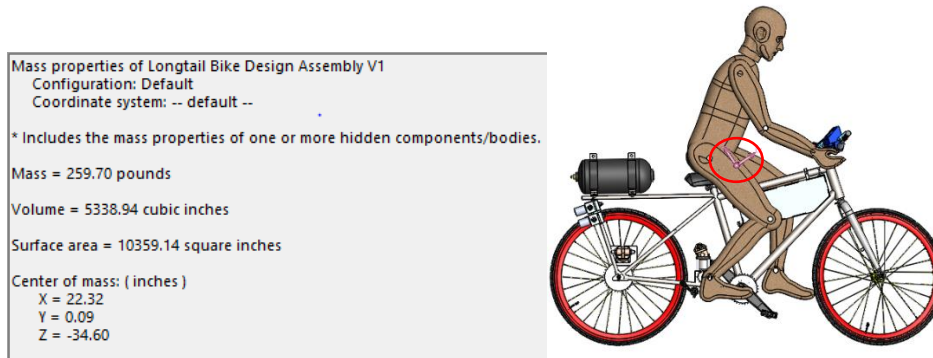


Figure 66. Mass of the bike and location of CG with 180lb rider

To make sure that the bike would be strong enough for standard driving, the frame was designed to meet 2 G's of acceleration in the Z direction. The bike frame was then simplified to a simple truss model. The bump load was then separated in to components and placed at the appropriate nodes. The weight of the accumulator was placed at the farthest back node. Then the weight of the rider and the rest of the bike was located between the seat tube and the handle bars. The developed FBD can be seen in Figure 67.

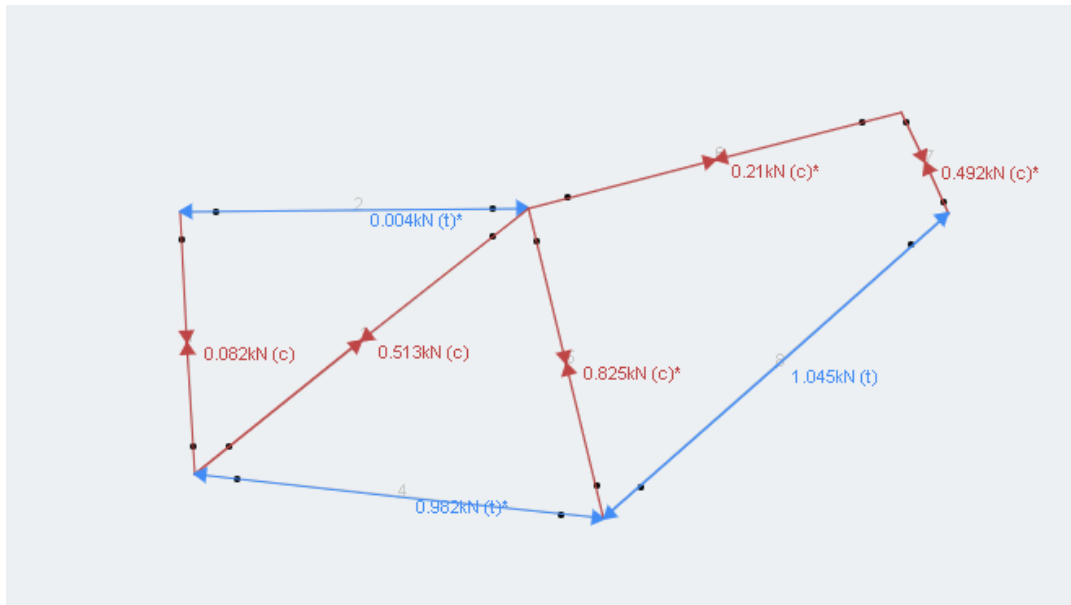


Figure 67. Truss analysis of bike frame

These forces were then used to find normal stress in each section of piping. For the analysis it was assumed that all the tapered tubes were just constant ID with the smallest wall thickness present across the length of the tube. The resulting factor of safety per tube was calculated and can be seen in Table 13.

Table 13. Tube Factor of safety based on truss analysis

<b>Tube</b>	<b>Factor of Safety</b>
Chainstay	15.95
Down Tube	14.83
Head Tube	79.46
Horizontal Support	3900
Seat Tube	13.44
Seatstay	25.28
Top Tube	51.16
Vertical Support	191.11

## 5.2 Hydraulics

### 5.2.1 Hydraulic Circuit

Four drive modes were implemented in the hydraulic circuit to meet both the competitions and the team's personal requirements: direct drive, accumulator discharge, accumulator regenerative braking, and coast mode. All hydraulic modes were approved by both Dr. James Widmann and Earnest Parker (the technical liaison for the NFPA).

#### 5.2.1.1 Direct Drive Mode

Direct drive mode connects the pump and the motor via the reservoir and two valves as shown in Figure 68. This mode allows for pressure generated from the rider through the pump to be utilized directly by the motor. In this mode, fluid flows from the pump through two solenoids before reaching the reservoir; each valve has a pressure drop of 15 psi when the bike is traveling at its top speed of 31 miles per hour and pumping at 2.7 gallons per minute. The pump not only needs to be connected to the motor but also must have the suction side directly connected to the reservoir to pull fluid and avoid air entering the system.

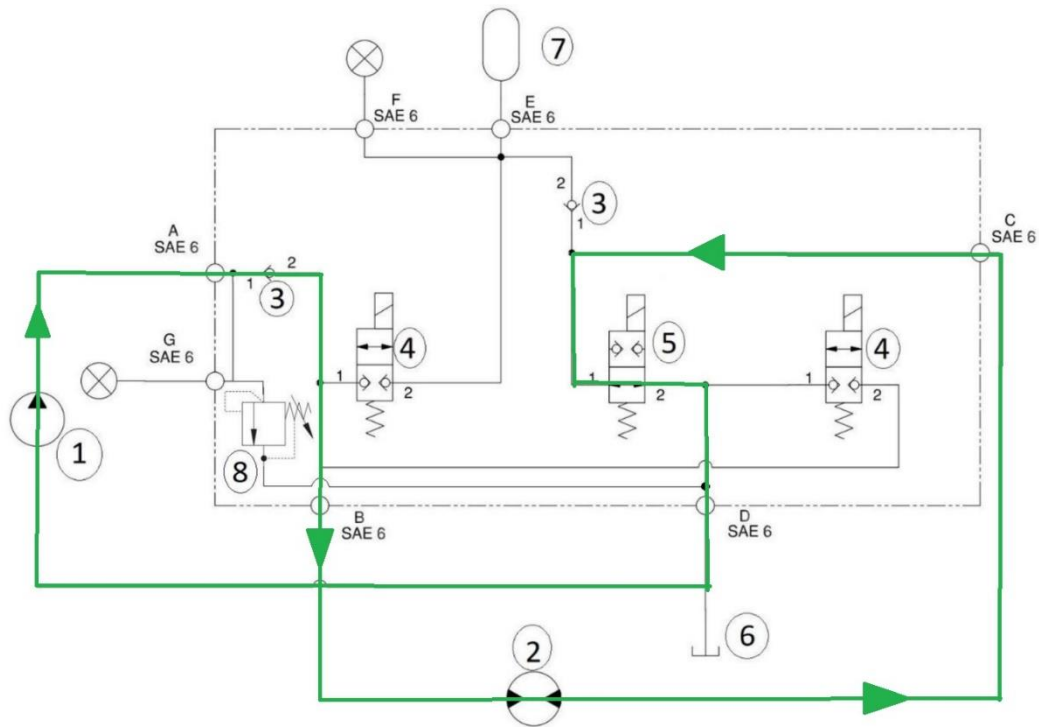


Figure 68. Direct Drive Mode Hydraulic Diagram

### 5.2.1.2 Discharge Mode

Discharge mode allows for the pressurized fluid stored in the accumulator to discharge through the motor to propel the bicycle forward. Fluid travels from the accumulator through one valve to the motor, then through a second valve to the reservoir, as seen in Figure 69. Comparatively, the pressure drop throughout the 2 solenoids in discharge mode is small when considering the high operating pressure of the accumulator. It should be noted that the 15-psi loss through each solenoid happens only when the bike is travelling at its top speed, the majority of the bikes operating life will take place at about half of that speed resulting in roughly half the pressure loss. Please see our pulse strategy for more information on the bikes expected operating speed.

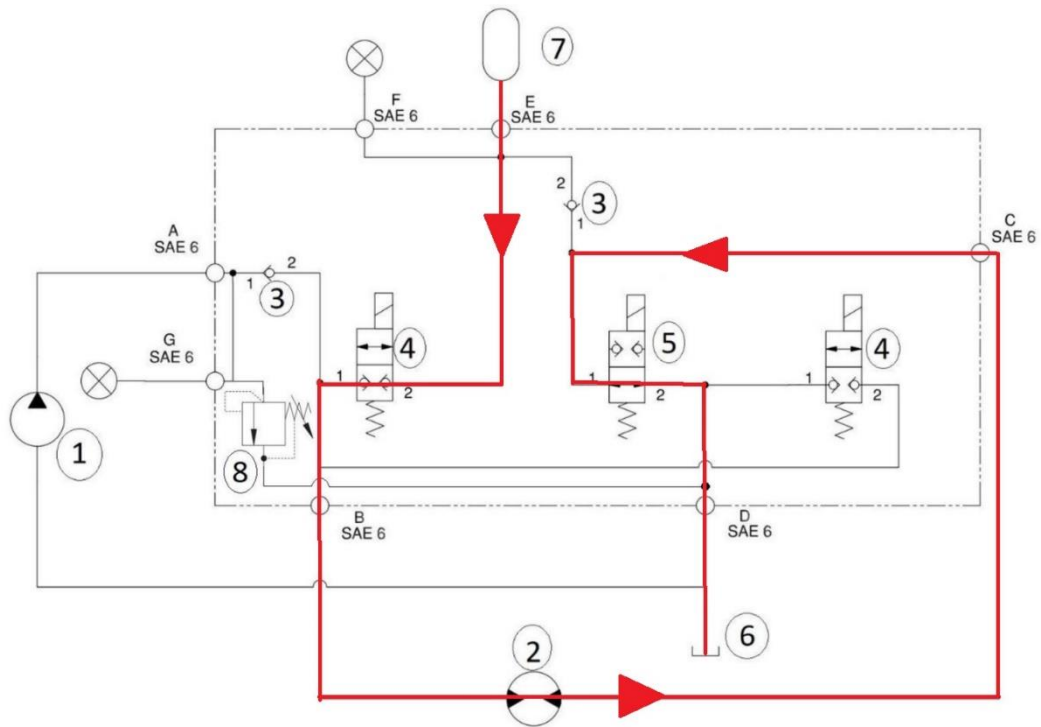


Figure 69. Discharge Mode Hydraulic Diagram

### 5.2.1.3 Regenerative Braking Mode

Regenerative braking mode utilizes the energy associated with the motion of the bike to build pressure in the accumulator. When this mode is engaged, the motor at the rear wheel acts as a pump, increasing the pressure and volume of the hydraulic fluid in the accumulator. Fluid flows from the motor through a check valve into the accumulator; about 8 psi of drop losses is experienced when fluid is flowing through the check valve, with 5 psi of loss resulting from cracking pressure. See Figure 70 for the schematic.



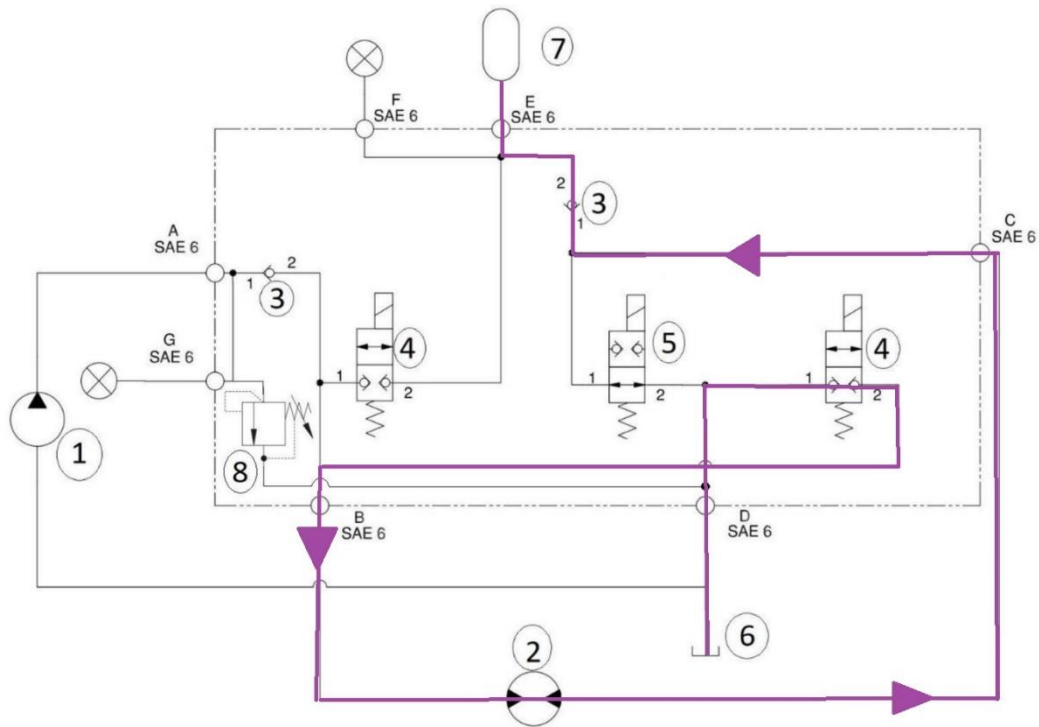


Figure 70. Regenerative Braking Mode Hydraulic Diagram

#### 5.2.1.4 Coast Mode

Last year's team attempted to incorporate a multiple-plate motorcycle friction clutch in the rear drivetrain, unfortunately they ran out of time and were not able to properly implement it. To avoid the same issue the Incompressibles investigated using a hydraulic coast mode to be used in place of the clutch that creates a closed loop through the motor and allows fluid to flow freely. Investigation of the validity of utilizing this mode in place of a clutch was done by testing last year's bicycle versus a conventional bicycle. A completely bled loop was created through the motor of the 805 Hubmasters' bicycle, this bicycle and a conventional bicycle were weighed down so the two bicycles' weight was comparable. Figure 72 and Figure 73 show the testing where both bikes were brought to the same speed and released at the same point while the distance travelled was recorded. The test was performed at 3 different speeds, the results can be found in

Table 14. The distance travelled by the hydraulic bike was surprisingly further than the conventional bicycle, we suspect this is because the hydraulic bicycle weighed slightly more. Although the results were not perfect the test gave validation that the hydraulic coast mode would be an acceptable alternative to the mechanical clutch and decrease the complexity of the bicycle greatly. The final schematic for the PIT or coast mode is shown below in Figure 71.

Table 14: Coast Mode Test Results

Speed Case	Previous Year Hydraulic Bike	Standard Road Bike
2 mph	33.5 ft	28.5 ft

4 mph	60 ft	47 ft
6 mph	158 ft	119 ft

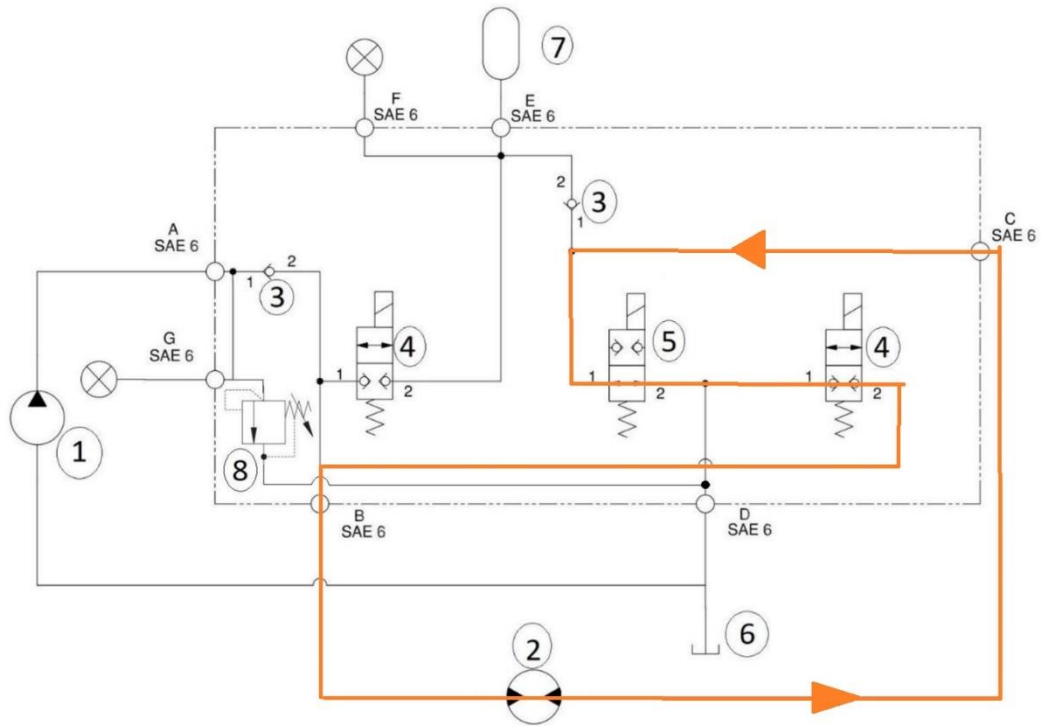


Figure 71. PIT Mode Hydraulic Diagram



Figure 72: Testing Hydraulic Coast Mode.



Figure 73: Coast Test Track

The line losses for all of the above modes were evaluated at the bicycles top speed, the losses are similar through all 4 of our modes with about 15 psi loss per solenoid, 8 psi loss from the check valve, and 0.2 psi of line loss. Table 15 tabulates the losses in each mode.

Table 15: Hydraulic Mode Losses (@ top speed)

<b>Mode</b>	<b>Pressure Loss (psi)</b>
Direct Drive	30.2
Discharge	30.2
Regen.	23.2
Coast	30.2

### 5.2.2 Solenoids

The NFPA sponsors a large list of hydraulic components manufactured by both Eaton and Sun Source. This list contains one Poppet-Type solenoid, manufactured by Eaton, the loss curve associated with the SBV1-10-C solenoid can be seen in Figure 74. Considering our maximum bicycle speed corresponds to a fluid flow rate of 2.7 gallons per minute and only 15 psi of loss we determined this solenoid is acceptable.

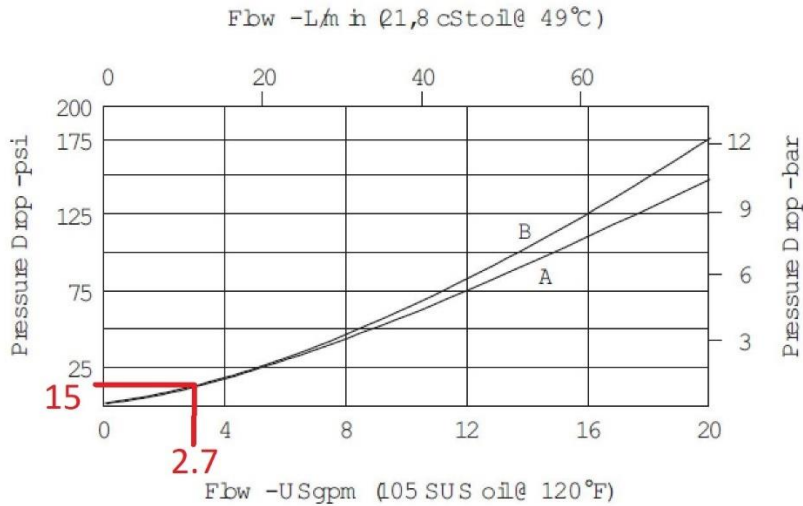


Figure 74: Eaton SBV1-10-C Solenoid Pressure Loss

The SBV1-10-C solenoid must be accompanied by a manufacturer specified line block that has multiple options for fitting style and size that can be seen in Figure 75. Both BSPP and SAE are compatible types of fitting styles for the acceptable line block, however the competition rules mandate that no pipe thread be use on high pressure side of the hydraulic circuit this disqualifies the use of BSPP fittings. Line loss between SAE 6 and 8 fittings are negligible, 0.0013 and 0.0006 psi/in respectively, and the line block weights are the same. The only discernable advantage of running the SAE 6 line is that we save about 1 pound of both line and fluid weight, this makes the SAE 6 size the prevailing option.

**6** Port Size

Code	Port Size	Housing Number	
		Aluminium	Steel
0	Cartridge only		
2G	1/4" BSPP	876702	02-175102
3G	3/8" BSPP	876703	02-175103
3B	3/8" BSPP	02-175462	-
6H	SAE 6	876700	-
6T	SAE 6	566151	02-175100
8H	SAE 8	876701	-
8T	SAE 8	-	02-175101

See section J for housing details.

**7** Voltage Rating

00 -	No coil	24A -	24VAC
12D -	12VDC	115A -	115VAC
24D -	24VDC	230A -	230VAC
36D -	36VDC	12B -	12VDC/w diode*
		24B -	24VDC/w diode*

\*Optional arc suppression diode.

Figure 75: SBV1-10-C Acceptable Line Block Options

Historically hydraulic lines are notoriously difficult to bend accurately, because of this we require a solenoid block mounting solution that is mobile. We will be clamping the solenoids and blocks in pairs to the rear of the bicycle frame as seen in Figure 76, the mounts will allow for rotation and translation of the components on the frame.



Figure 76: Hydraulic Mounting Position

The components will be mounted to the rear of the frame via a tapped aluminum plate shown in Figure 77. 0.375" aluminum sheet will be purchased from Online Metals and waterjet to the desired position with correctly sized and place mounting holes. Two Alan-head bolts accompanied by nylon-lock nuts will secure the line blocks to the mount, the mount will have ¼"-20 threaded holes that allow mounting to the frame. One half of a purchased shaft collar will accompany the mount and thread into the aluminum to tighten the mount on the frame rail while allowing for translation and rotation.

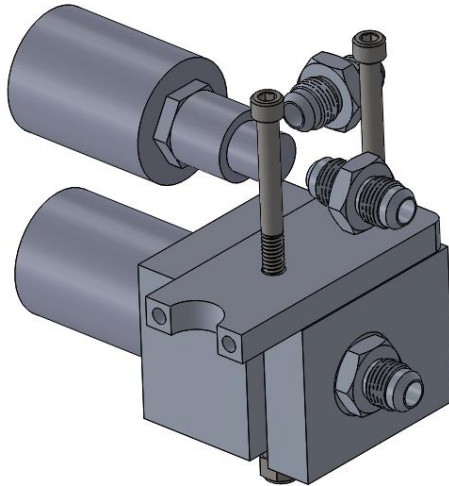


Figure 77: Solenoid Mounting Solution

### ***5.2.3 Manifold***

Once testing and verification of the hydraulic circuit has been completed, a single aluminum manifold block will be implemented. The block will contain all the solenoids and simplify the circuit to five ports. The check valve and accumulator pressure sensor will also be integrated into the block. The internal design can be seen in Figure 78 and all port locations are expanded upon in attachment 7. Although the new manifold will incur a similar level of losses, replacing the individual solenoid blocks will save approximately 2.5[lbs] in line and fluid weight.

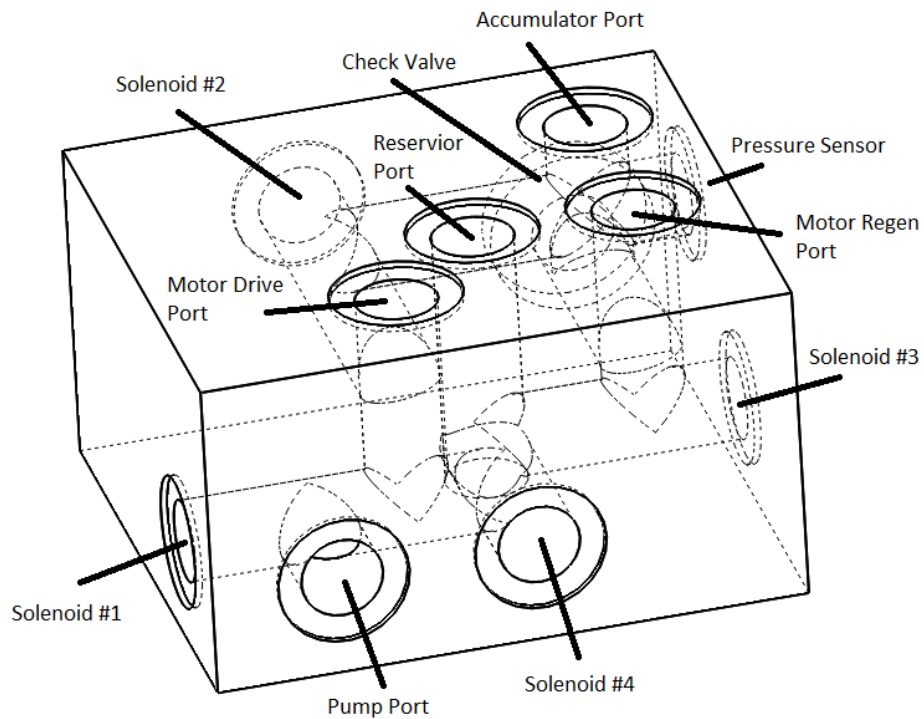


Figure 78. Representative wire frame of hydraulic manifold design showing internal features.

Holes will be tapped to the back of the manifold and a tube mount will be bolted on. The manifold will be mounted to the side of the bike on the seat stay to limit the length of lines to all components. See the mounting location and line placement in Figure 79 and mounting bracket in Figure 80.

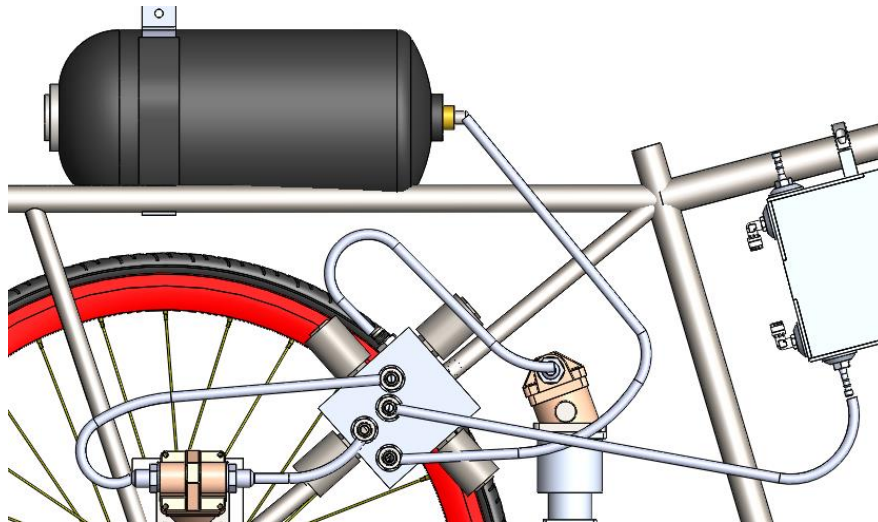


Figure 79. Line configuration of hydraulic manifold

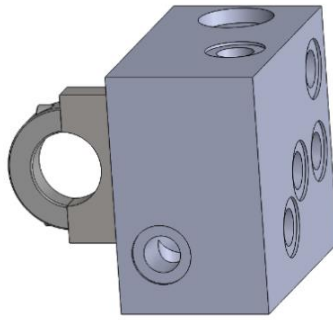


Figure 80. Hydraulic manifold mounting bracket.

The five line ports will be tapped for 6AN fitting along with the pressure sensor port which will use an adapter to allow 1/4" BSPP (Note that pipe thread is only allowed for small instrumentation on high pressure lines by competition rules). The solenoids will meet junctions at a depth of 0.75" whereas the check valve requires a depth of 0.61". This requires that the check valve port be counter bored for channel alignment. A sufficient portion of unused space is reserved for mounting the tube clamp to the block. At this point no dimensions are final until a technical advisor has reviewed the design.

#### 5.2.4 Accumulator

The hydraulic accumulator will be a 4[L] composite shelled bladder accumulator rated at 3000[psi]. The unit will be 6.5[in] in diameter, 15.7[in] long and weight 10.8[lbs]. The unit will be fixed in accumulator mounts which are bolted to tabs welded onto the tail of the frame as seen in Figure 81.

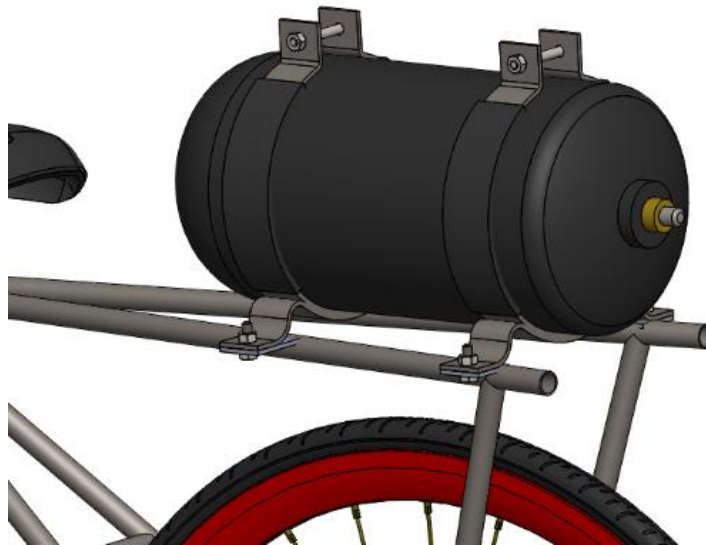


Figure 81. Mounting configuration of hydraulic accumulator.

This accumulator volume was chosen based upon the results produced from our Simscape accumulator discharge model. The model, described in more detail in section 5.7.2, predicts the



distance traveled, speed and efficiency challenge score with different accumulator sizes and pre-charge pressures. We initially swept through different accumulator sizes and completely discharged the accumulator then allowed the bike to coast to a stop using the hydraulic bypass circuit. This model predicted that larger accumulator sizes would reduce the efficiency challenge performance, see Figure 128, which seemed contrary to the previous year's competition results. Using a smaller accumulator compared to last year in theory should increase our efficiency score but at the cost of our sprint time. Increasing the accumulator volume would exceed our weight target, greatly modify our bike's packaging efficiency and reduce our efficiency score. In order to meet our weight goal and still achieve our efficiency score and sprint time requirements, we opted to switch to a PWM-like discharge. This modification would keep the bike at a certain speed range instead of fully discharging at once. The model was modified to discharge the accumulator up to 14[mph] then allow the bike to coast down to 9[mph] before discharging again and repeating until the accumulator was completely discharged. Completely discharging the accumulator led to an efficiency score of approximately 44, however, the model produced a efficiency score of 91 with the PWM-like control. See Figure 83 for the performance results of the 4[L] accumulator. This control allowed us to use a medium sized accumulator to keep sprint time low while allowing us to greatly increase our efficiency score. The speed at the upper bound of the discharge will be determined through a loss model which quantifies the relationship between pressure drop and speed gain. This speed is currently estimated to be approximately 10[mph]. The Patterson Control model has already indicated that the lower bound should not drop below 6.2[mph] in order to maintain bike stability.

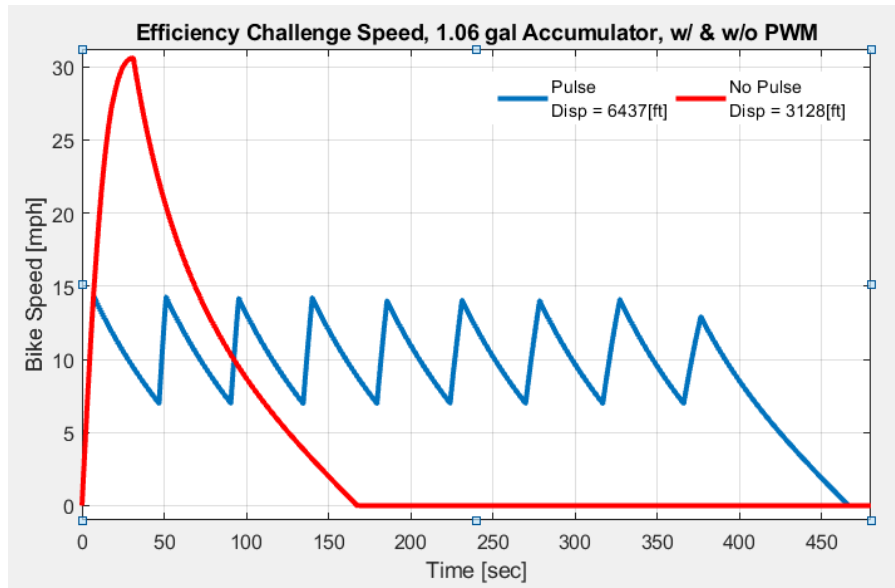


Figure 82. Pulsing discharge compared to complete discharge of the accumulator

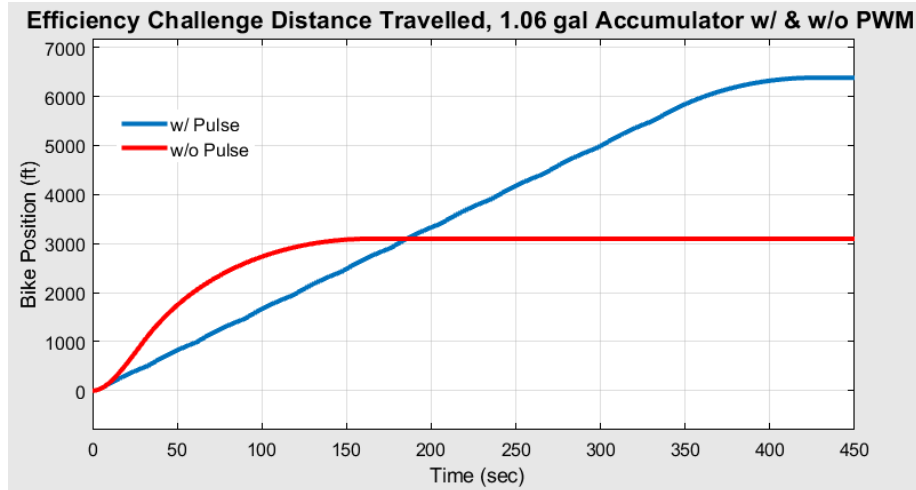


Figure 83. Distance traveled based on discharge technique.

During the sprint challenge the large accumulator will completely discharge resulting in a top speed of approximately 31[mph] and reaching 600[ft] around 21[sec]. Varying pre-charge pressures still need to be tested to achieve the lowest possible sprint time.

### 5.2.5 Pump/Motor

Based on exceptional performance during the endurance challenge, which relies solely on the pump and motor, the same unit will be implemented again. Its small profile and light weight also prove easy to integrate into the bikes packaging. Figure 84 displays the current pump. Mounting locations and coupling methods will be further developed in sections 5.3 Front Drive Train and 5.4 Rear Drive Train.

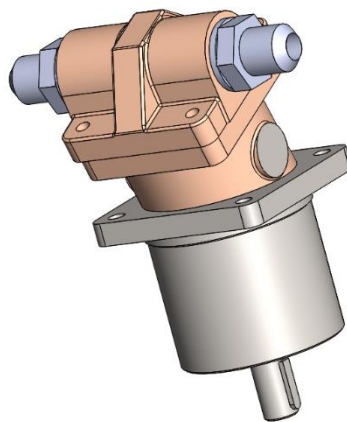


Figure 84. Bosh bent axis pump

### 5.2.6 Reservoir

The reservoir shown in Figure 85 will consist of seven 0.125” thick 6061-T6 aluminum sides that will be waterjet to incorporate locating ears to allow for accurate positioning relative to each other. The correct sides will also incorporate holes that position purchased aluminum weld bungs that

allow us to thread in the drain, fill, vent, and sight tube. Mounting is similar to that of the solenoids with a threaded aluminum mount that utilize one half of a purchase shaft collar to secure to the bicycle's top tube. The reservoir will have a capacity of 1.25 gallons to accommodate the full volume of fluid held in the accumulator after discharge, an additional 0.25 gallons of capacity is to ensure that during operation the hydraulic circuit doesn't ingest air.

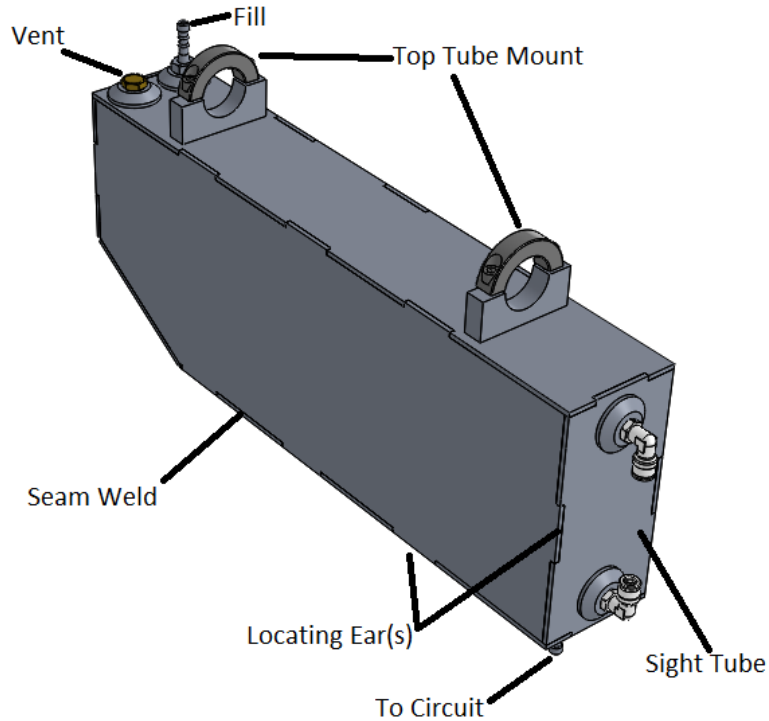


Figure 85: Reservoir

### 5.3 Front Drivetrain

The front drivetrain was a large area of focus for this year's FPVC design, as last year's front drivetrain exhibited some areas of concern. This year, the front drivetrain will consist of a chain and sprocket assembly at the pedals, the rear sprocket of which will be mounted to a planetary gearbox which will then be mounted to the pump. This drivetrain setup allows for improved packaging and weight reduction without sacrificing functionality. The overall front drivetrain assembly is shown in Figure 86, and is described in detail in the following subsections.

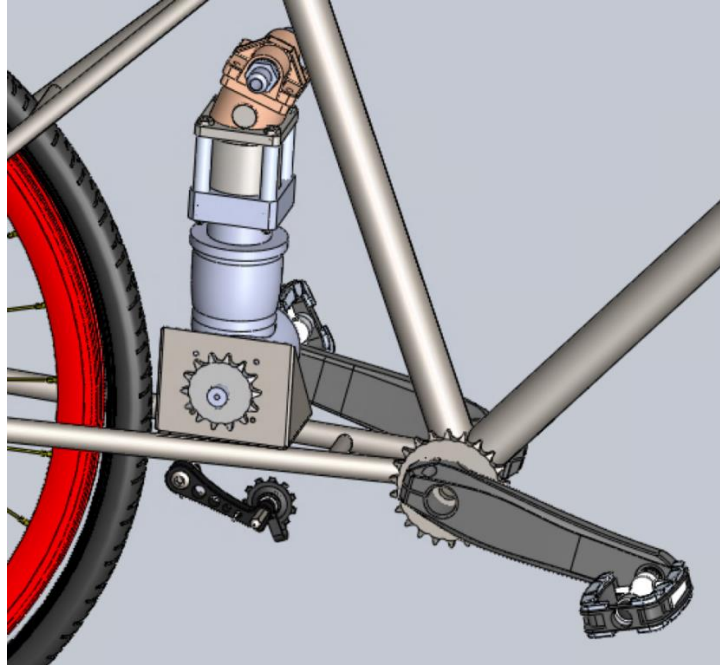


Figure 86. Front drivetrain assembly

### ***5.3.1 Chain and Sprockets***

As mentioned previously, The Incompressibles decided to stray from the previous bevel gear set used in last year's front drivetrain assembly. Instead, a chain and sprocket set will be implemented in order to reduce weight and allow for variable gearing. In order to determine the size of the crankset sprockets, it was first necessary to find the desired overall gear ratio for the front drivetrain. The Simscape direct drive model was used to conduct a gear ratio parametric study, ultimately giving mile time as a function of gear ratio as seen in Figure 87. The trend is seen to reach a minimum value of mile time below a gear ratio of  $(1/10.3):1$ , which is lower than last year's ratio of  $(1/15):1$ . However, after riding last year's bike, it was clear that pedaling up to speed and even at speed was quite difficult. Thus, The Incompressibles decided to use a ratio of  $(1/6.3):1$  to get the vehicle up to speed and switch over to  $(1/10.3):1$  once the bike was at steady state speed.

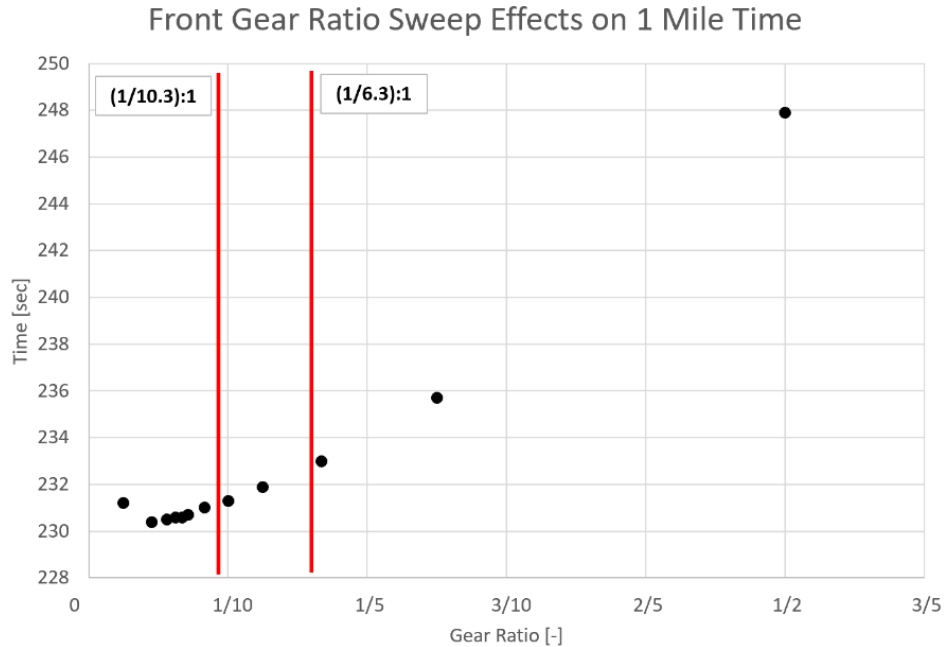


Figure 87. Single mile time sweep over different gear ratios for front drivetrain.

The crankset that was ultimately chosen to achieve the desired gear ratio was the Shimano Acera FC-M3000-B2, as previewed in Figure 88. This model has two chain rings, the larger having 36 teeth and the smaller having 22 teeth. Since there are many cranksets available, the initial scope was narrowed by deciding to use a square tapered bottom bracket, as recommended by Bike Builders, which requires a matching crankset. The model chosen was a BB-UN26 square tapered bottom bracket from Shimano. The following process to determine the exact crankset model was then iterative, as the rear sprocket and planetary gearbox sizes were also variable parts of the drivetrain. Ultimately, using a rear sprocket with 14 teeth and a planetary gearbox with a 4:1 ratio, the crankset was approved, achieving an overall front drivetrain ratio of (1/10.3):1 for the high gear chain ring. The overall ratio using the low gear chain ring is (1/6.3):1, which will ease pedaling up to speed.



Figure 88. Shimano Acera FC-M3000-B2 crankset & BB-UN26 square taper bottom bracket.

The chain and derailleur were selected by recommendation from Shimano for use on this particular crankset. The chain used will be the CN-HG93 Ultegra/XT, which will have to be shortened as the chain and sprocket assembly is much smaller than on a standard bicycle. The derailleur used is the M4020-M-B from Shimano. This derailleur is mounted via an adjustable clamp that mounts to the

seat tube and can easily be removed if the variable gearing is later abandoned. The SL-M3010-L-B Shimano Acera Mountain Bike Shifter will actuate the front derailleur.

A large concern in the chain and sprocket assembly design was determining a chain tensioning method. With the use of variable gearing, it is necessary to maintain chain tension at each gear. However, since this chain and sprocket assembly only incorporates variable gearing on the front chain rings, a standard rear derailleur—which also acts as a chain tensioner—would not be necessary. Thus, the Incompressibles decided to use a simple spring loaded chain tensioner to be mounted under the rear sprocket of the front drivetrain, as seen in Figure 89. The chain tensioner mounted via its M10x1.0 bolt into a machined aluminum tab mounted on the underside of the planetary gearbox mount. Because the chain tensioner will be fixed in the y-direction (SAE J670e coordinates), the chain will be at a slight angle with respect to the center line of the bike while engaged with one of the front chain rings, preferably the low gear chain ring. After observing the drivetrain of some standard bicycles while in use, it was clear that a slight angle of the chain does not drastically affect functionality, however it may slightly reduce efficiency. This reduction is tolerable since the chain will only be angled for a short period of time when in low gear.



Figure 89. Simple chain tensioner mounted on right chainstay.

As will be discussed further in the testing section, the chain tensioner that was initially selected did not allow for enough chain wrap around the rear sprocket while in low gear, thus it was necessary to reconsider this component. Ultimately, it was decided to instead use a dual jockey wheel chain tensioner, seen in Figure 90, which allowed for constant and sufficient chain wrap around the rear sprocket in both gears.



Figure 90. Dual jockey wheel chain tensioner to update previous single jockey wheel version

The final component of the chain and sprocket assembly is the rear sprocket that will be mounted on the planetary gearbox. As stated previously, this sprocket will have 14 teeth in order to achieve the desired overall gear ratio. To mount this sprocket to the planetary gearbox, it is necessary that it have a keyed hole to fit a shaft size of 16mm h6. Machinable bore sprockets are available through McMaster-Carr, although these sprockets are sized for ANSI roller chains only, not standard bicycle chains. Standard bicycle chains for use with derailleurs are  $\frac{1}{2}$ " in pitch and  $\frac{3}{32}$ " in inner width. ANSI 40 is the only size for  $\frac{1}{2}$ " pitch, but the chain inner width is  $\frac{5}{16}$ ". However, The Incompressibles were able to find an externally threaded freewheel shaft adapter, seen in Figure 91, which allowed the coupling of a standard fixie sprocket with the planetary gearbox shaft. The freewheel adapter also includes two set screws that will be used to secure its position on the planetary gearbox shaft.



Figure 91. Freewheel to Axle Adapter with Right Hand Threads for 5/8" Axle from [electricscooterparts.com](http://electricscooterparts.com)

### 5.3.2 Planetary Gearbox

One of the large purchases with this year's fluid powered vehicle was a new planetary gearbox. The Incompressibles decided a new, right-angle, planetary gearbox was necessary in order to improve the packaging of components for the desired chain and sprocket assembly. As seen in Figure 92, the right-angle planetary gearbox allows the pump to be placed vertically in the rear triangle of the bicycle frame, rather than protruding out laterally.

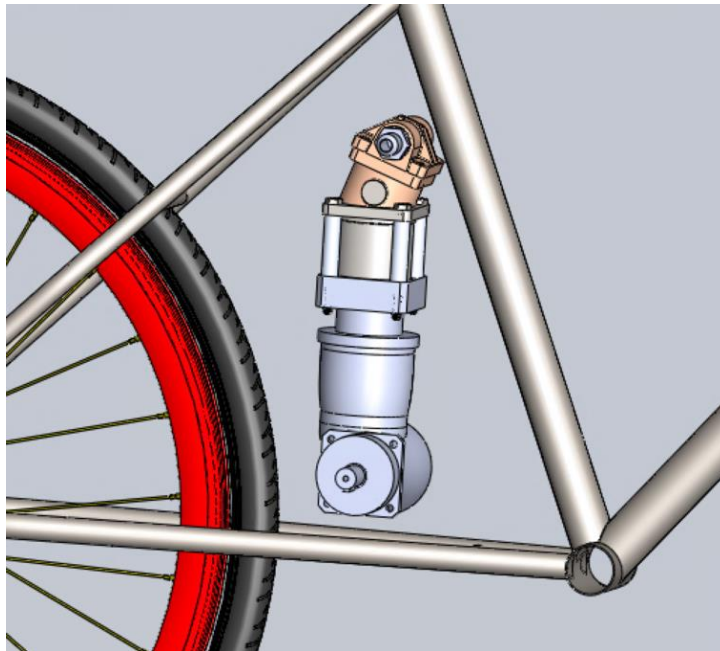


Figure 92. Planetary gearbox and pump orientation on bicycle

The gearbox initially selected for this year's bike was the Neugart WPLPE 50, as opposed to last year's Harmonic Drive HPG-14A. Figure 93 highlights some of the component specifications that were of interest while selecting a new planetary gearbox. Apart from allowing the improved packaging of drivetrain components, the WPLPE 50 is both lighter and smaller than the HPG-14A. Additionally, Neugart provides a compact shaft coupler that will enable the pump and gearbox to interact without taking up much extra space. This would be a large improvement to last year's shaft coupler, which was unnecessarily oversized.

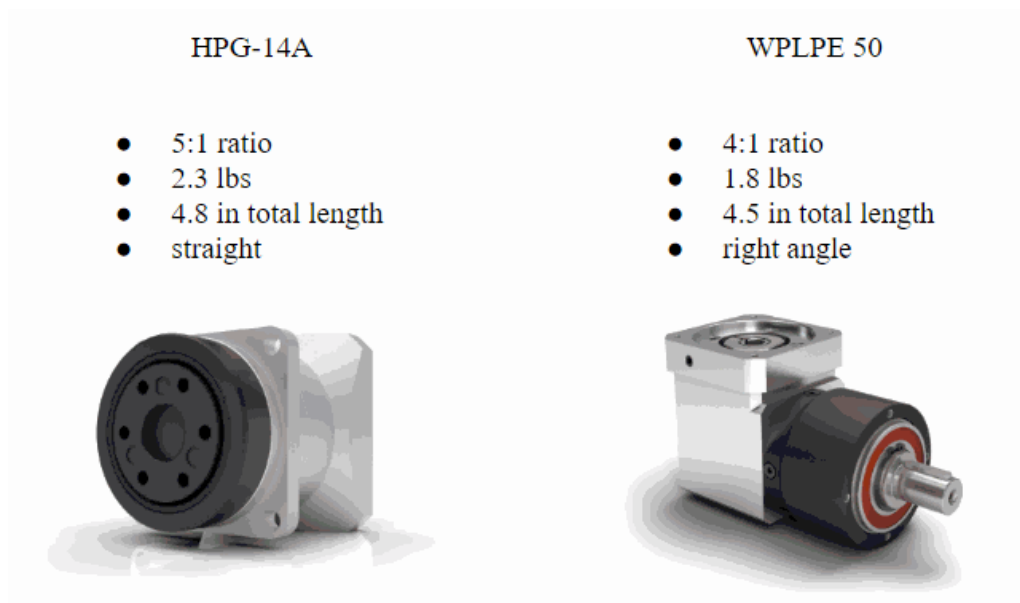


Figure 93. Comparison of previous and current planetary gearbox models.



At the Incompressible's critical design review, Dr. Widmann suggested that the rated overhanging load on the Neugart gearbox shaft be checked to ensure that the bearings could sustain the maximum operating load introduced by the rider. After performing simple load analysis, it was determined that the Neugart gearbox would not accommodate the maximum radial load applied on its shaft from the chain. This radial load was calculated using the weight of the heaviest rider applied to one pedal in the high gear, which could theoretically be seen while pedaling from a dead stop. To solve this issue, it was decided to use another gearbox with a rated overhanging load that sufficiently exceeded the theoretical maximum radial load that the gearbox shaft would see. The gearbox ultimately chosen was the KF060-004-S2 from Apex Dynamics, shown in Figure 94, which has a 4:1 ratio, weighs 7 lbf, and is 5.3 in in length. Although this gearbox is larger and heavier than desired, it was ultimately necessary to accommodate the front drivetrain packaging design. Apex Dynamics also provided a customer mounting plate allowing the direct attachment of the pump without additional coupling components.



Figure 94. KF060-004-S2 planetary gearbox from Apex Dynamics.

### ***5.3.3 Mounting***

The mount for the planetary gearbox consisted of two pieces. The first piece was an L-bracket made from folded 0.063" steel sheet metal. The second piece was a flat cutout of 0.063" steel sheet metal that was welded atop the chain stay tubes, between the crankset and the rear wheel. The L-bracket was bolted to the flat cutout, and the planetary gearbox was bolted to the L-bracket. Finally, the pump was mounted directly to the planetary gearbox via a custom mounting plate provided by Apex Dynamics. The patterns for both mount components were cut using a waterjet, which will be discussed further in the manufacturing section. Both the flat and folded mount pieces may be seen in Figure 95.

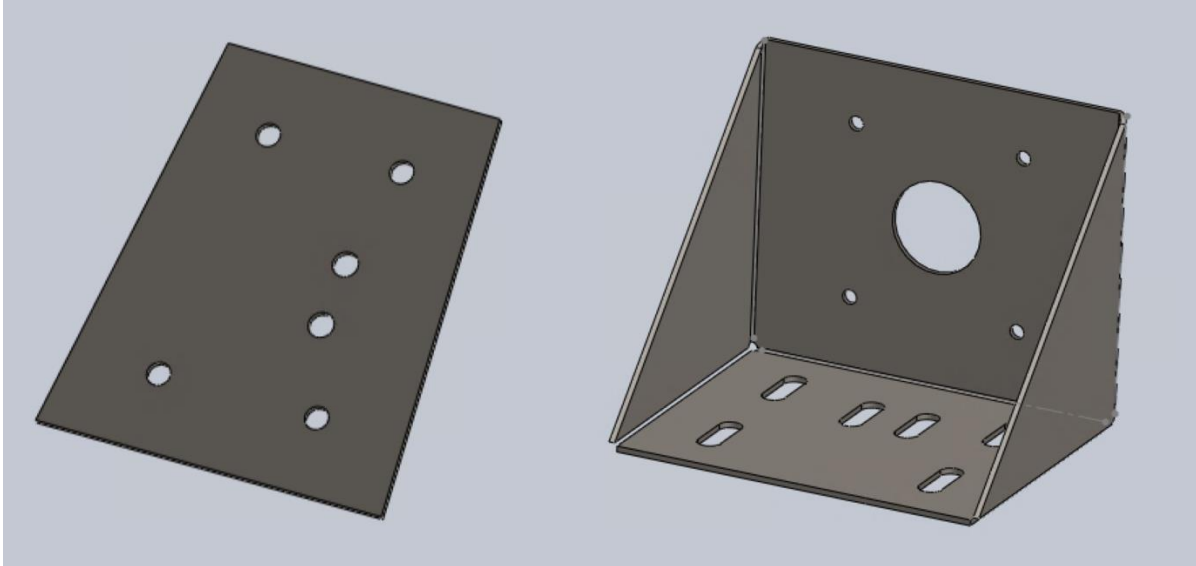


Figure 95. Front drivetrain mounting bracket.

## 5.4 Rear Drivetrain

The final design of the rear drivetrain this year was a chain driven sprocket from the rear pump to the rear wheel. The rear wheel was a standard fixie 700c x 32c with a machinable bore sprocket from McMaster adapted to fit onto the threads of the fixie wheel. The motor and sprocket is bolted onto the frame at a welded plate, located between the rear vertical support tube and the seat stay (on the right hand side of the rider). This whole assembly can be viewed below in Figure 96. The rear drivetrain is one of the largest changes to the bike from last year, specifically with the removal of a rear mechanical clutch, instead choosing to use a hydraulic coast mode.

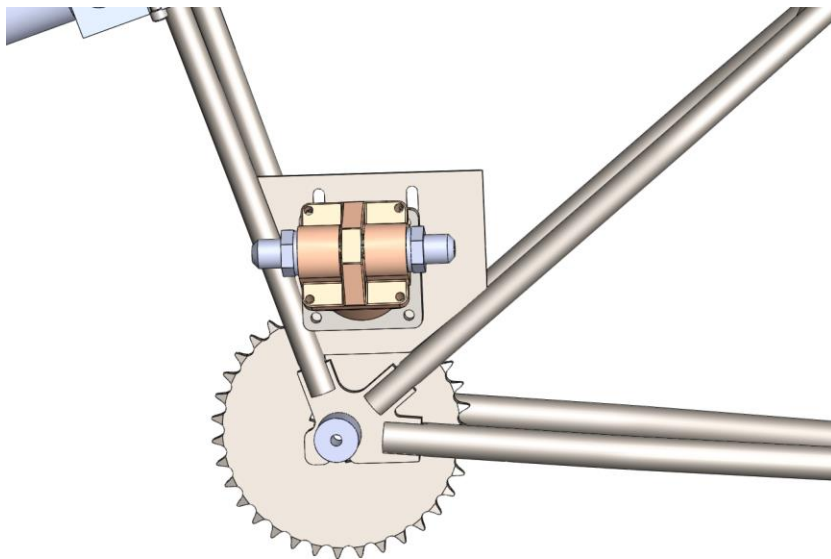


Figure 96. Rear drivetrain assembly

### 5.4.1 Mounting

To mount the motor and the sprockets to the bike frame a simple single shear plate is welded between the seat stay and rear vertical support tube. Adjustments were made to the position of the seat stay and vertical support tube, such that they are both more vertical (flat with the XY plane). This was done by adding a single bend to both of the tubes, using a bending die. The single shear mount will be 0.1” thick and this was determined using stress analysis (see analysis section).

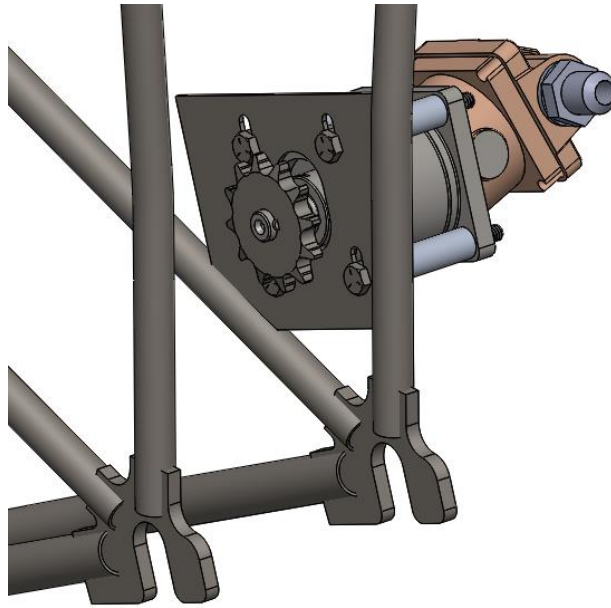


Figure 97. Rear drivetrain mounted to the back of the bike

### 5.4.2 Sprockets

The sprockets selected are sprockets purchased from McMaster with the internal bore adjusted for the mounting mechanism. The motor sprocket required a keyway broached into the ID of the gear, while the wheel sprocket required threading such to mount on to threading on the fixie wheel. The Sprocket attached to the motor is a 13-tooth sprocket while the one connected to the wheel is a 35 tooth sprocket. An ANSI 40 roller chain was used to transfer the torque between the sprockets.

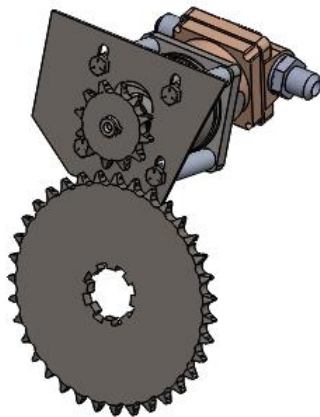


Figure 98. Rear Drivetrain with frame hidden

### 5.4.3 Analysis

#### 5.4.3.1 Drivetrain Ratio

The most important question when it came to the rear drivetrain design was finding the best gear ratio. In order to determine this sizing, we utilized the Simscape direct drive model to perform a parametric study. We used the model to find the amount of time that it would take for the bike to complete a single mile in a straight line at different gear ratios with a constant power input. The results from this sweep and can be seen in Figure 99.

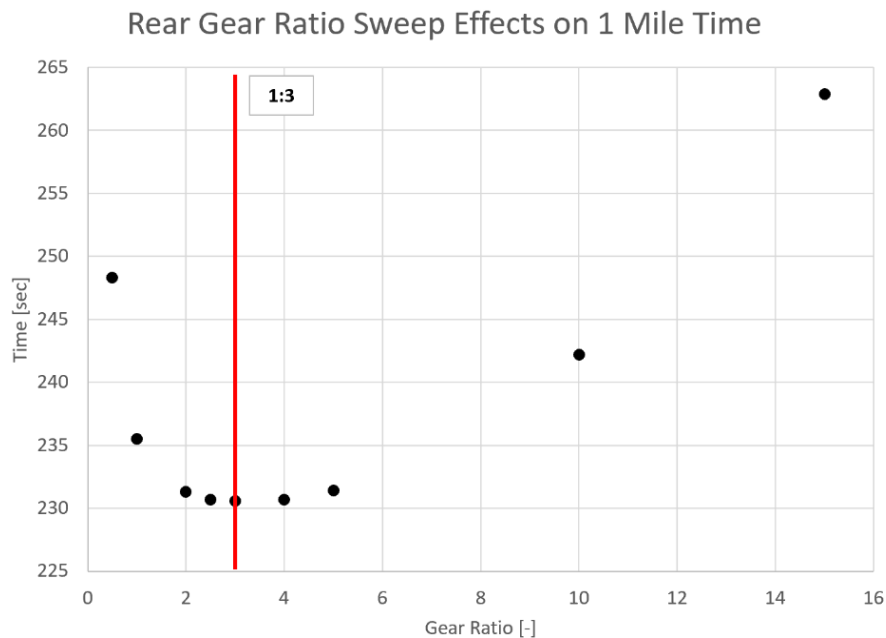


Figure 99. Single mile time sweep over different gear ratios for rear drive train

The sweep showed a clear local minimum that developed at a gear ratio of 1:3, meaning that at a rear gear ratio of 1:3 we would have the fastest single mile time. This result make sense due to the increase in efficiency at higher motor speeds. With this result it was only a matter of finding sprockets that match this ratio. For more details about selected sprockets see section 5.4.3 Sprockets.

#### 5.4.3.2 Stress analysis

To find the thickness of the plate used for the rear drivetrain mounting, we used stress analysis of a worst-case scenario situation. The first step was to find the load that would normally be placed into the sprockets and the mounting plate. The peak load case for this was determined to be during the initial acceleration of the bike from stand still. Using the Simscape model talked about earlier in the report. This torque was 53 ft-lbs at the rear axle. In order to get the force applied we did a simple torque calculation with the radius of our sprocket. This intail FBD can be seen in Figure 100. Driving force on rear drive train sprockets.

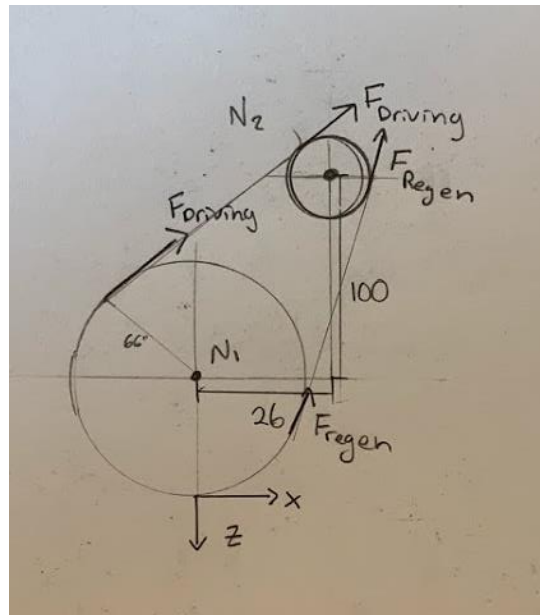


Figure 100. Driving force on rear drive train sprockets

With these forces defined at the sprockets this information was then translated into a shear force applied at the center of the mounting face, a torque in the Y axis and a moment about the X axis. These loads can be seen summarized in Table 16. Rear drivetrain load.

Table 16. Rear drivetrain loads into mounting plate

Load	Amount	Units
Fz	113.99	lbs
Fx	-113.99	lbs
Mx	128.00	in-lb
Ty	235.20	in-lb
Mz	128.00	in-lb

With these loads defined the factor of safety was determined in the plate with a simplified model. The assumption made was that all of these loads were applied at the center of the mount, and the mount was rigidly mounted at the bottom of the plate to the frame. This produced a FOS of 3.1 with the combined loading case. This loading case can be seen in Figure 101. Rear drivetrain mount with loads applied

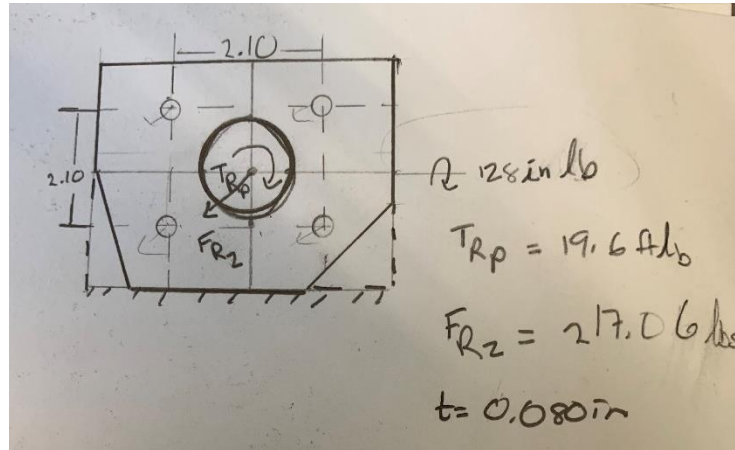


Figure 101. Rear drivetrain mount with loads applied

With this load case established a more complicated loading case was designed for the plate utilizing solid works FEA. For this case the mount would be fixed at both welding faces. The torque of the motor would all be placed at two of the bolt holes. Simulation a loose bolted connection (shear pins instead of a friction contact). It is important to note that this model is not completely indicative of how the plate will act in real life. It is rough approximation of the strength of the member, and for this reason a large factor of safety was required. The final FOS was 3.01 with 4130 steel, and can be seen in Figure 102. Solidworks FEA for rear drivetrain mount.

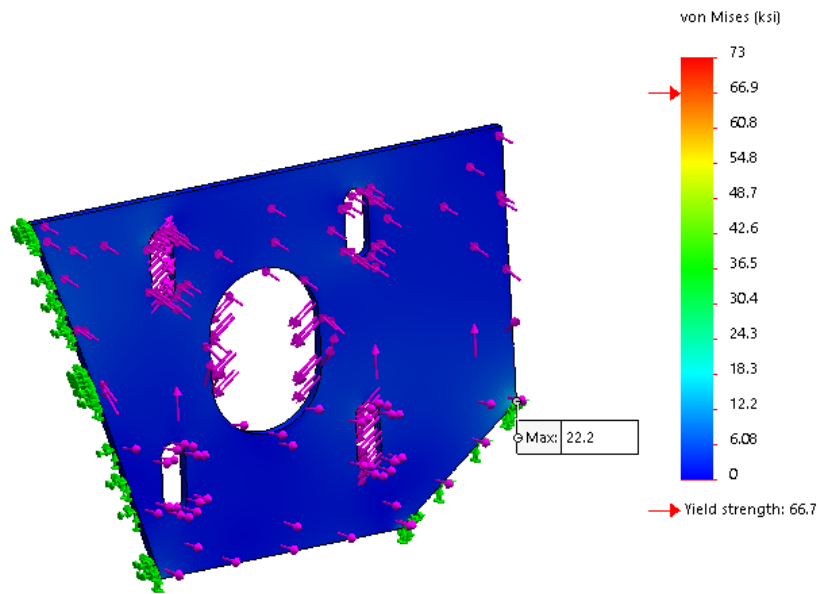


Figure 102. Solidworks FEA for rear drivetrain mount

## 5.5 Mechatronics

### 5.5.1 Functionality

The mechatronics system will allow for selection of the drive mode and the display of relevant metrics to the rider with a low latency. It is our intent to measure bike velocity, pedaling cadence, accumulator pressure, and line pressure. A microcontroller will gather data from various sensors and inputs, analyze the information, and display selected values on a LCD screen. Shown below is a simple schematic of the mechatronics circuit.

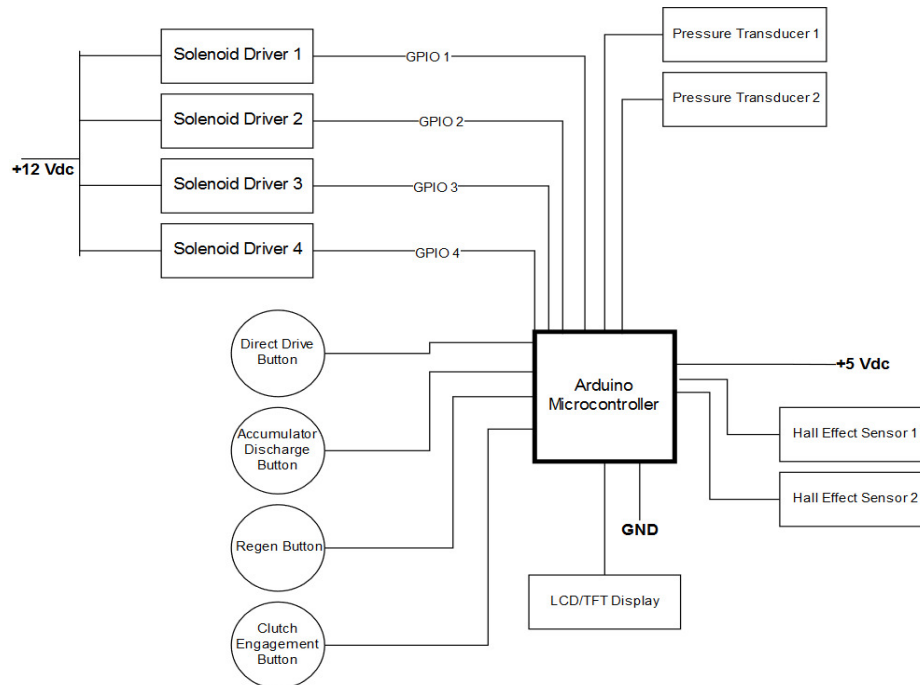


Figure 103. Mechatronics Circuit Layout

### 5.5.2 Platform

The Mechatronics system this year will be run on an Arduino platform. As discussed in the Background, last year's team opted to design their own circuit board as part of the ME 507 project. This approach ended up being very complicated and resulted in the team not having a functional display or sensors at competition. In contrast to a bespoke circuit board, the Arduino environment is accessible and easy to prototype with. Being an open-source project, Arduino has many integrated libraries that greatly simplify certain programming tasks such as writing values to a LCD display. These libraries make it possible to purchase compatible hardware that can be integrated very easily. The specific microcontroller chosen was the Arduino Uno R3. This is an inexpensive, entry level board that features sufficient I/O and is fast enough for our purposes.

### 5.5.3 Components

There are a number of hardware components that will be necessary to accomplish the intended system functionality. The heart of the system is the aforementioned Arduino Uno R3 and peripheral components include:

#### 5.5.3.1 Display

The display chosen was a 2.8 TFT LCD screen. This display is inexpensive and is the perfect size for our application. The display also features an SPI peripheral interface which allows connectivity using only four wires instead of the usual eight for a parallel LCD interface. Additionally, this display is compatible with the ILI9341 Adafruit LCD library. This will allow us to write text to the display without having to write tedious code that would be otherwise necessary.





Figure 104. 2.8” LCD Screen

### 5.5.3.2 Buttons

Drive-mode selection will be accomplished through the pressing of buttons. Currently there are four drive modes and the intent is to have one button assigned per mode. The buttons are momentary switches, meaning that they can be configured to select a drive mode either by pressing the button, or by having to hold it.



Figure 105. Momentary Button

### 5.5.3.3 Pressure Transducer

A transducer will be necessary to measure both accumulator and line pressure. The accumulator pressure will reach up to 3000psi and requires a specialty sensor. Appropriately, we have chosen a 3000psi/5V transducer from Honeywell. This sensor features an accuracy of 0.25%, which corresponds to approximately 7.5psi. This resolution is very much adequate for the application. It is also important to note that this component is \$125.00 and the largest expense of the mechatronics subsystem. The line pressure measurement will be taken between the pump and the motor and will tell us the pressure that the pump produces during direct drive operation. This pressure is calculated to be low (<150 psi), and therefore, this transducer will be a less expensive, lower pressure model.



Figure 106. 3000psi Pressure Transducer

#### 5.5.3.4 Speed Sensor

Bike velocity and pedal cadence will both be measured using Hall Effect sensors. These sensors consist of a transducer that varies its output voltage in response to a magnetic field. The sensors will be mounted on the front fork and down tube respectively. Then, a magnet can be mounted on the rotating component (wheel and crank), and the sensor will output a signal every rotation of the magnet. This will give the angular velocity of the wheel and crank, and can be used to calculate velocity.

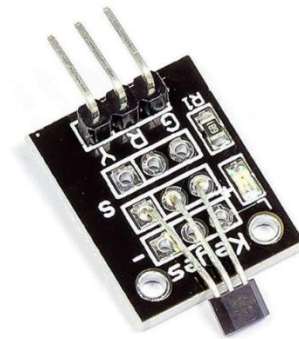


Figure 107. Hall Effect Sensor

#### 5.5.3.5 Solenoid Driver

Arguably the most vital function of the mechatronics system will be to actuate the solenoids that control the hydraulic circuit. These solenoids are 12V/2A coils that sit inside and regulate a poppet valve. This power draw is too high for the Arduino to supply and must therefore be powered by an external battery. As a result, some type of transistor circuit will be necessary to power the solenoids on and off. We've decided to go with the ULN2803 Darlington Transistor Arrays. These chips are rated for 4 amps each and include open-collectors/freewheeling clamp diodes for transient suppression. This is necessary to account for the back EMF generated by electromagnets such as solenoids. The drivers have eight total outputs, but because they are only rated for 4 Amps, we will need to use two of them.



Figure 108. Solenoid Driver IC

#### 5.5.3.6 Battery

We have chosen to go with a 12V/10000mAh rechargeable battery pack. This is an identical battery pack to last year's, with the exception of having a slightly larger capacity. The 12 Volts will be perfect for running the solenoids, and a linear voltage regulator can be attached in order to also power the Arduino. Calculations indicate that, assuming all solenoids are powered on the entire time, the battery will last for a full hour. The peak discharge rating of 5 Amps is also within specification.



Figure 109. 12V/10000mAh Battery

### **5.5.4 Packaging**

The entirety of the mechatronics system will be attached to the bike using 3D printed parts.

#### 5.5.4.1 Button Enclosure

The buttons will be mounted in their own housings. These housings fit two buttons, and there will be a housing on either side of the handlebars. The buttons will be located just inward from the grips and will be operable using your thumbs. The housing is attached to the handlebars by means of zip ties that thread through the included grooves. This method of attachment is lightweight and very adaptable.

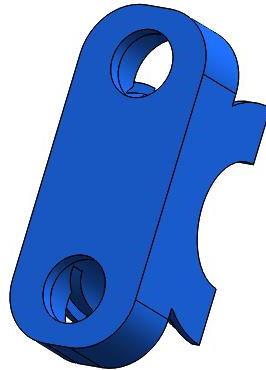


Figure 110. Button Enclosure

#### 5.5.4.2 Display Enclosure

The main enclosure for the mechatronics system will sit on the handlebars directly facing the rider. This enclosure will house the display, controller, and necessary circuitry to interface components. The enclosure will sit contacting the handlebars and stem, and will also be attached using zip ties.

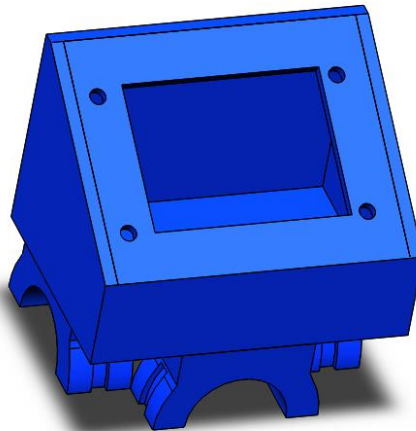


Figure 111. Display Enclosure

#### 5.5.4.3 Packaging Proof of Concept

Here is a picture showing the printed parts mounted on a set of standard mountain bike handlebars. The parts fit well and are held securely into place by the zip ties. The size and positioning are very representative of the final product and show that the 3D printed components will easily be able to integrate with bike.



Figure 112. Mechatronics Mounted on Test Bike

### ***5.5.5 Current Design Progress***

Many of the components have already been received, and work on a preliminary circuit has begun. The current circuit and display progress can be seen below.

#### **5.5.5.1 Circuit**

The entire mechatronics system as it currently stands is shown below. The circuit is mounted on a breadboard with all the testing components attached. The LED's represent the four solenoids and light up to correctly show which solenoids would be powered in each drive mode. The buttons allow selection of the drive mode, and the Hall Effect sensor can detect the speed at which a magnet is waved in front of it. The pressure transducer (3000psi ) was also connected and is operational.

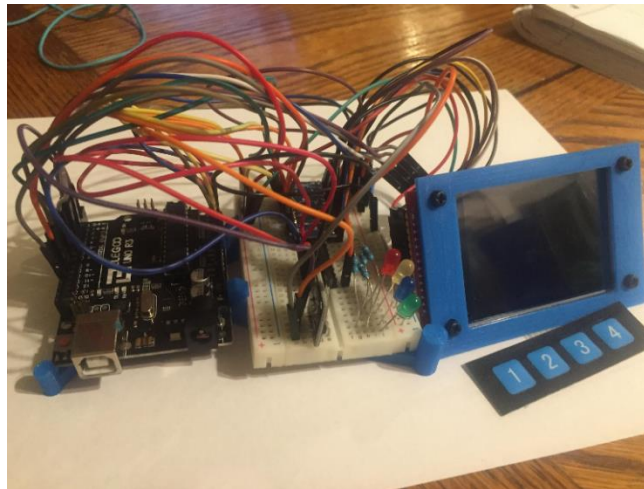


Figure 113. Breadboard Prototype Circuit

#### **5.5.5.2 Software**

The entirety of the code is written in C++ using the Arduino IDE and a handful of downloaded libraries. The full, commented code can be seen in the Appendix in Attachment 5.

### 5.5.5.3 Display Functionality

The display is also coming along nicely. It currently displays the selected drive mode, has a tachometer, and can display the max speed. All the critical features of the display have been programmed and it is ready for the final rendition. The only thing remaining is to decide on a layout and mess around with formatting of the different elements.

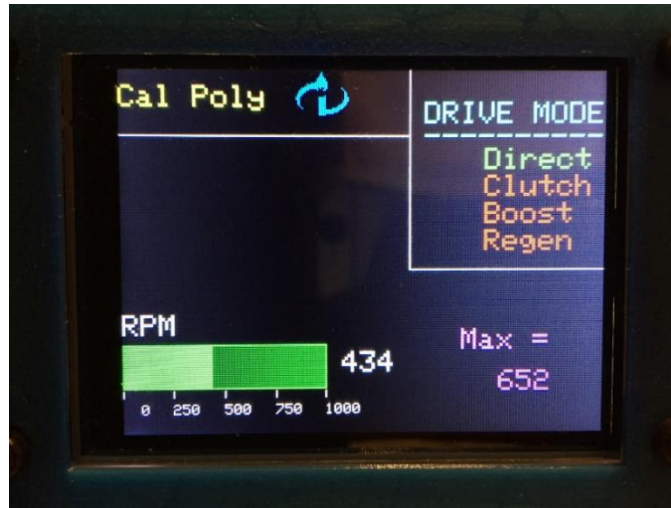


Figure 114. Display Functionality

## ***5.5.6 Final Design Plan***

### 5.5.6.1 Hardware

The current circuit is mounted on a breadboard and takes up a lot of space. A major reason for this is the use of a breadboard and the multitude of wires that go along with it. In order to save space, we must make some changes to the hardware.

First, the Arduino Uno will be replaced by an Arduino Pro Micro. This is a more powerful, but much smaller microcontroller that the same functionality and compatibility as the Uno.

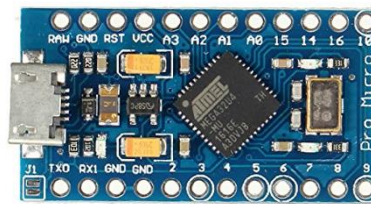


Figure 115. Arduino Pro Micro

By switching to a smaller microcontroller that does not have female pin headers, we are free to design our new circuit on a prototype board. This board will house all the components, have a

small profile, and won't need any bulky wires. Shown on the left is an example prototype board with an Arduino Nano, and shown on the right is the bottom side of a properly soldered prototype board.

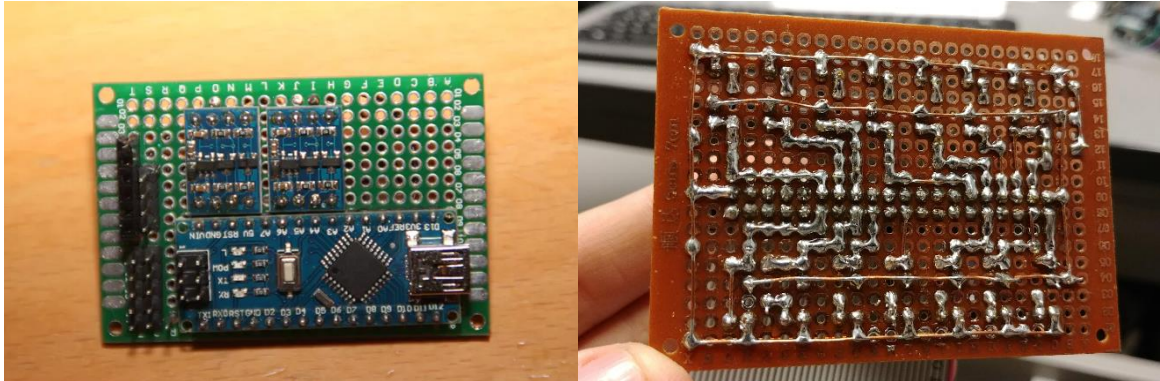


Figure 116. Example of a Finished Perfboard

#### 5.5.6.2 Software

The majority of the software has already been written. The major addition to the code will be support for a PWM discharge mode. This will allow pulsed discharge of the accumulator at an optimized rate in order to greatly increase accumulator efficiency. Some smaller changes will be finalizing display formatting and implementing a voltage to pressure conversion for the transducer.

#### ***5.5.7 Final Design Prototype***

As intended in the final design plan, a new circuit was designed and soldered onto a prototype board.

##### 5.5.7.1 Solenoid Driver

During testing of the breadboard circuit, it was found that the chosen solenoid drivers – the uln2003 – were not powerful enough to actuate the 2.5 Amp poppet type solenoids. A new solenoid driver was designed that would be able to handle much larger current loads. The driver consisted of a logic level, N-type, power MOSFET and a Schottky flyback diode.

##### 5.5.7.2 Microcontroller

A new, smaller microcontroller was chosen to replace the original Arduino Uno board. This new controller was the Node MCU 32-S. This board featured a 32-bit processor with Wi-fi and Bluetooth capabilities.

### 5.5.7.3 Packaging

The new development board, solenoid driver circuits, and screw terminals were soldered together onto a prototype board. This design was very compact and robust compared to the breadboard circuit.

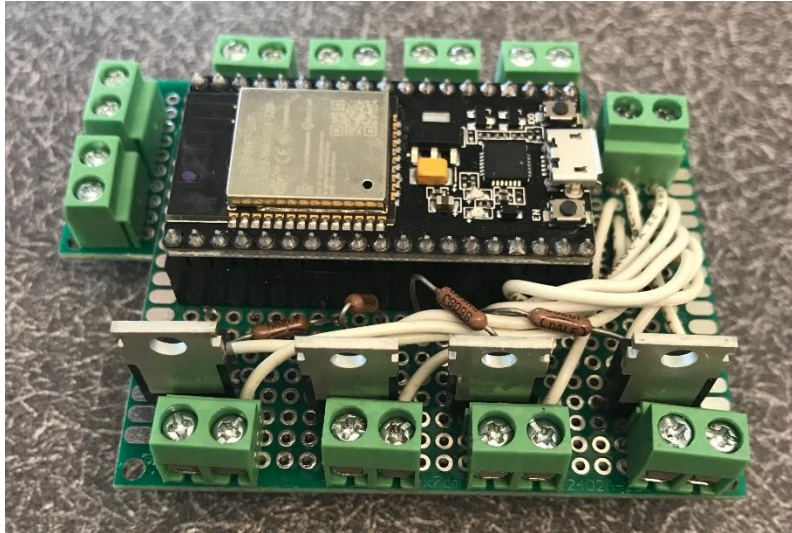


Figure 117. Final Design Prototype on Perf-Board

### 5.5.7.2 Software

Most of the code remained the same, with the only addition being Bluetooth control. An Android app was developed that allowed manipulation of the drive modes, display of speed and pressure, and data logging.

### ***5.5.8 Actual Final Design***

The final design prototype did not operate as desired due to unforeseen complications, so it was decided to design a printed circuit board with new, surface-mount, solenoid drivers. The new development board, the Node MCU, was also replaced with an Arduino Nano.

#### 5.5.8.1 Solenoid Driver

The new solenoid drivers chosen were the Texas Instruments DRV-103H. These were surface-mount, 3 Amp drivers with an automatic current limiting feature. They could provide an initial starting current to actuate the solenoid, then lowering the current to a minimum holding value through PWM in order to save power.

#### 5.5.8.2 Microcontroller

The Arduino Nano was chosen to replace the Node MCU-32S from the final design prototype. It was found that the MCU board did not operate correctly from battery power, whereas the more robust Arduino Nano did. Another reason for replacing the microcontroller was the lack of an



existing Eagle footprint and schematic for the MCU. Ultimately the result of this change was the loss of Bluetooth capability and the associated data logging functionality. This was an acceptable tradeoff for reliable performance.

### 5.5.8.3 Printed Circuit Board

The new solenoid drivers, being surface mounted components, necessitated the switch from perf-board to a printed circuit board. A PCB was designed using the Autodesk Eagle software and was manufactured by JLCPCB. The board layout can be seen below.

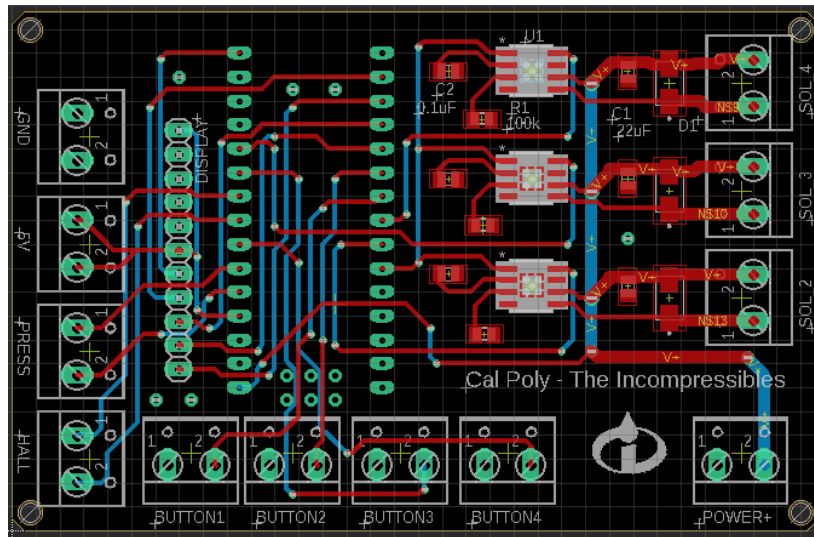


Figure 118. Printed Circuit Board Layout

## 5.7 Modeling

### 5.7.1 Direct Drive Model

Further refinements were made to earlier revision of the Simscape direct drive model such as: accounting for the cyclic torque application from the rider, adding finer efficiency tables for the Bosch bent axis pump and motor, adding aero drag, and incorporating weight transfer effects to the bike. Figure 119 shows an overview of the direct drive model, with rider power being the input and bike velocity as the output.

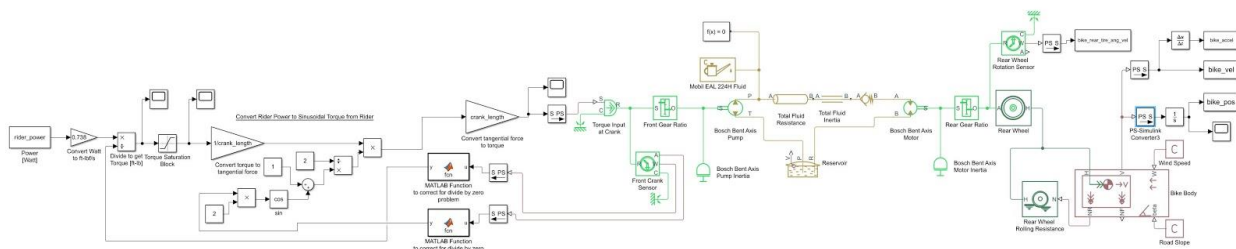


Figure 119. Overview of Simscape direct drive model

The input into the model is constant rider power, but due to the cyclic motion of the pedal crank, torque is applied through the crank in a cyclic motion. Constant power is converted to torque by dividing by angular velocity of the crank, then converted to a normal force on the crank arm. This value is modified to represent sinusoidal force application through each crank arm and converted back to torque. The sinusoidal torque conversion, Figure 120, was taken from Jason Thomas Parks' master's thesis where he simulated the riding motion of a bicycle using Simulink.

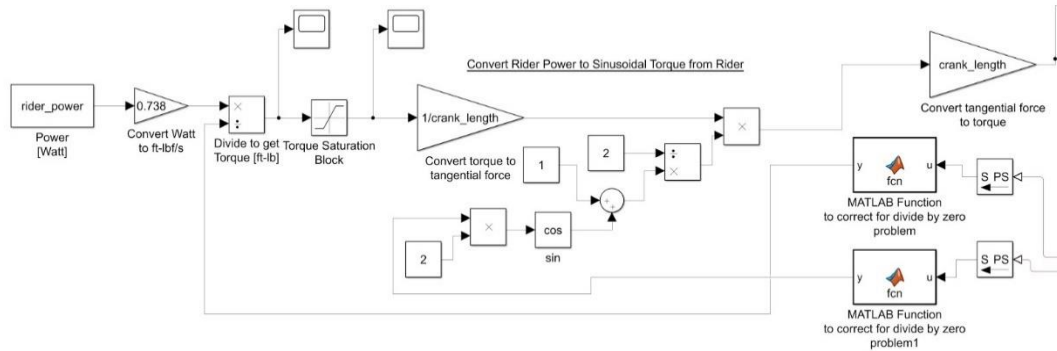


Figure 120. First portion of direct drive model showing cyclic pedal force conversion

The sinusoidal torque is inputted through the pump, lines and motor to the rear wheel. The addition of the vehicle body block in Simscape allows for wind speed and road slope inputs while accounting for aero drag and longitudinal load transfer.

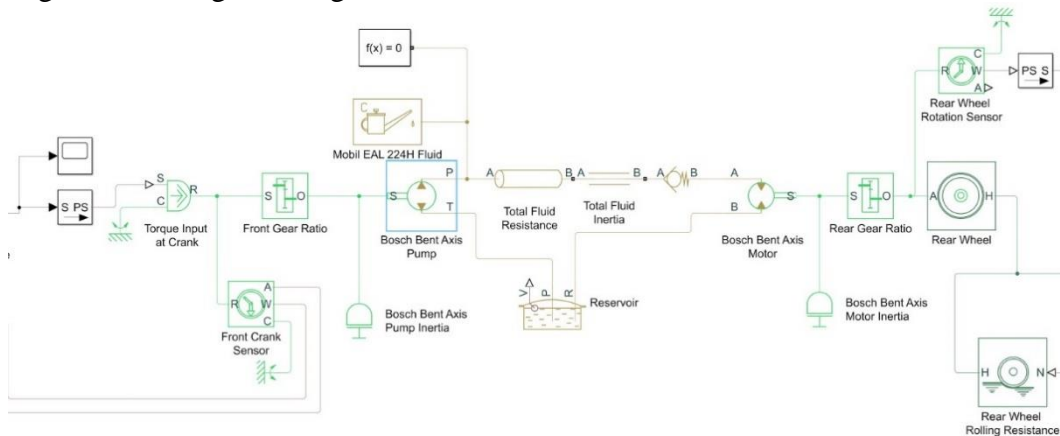


Figure 121. Close up view of motor to pump portion of direct drive model

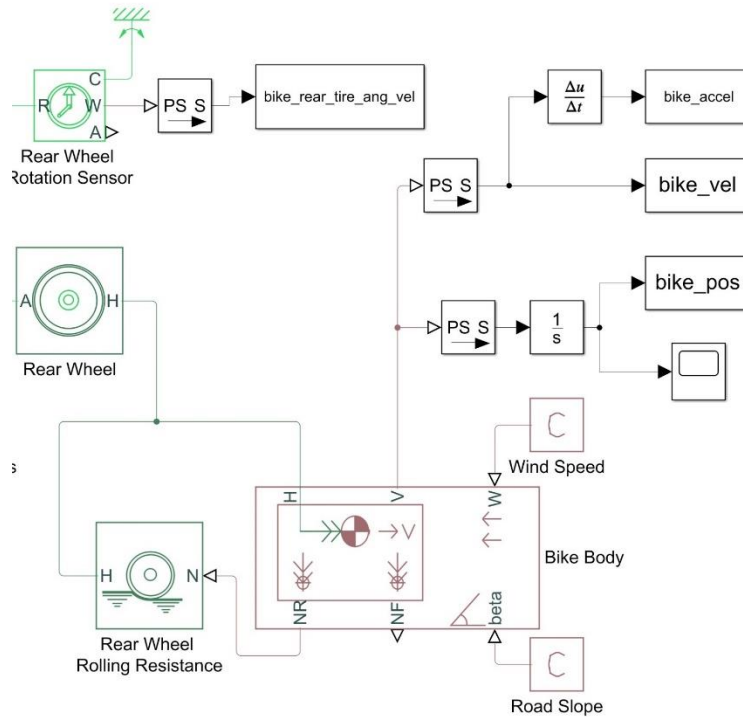


Figure 122. Close up view of vehicle body block and outputs to workspace of direct drive model

The final direct drive model was validated against the previous year's Simulink model using the same input parameters to make sure the Simscape model functioned properly. The Simscape model was determined valid compared to the Simulink model as it had a 1.43% difference in distance traveled and a 2.48% difference in steady state speed.

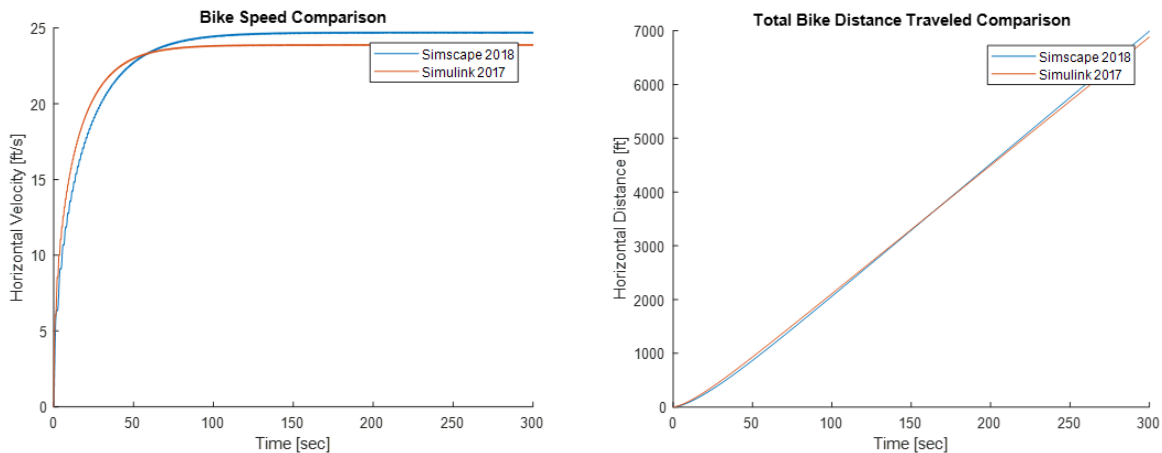


Figure 123. Bike speed and distance traveled comparison between the 2018 Simscape and 2017 Simulink direct drive models

After validating the model to last year's, front and rear gear ratio sweeps were performed and plotted against the time to travel one mile, refer to Figure 87 and Figure 99, to determine the set of gear ratios which gave the lowest time to mile. From the sweeps, a gear ratio of 10.3:1 and 6.3:1 were selected for the front and a 3:1 was selected for the rear. These gear ratios were inputted into the direct drive model and produced the following results shown in Figure 124 and Table 17. These

gear ratios gave a final time to mile of 3 minutes 46 seconds which exceeded our 4 minute requirement.

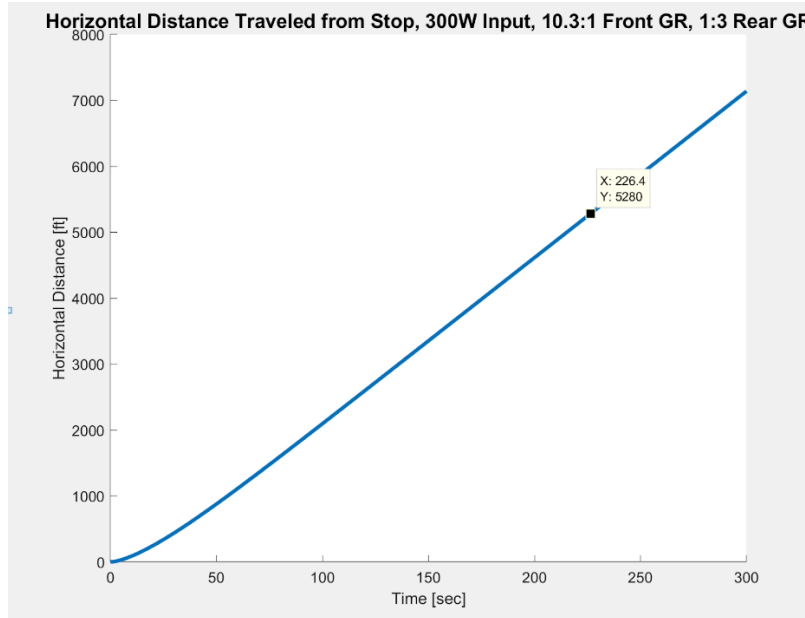


Figure 124. Horizontal distance traveled from stop with a 300W input, 10.3:1 front GR, 1:3 rear GR using Simscape direct drive model

Table 17. Summary table of above analysis with major inputs and outputs with Simscape direct drive model

Model Inputs/Outputs	Value
Power Input	300 Watts
Total Weight	256 lb
<b>Front Gear Ratio</b>	<b>10.3:1</b>
Rear Gear Ratio	1:3
<b>Peak Pedal Torque</b>	<b>192.8 ft-lbf</b>
Steady-State Average Cadence	67.5 rpm
Steady-State Max Pedal Torque	30.3 ft-lbf
Steady State Speed	17.2 mph
<b>Time to Mile</b>	<b>3 minutes 46 seconds</b>

Although the 10.3:1 front gear ratio and 1:3 rear gear ratio combination exceeds our time to mile requirement, there is an excessive amount of initial pedal torque, 193 ft-lbf. This led to the design decision of running a lower gear ratio to reduce initial pedal torque, then switch to the higher gear once the bike is up to speed. A 6.3:1 front gear ratio was selected to reduce the pedal torque by half.

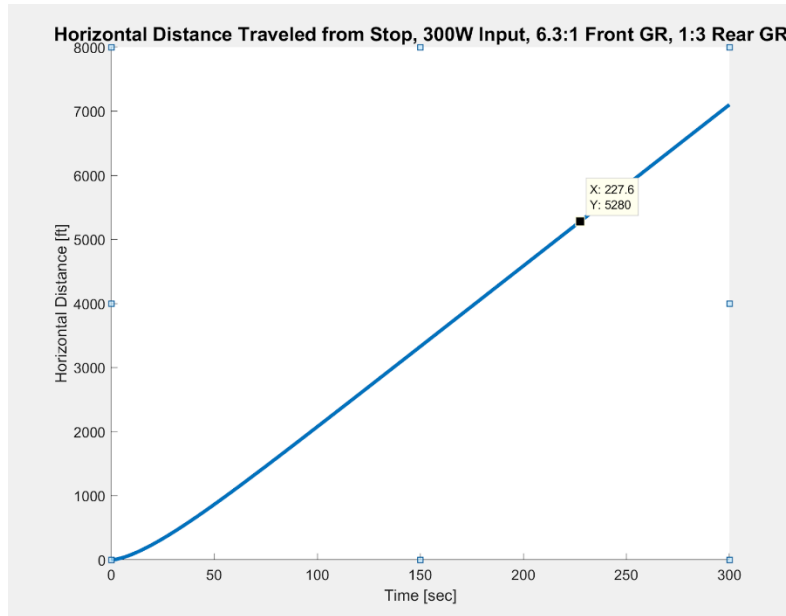


Figure 125. Horizontal distance traveled from stop with a 300W input, 6.3:1 front GR, 1:3 rear GR using Simscape direct drive model

Table 18. Summary table of above analysis with major inputs and outputs with Simscape direct drive model

Model Inputs/Outputs	Value
Power Input	300 Watts
Total Weight	256 lb
<b>Front Gear Ratio</b>	<b>6.3:1</b>
Rear Gear Ratio	1:3
<b>Peak Pedal Torque</b>	<b>99.8 ft-lbf</b>
Steady-State Average Cadence	113.2 rpm
Steady-State Max Pedal Torque	18.3 ft-lbf
Steady State Speed	17.2 mph
<b>Time to Mile</b>	<b>3 minutes 47 seconds</b>

Both of these front gear ratio combinations allow our bike in its current configuration to complete the mile well below the 4-minute requirement.

### 5.7.2 Accumulator Discharge Model

The accumulator discharge model in Simscape was modified to reflect similar changes made in the direct drive model. Figure 126 shows the final accumulator discharge model. A vehicle body block was added to incorporate the effects of aero drag and longitudinal weight transfer. The model also incorporates switches to control the 3-way valve to allow the bike to coast after discharge and to model a PWM-like discharge mode to maintain the bike at a specified range of speeds. The model also needed the addition of a needle valve at the accumulator discharge exit in order to reduce the water hammer effect on the motor, which crashed the model. The input into the model is the bladder accumulator volume, precharge pressure, and max pressure, and the output is bike distance.

This model was used to perform accumulator volume sweeps varying the accumulator volume, while leaving the max pressure constant at 3000 psi and the precharge pressure constant at 900 psi.

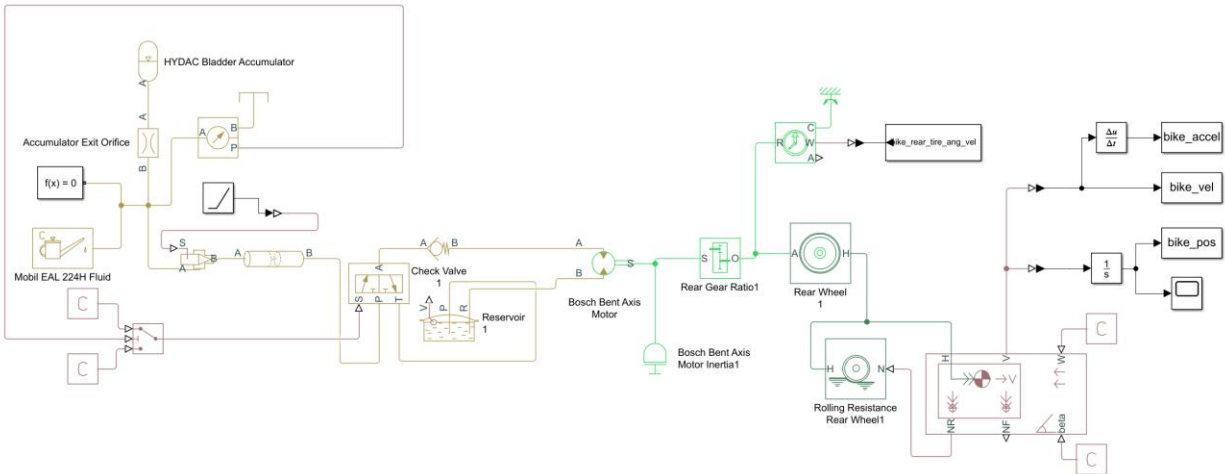


Figure 126. Simscape accumulator discharge model.

From the accumulator volume sweep results in Figure 128 below, it shows that a large accumulator reduces the efficiency score, which seemed contrary to the previous year's results as larger accumulators were favored. The efficiency score is calculated from the total distance traveled, the total weight of the bike, the pre-charge pressure and volume of accumulator, see Figure 127. According to the model's results having a smaller accumulator would yield the higher efficiency score but the cost of a poor sprint time. In order to achieve our efficiency score and sprint time requirements, we changed to a PWM-like discharge method with a medium sized accumulator. The PWM-like switching is performed while the accumulator is discharging, turning it on and off periodically, the efficiency score drastically increases. The PWM control maintained the bike's speed between 9 and 14 mph. This effectively doubled the bike's efficiency score and allowed us to keep a relatively large accumulator for low sprint times.

$$\text{Scoring Ratio} = \frac{[W * L]}{[P * V]}$$

- L = total distance traveled [in]
- W = weight of bike [lbs]
- P = pre-charge pressure [psi]
- V = volume of accumulator [in<sup>3</sup>]

Figure 127. FPVC efficiency challenge score

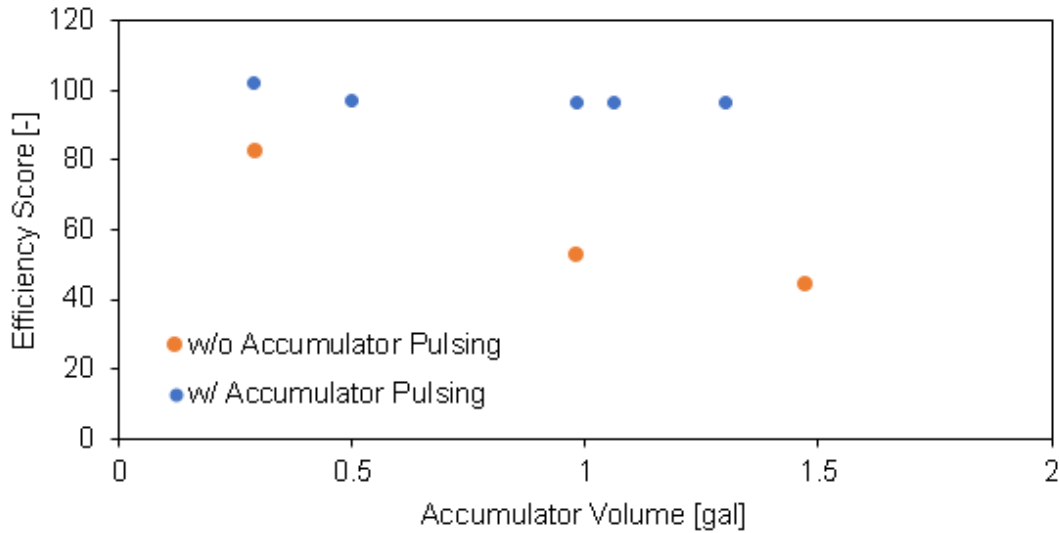


Figure 128. Graph of various accumulator sweeps and effect on efficiency challenge score with and without PWM-like pulsing

These results also show diminishing returns if the accumulator volume is increased while using the PWM-like discharge mode. A 1.06 gal accumulator was selected and achieved an efficiency score of 44.8 without the pulsing action and 92.4 with the pulsing action. This efficiency score well exceeds the requirement of 25 points. See Figure 82 and Figure 83 for the final accumulator discharge results.

### 5.7.3 Accumulator Recharge/Regen Model

A derivative of the accumulator discharge model was created to determine whether the bike met the accumulator recharge/regen time requirement. Rear wheel speed is the input into the model, pressurizing the accumulator from the pre-charge pressure to the max pressure, see Figure 129 for the model. This emulates the rider rolling the bike around at 5 mph to recharge the accumulator.

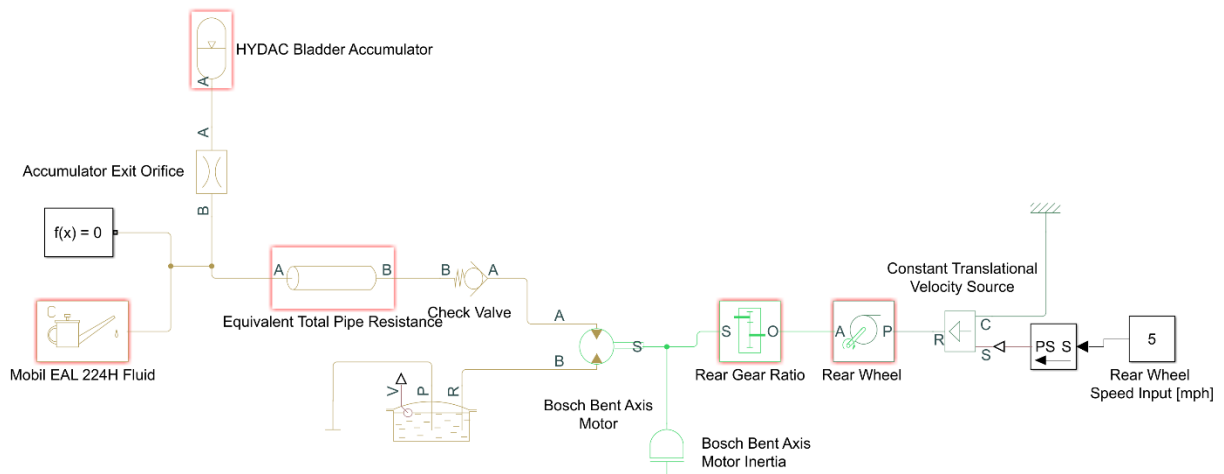


Figure 129. Simscape model of accumulator recharge/regen

A plot of time to recharge the accumulator to a max pressure of 3000 psi from a pre-charge pressure of 900 psi for the chosen 1.06 gal accumulator was generated and showed a full recharge of the accumulator in 2 minutes and 24 seconds exceeding our requirement of 5 minutes to recharge.

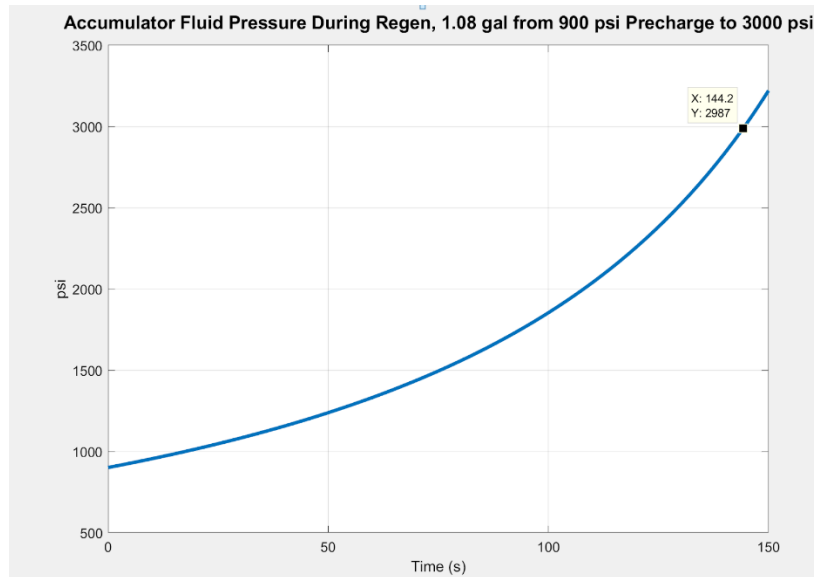


Figure 130. Plot of accumulator pressure over time for a 1.06 gal accumulator

#### 5.7.4 Loss and User Requirements

The loss model is used to determine the upper speed bound of the accumulator discharge pulse. As seen in Figure 131, the aerodynamic drag and hydraulic inefficiency begin to surpass road friction around 10[mph]. Any speed above this point proves to be a wasteful use of accumulator pressure. Knowing that the bike is restricted to above 6.2[mph] by the Patterson model the discharge will be controlled approximately between 7[mph] and 10[mph].

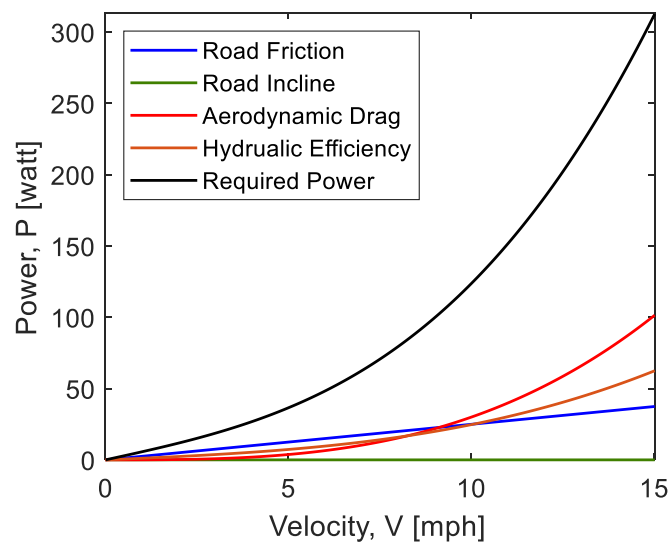


Figure 131. Power losses at steady state operation for various speeds



The past efficiency challenge had competitors negotiate a slight grade during their discharge resulting in many teams being unable to meet the minimum distance requirement. The loss model also quantifies the discharge limit under these conditions. Although the losses are far greater due to an incline, as seen in Figure 132, the domination of the gravitational losses creates a much more linear loss curve. This indicates a larger range of effective accumulator pressure use. Thus, the bike can be pulsed between higher speeds to reduce momentum losses. Ultimately this model will describe the relationship between change in pressure and change in speed over a range of bike speeds to more effectively utilize the accumulator in the efficiency challenge.

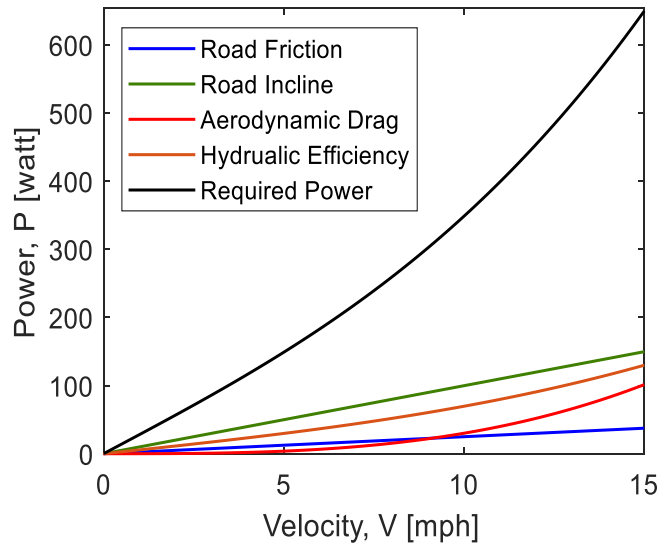


Figure 132. Power losses when traveling up a 2% grade.

## 6 MANUFACTURING

### 6.1 Procurement

Table 19 outlines the tentative budget for the 2018-2019 hydraulic bicycle. Notable purchases this season include a right-angle planetary gearbox for the front drivetrain and a new composite hydraulic 1-gallon accumulator for the hydraulic system. The Incompressibles will be reusing the hydraulic motors from the previous year's bicycle, this will result in a savings of about \$3000. The Incompressibles were also able to secure power measuring bike pedals through MESFAC funds, the purpose of these pedals is to measure power output by the rider to characterize drivetrain losses and validate the bicycle model.

Table 19: 2018-2019 Hydraulic Bicycle Budget

System	Cost (USD)
Frame	\$340.89
Front Drivetrain	\$1031.00
Rear Drivetrain	\$111.67
Mechatronics	\$263.00
Hydraulics	\$1102.02
Auxiliaries	\$505.06
<b>Total</b>	<b>\$2,210.97</b>

#### 6.1.1 Frame

##### 6.1.1.1 Frame Tubes

Our frame steel tubes were purchased from Nova Cycles Supply Inc. and Online Metals. The front polygon of the frame was manufactured from purchased tubes from Nova Cycles Supply whereas the rear of the frame including the chainstays, seatstays, and support tubes was from Online Metals. We were not able to use chainstay and seatstay tubes from Nova because of our extended lengths. We also needed to make custom single bends in each of those tubes different from what is provided by standard frame builder suppliers.

##### 6.1.1.2 Frame Auxiliaries

As well as purchasing the frame tubes, the bike required auxiliary components such as handlebars, front fork, seat and wheels to operate properly. The handlebars, seat, seatpost, wheels and stem were purchased from the local SLO Bike Kitchen. They were able to supply us with quality parts

at an inexpensive price. The bottom bracket, crankset, headset and fork were purchased online from Amazon, Chain Reaction Cycles and Bikeparts.com. Most of these parts contain limited life-span components such as bearings and purchasing these components new eliminated possible reliability problems.

## **6.1.2 Hydraulics**

### 6.1.2.1 Solenoids

The largest part of the hydraulic sub-system, the manifold, was designed and manufactured by SunSource to accept the Eaton-sponsored solenoids outlined in our manifold design. A proportional needle valve was later implemented to control the flow of fluid to the rear motor during discharge. This needle valve was purchased from Contractor Maintenance in SLO and plumed into the hydraulic circuit.

### 6.1.2.2 Reservoir

0.125" thick aluminum sheet stock was purchased from Online Metals while the remaining components including the weld bungs will be purchased from McMaster Carr.

### 6.1.2.3 Accumulator

The hydraulic accumulator, which is an off the shelf option, will be ordered from Steelhead Composites. The unit will take around a week to ship.

### 6.1.2.4 Lines/Fittings

Six, 3/8" diameter lines were supplied by Eaton in multiple lengths all with -6 JIC fittings. A large quantity of fittings were supplied by NFPA.

## **6.1.2 Front Drivetrain**

### 6.1.2.1 Front Crank

The crankset along with the bottom bracket, pedals, chain, and chain tensioner are available online through Amazon and other bicycle component websites such as Blue-Sky Cycling. The rear sprocket was purchased from Ebay, and the freewheel adapter was purchased from electric scooter part.com.

### 6.1.2.1 Planetary Gear Set

The right-angle planetary gearbox was ordered directly from Apex Dynamics. A mounting plate with shaft coupler was also provided with the order. The lead time for this component was approximately 2 weeks, and Apex Dynamics did provide a university discount.

## **6.1.3 Rear Drivetrain**

The majority of the components for the rear drivetrain was purchased from McMaster Carr. This includes the sheet metal for the motor mounting, the standoffs for mounting the motor, the bolts to mount the motor, the sprockets and the roller chain. The rear fixie wheel was purchased from the bike kitchen in San Luis Obispo and included the fixed gear sprocket that was used to mount the McMaster sprocket to the rear wheel.

### 6.1.4 Mechatronics

The majority of the components were purchased from Amazon and Digikey. The only exception was the PCB, which was ordered from JLCPCB. The Amazon components included the microcontroller, display, hall effect sensors, and screw terminals. The Digikey components included the solenoid drivers, diodes, capacitors, resistors, and pressure transducers.

## 6.2 Manufacturing

### 6.2.2 Frame

#### 6.2.2 Frame Tube Machining

Frame manufacturing started with developing miter drawing for each tube. The critical dimensions needed are cut orientation, hole saw cut diameter, and tube length. For the front triangle, BikeCAD was able to output miter drawing templates that could be cut out and taped to the end of each tube, see Figure 133. Each template has lines indicating the up or down orientation. We used a straightedge to correctly orient each cut template with its pair and spaced them apart based on the cut-to-cut distance



Figure 133. Unmachined tubes with miter templates taped on each end

The Anvil Universal Mitering Jig was fixtured to a rotary vice attached to a 3-axis manual mill. Each tube was placed in the fixture and the angle of the cut was changed with the rotary vice angle. Before each tube could be mitered, they had to be cut to rough length using the horizontal saw in order to minimize the depth of cut for the hole saw. It was recommended to us to engage only half of the teeth on the tool and maintain a low speed. See Figures Figure 134Figure 135Figure 136 showing some of the processes.



Figure 134. Anvil Universal Mitering Jig attached to a rotary vice on a mill



Figure 135. Russell showing how mitering is done



Figure 136. Close up of hole saw miter in tube

The front triangle utilized the above process, whereas the seatstays, chainstays and rear support tubes required additional fixtures. Depending on the orientation of the tubes, two different fixtures were used. The fixture shown in Figure 137 was used for tubes attached to the bottom bracket. Figure 138 shows another fixture for tubes attached to the seat tube.



Figure 137. Another Anvil fixture used for the tubes attached to the bottom bracket

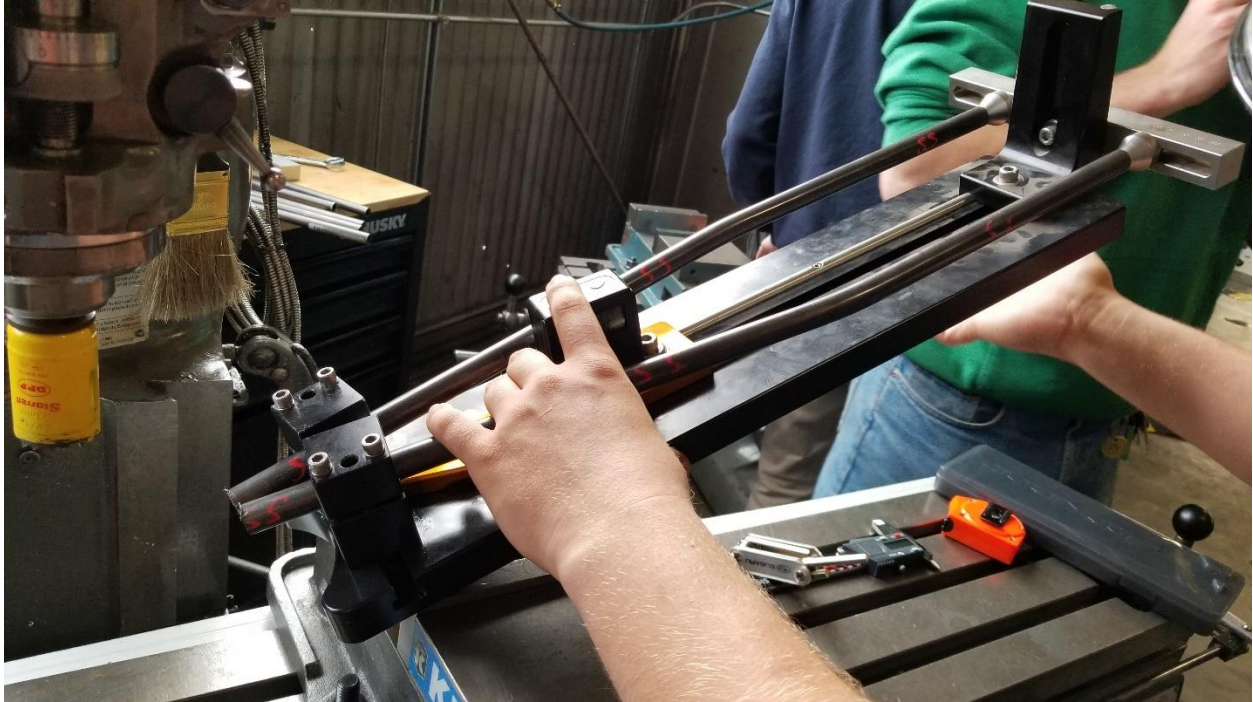


Figure 138. Another Anvil fixture used for tubes attached to the seat tube

Once all the tubes were mitered, the seatstays, chainstays and rear support tubes had to be bent. We utilized a Anvil tube bender attached to a table, see Figure 139, and marked on each tube where each bend started. An angle finder was attached to the end of each tube to determine the angle the bend.



Figure 139. Anvil tube bender

Once each tube was mitered and bent, they were placed on the Anvil Type 3.1 Journeyman fixture for welding, see Figure 140. We did have to grab specific dimensions from BikeCAD to properly set the fixture in position. See Figure 141 for the needed dimensions to setup the Journeyman fixture.

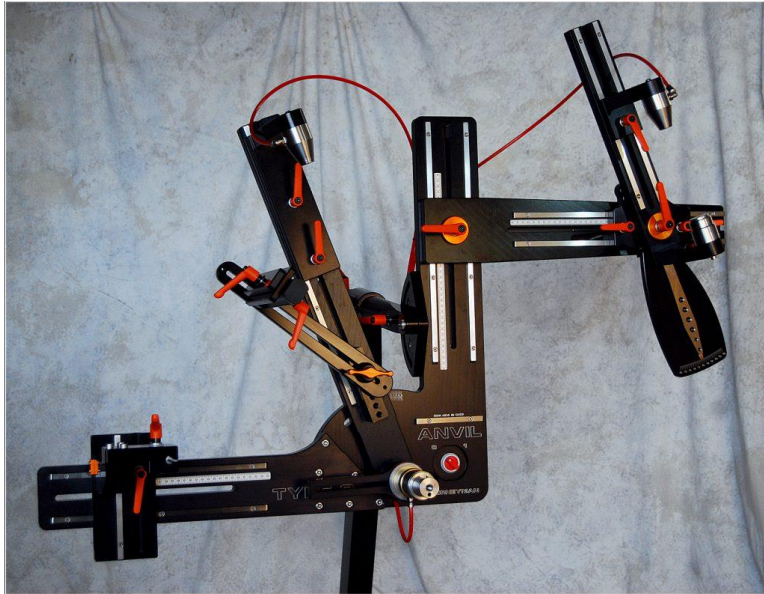


Figure 140. Anvil Bikeworks Type 3.1 Journeyman bicycle frame fixture

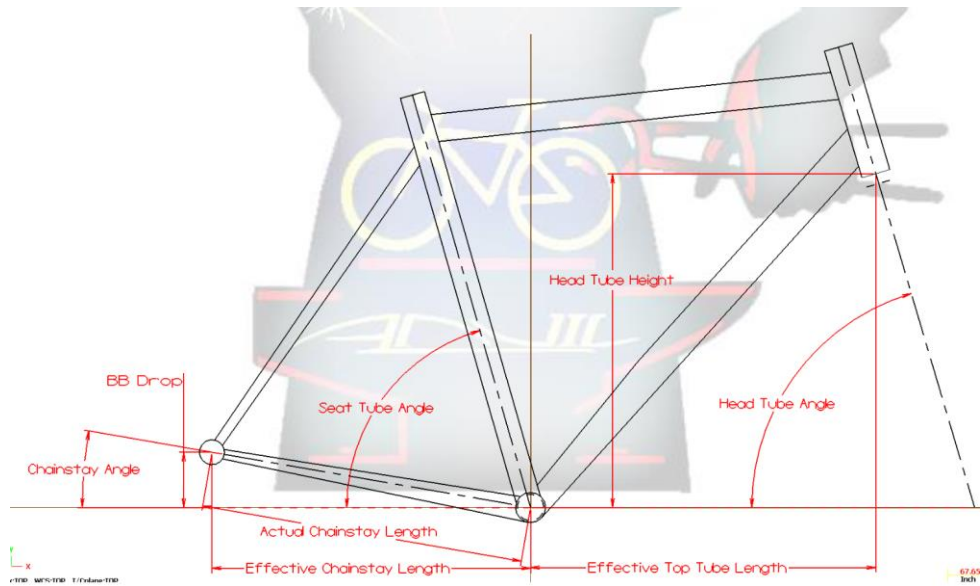


Figure 141. Dimensions needed to setup Anvil Journeyman fixture

We needed to make holes in each weld location order to allow argon purge for welding. Tubes were placed on the fixture and each hole was marked with a sharpie. Then holes were drilled with a center drill and a small drill bit, see Figure 142 for an example.





Figure 142. Example of the bottom bracket purge hole process

Once purge holes were made, the frame was tacked on the fixture then pulled off for final welding. We did, however, have a problem where the Anvil fixture couldn't accommodate the larger chainstay length. We had to adjust the rear dummy axle piece rearward but held it on to the assembly with a c-clamp, see Figure 143. It is recommended that the next team make sure the fixture can accommodate their bike's wheelbase properly.



Figure 143. We had to move the rear portion of the Anvil fixture holding the rear dummy axle backwards past the normal limits of the fixture to weld the bike. We held the fixture piece to the assembly with a c-clamp.

After the frame was fully welded, the rear brake bosses were brazed onto the rear seatstays. This required another fixture which attached to the rear dropouts, see Figure 144.



Figure 144. Image of rear brake boss brazing fixture attached to the rear dropouts

Once the brake bosses were brazed on and the mounts welded, the frame went into the paint booth. Formula SAE was gracious enough to use our bike as their test piece for their cars' paint scheme. We sanded the frame, painted it with primer then finished it with paint and clear coat in the Hangar's paint booth. See Figure 145 for the final version of the frame with paint.



Figure 145. Final version of the frame with paint

The final step left for frame manufacturing was post machining the head tube, seat tube and bottom bracket to properly accept the bike components. We again utilized Bike Builder's tools to face and ream the head tube, face and chase the threads on the bottom bracket, and face and ream the seat tube, see Figure 146, Figure 147, and Figure 148. Once these steps were complete, the frame was finally ready for component installation.



Figure 146. Facing the bottom bracket and chasing the threads



Figure 147. Reaming the seat tube



Figure 148. Facing and reaming the head tube

## **6.2.2 Hydraulics**

### **6.2.2.1 Solenoids**

The sponsored solenoids and manifold arrived ready to be assembled, the solenoid valves and fittings required proper torque into the manifold. The manifold incorporated drilled and tapped holes for mounting purposes, an aluminum plate was cut with the shear and properly placed holes were stamped to allow for the plate to bolt to the manifold and to the frame. Tube collar halves were utilized to secure the aluminum plate to the bicycle frame directly behind the seat.

### **6.2.2.2 Reservoir**

The reservoir is the most manufacturing-heavy item in the hydraulic assembly, seven sides will be waterjet from 0.125" aluminum stock in a pattern incorporating locating ears and holes for weld bungs. Once waterjet the sides and the bungs can be welded together with the frame mounts.



Figure 149. Final reservoir getting welded

## 6.2.3 Front Drivetrain

### 6.2.3.1 Planetary and Pump Mount

The two mount patterns, shown in , were waterjet from 0.063” 4130 CR steel sheet metal. The L-bracket piece was then bent using the sheet metal brake in the aero hangar shop and welded down the mating edges of the fold, as shown in Figure. The mounting plate was welded directly to the top of the chain stays.



Figure 150. Front drivetrain mounting bracket flat pattern and mounting tab



Figure 151. Bending the front drivetrain mounting bracket on the sheet metal brake

Since the mounting method for the chain tensioner was altered after the front drivetrain mounting pieces were waterjet, two extra slots had to be machined in the mounting bracket, shown in Figure 152, to accommodate the new chain tensioner mounting block, as well as two extra holes drilled in the mounting plate.



Figure 152. Machining additional slots into the front drivetrain mounting bracket using the mill in Mustang 60

The front drivetrain mounting plate was welded directly to the frame, located in between and on top of the chain stays. A fixture was designed to locate the mounting plate using the axis of the bottom bracket as a datum. The fixture is shown in Figure 153.



Figure 153. Fixture to locate the front drivetrain mounting plate

#### 6.2.3.2 Chain Tensioner Mount

A small aluminum block was machined to serve as a mount for the chain tensioner, located on the underside of the flat planetary and pump mounting plate. The block was machined from leftover 0.125" aluminum stock. Two holes on the top of the block were drilled and tapped to accommodate two 1/4-20 bolts that would fix the block to the planetary and pump mounting plate. Another hole was drilled and tapped on the face of the block to accommodate the M10x1.0 bolt on the chain tensioner itself. Finally, a 2mm hole was drilled near the M10x1.0 threaded hole to fix the small pin protruding from the chain tensioner, critical to allowing the chain tensioner to function correctly.

#### **6.2.3 Rear Drivetrain**

The rear mounting plate and slots will be waterjet from 0.10" 4130 CR steel sheet then welded vertically between the right hand seatstay and vertical tail support tube. In order to locate the final position of the plate, a fixture was used that attached to the rear axel.



Figure 154. Rear drivetrain mount welded in place

One of the more difficult challenges with the rear drivetrain was the simple matter of how to attach the McMaster sprocket that we wanted on to the rear wheel. The sprocket needed a large thread on the ID for it fit onto the wheel, and we were not able to get ahold of a tap for that thread. Additionally, we were worried about single point threading it on the lathe because of the quality of the lathes we had available to us. We ended up taking the fixie sprocket that came with the wheel that we bought and machining the teeth off the ID. Then using this toothless sprocket as a hub with the ID thread that we wanted. The machined down sprocket can be seen in Figure 155. Fixie sprocket with teeth machined down



Figure 155. Fixie sprocket with teeth machined down



With the teeth machined down we then had to increase the ID of the McMaster sprocket such that the new “hub” could fit inside. The two parts were welded together and can be seen below in Figure 156. Rear fixie sprocket components welded together.



Figure 156. Rear fixie sprocket components welded together.

The rear sprocket was then fit onto the rear wheel, and held in place with a lock ring. The final assembly can be seen in Figure 157.



Figure 157. Final rear wheel and sprocket

Another part of the manufacturing of the rear drivetrain involved broaching the keyway for the motor onto the sprocket that would mount there. We were able to utilize the tools at the Mustang machine shop at Cal Poly to broach the keyway on a hydraulic press.



Figure 158. Broached keyway on McMaster sprocket

#### ***6.2.4 Mechatronics***

The printed circuit board was manufactured overseas through the company JLCPCB. The Gerber files generated from the Eagle design were uploaded through their website, and the completed PCB was shipped a week later. All the components were then soldered onto the board in the mechatronics lab. Additional manufacturing for mechatronics consisted of 3D printing mounts and making wires of the appropriate size. The 3D printed components were printed at the home of one of the team members, and the wire cutting/stripping was done on campus.

## 6.3 Assembly

After the frame was manufactured all of the subassemblies were added to the frame



Figure 159. Completed bike assembly

- The mechatronics interface will be attached to the handle bars with the two buttons near each hand location and a screen directly in front of the user.
- The 1.25[gal] reservoir will be hung from the top tube in the front triangle.
- The planetary set and pump will be mounted on the chain stays behind the user's feet.
- The individual manifold blocks will be mounted on the vertical tubes of the tail, whereas the single manifold will be mounted on the right seat stay tube.
- The accumulator will be bolted the top of the rear support tubes with enough room behind the seat to allow for line routing.
- The motor mount will be welded between the right seat stay and vertical tail tube.

### 6.3.1 Frame

Frame installation started with the headset and bottom bracket installation. The headset cups were pressed into the headtube and the crown race was installed onto the fork. The fork stem length was cut to match the necessary stem height with spacers, see Figure 160. After the stem, spacers and fork was installed, we had to install the star nut into the fork tube for the stem cap.



Figure 160. Fork, handlebar and stem installation

The bottom bracket, crankset and brakes were installed, following their respective instructions, and we were able to get a rolling bike, see Figure 161.



Figure 161. Frame with all bike auxillaries installed

## **6.3.2 Hydraulics**

### 6.3.2.1 Solenoids

Items in the solenoid assembly arrived ready to be assembled. Solenoids and the respective fittings were threaded into the line blocks and torqued to the proper specification, a small amount of grease is recommended to insure the o-ring seat properly.

### 6.3.2.2 Reservoir

With a fully welded reservoir both the barbed fittings, the vent, and the sight tube push fittings were threaded in. The reservoir was mounted to the top tube of the bicycle by threading the purchased shaft collars into the ¼"-20 tapped holes on the reservoir mount.

### 6.3.2.3 Fittings

All fittings are 3/8 JIC and were assembled using proper torque specifications while ensuring the hydraulic lines are straight to avoid loosening during useage.

## **6.3.3 Front Drivetrain**

### 6.3.3.1 Planetary and Pump

The planetary gearbox and the pump were mounted to each other before being attached to the mounting bracket on the frame. This was done because of space limitations within the rear triangle of the frame. If the planetary gearbox was mounted alone, there would not be enough vertical space to then mount the pump, as its shaft must be slid into the gearbox mounting plate. The pump shaft key was removed before inserting it into the shaft collar on the gearbox mounting plate, as advised by the installation instructions provided from Apex Dynamics. Next, four male-female hex standoffs were threaded into the four mounting holes on the planetary mounting plate. The pump shaft was then inserted into the shaft collar on the planetary mounting plate. The shaft collar was tightened using an Allen key through the sight hole on the side of the planetary mounting plate. Finally, four socket head screws were inserted through the pump mounting plate holes to meet the female end of the hex standoffs. The pump-planetary assembly is shown in Figure 162.



Figure 162. Planetary gearbox mounted to pump

After mounting the pump to the planetary gearbox, the gearbox was attached to the mounting bracket. Four M5 bolts along with standoffs, washers, and nuts were used to mount the input side of the planetary gearbox to the mounting bracket, as shown in Figure 163.



Figure 163. Planetary gearbox and pump attached to mounting bracket

#### 6.3.3.2 Chain and Sprocket Assembly

The fixie sprocket obtained for the front drivetrain was first threaded onto the freewheel adapter from [electricscooterparts.com](http://electricscooterparts.com). The keyway of the freewheel adapter had to be filed down slightly

to fit the planetary keyed shaft. The sprocket and freewheel adapter were then slid onto the shaft of the gearbox and the two set screws on the freewheel adapter were tightened with an Allan key to fix the sprocket axially. The chain tensioner block was also attached to the planetary mounting plate, and the chain tensioner itself was mounted to the block via its M10x1.0 bolt. In order to size the chain for both speeds of the crankset, the chain was wrapped around the larger of the two sprockets, the planetary sprocket, and the chain tensioner jockey wheels, with the chain tensioner twisted until it nearly touched the bottom of the chainstay. Sizing the chain in this configuration would ensure the chain tensioner would be able to pull back and provide tension when shifting to the smaller of the two chain rings. The front drivetrain is shown in action in Figure 164.



Figure 164. Front drivetrain assembly in motion

#### ***6.3.4 Rear Drivetrain***

After the rear drivetrain mount was welded into place, the components were then mounted. A set of aluminum standoffs were put in place for the motor to be mounted with long bolts from near the top of the motor. ANSI roller change was also fit around the motor at the smallest distance between the pump and the rear axle such that tension could be placed in the chain when they were moved apart. This moving apart was achievable because of the slots in the motor mount and the vertical dropouts for the rear axle.



Figure 165. Rear drivetrain assembled and chain being sized



Figure 166. Rear drivetrain assembled and chain being sized 2

### ***6.3.5 Mechatronics***

The components were soldered onto the PCB, the display was attached, and this system was placed into the 3D printed enclosure. The enclosure was then mounted to the bike using zip-ties. The buttons were also placed into their 3D printed mounts and attached in a similar fashion. The



pressure transducer attached to the manifold and the battery was secured to the frame using Velcro straps. All these peripheral components were then connected to the screw terminals on the PCB using the previously manufactured wires.

## **6.4 Outsources**

### ***6.4.1 Frame***

We outsourced the frame welding to the Bike Builders club on campus, and specifically, Greg Ritter was gracious enough to completely weld our bike for no charge. The rear dropouts were outsourced to Waterjet Central in Paso Robles.

### ***6.4.2 Manifold***

A free custom manifold was provided through the NFPA by SunSource. However, SunSource will only provide a single block so the circuit design must be tested before the block is ordered. The block schematic was designed by the Incompressibles and tested prior to the finalization of the manifold schematic using individual solenoid blocks. The design of the block itself was performed by Jeff McCarthy of Sunsource. The block is aluminum and rated at 3000[psi]. Lead time on the manifold was estimated to be around two weeks, however it took much longer at around 2 months.

### ***6.4.3 Waterjet***

The front drivetrain, rear drivetrain and aluminum reservoir all relied on waterjet sheet metal in order to mount the pump, motor and planetary gearbox to the bike frame. All the waterjet cutting for this project was completed by Waterjet Central in Paso Robles.

## 7 DESIGN VERIFICATION

After predicting the performance of the bike with simulations and calculations to determine whether it met our initial requirements, we tested the bike using various methods to verify if the final vehicle met our initial design specifications. Table 20 shows our requirements table with the bike predicted performance and the actual bike performance at competition. Rows highlighted in green indicate the bike meets or exceeds our targets. Cells in red indicate the bike did not meet the targets and rows in yellow indicate requirements that could not be predicted with simulation and require testing once the final product is made.

Table 20. Design specifications table with predicted performance with current design

Spec #	Parameter Description	Requirement or Target	Tolerance	Risk	Predicted Performance	Vehicle Testing	Actual Results @ Competition
1	Endurance Time (1 mile)	4 minutes	Max	H	3 min. 46 sec.	4 min. 15 sec.	4 min. 50 sec.
2	Efficiency Score	25 points	Min	H	44.8 w/o PWM, 91.4 w/ PWM	54.5	7.53
3	Sprint Time (600 ft)	18 seconds	Min	H	20.9 sec.	21.5 sec.	23.1 sec
5	Top Speed	40 mph	Max	M	32 mph	--	--
7	Time to Assemble Completely	1 hour	Max	M	--	--	--
8	Time to charge accumulator	5 minutes	Max	L	2 min. 24 sec.	3 min.	3.5 min.
9	Drive mode selection latency	1 second	Max	M	0.1 sec.	--	--
11	System Lifespan	2 years	Min	M	--	--	--
12	Number of CNC Components	8 parts	±2	H	1 part	1 part	1 part
13	Internal Leakage	2 psi/s	Max	H	0.1 psi/s	--	--
14	Braking Torque	Max. torque of accumulator	Min	H	--	Completed	Completed
15	Weight	85 lbs	Max	H	69.3 lbf	100 lbf	96 lbf
17	External Leakage	0 drips	Max	H	--	0 drips	0 drips
18	Coast Compared to Regular Bike	90%	Min	M	--	Yes	Yes

## 7.1 Initial Bike Performance Testing

The main dynamic events in the Fluid Power Vehicle Challenge are the endurance, efficiency and sprint challenges. Once the bike was rolling and we were able to select drive modes, we developed a mock competition to test the bike's dynamic performance.

### 7.1.1 Mock Dynamic Bike Challenges

#### 7.1.1.2 Mock Endurance Challenge

We setup a mock endurance course around the perimeter of the H1 parking lot, see Figure 167, and ~5.5 laps around it, totaled 1 mile. We started from a standstill, had no accumulator charge and used the clipless pedals. Nicholas was able to complete the course around 4:15 minutes which was less than our expected performance, but it was noted that sustaining 300 watts of power for 4 minutes was unfeasible compared to our initial assumptions. Testing with power pedals needs to be conducted to see the actual power output of a rider over time. The 4:15 minute completion time was deemed acceptable because it was a competitive time compared to the previous year's competition.



Figure 167. Mock endurance course in the H1 parking lot on campus

#### 7.1.1.2 Mock Efficiency Challenge

The mock efficiency challenge utilized the same course as the endurance challenge seen in the above figure. The accumulator had a precharge of 900 psi and was fully charged to 3000 psi for each test. Each rider was supposed to modulate the discharge mode to maintain a fast-enough speed to prevent stopping while maximizing the distance traveled. The results are outlined in Table 21 below. We were able to achieve an efficiency score ~50 which exceeded our goal of 25 points.

Table 21. Mock efficiency challenge results

Rider Name	Rider Weight [lbf]	Bike Weight [lbf]	Distance Traveled [in]	Efficiency Score [-]
Alex	180	100	38,000	52.2
Nicholas	175	100	40,400	54.5

7.1.1.3 Mock Sprint Challenge

The final mock dynamic challenge we completed was the sprint event. We utilized the street adjacent to the H1 parking lot and measured a straight course, 600 ft long, see Figure 168. We fully charged the accumulator to 3000 psi with a precharge of 900 psi. We tested various opening positions for the flow control valve to see its effect on sprint time and whether the pump experienced any water hammering. We had to add the flow control valve after experiencing massive amounts of fluid blowby through the motor into the reservoir in the case drain line. Russell was able to complete the sprint event in 21.5 sec. This time could have been improved if we fine tuned the valve more and if it could open gradually over time ending at fully opened, similar to a proportional valve. See

Table 22 for specific results.



Figure 168. Mock sprint course adjacent to H1 parking lot on campus

Table 22. Mock sprint challenge results

Rider Name	Rider Weight [lbf]	Bike Weight [lbf]	Flow Control Valve [Turns Opened]	Sprint Time [sec]
Russell	170	100	4	22.4
Russell	170	100	3.5	21.5

## 7.2 Competition Bike Performance Testing

The 2019 NFPA FPVC was held in Littleton, Colorado at IMI Precision Engineering from April 10, 2019 to April 12, 2019. The event consisted of completing the three dynamic challenges in IMI's parking lot, giving a design presentation and showing our bike to the judges for safety/design critique. The top 5 results for each dynamic event from the competition are shown below. The complete dynamic results are in Appendix 14. We were able to achieve 2<sup>nd</sup> overall, 1<sup>st</sup> in endurance, 3<sup>rd</sup> in efficiency and 5<sup>th</sup> in sprint. The specific results and takeaways from each challenge are outlined below. The design presentation and critique scores are in appendices

### 7.2.1 Dynamic Bike Challenges

#### 7.2.1.1 Sprint Challenge

The sprint challenge consisted of two vehicles starting on the side of the IMI building, traveling along a path of cones, and finishing at the end of the parking lot. Each team was allowed two chances to secure their best time. This challenge favored vehicles with a fast acceleration (low weight & large accumulators) and some teams made last minute changes to their accumulator pre charge settings to maximize their energy release. The top 5 results for this challenge are below in Figure 169.

<b>Sprint Challenge</b>		
	<b>University Name</b>	<b>Best Time (sec)</b>
1st	Cleveland State	14.71
2nd	Murray State University	14.94
3rd	Western Michigan University	21.75
4th	Purdue University	22.24
5th	California Polytechnic State University, San Luis Obispo	23.09

Figure 169. 2019 competition sprint challenge top 5 results

While the first teams were competing in the event, we charged our accumulator and tested the settings on the flow control valve before we started our first trial. We found through that we lost accumulator pressure momentarily after selecting discharge mode. We remedied this issue by placing the bike in direct drive and cycling the system for a minute before discharging. This seemed fill the lines preemptively and reduced pressure loss as the solenoids clicked over. More accumulator pre charge testing should have been completed prior to competition to determine the best pressure to maximize sprint performance.

#### 7.2.1.2 Efficiency Challenge

The efficiency challenge circuit was set up similar to our H1 testing layout with a circular loop around the IMI parking lot. Teams were allowed to complete two trials for their best. Although we were under the impression the bike's setup couldn't be changed for the efficiency challenge, we noticed teams swapping accumulators and changing pre charge pressure before the event. We found that due to the design of the efficiency equation, we could greatly increase our score if we dropped our pre charge pressure to the minimum required, 100 psi, compared to leaving it at 900

psi. We also placed our heaviest driver on the bike to maximize the weight variable, increasing our score. We knew that that our distance may decrease due to the increased weight and low accumulator torque output but believed that the weight increase and pre charge decrease would still amplify our score. However, this will most likely not be a valid strategy for next year as Ernie Parker expressed his criticism that the equation doesn't actually measure the efficiency of the vehicle. The top 5 teams in this challenge are shown in Figure 170 below.

<b>Efficiency Challenge</b>		
	<b>University Name</b>	<b>Score</b>
1st	Western Michigan University	31.63
2nd	Cleveland State	10.46
3rd	Cal Polytechnic State University	7.54
4th	Montana State University	4.16
5th	Purdue University	3.32

Figure 170. 2019 competition efficiency challenge top 5 results

### 7.2.1.3 Endurance Challenge

The final dynamic challenge, endurance, utilized the same track as the efficiency challenge. Only one trial was allowed and teams went on the track in waves. Teams were also required to make a stop during the event using only the force from the accumulator regen circuit and restart using only accumulator discharge. We were also under the assumption that vehicles weren't allowed to have any accumulator charge before starting the event. We later found the rules never stated you could or couldn't have any charge beforehand. Each team was allowed five minutes to charge their accumulator before starting. We initially thought this would put us at a significant disadvantage compared to teams with very large accumulators. Our results refuted this claim and reaffirmed that a competitive bike also needs to perform well in direct drive. Teams that relied solely on the accumulator discharge to propel their vehicle had significantly slower times because they stopped mid event to recharge then discharged again, and repeated this cycle till the finish. Our bike was relatively easy to ride and capitalized on human power rather than accumulator power. Having two selectable gear ratios also helped during the hill ascents when the rider became fatigued. The top 5 results from the challenge are shown in Figure 171 below.

<b>Endurance Challenge</b>		
	<b>University Name</b>	<b>Time</b>
1st	California Polytechnic State University, San Luis Obispo	4:50:45
2nd	Cleveland State	5:40:00
3rd	Montana State University	5:45:48
4th	West Virginia University Inst. Of Tech	6:40:00
5th	Purdue Northwest	10:42:00

Figure 171. 2019 competition endurance challenge top 5 results

## 7.3 Drivetrain

### 7.3.1 Front Drivetrain

Upon preliminary testing of the bicycle, the team quickly ran into issues regarding chain tensioning. With the initial configuration of the chain and sprocket assembly, it was realized that there was not enough chain wrap around the driven sprocket mounted on the planetary gearbox shaft, as illustrated in Figure 172. As a result, the chain would occasionally skip over the sprocket under high load. The chain skip served to exacerbate the already non-uniform pedaling motion of the bicycle. Research showed that it was necessary to have 180° of chain wrap on any driving or driven sprocket to provide sufficient power transfer. However, with this chain tensioner in this configuration, it was not possible to achieve the desired amount of chain wrap. Thus, a dual jockey wheel chain tensioner was procured, which allowed for sufficient chain wrap.



Figure 172. Demsontration of lack of chain wrap and chain tension in front driveetrian

Although the dual jockey wheel chain tensioner allowed for sufficient chain wrap around the rear sprocket of the front drivetrain assembly, there was still occasional skipping. It was deduced that the spring in the chain tensioner was not providing enough force to maintain tension. As a last ditch effort to provide increased tension in the chain, the team implemented a bungie cable hooked from the chain tensioner to the bridge of the rear horizontal tubes. In the future, a more elegant and effective solution should be determined.

## 7.4 Hydraulics

### 7.4.1 Solenoids

During the 2019 competition we experienced a small amount of internal leakage but it was far from detrimental. The accumulator lost 100 psi of pressure (3000 to 2900 psi) in 30 seconds. This was not insignificant but was small relative to our goal. It should be noted that at lower pressures the pressure drop would slow drastically. An unforeseen issue encountered was massive blow-by in the rear motor during fast accumulator discharge. When discharging at 3000 psi the hydraulic fluid hitting the rear motor created a pressure spike forcing a substantial amount of fluid past the cylinder seals in the motor and into the case drain, effectively wasting that energy. We implemented a manual needle proportional valve in-between the accumulator and the rear motor, this valve acted as a check valve in one direction (into the accumulator) and a proportional valve in the other. This slowed the flow of fluid to the rear motor drastically preventing the motor blow-by, however it introduced another pressure loss in the system and increased our sprint time. Later it was discovered that if we pedaled the bike in direct drive mode prior to discharge we would not experience this water hammer effect even when the needle valve was fully open. This leads us to believe that the lines may have been void of fluid prior to discharge and pedaling during direct drive filled them again, not giving the fluid room to accelerate.

Both the pump and motor experienced cavitation during high-load situations, the pump when in direct drive mode and the motor in regen mode. We found that during regen if we turned the pedals (pumped the pump) the cavitation noise disappeared. We suspect that the valve circled in red was not opening enough for some reason, or the pressure loss through the valve proved to be too high. Please investigate in the future.

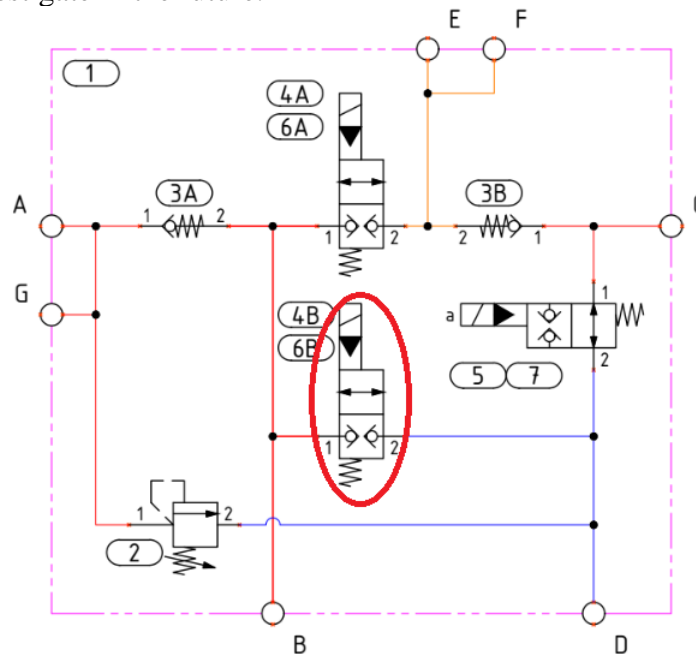


Figure 173. Schematic of hydraulic circuit with the specific solenoid in question circled in red



## 7.5 Mechatronics

The requirements of the mechatronics system were as follow. 1: Be able to actuate the solenoids to change drive modes. 2: Display relevant information to the rider. 3: have a latency of less than one second. 4: Have a sufficiently large battery. The solenoid performance was tested and found to have a response time of less than 0.1 seconds. On the bike, the mechatronics system was able to successfully switch between drive modes and reproduce this speed The drive modes were each tested in quick succession and all four were found to be in working order and capable of routing fluid through the correct pathway. The displayed metrics to the rider in the final iteration of the system were limited to the pressure value in the accumulator. Nonetheless, this reading was compared with an analog pressure gauge on the accumulator and confirmed to be accurate. The overall speed of the system, including the display refresh rate, was far below the goal of one second and met the requirement for system latency. The battery, a 40,000 mAh NiMh 12v assembly, was tested for longevity and found to exceed requirements for battery life. The system was able to be powered for a time period of over three hours, with a predicted lifetime of 2.5 hours, and met the required timeframe for completing the necessary competition events on one charge.

## 7.6 Modeling

Validation of the Simscape models are critical so future teams can use these tools to predict the bike's performance without having to remake models again or use them knowing the results could be inconclusive. Although we planned to add pressure transducers and hall effect sensors in the mechatronics circuits, we were not will be able to validate the direct drive and accumulator discharge models. The mechatronics circuit had some development complications and we were not able to implement all of the desired sensors or data collection during testing. Future teams should take the opportunity to add the power pedals, pressure transducers and hall effect sensors to collect data and validate the model. Once the data is collected, the same bike parameters for the actual bike should be copied into the Simscape models and the results of both real life testing and the models will need to be compared for discrepancies. The power input into the direct drive model can be validated with the addition of power tapping pedals. These pedals calculate the power input from the rider and can be used to validate whether the constant 300W power input into the direct drive model is correct. The hall effect sensor data should validate whether the bike gets up to speed and achieves the same top speed as the model. For the accumulator discharge model, total bike distance traveled and the accumulator discharge profile acquired from pressure sensor data should be compared and analyzed for discrepancies. The accumulator regen model can be validated by pushing the bike around an open area at a constant 5 mph and comparing the pressurization curve of the model to the collected bike data. If the model is able to produce results with 5-10% of error compared to the real bike, it is reasonable to say it accurately represents the bike's performance.

## 8 PROJECT MANAGEMENT

### 8.1 Roles and Responsibilities

In order to stay on track and successfully bring our project to fruition, we have developed a structured plan for the division of labor to complete tasks and meet deadlines. Each member of the team has been assigned a specific role relating to team logistics as well as been given responsibilities involving their technical areas of interest. The individual roles and responsibilities can be found in Table 23. Another critical component of our management plan was the development of a team contract. This contract establishes procedures for deadlines, responsibilities, communication, conflict resolution, and violations of contract. The document, signed by each member, clearly defines rules set by the team and guarantees a mutual understanding of the expectations.

Table 23. Individual Roles and Responsibilities

<b>Team Member</b>	<b>Logistical Roles</b>	<b>Subsystem Responsibilities</b>
Nicholas Gholdoian	Sponsor Contact, Editor	Modeling and Mechatronics
Julian Rodkiewicz	Testing Facilitator	Modeling, Mechatronics, and Manufacturing
David Vitt	Vendor Contact, Manufacturing Coordinator	Mechatronics, Manufacturing and Frame
Kyle Franck	Secretary, Editor	Hydraulics and Modeling
Russell Posin	Project Planner	Frame, Power Transfer, and Manufacturing
Alex Knickerbocker	Treasurer, Manufacturing Coordinator	Hydraulics, Power Transfer

### 8.2 Project Timeline

In addition to specific obligations of each team member, we created a general timeline for our project using a Gantt chart. Figure 174 shows a segment of the TeamGantt utility we were using for general time management. The intent of this plan is to provide a clear timeframe and establish team member accountability for necessary tasks and milestones. Through visual representation of our due dates, individual contributions, and milestone progress, we will be able to effectively stay on track throughout the duration of the project. Important milestones for the project include: PDR, CDR, rolling bike, and competition. Beginning mid-September, detailed design began with priority set on frame, hydraulic circuits and power transmission. Final design was completed for CDR, but we had to make corrections after the presentation based on the feedback from our advisor

and sponsor. After correcting our design, we heading into the manufacturing phase starting in December. Once manufacturing was completed in February, we started testing the bike stationary and transitioned into completed mock dynamic challenges. Finally, the competition took place from April 10<sup>th</sup> – 12<sup>th</sup>, 2019.

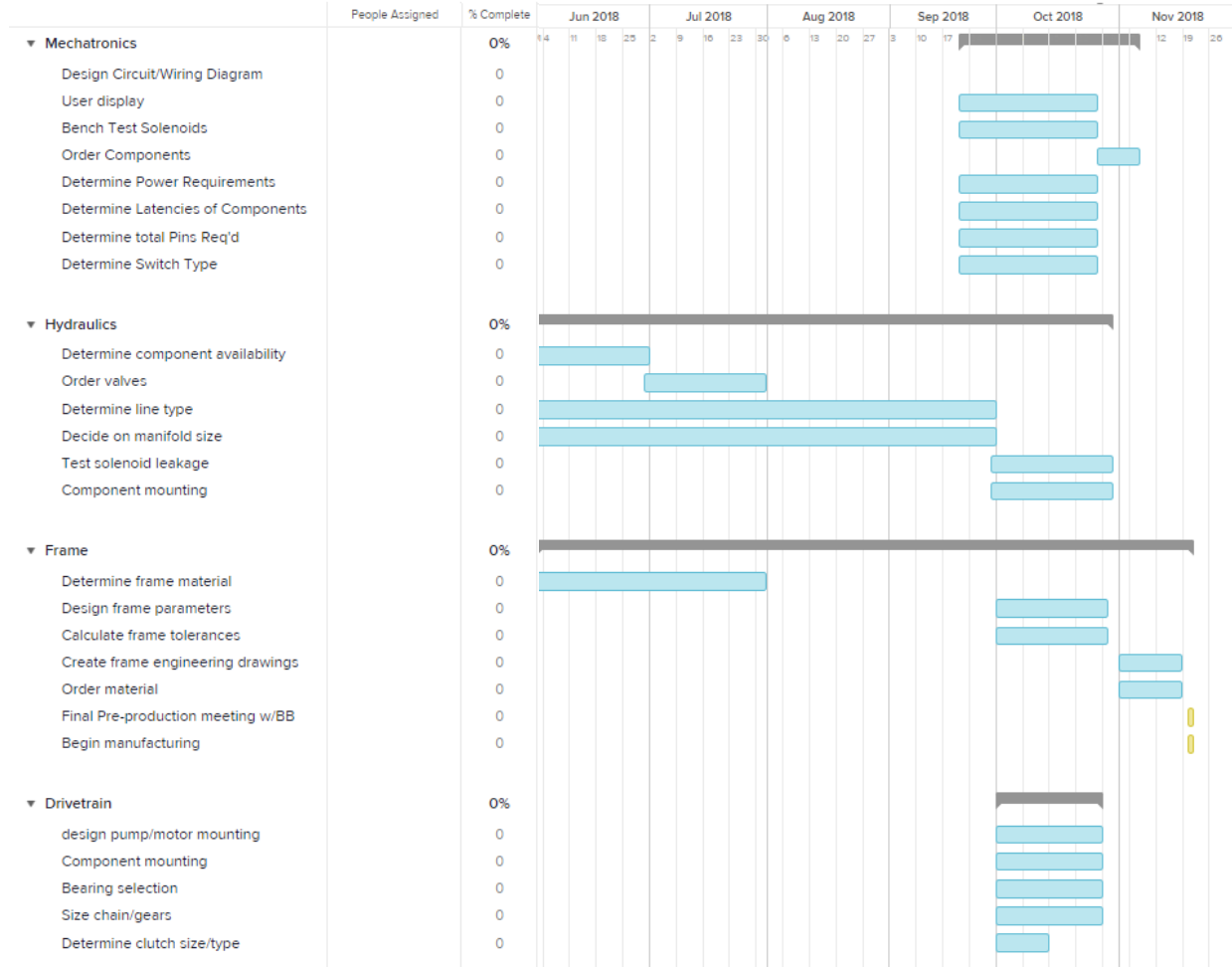


Figure 174. Gantt Chart Excerpt

### 8.3 Project Management Recommendations

Although each person had definitive roles that we decided on early in the design phase, we soon had to transition into different positions based on where work was needed. Even though people have assigned positions, it wasn't rare for team members to step out of their subsystem to assist another team member. Don't place strict guidelines on the team member responsibilities as they may have to be adaptable to help when necessary but make sure to hold each member accountable for the work they are assigned. It also seemed necessary to assign a single person as the team manager or leader. Even though a group of six people doesn't seem large, with a project that encompasses many different aspects of engineering that needs to meet stringent deadlines, there needs to be a member in charge of keeping the project on track and holding members accountable. If team members are allowed to have fluid deadlines, then the team may not be able to meet deadlines on time because each member isn't made aware of the overall project progress or where

the project needs to be. Having the ability to see a gantt chart of gain some visibility of project progress is vey beneficial at providing a self-check on whether you are completeing you work on time or need more time.

## **9 RECOMMENDATIONS**

### **9.1 Design Recommendations**

Overall, we determined that the next team needs to read the rules carefully so you can capitalize on any opportunities or loopholes to increase the vehicle's performance. We had assumed that you weren't able to change the vehicles configuration during the events and quickly adapted to other teams to stay competitive during the dynamic events. If conceptual design started with the notion that bike components such as accumulator size and pre charge pressure could be changed during competition, our bike could have better tailored to each event.

#### ***9.1.1 Frame***

An area of improvement for the frame could be the weight and selection of bike tubes. The bike was designed as an oversized mountain bike, but more analysis should be done to determine how oversized the frame is for the loads and reduce tube wall thickness or OD and reduce accordingly. We were able to decrease frame weight compared to last year, but a couple of pounds could be shaved if the frame was designed closer to a FOS = 1.

#### ***9.1.2 Front Drivetrain***

The front drivetrain as we mentioned earlier, had chain tensionsing problems while the bike was in the lowest gear and pedaling under load. We were able to remedy the problem of the chain skipping off the planetary sprocket by replacing the single jockey wheel tensioner to the dual jockey setup and adding a bungee cord for more tension. This gave us the ability to pedal aggressively in the lowest gear without skipping. This solution should not be permanent and should be fixed by changing the front drivetrain system to allow for more chain wrap and integrating a stronger chain tensioner, like a rear bike derailleur.

#### ***9.1.3 Modeling***

One of the areas for improvement in regards to modeling is validation. As the report mentioned previously, utilizing data collected from a DAQ during testing would allow teams to see how accurate the model is and correct or adjust accordingly. One area of the model that we had to assume was the Bosch pump mechanical and volumetric efficiency. We were not able to obtain efficiency data for our pumps so we had to use curves from a similar Parker bent axis pump. We felt this would be the best way to characterize the pumps for the model, but time should be spent actually finding and inputting efficiency data for the Bosch pumps on the bike.

#### ***9.1.4 Hydraulics***

Routing of the hydraulic circuit was correct however component selection should be audited with special attention paid to pressure losses. Cavitation occurred in both the pump and motor during the regeneration mode, this could be due to the spring on the check valve prior to the pump/motor being too stiff. An additional check valve should also be incorporated into the hydraulic circuit that allows for pedaling during discharge and regen to add pressure to the accumulator.

#### ***9.1.5 Mechatronics***

Erroneous switching of drive modes came as a result of thin wires and loosely soldered connections. It would be advantageous to use lower gauge wire, utilize more solder, and tie down wires near the connection points. The mechatronics system did not have the desired capability to record data for further testing analysis. Originally this was to be done through Bluetooth and a mobile app on the MCU-32s, but complications resulted in the use of a different control.

### **9.2 Manufacturing Recommendations**

#### ***9.2.1 Frame***

A recommendation for any team that would like to make their own custom frame is to make sure they have an experienced welder on their team. We were gracious enough to have Greg Ritter weld our entire bike frame and mounts but if he didn't help us out then we wouldn't have a bike. A team who is considering making their own frame should factor in whether they have a welder on their team.

#### ***9.2.2 Hydraulics***

One issue that we encountered this year is loosening of the hydraulic lines through normal use. When installing the hydraulic lines ensure that there is no compliance in the component mounting and if there is that there is no movement in the hydraulic fittings. Welders should be outsourced way in advance to manufacturing deadlines.

### **9.3 Testing Recommendations**

We were not able to test different pre charge pressures to see their effects on the sprint and efficiency challenge. We observed at competition that teams were adjusted their pre charge specifically for each event which could improve the bike's performance. Next year's team should invest into making a nitrogen tank refilling system so they can test different pressures rapidly instead of having to travel to Contractor's Maintenance to change the accumulator pre charge

pressure. As noted previously, the next team should implement a DAQ system with the appropriate sensors to collect driver data and validate the Simscape models.

Another improvement to the overall hydraulic circuit is to reduce the amount of fittings necessary and replace the soft line with hard line. Both of these would reduce the fluid losses and weight. We were not able to complete these tasks due to diagnosing higher priority issues during testing, but next year's team could implement this fairly easy and quickly.

## 10 CONCLUSION

This Final Design Review document outlines in detail the final design of the 2018-2019 hydraulic bicycle and The Incompressibles' results through testing and at competition. This document includes justification for why key design parameters were chosen and how they are expected to achieve our performance goals. The hydraulic bicycle for the 2018-2019 season incorporated the same style characteristics as the previous year's team but were designed in a simpler fashion to increase the likelihood of success. The bike frame was modeled after a Trek bike to emulate a middle-ground performance bicycle and was designed to package the hydraulic components more efficiently. The bicycle was controlled with computer driven solenoids and utilize two chains, one before the pump and one after the motor. The bike benefited from the new hydraulic system that utilizes more appropriate poppet-style solenoid-driven valves to reduce internal leakage and the same bent-axis style pump and motor combination as in previous years due to their efficiency at our operating speeds. The mechatronics system was based on an Arduino system, using a pre-designed computer system to expedite the development time and ensure a properly controlled bicycle early in build season. A large majority of manufacturing was completed in house with the help of the Bike Builders club who let us borrow their bike frame fixtures, and guided us through the bike frame manufacturing process. Once the frame was manufactured, the hydraulic and mechatronics components were attached yielding a bike ready for preliminary testing. Testing the bike during the early Winter quarter months allowed us to diagnose and solve initial problems with the bike so it had a solid reliability during competition. We ran into drivetrain rideability problems, leaking fittings and mechatronics faults, but were able to solve them in time to have a ready bike for competition. Testing results showed that our bike deviated slightly with our initial performance estimates and goals, but our competition results of 2<sup>nd</sup> overall proved that our bike was still competitive and our design was solid. Overall, we were able to develop a bike starting with a design concept and following the design process through, to produce a competitive vehicle which yielded great results at competition and can serve as a foundation for the next team to continue.



## REFERENCES

“Fluid Power Vehicle Challenge | Interactive Science.” *Fluid Power Challenge*,  
nfpahub.com/fpc/vehicle-challenge/.

“Online Gantt Chart Software” *TeamGantt*, www.teamgantt.com/.

“Student Success Guide,” Department of Mechanical Engineering  
California Polytechnic State University – San Luis Obispo, April 2018

## APPENDIX

### Attachment 1: Summary of Customer Needs

Summary of Customer Needs
The Vehicle Must Utilize Human Power and Use Fluid as Method of Transfer
The Vehicle Must Obey All NFPA Rules and Regulations
The Vehicle Must Be Safe
The Team Will Win Overall First Place
The Team Will Obtain the Fastest Endurance Time
The Team Will Obtain the Fastest Sprint Time
The Team Will Obtain the Highest Efficiency Score

# Attachment 2: Quality Function Deployment - House of Quality

QFD: House of Quality  
 Project: The Incompressibles  
 Revision: V1  
 Date: 4/23/2018

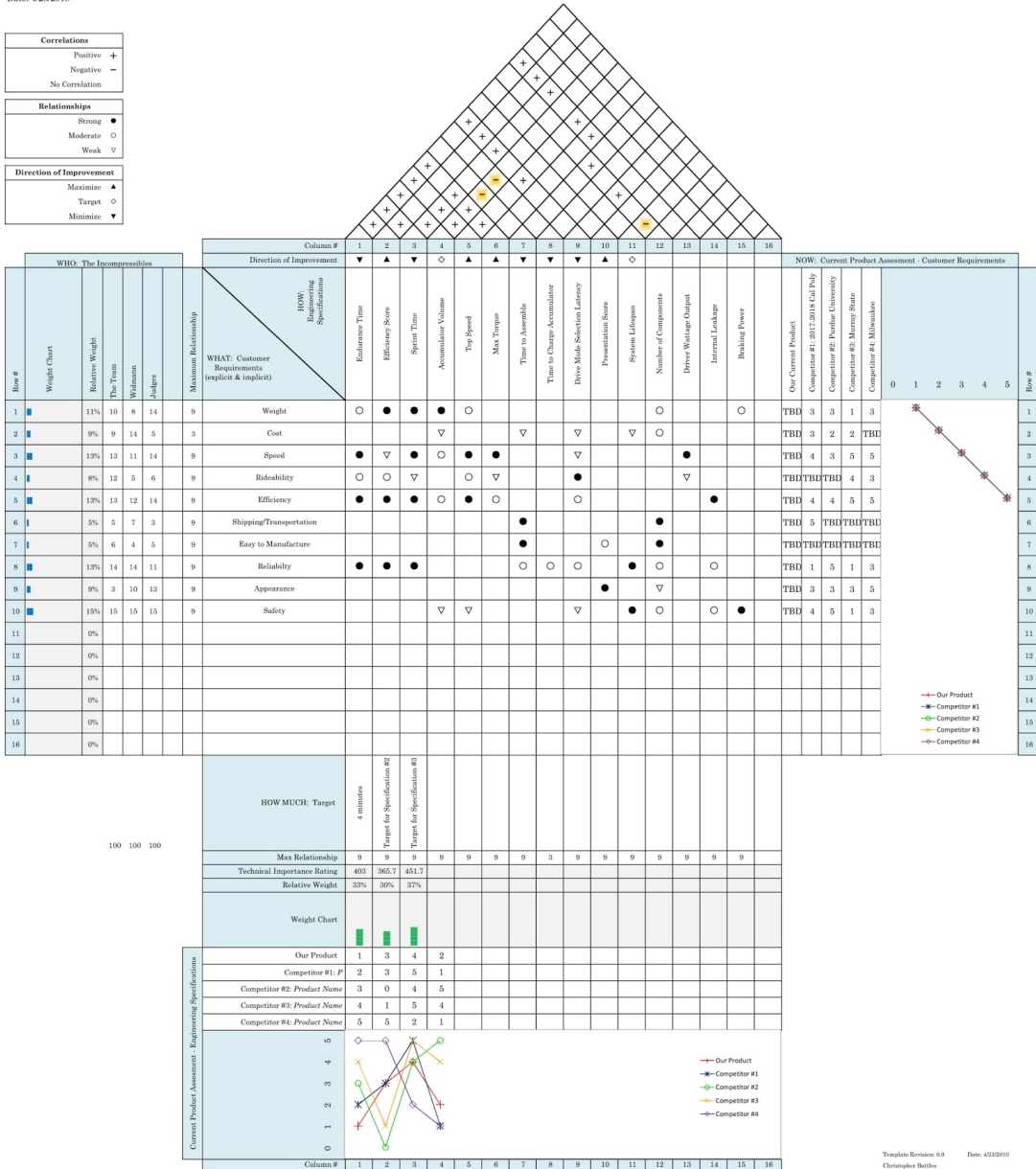
Correlations	
Positive	+
Negative	-
No Correlation	

Relationships	
Strong	●
Moderate	○
Weak	▽

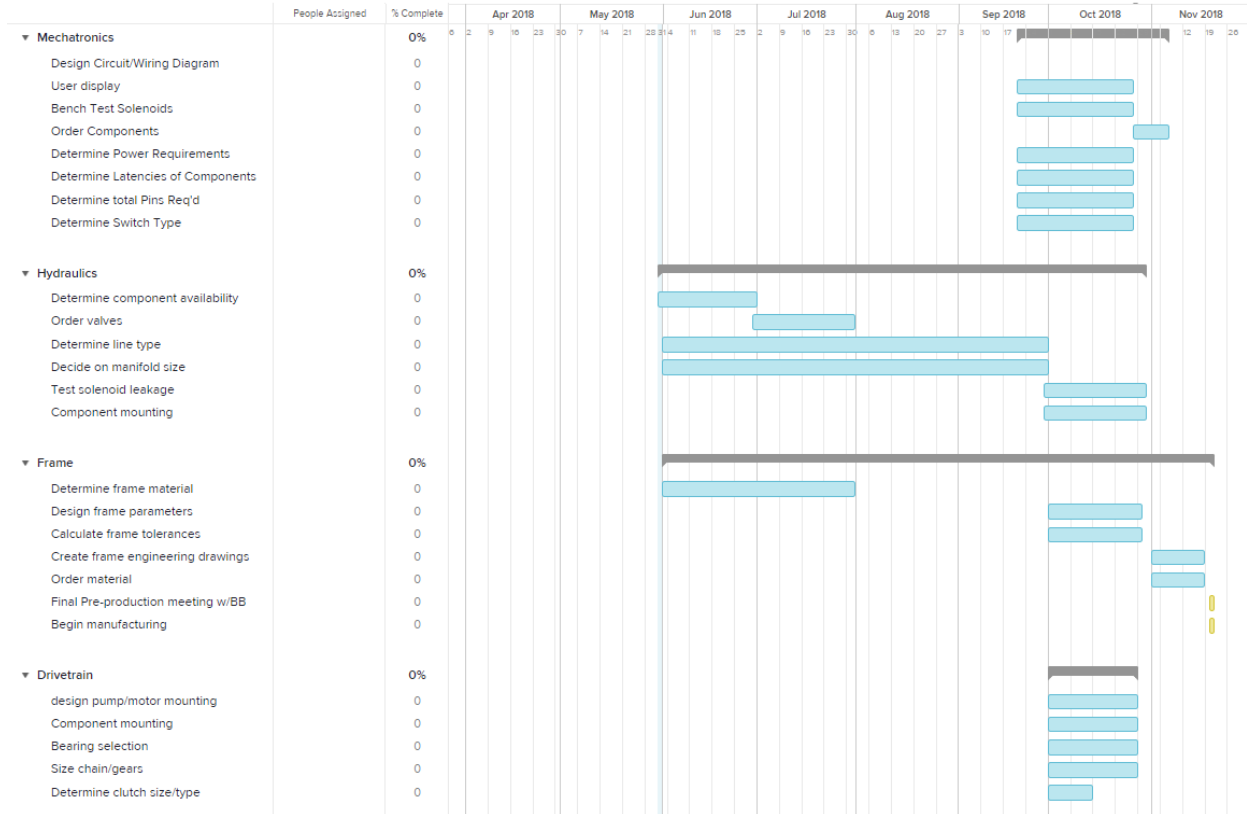
  

Direction of Improvement	
Maximize	▲
Target	○
Minimize	▼



Template Revision: 0.9 Date: 05/20/10  
 Christopher Bartke

# Attachment 3: Comprehensive Gantt Chart



## Attachment 4: Decision Matrices

### *Weighted design matrix for different types of bikes*

Criteria	Weight (0-5)	Frame Concept				
		Upright Standard	Recumbent	MonoWheel	Prone Bike	Velomobile
Weight	4	Datum	-4	-4	0	0
Cost	3		-3	-3	-3	-3
Reliability	5		0	0	0	0
Handling	3		-3	-3	-3	-3
Manufacturability	3		-3	-3	-3	-3
Packaging Flexibility	3		3	-3	0	-3
Driver Comfort	2		0	-2	-2	0
Aero Dynamics	2		2	-2	2	2
<b>Total</b>				-8	-20	-9

### *Weighted design matrix for drivetrain connections*

Criteria	Weight (0-5)	Power Transmission		
		Planetary Gearbox	Sprocket & Chain	Gear Train
Weight	3	Datum	0	-3
Size/packaging	4		-4	-4
Cost	3		3	0
Reliability	5		0	0
Efficiency	5		0	0
<b>Total</b>				-1

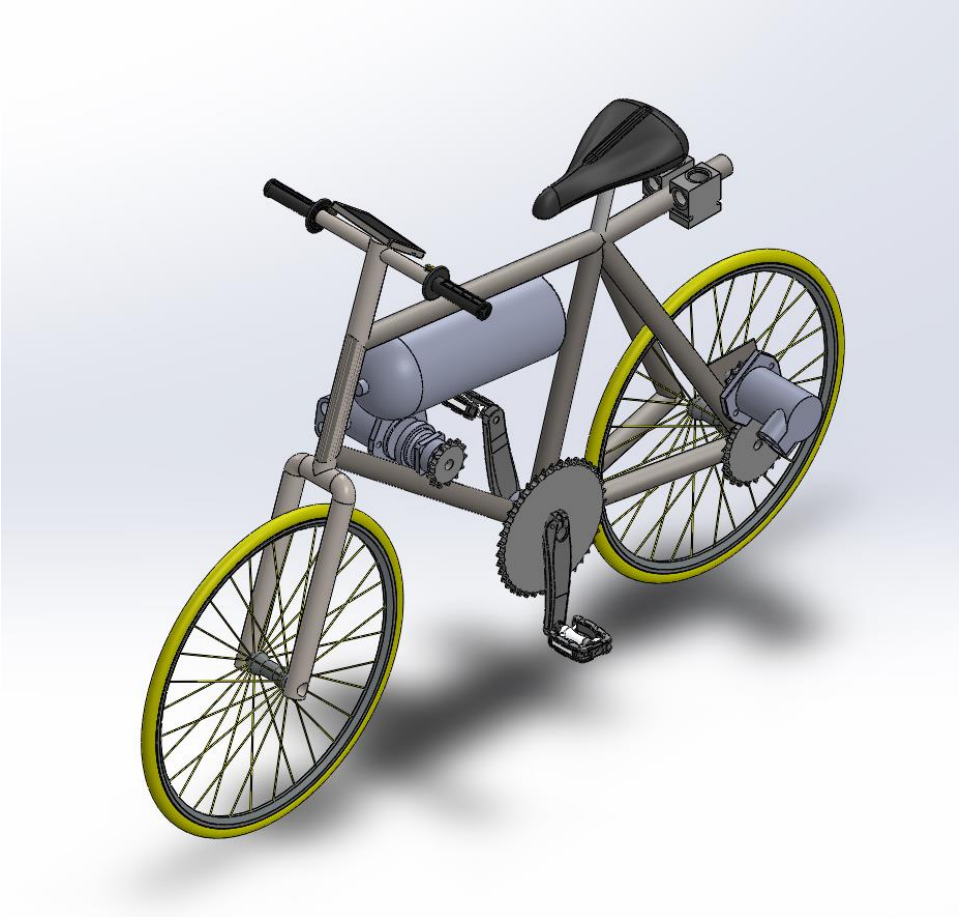
*Weighted decision matrix for mechatronics controller selection*

Criteria	Weight (0-5)	Mechatronics Controller Board		
		Custom In-House	Arduino	Raspberry Pi
Cost	2	Datum	0	0
Implementation Time	5		5	5
Simplicity	3		3	0
Reliability	5		5	5
Support	3		3	3
Versatility/Robustness	4		4	4
<b>Total</b>				20

*Weighted design matrix for power decoupling mechanism*

Criteria	Weight (0-5)	Power Transmission		
		Planetary Gearbox	Sprocket & Chain	Gear Train
Weight	3	Datum	0	-3
Size/packaging	4		-4	-4
Cost	3		3	0
Reliability	5		0	0
Efficiency	5		0	0
<b>Total</b>				-1

**Attachment 5: Concept Drawing**



Conceptual Bike Layout

## Attachment 6: Mechatronics Code

```
#include <SPI.h> //serial interface library
#include <Adafruit_GFX.h> //graphical element library
#include "Adafruit_ILI9340.h" //LCD library

#define _sclk 13 //these are the LCD inputs
#define _miso 12
#define _mosi 11
#define _cs 10
#define _dc 9
#define _rst A0

Adafruit_ILI9340 tft = Adafruit_ILI9340(_cs, _dc, _rst); //instantiating an
LCD object

#define key4 4 //assigning names to pins
#define key2 5
#define key3 6
#define key1 7

#define relay1 A0
#define relay2 A1
#define relay3 A2
#define relay4 A3

//naming some colors

#define LTBLUE 0xB6DF
#define LTTEAL 0xBF5F
#define LTGREEN 0xBFF7
#define LTCYAN 0xC7FF
#define LTRED 0xFD34
#define LTMAGENTA 0xFD5F
#define LTYELLOW 0xFFF8
#define LTORANGE 0xFE73
#define LTPINK 0xFDDF
#define LTPURPLE 0xCCFF
#define LTGREY 0xE71C

#define BLUE 0x001F
#define TEAL 0x0438
#define GREEN 0x07E0
#define CYAN 0x07FF
#define RED 0xF800
#define MAGENTA 0xF81F
#define YELLOW 0xFFE0
#define ORANGE 0xFD20
#define PINK 0xF81F
#define PURPLE 0x801F
#define GREY 0xC618
#define WHITE 0xFFFF
#define BLACK 0x0000

#define DKBLUE 0x000D
```



```

#define DKTEAL          0x020C
#define DKGREEN         0x03E0
#define DKCYAN          0x03EF
#define DKRED           0x6000
#define DKMAGENTA       0x8008
#define DKYELLOW        0x8400
#define DKORANGE        0x8200
#define DKPINK          0x9009
#define DKPURPLE        0x4010
#define DKGREY          0x4A49

//#define hallSensor 3

int currentSpeed = 0;           //initializing variables
int mode = 0;
int newMode = 0;

int lastKey = 0;
long count = 0;

int pressureVoltage = 0;

int hallState = 0;
int hallCounter = 0;

boolean graph_1 = true;
boolean graph_2 = true;
boolean graph_3 = true;
boolean graph_4 = true;
boolean graph_5 = true;
boolean graph_6 = true;
boolean graph_7 = true;

//hall effect stuff -----

int REV = 0;                    //more variables
//int RPM = 0;
unsigned long rpm = 0;
//long rpmConstant = 60*1000*5;

//long time = 0;
int flag = 1;

unsigned long currentTime = 0;
unsigned long previousTime = 0;
unsigned long idleTime = 0;

int maxRPM = 0;

//this is our logo

```

```

const unsigned char myBitmapBitmap2 [] PROGMEM = {
  // 'incompressibles_logo_small_V1, 35x29px
  0x00, 0x00, 0x00, 0x00, 0x00, 0x00, 0x00, 0x40, 0x00, 0x00, 0x00, 0x00,
  0xc0, 0x00, 0x00, 0x00,
  0x00, 0xc0, 0x00, 0x00, 0x00, 0x01, 0xe0, 0x00, 0x00, 0x00, 0x03, 0xf0,
  0x00, 0x00, 0x00, 0x03,
  0xf0, 0x00, 0x00, 0x00, 0x07, 0xf8, 0x00, 0x00, 0x00, 0x3f, 0xf8, 0x00,
  0x00, 0x00, 0xff, 0xf8,
  0x00, 0x00, 0x03, 0xff, 0xf8, 0x00, 0x00, 0x0f, 0xfe, 0x98, 0x02, 0x00,
  0x1f, 0x82, 0x30, 0x01,
  0x00, 0x3e, 0x00, 0x00, 0x00, 0x80, 0x3c, 0x00, 0x00, 0x00, 0xc0, 0x78,
  0x00, 0x00, 0x00, 0xc0,
  0x70, 0x00, 0x10, 0x00, 0xc0, 0xe0, 0x01, 0xf0, 0x00, 0xe0, 0xe0, 0x01,
  0xf0, 0x00, 0xe0, 0x60,
  0x01, 0xf0, 0x01, 0xe0, 0x60, 0x01, 0xf0, 0x01, 0xc0, 0x60, 0x01, 0xf0,
  0x03, 0xc0, 0x20, 0x01,
  0xf0, 0x0f, 0x80, 0x10, 0x01, 0xf0, 0x1f, 0x00, 0x08, 0x01, 0xf0, 0xfe,
  0x00, 0x00, 0x01, 0xff,
  0xf8, 0x00, 0x00, 0x01, 0xff, 0xf0, 0x00, 0x00, 0x01, 0xff, 0x80, 0x00,
  0x00, 0x01, 0xf0, 0x00,
  0x00
};

//-----

void setup() {
  // put your setup code here, to run once:

  Serial.begin(9600); //initializes serial connection
  to computer
  Serial.println("wassup tho...");

  pinMode(key1, INPUT_PULLUP); //set pins allocated to the buttons
  as inputs pullups
  pinMode(key2, INPUT_PULLUP);
  pinMode(key3, INPUT_PULLUP);
  pinMode(key4, INPUT_PULLUP);

  //pinMode(hallSensor, INPUT_PULLUP);

  //pinMode(2, OUTPUT);

  pinMode(relay1, OUTPUT); //set pins for solenoids as outputs
  pinMode(relay2, OUTPUT);
  pinMode(relay3, OUTPUT);
  pinMode(relay4, OUTPUT);

  Serial.println("Starting Program...");
}

```

```

tft.begin(); //begin writing to display
tft.setRotation(3);
tft.fillScreen(ILI9340_BLACK);

digitalWrite(relay1, LOW); //start in direct drive mode
digitalWrite(relay2, LOW);
digitalWrite(relay3, LOW);
digitalWrite(relay4, LOW);

//Serial.println(testFilledCircles(10, ILI9340_MAGENTA)); //starting
screen animation
//Serial.println(testCircles(10, ILI9340_WHITE));
//delay(500);

tft.fillScreen(ILI9340_BLACK);

tft.drawBitmap(0, 0, myBitmapBitmap, 321, 240, TEAL); //OUR LOGO SO
COOL HECK YA

delay(2000);
tft.fillScreen(ILI9340_BLACK);

tft.drawLine(190, 0, 190, 130, ILI9340_WHITE); //setting up
all the static LCD elements
tft.drawLine(190, 130, 340, 130, ILI9340_WHITE);

tft.setCursor(20,70);
tft.setTextColor(ILI9340_WHITE);
tft.setTextSize(2);
//tft.print("Pressure");

tft.setCursor(200,20);
tft.setTextColor(CYAN);
tft.setTextSize(2);
tft.print("DRIVE MODE");
tft.setCursor(200,35);
tft.print("-----");
//tft.setTextColor(ILI9340_RED);

tft.setTextColor(ILI9340_GREEN);
tft.setCursor(240,50);
tft.print("Direct");

tft.setTextColor(ILI9340_RED);
tft.setCursor(240,68);
tft.println("Clutch");

tft.setCursor(240,86);
tft.println("Boost ");

tft.setCursor(240,104);
tft.println("Regen ");

```

```

tft.setCursor(20,170);
tft.setTextColor(ILI9340_MAGENTA);
tft.setTextSize(2);
//tft.print("Speed (RPM) = ");

tft.setCursor(225,170);
tft.print("Max = ");

tft.setCursor(0,10);
tft.setTextColor(ILI9340_YELLOW);
tft.setTextSize(2);
tft.print("Cal ");
tft.println("Poly");

tft.drawLine(0, 42, 190, 42, ILI9340_WHITE);

tft.drawBitmap(115, 0, myBitmapBitmap2, 35, 29, TEAL);

//tft.setTextColor(ILI9340_BLACK,ILI9340_WHITE);
//tft.setTextSize(2);
//tft.println("GROOP");

attachInterrupt(digitalPinToInterrupt(2), RPMCount, FALLING);

//configures pin 2 as an interrupt for FALLING inputs
//upon interrupt, the function RPMCount will be run

}
//-----

void loop() {
  // put your main code here, to run repeatedly:

  if (flag==1) //once a new RPM has
  been calculated, print it
  {
    tft.setTextColor(ILI9340_WHITE, ILI9340_BLACK);
    tft.setCursor(200,170);

```

```

//tft.print("  ");
//tft.drawRect(200, 200, 100, 100, ILI9340_BLACK);

tft.setCursor(200,170);
tft.setTextColor(ILI9340_MAGENTA);
tft.setTextSize(2);
//tft.print(rpm);

DrawBarChartH(tft, 0, 180, 135, 30, 0, 1000, 250, rpm, 3, 0, GREEN,
DKGREEN, GREEN, WHITE, BLACK, "RPM", graph_1);

if(rpm>maxRPM) //also update the max
RPM when necessary
{
  maxRPM = rpm;
  tft.setTextColor(ILI9340_WHITE, ILI9340_BLACK);
  tft.setCursor(250,198);
  tft.print("  ");
  tft.setCursor(250,198);
  tft.setTextColor(ILI9340_MAGENTA);
  tft.setTextSize(2);
  tft.print(maxRPM);
}

flag = 0;
rpm = 0;
}

int key1S = digitalRead(key1); //read the button pins to check
for any button presses
int key2S = digitalRead(key2);
int key3S = digitalRead(key3);
int key4S = digitalRead(key4);

if(!key1S){ //if key 1 is low, set mode to
be 1 (remember INPPUT_PULLUP)
  //Serial.println("key 1");
  mode = 1; //also checks for repeat button
presses and ignores them
  if (lastKey !=1){
    newMode = 1;
    lastKey = 1;
  }
}

if(!key2S){
  //Serial.println("key 2");
  mode = 2;
  if (lastKey !=2){
    newMode = 1;
  }
}

```

```

        lastKey = 2;
    }
}

if(!key3S){
    //Serial.println("key 3");
    mode = 3;
    if (lastKey !=3){
        newMode = 1;
        lastKey = 3;
    }
}

if(!key4S){
    //Serial.println("key 4");
    mode = 4;
    if (lastKey !=4){
        newMode = 1;
        lastKey = 4;
    }
}

if (newMode==1){

//if a new mode has been set, make the
appropriate changes

    if(mode==1){

        tft.setCursor(240,50);
        tft.setTextColor(ILI9340_GREEN);
        tft.print("Direct");

        digitalWrite(relay1, LOW); //if its mode 1, print the text in
green, otherwise print it in red
        digitalWrite(relay2, LOW);
        digitalWrite(relay3, LOW);
        digitalWrite(relay4, LOW);

        //Serial.println("printing");
    }
    else {

        tft.setCursor(240,50);
        tft.setTextColor(ILI9340_RED);
        tft.print("Direct");

        //digitalWrite(relay1, LOW);
    }

if(mode==2){

```

```

tft.setCursor(240,68);
tft.setTextColor(ILI9340_GREEN);
tft.println("Clutch");

digitalWrite(relay1, HIGH);
digitalWrite(relay2, LOW);
digitalWrite(relay3, LOW);
digitalWrite(relay4, HIGH);

}
else{

tft.setCursor(240,68);
tft.setTextColor(ILI9340_RED);
tft.println("Clutch");

//digitalWrite(relay2, LOW);
}

if(mode==3){

tft.setCursor(240,86);
tft.setTextColor(ILI9340_GREEN);
tft.println("Boost ");

digitalWrite(relay1, HIGH);
digitalWrite(relay2, HIGH);
digitalWrite(relay3, LOW);
digitalWrite(relay4, LOW);
}
else {

tft.setCursor(240,86);
tft.setTextColor(ILI9340_RED);
tft.println("Boost ");

//digitalWrite(relay3, LOW);
}

if(mode==4){

tft.setCursor(240,104);
tft.setTextColor(ILI9340_GREEN);
tft.println("Regen ");

digitalWrite(relay1, HIGH);
digitalWrite(relay2, LOW);
digitalWrite(relay3, HIGH);
digitalWrite(relay4, HIGH);
}
else {

tft.setCursor(240,104);

```

```

    tft.setTextColor(ILI9340_RED);
    tft.println("Regen ");

    //digitalWrite(relay4, LOW);
}

newMode = 0;
}

}
//-----

unsigned long testFilledCircles(uint8_t radius, uint16_t color) {
    unsigned long start;
    int x, y, w = tft.width(), h = tft.height(), r2 = radius * 2;

    tft.fillScreen(ILI9340_BLACK);
    //startup animation
    start = micros();
    for(x=radius; x<w; x+=r2) {
        for(y=radius; y<h; y+=r2) {
            tft.fillCircle(x, y, radius, color);
        }
    }
}

unsigned long testCircles(uint8_t radius, uint16_t color) {
    unsigned long start;
    int x, y, r2 = radius * 2, //also a
    startup animation
        w = tft.width() + radius,
        h = tft.height() + radius;

    // Screen is not cleared for this one -- this is
    // intentional and does not affect the reported time.
    start = micros();
    for(x=0; x<w; x+=r2) {
        for(y=0; y<h; y+=r2) {
            tft.drawCircle(x, y, radius, color);
        }
    }
}

void RPMCount() // this gets called as an interrupt when pin two goes
from HIGH to LOW
{
    REV++;

    currentTime = millis() - previousTime;
    previousTime = millis();
}

```



```

idleTime += currentTime;

if (REV >=3)
{
    rpm = (1000UL*60*REV)/idleTime;

    REV = 0;
    idleTime = 0;
    flag = 1;
}
}

void DrawBarChartH(Adafruit_ILI9340 & d, double x , double y , double w,
double h , double loval , double hival , double inc , double curval , int
dig , int dec, unsigned int barcolor, unsigned int voidcolor, unsigned int
bordercolor, unsigned int textcolor, unsigned int backcolor, String label,
boolean & redraw)
{
    double stepval, range;
    double mx, level;
    double i, data;

    // draw the border, scale, and label once
    // avoid doing this on every update to minimize flicker
    // draw the border and scale
    if (redraw == true) {
        redraw = false;
        d.drawRect(x , y , w, h, bordercolor);
        d.setTextColor(textcolor, backcolor);
        d.setTextSize(2);
        d.setCursor(x , y - 20);
        d.println(label);
        // step val basically scales the hival and low val to the width
        stepval = inc * (double (w) / (double (hival - loval))) - .00001;
        // draw the text
        for (i = 0; i <= w; i += stepval) {
            d.drawFastVLine(i + x , y + h + 1, 5, textcolor);
            // draw lables
            d.setTextSize(1);
            d.setTextColor(textcolor, backcolor);
            d.setCursor(i + x , y + h + 10);
            // adding a small value to eliminate round off errors
            // this val may need to be adjusted
            data = ( i * (inc / stepval)) + loval + 0.00001;
            d.println(Format(data, dig, dec));
        }
    }
    // compute level of bar graph that is scaled to the width and the hi and
low vals
    // this is needed to accomodate for +/- range capability

```

```

    // draw the bar graph
    // write a upper and lower bar to minimize flicker cause by blanking out
bar and redraw on update
    level = (w * (((curval - loval) / (hival - loval))));
    d.fillRect(x + level + 1, y + 1, w - level - 2, h - 2, voidcolor);
    d.fillRect(x + 1, y + 1, level - 1, h - 2, barcolor);
    // write the current value
    d.setTextColor(textcolor, backcolor);
    d.setTextSize(2);
    d.setCursor(x + w + 10, y + 5);
    d.println(Format(curval, dig, dec));
}

```

```

String Format(double val, int dec, int dig ) {
    int addpad = 0;
    char sbuf[20];
    String condata = (dtostrf(val, dec, dig, sbuf));

    int slen = condata.length();
    for ( addpad = 1; addpad <= dec + dig - slen; addpad++) {
        condata = " " + condata;
    }
    return (condata);
}

```

# Attachment 7: Safety Hazard Checklist

## DESIGN HAZARD CHECKLIST

Team: The Incompressibles Advisor: John Fabijanac Date: 5/29/2018

- Y N
- 1. Will the system include hazardous revolving, running, rolling, or mixing actions?
  - 2. Will the system include hazardous reciprocating, shearing, punching, pressing, squeezing, drawing, or cutting actions?
  - 3. Will any part of the design undergo high accelerations/decelerations?
  - 4. Will the system have any large (>5 kg) moving masses or large (>250 N) forces?
  - 5. Could the system produce a projectile?
  - 6. Could the system fall (due to gravity), creating injury?
  - 7. Will a user be exposed to overhanging weights as part of the design?
  - 8. Will the system have any burrs, sharp edges, shear points, or pinch points?
  - 9. Will any part of the electrical systems not be grounded?
  - 10. Will there be any large batteries (over 30 V)?
  - 11. Will there be any exposed electrical connections in the system (over 40 V)?
  - 12. Will there be any stored energy in the system such as flywheels, hanging weights or pressurized fluids/gases?
  - 13. Will there be any explosive or flammable liquids, gases, or small particle fuel as part of the system?
  - 14. Will the user be required to exert any abnormal effort or experience any abnormal physical posture during the use of the design?
  - 15. Will there be any materials known to be hazardous to humans involved in either the design or its manufacturing?
  - 16. Could the system generate high levels (>90 dBA) of noise?
  - 17. Will the device/system be exposed to extreme environmental conditions such as fog, humidity, or cold/high temperatures, during normal use?
  - 18. Is it possible for the system to be used in an unsafe manner?
  - 19. For powered systems, is there an emergency stop button?
  - 20. Will there be any other potential hazards not listed above? If yes, please explain on reverse.

For any "Y" responses, add (1) a complete description, (2) a list of corrective actions to be taken, and (3) date to be completed on the reverse side.

Description of Hazard	Planned Corrective Action	Planned Date	Actual Date
Hazardous revolving, running, rolling, reciprocating, shearing, revolving actions	Chain guards blocking gears/chains Place components away from limb extremities		
High accelerations/ decelerations	Have easy/sturdy way for rider to grip handlebars to control bike and restrain feet for pedaling		
Large moving masses/forces	Stay a safe distance away from bike while its operating		
Projectile	Make sure lines are bled properly & energy storage devices are pointed away from the rider.		
stored energy	Do not over-fill accumulator. Make sure deactivated solenoids do not discharge occur.		
System Used in unsafe manner	Take proper precautions to ride bike correctly and carefully		
Emergency stop	Implement sufficiently strong brakes and emergency accumulator discharge		

# Attachment 8: Drawings

ITEM NO.	PART NUMBER	QTY.
1	Seat Tube	1
2	Head Tube	1
3	Bottom Bracket	1
4	Top Tube	1
5	Down Tube	1
6	Seatstay - Right Tube	1
7	Chainstay - Right Tube	1
8	Vertical Support Tube - Right	1
9	Upper Support Tube - Right	1
10	Rear Dropout - Right	1
11	Rear Dropout - Left	1
12	Vertical Support Tube - Left	1
13	Seatstay - Left Tube	1
14	Chainstay - Left Tube	1
15	Rear Brake Bridge	1
16	Chainstay Bridge	1
17	Upper Support Tube - Left	1

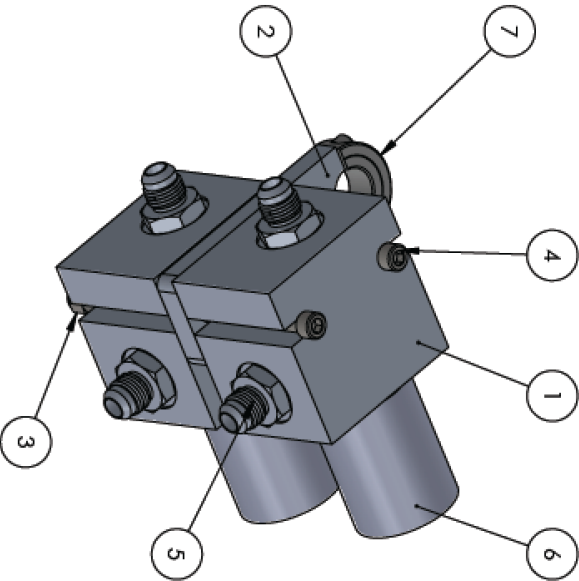
Drawn By: _____ Checked By: _____ Start Date: 10/27/18 Requested End Date: xx/xx/xx	Nicholas Choidolan Mechanical Engineering
--	--

DIMENSIONS ARE IN INCHES TOLERANCES: FRACTIONAL: ± 1/8 ANGULAR: MACH ± 1° 8RD ± 2° TWO PLACE DECIMAL: ± 0.05 THREE PLACE DECIMAL: ± 0.005 TOLERANCED PARTS: MFG	TITLE: <b>Frame Assembly BOM</b>	REV: <b>A</b>
SCALE: 1:7	MATERIAL: 4130 Steel	1 OF 1

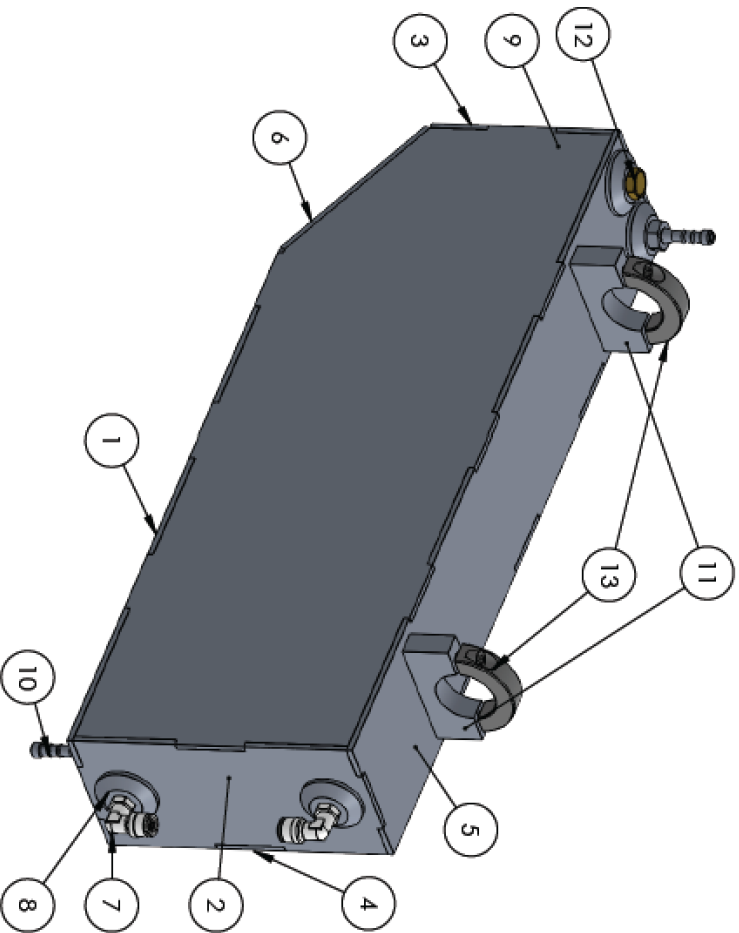
SOLIDWORKS Educational Product. For Instructional Use Only.

Part Name	P/N	Balloon #
Line Body	700-01	1
Mount	700-02	2
1/4" Bolt	700-03	3
1/4" Nut	700-04	4
SAE -6AN	700-05	5
Solenoid	700-06	6
Upper Mount	700-07	7



<b>The Incompressibles Senior Project</b> California Polytechnic State University - San Luis Obispo Mechanical Engineering		Drawn By: ALEX KNICKERBOCKER Checked By: JOHN FABULANIC	Start Date: 10/26/18 Requested End Date: 10/27/18	UNLESS OTHERWISE SPECIFIED: DIMENSIONS ARE IN INCHES TOLERANCES: FINISHES: RADIUSES: 1/8" ANGLES: 45° HOLE FINISH: 2:1 BRND 2° THREADS: 2:1 THREE PLACE DECIMALS: ± 0.005 TOLERANCING PER: MMC	TITLE: <b>700</b>	REV <b>A</b>
		SCALE: 1:2	MATERIAL: -	1 OF 1		

Part Name	P/N	Balloon #
Res. Bot. Panel	500-01	1
Res. Rear Panel	500-02	2
Res. Front Panel	500-03	3
Res. Right Panel	500-04	4
Res. Top Panel	500-05	5
Res. Angle Panel	500-06	6
1/4" 90Deg Push Fit.	500-07	7
1/4" NPT Weld Bung	500-08	8
Res. Left Panel	500-09	9
1/4" Barb Fit.	500-10	10
Weld Mount	500-11	11
1/4" Vent	500-12	12
Upper Mount	500-13	13



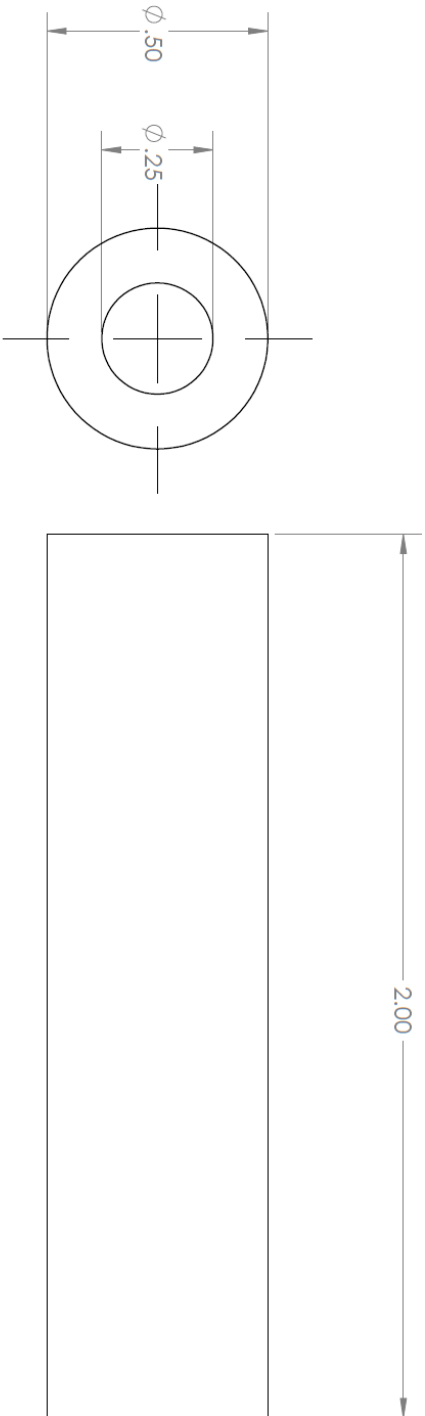
The Incompressibles Senior Project California Polytechnic State University - San Luis Obispo Mechanical Engineering		Drawn By: ALEX KNICKERBOCKER Checked By: JOHN FABLIANIC	Start Date: 10/26/18 Requested End Date: 10/27/18	UNLESS OTHERWISE SPECIFIED: DIMENSIONS ARE IN INCHES TOLERANCES: FINISHES: 1/8" ANGLES: ALL: 45° TWO PLACE DECIMAL: ±.005 THREE PLACE DECIMAL: ±.0005 TOLERANCING PER: ASME	TITLE: <h1>500</h1>	REV <h1>A</h1>
SCALE: 1:3		MATERIAL: 6061-T6		1 OF 1		

ITEM NO.	PART NUMBER	DESCRIPTION	QTY.
1	Wheel	Fixie Rear Wheel	1
2	Motor	Bent Axis Motor	1
3	Mounting Plate Motor	Rear Drivetrain Mounting Plate	1
4	2299K18	McMaster 12 tooth sprocket	1
5	2299K35	McMaster 35 tooth sprocket	1
6	92511A085	Motor Standoffs	4
7	91247A553	1/4"-20 2 3/4" Bolt	4

The Incompressibles Senior Project California Polytechnic State University - San Luis Obispo Mechanical Engineering		Drawn By: <b>David Vitt</b>	Start Date: Requested End Date:
DIMENSIONS ARE IN INCHES TOLERANCES: FRACTIONAL: ± 1/8 ANGULAR: MACH ± 1° BEND ± 2° TWO PLACE DECIMAL: ± 0.05 THREE PLACE DECIMAL: ± 0.005 TOLERANCING PER: MMC		TITLE: <b>Rear Drivetrain</b> SCALE: 1:1 MATERIAL: N/A	
		REV	1 OF 1



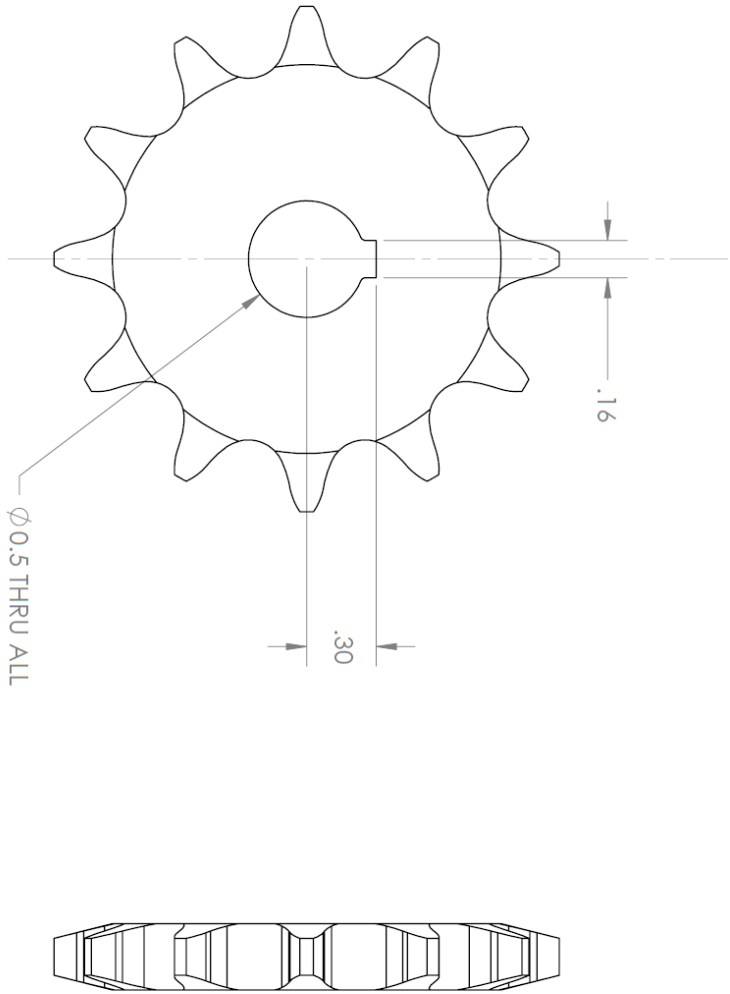


UNLESS OTHERWISE SPECIFIED:

DIMENSIONS ARE IN INCHES  
 TOLERANCES:  
 FRACTIONAL:  $\pm 1/8$   
 ANGULAR: MACH  $\pm 1^\circ$  BEND  $\pm 3^\circ$   
 TWO PLACE DECIMAL:  $\pm 0.005$   
 THREE PLACE DECIMAL:  $\pm 0.0005$   
 TOLERANCING PER: MMC

TITLE:	Standoff	REV
SCALE: 1:1	MATERIAL: Aluminum	A
		1 OF 1

The Incompressibles Senior Project	Drawn By:	David Vitt	Start Date:	
California Polytechnic State University - San Luis Obispo	Checked By:		Requested	End Date:
Mechanical Engineering				



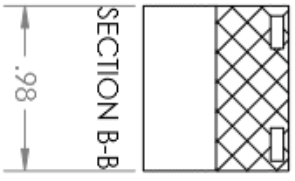
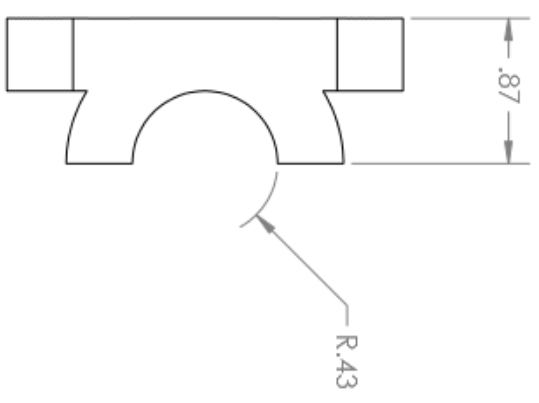
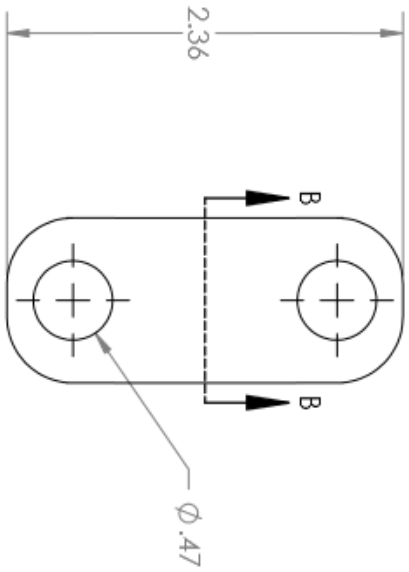
UNLESS OTHERWISE SPECIFIED:

DIMENSIONS ARE IN INCHES  
 TOLERANCES:  
 FRACTIONAL:  $\pm 1/8$   
 ANGULAR: MATCH  $\pm 1^\circ$  BEND  $\pm 2^\circ$   
 TWO PLACE DECIMAL:  $\pm 0.005$   
 THREE PLACE DECIMAL:  $\pm 0.0005$   
 TOLERANCING PER: MMMC

TITLE: **13 Tooth Sprocket**  
 SCALE: 1:1 MATERIAL: Steel  
 REV **A**  
 1 OF 1

**The Incompressibles Senior Project**  
 Drawn By: **David Vitt**  
 Checked By:  
 Start Date:  
 Requested End Date:

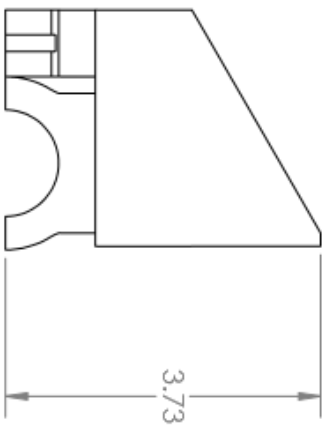
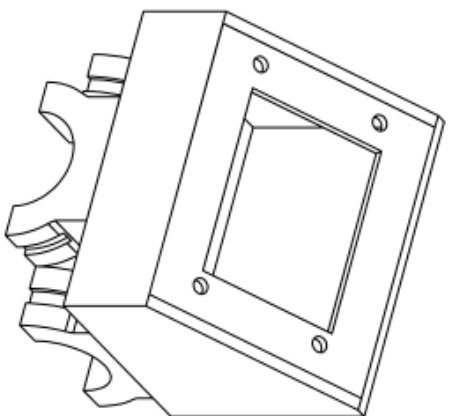
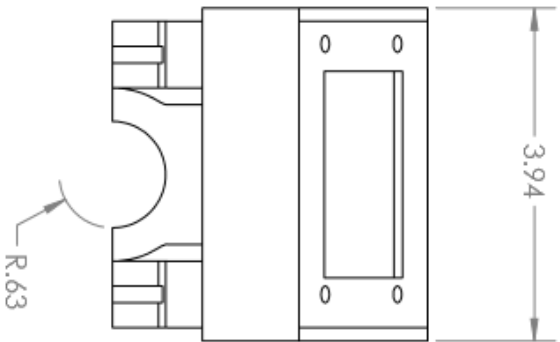
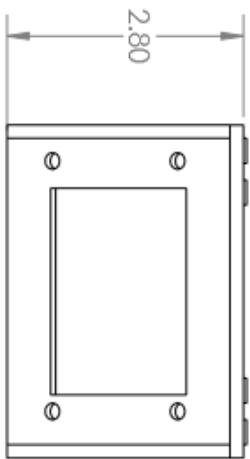
California Polytechnic State University - San Luis Obispo  
 Mechanical Engineering



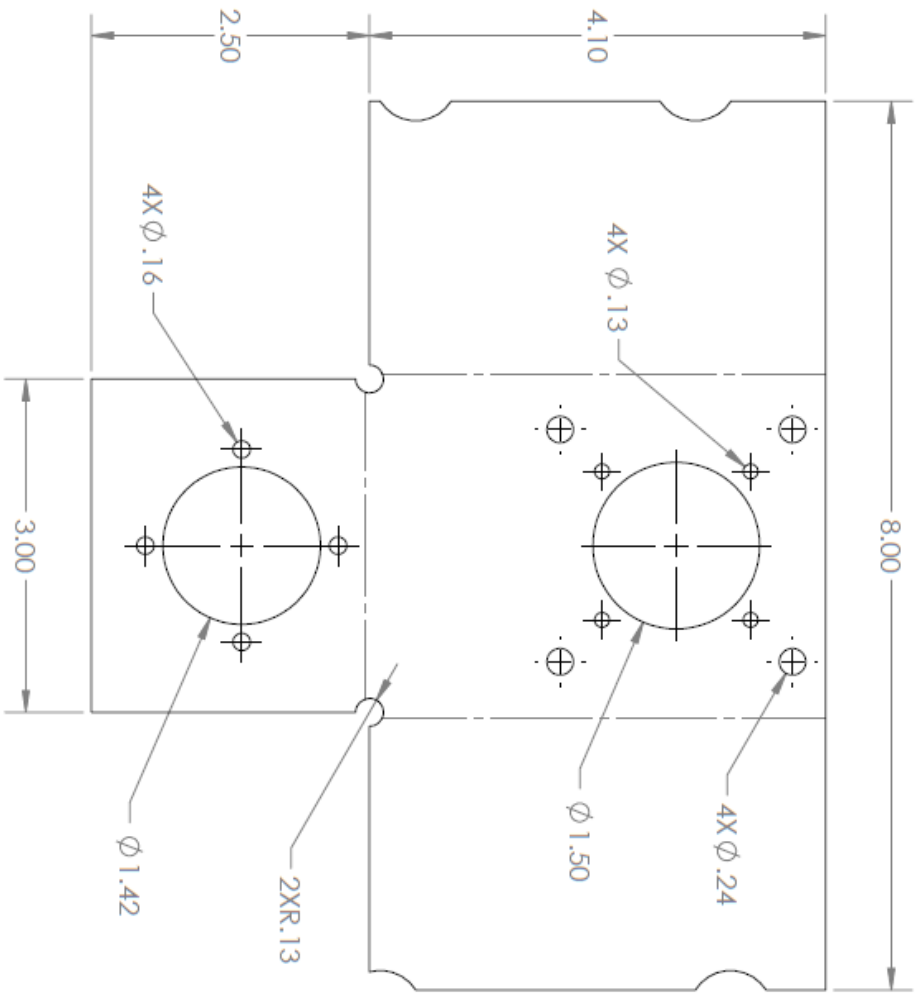
UNLESS OTHERWISE SPECIFIED:  
 DIMENSIONS ARE IN INCHES  
 TOLERANCES:  
 FRACTIONS:  $\pm 1/8$   
 ANGULAR: MACH  $\pm 1^\circ$  BEND  $\pm 2^\circ$   
 TWO PLACE DECIMAL:  $\pm 0.05$   
 THREE PLACE DECIMAL:  $\pm 0.005$   
 TOLERANCING PER: MVIC

TITLE:	REV
Button Enclosure	A
SCALE: 1:1	1 OF 1
MATERIAL: xxxxx xxx	

The Incompressibles Senior Project	Drawn By:	Julian Rodkiewicz	Start Date:
California Polytechnic State University - San Luis Obispo	Checked By:		Requested End Date:
Mechanical Engineering			



<p>UNLESS OTHERWISE SPECIFIED:</p> <p>DIMENSIONS ARE IN INCHES</p> <p>TOLERANCES:</p> <p>FRACTIONS: ± 1/8" BEND ±2°</p> <p>ANGULAR: MACH ±1°</p> <p>TWO PLACE DECIMAL: ± 0.05</p> <p>THREE PLACE DECIMAL: ± 0.005</p> <p>TOLERANCING PER: N/MC</p>		<p>TITLE:</p> <p><b>Display Enclosure</b></p> <p>SCALE: 1:1</p>	<p>REV</p> <p><b>A</b></p>
<p>California Polytechnic State University - San Luis Obispo</p> <p>Mechanical Engineering</p>	<p>Drawn By: <b>Julian Rodkiewicz</b></p> <p>Checked By:</p>	<p>Start Date: <b>xx/xx/xx</b></p> <p>Requested End Date: <b>xx/xx/xx</b></p>	<p>1 OF 1</p>
<p><b>The Incompressibles Senior Project</b></p>			

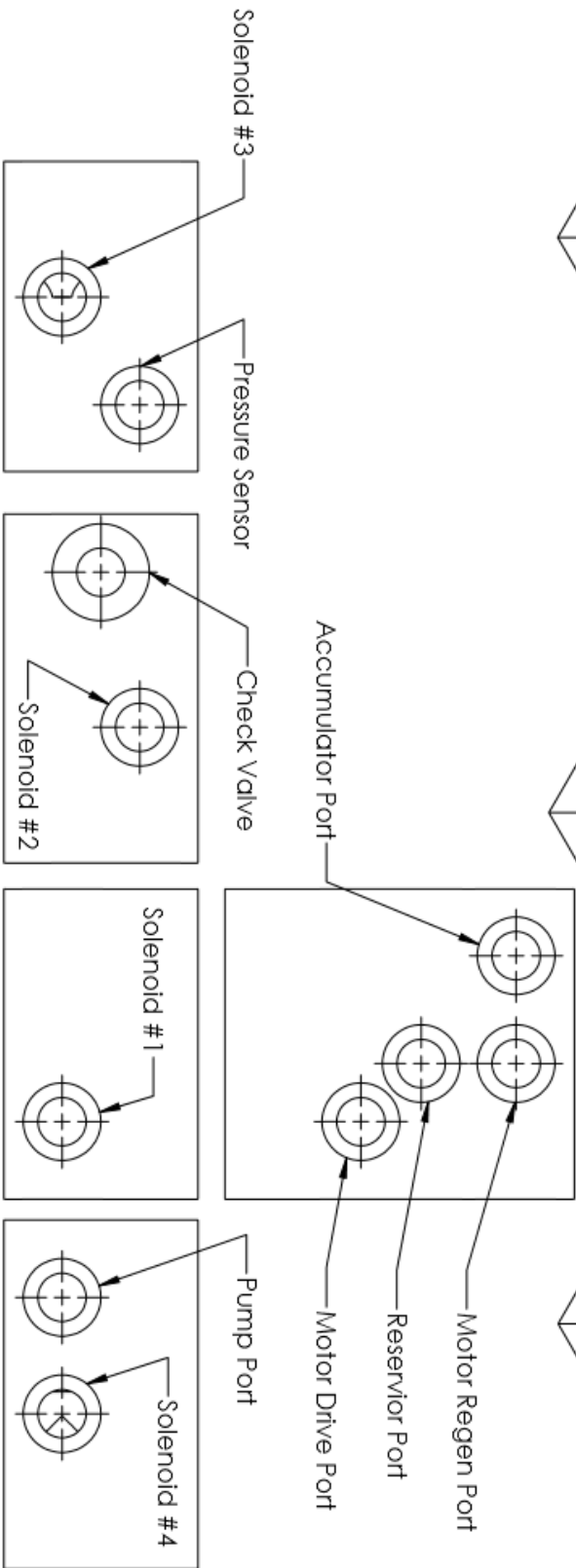
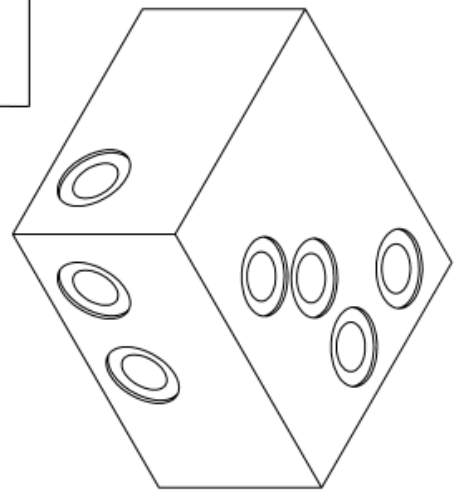
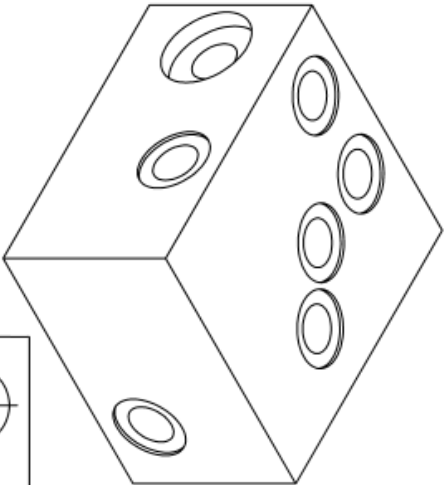
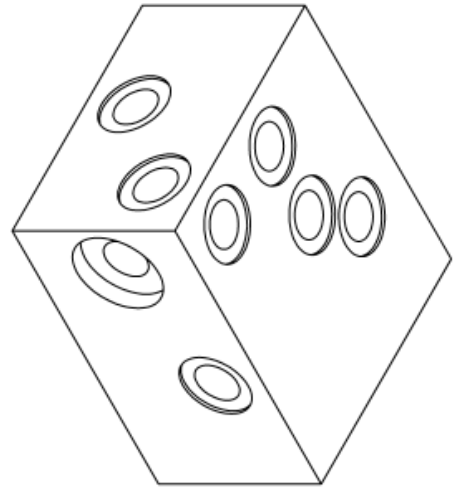


UNLESS OTHERWISE SPECIFIED:

DIMENSIONS ARE IN INCHES  
 TOLERANCES:  
 FRACTIONAL: ± 1/8  
 ANGULAR: MACH ± 1° BEND ± 2°  
 TWO PLACE DECIMAL: ± 0.05  
 THREE PLACE DECIMAL: ± 0.005  
 TOLERANCING PER: M/MC

The Incompressibles Senior Project		Drawn By:	Russell Posin	Start Date:	10/26/18
California Polytechnic State University - San Luis Obispo	Checked By:			Requester End Date:	xx/xx/xx

TITLE:	Front Drivetrain Mounting Bracket	REV	A
SCALE:	2:3	MATERIAL:	Alloy 4130 Annealed
			1 OF 1



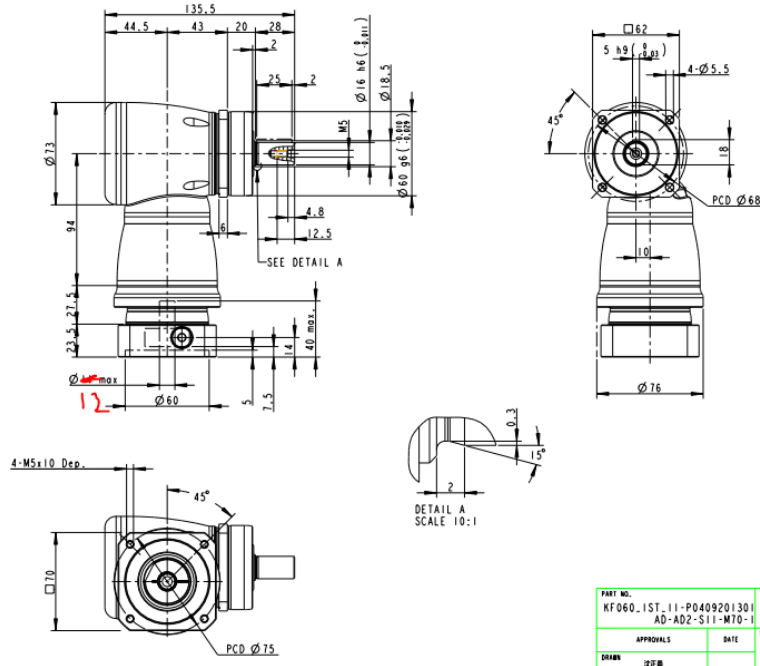
UNLESS OTHERWISE SPECIFIED:

- DIMENSIONS ARE IN INCHES
- TOLERANCES:
- FRACTIONAL: 1/8
- ANGULAR: MACH ±1° BEND ±2°
- TWO PLACE DECIMAL: ± 0.05
- THREE PLACE DECIMAL: ± 0.005
- TOLERANCING PER: MVIC

<b>The Incompressibles Senior Project</b>		Drawn By:	<b>Kyle Franck</b>	Start Date:	
California Polytechnic State University - San Luis Obispo		Checked By:		Requested End Date:	
		TITLE:		REV	
		<b>Manifold</b>		<b>A</b>	
		SCALE:	MATERIAL:	1 OF 1	

# Attachment 9: Specification Sheets

KF060 - 004 - S2 / ~~ATTENB...~~



PART NO. KF060_IST_11-P0409201301 AD-AD2-S11-M10-1			
APPROVALS	DATE	TITLE KF060_1 S10e_S11_RATIO: 3-10 AND MOTOR FLANGE MOUNTING	
DRAWN JZEM		DWG NO. KF060_IST_11-P0409201301	
CHECKED		SIZE A1	SCALE 1:1
APPROVED		REV	

## Attachment 10: Bill of Materials

Bill of Materials (BOM) - Frame The Incompressibles										Total Sub-System:	Total Project:
										\$340.89	\$2,516.95
Item #	Description	Material	Manufacturer PN	Manufacturer	Link	Qty.	Cost.	Price Extended	Date Received	Invoice Number	
1	Head Tube	Steel	NOV_COHT_46.4_220	Nova	<a href="https://www.cycle">https://www.cycle</a>	2	\$10.25	\$20.50	11/26/18	42883	
2	Top Tube	Steel	NOV_COTT_858	Nova	<a href="https://www.cycle">https://www.cycle</a>	2	\$16.50	\$33.00	11/26/18	42883	
3	Down Tube	Steel	NOV_CODT_38_969	Nova	<a href="https://www.cycle">https://www.cycle</a>	2	\$18.45	\$36.90	11/26/18	42883	
4	Seat Tube	Steel	NOV_COST_33.5_560	Nova	<a href="https://www.cycle">https://www.cycle</a>	2	\$18.80	\$37.60	11/26/18	42883	
5	Bottom Bracket Tube	Steel	NOV_LLBB_SL_73M	Nova	<a href="https://www.cycle">https://www.cycle</a>	2	\$6.00	\$12.00	11/26/18	42883	
6	Chain Stay Tube	Steel	6' of 0.75" X 0.065" 4130 Tub	Online Metals	<a href="https://www.onlin">https://www.onlin</a>	2	\$24.18	\$48.36		2340786	
7	Seat Stay Tube	Steel									
8	Support Tube	Steel	6' 0.625" X 0.065" 4130 Tube	Online Metals	<a href="https://www.onlin">https://www.onlin</a>	4	\$31.43	\$125.72		2340786	
9	Upper Support Tube	Steel									
10	Tube Bridges	Steel	1' 0.5" X 0.065 4130 Tube	Online Metals	<a href="https://www.onlin">https://www.onlin</a>	1	\$9.26	\$9.26	11/26/18	2326586	
11	Rear Dropouts	Steel	2' of 0.25" x 3" 1018 Sheet	Online Metals	<a href="https://www.onlin">https://www.onlin</a>	1	\$14.93	\$14.93		2340786	
12	Cantilever Brake Studs	Steel	8mm Brake Stud	Nova	<a href="https://www.cycle">https://www.cycle</a>	2	\$1.31	\$2.62	11/26/18	42883	
13	Order Error	Steel	1' of 0.75" X 0.065" 4130 Tub	Online Metals	<a href="https://www.onlin">https://www.onlin</a>	2		\$0.00	11/26/18	2326586	
14	Order Error	Steel	1' 0.625" X 0.065" 4130 Tube	Online Metals	<a href="https://www.onlin">https://www.onlin</a>	4		\$0.00	11/26/18	2326586	
15	Order Error	Steel	1' of 0.25" x 3" 1018 Sheet	Online Metals	<a href="https://www.onlin">https://www.onlin</a>	1		\$0.00	11/26/18	2326586	

Bill of Materials (BOM) - Front Drivetrain The Incompressibles										Total Sub-System:	Total Project:
										\$1,031.00	\$2,516.95
Item #	Description	Material	Source PN	Source	Qty.	Cost.	Price Extended	Date Received			
1	Chain	Steel	CN-HG93	<a href="https://www.amazon.com">Amazon.com</a>	1	\$18.40	\$18.40		<a href="https://www.amazon.com">https://www.amazon.com</a>		
2	Sprocket	Steel	2299K21	McMaster	1	\$22.74	\$22.74		<a href="https://www.mcmaster.com">https://www.mcmaster.com</a>		
3	Planetary Gearbo	Steel	KF060-004-S2	Apex Dynamics	1	\$700.00	\$700.00		<a href="https://www.neuq.com">https://www.neuq.com</a>		
4	Standoff	Aluminum	92510A459	McMaster	4	\$6.39	\$25.56	11/26/18	<a href="https://www.mcmaster.com">https://www.mcmaster.com</a>		
5	Stock for Mount	Steel	9663	Online Metal	1	\$15.91	\$15.91		<a href="https://www.online.com">https://www.online.com</a>		
6	Shimano Alivio Si	Aluminum	FD-M4020-M-B	<a href="https://www.amazon.com">Amazon.com</a>	1	\$28.99	\$28.99		<a href="https://www.aliexpress.com">https://www.aliexpress.com</a>		
7	Chain Tensioner	Aluminum	CHA2281k	<a href="https://www.ebay.com">ebay.com</a>	1	\$16.99	\$16.99		<a href="https://www.ebay.com">https://www.ebay.com</a>		
8	Hex Head Screw	Steel	91247A555	McMaster	1	\$6.49	\$6.49	11/26/18	<a href="https://www.mcmaster.com">https://www.mcmaster.com</a>		
9	Hex Head Nut	Steel	95462A029	McMaster	1	\$4.40	\$4.40	11/26/18	<a href="https://www.mcmaster.com">https://www.mcmaster.com</a>		
10	White Plastic 5" x 20" Shim Sheet,		<a href="https://www.ebay.com">9513K24</a>	McMaster	1	\$4.90	\$4.90				
11	Aluminum Unthreaded Spacer, 8 mm O		94669A063	McMaster	4	\$2.02	\$8.08				
12	Aluminum Male-Female Threaded Hex		<a href="https://www.mcmaster.com">98952A429</a>	McMaster	4	\$3.62	\$14.48				
13	Aluminum Male-Female Threaded Hex		<a href="https://www.mcmaster.com">98952A430</a>	McMaster	4	\$3.72	\$14.88				
14	Zinc-Plated Steel Washer for M5 S		<a href="https://www.mcmaster.com">91166A240</a>	McMaster	1	\$2.31	\$2.31				
15	Zinc-Plated Steel Hex Nut, Medium-Stre		<a href="https://www.mcmaster.com">90591A260</a>	McMaster	1	\$2.80	\$2.80				
16	Medium-Strength Steel Nylon-Insert Loc		<a href="https://www.mcmaster.com">90576A104</a>	McMaster	1	\$4.50	\$4.50				
17	Zinc Yellow-Chromate Plated Grade 8 S		<a href="https://www.mcmaster.com">98023A029</a>	McMaster	1	\$7.70	\$7.70				
18	High-Strength Steel Nylon-Insert Lockn		<a href="https://www.mcmaster.com">97135A215</a>	McMaster	1	\$3.66	\$3.66				
19	Zinc Yellow-Chromate Plated Steel Thin		<a href="https://www.mcmaster.com">93839A805</a>	McMaster	1	\$11.45	\$11.45				
20	Aluminum Unthreaded Spacer, 8 mm O		<a href="https://www.mcmaster.com">94669A329</a>	McMaster	4	\$2.25	\$9.00				
21	<a href="https://www.fastenal.com">M5-0.8 x 20mm ISO 4762/DIN 91</a>		1139547	Fastenal	50	\$0.22	\$11.20				
22	<a href="https://www.fastenal.com">M5-0.8 x 35mm DIN 931 Class 8.8</a>		38548	Fastenal	5	\$0.54	\$2.69				
23	<a href="https://www.fastenal.com">M5-0.8 x 40mm DIN 931 Class 8.8</a>		38549	Fastenal	5	\$0.58	\$2.91				
24	<a href="https://www.fastenal.com">1/4"-28 x 1" Grade 8 Yellow Zinc</a>		18755	Fastenal	5	\$0.32	\$1.58				
25	<a href="https://www.fastenal.com">1/4"-28 Yellow Zinc Finish Grade</a>		36452	Fastenal	5	\$0.13	\$0.65				
26	<a href="https://www.fastenal.com">M5-0.8 DIN 439B Class 04 Zinc F</a>		141487	Fastenal	5	\$0.06	\$0.31				
27	<a href="https://www.fastenal.com">1/4"-20 x 1/2" Grade 8 Yellow Zin</a>		15001	Fastenal	3	\$0.19	\$0.56				
28	14 Tooth Threaded Track Cog, 3/32"			Surly	1	\$19.94	\$19.94				
29	Freewheel Adapter for 5/8" Axle wit		FWM-ADAPTER	Electric Scooter F	1	\$32.44	\$32.44				
30	Irwin 8338 10mm X 1.0 Metric Tap		8338	<a href="https://www.amazon.com">Amazon.com</a>	1	\$8.04	\$8.04				
31	Shimano Acero MTB Shifter		SL-M3010	<a href="https://www.amazon.com">Amazon.com</a>	1	\$27.44	\$27.44				

Bill of Materials (BOM) - Rear Drivetrain The Incompressibles										Total Sub-System:	Total Project:
										\$111.67	\$2,516.95
Item #	Description	Material	Source PN	Source	Qty.	Cost.	Price Extended	Date Received			
1	Motor Sprocket	Steel	6280K661	McMaster	1	\$16.15	\$16.15	11/26/18	<a href="https://www.mcmaster.com">https://www.mcmaster.com</a>		
2	Wheel Sprocket	Steel	2299K35	McMaster	1	\$33.71	\$33.71	11/26/18	<a href="https://www.mcmaster.com">https://www.mcmaster.com</a>		
3	Stock for Mount (12"x12")	Steel	<b>9665</b>	Online Metal	1	\$24.60	\$24.60	days	<a href="https://www.online.com">https://www.online.com</a>		
4	Standoff	Aluminum	92511A085	McMaster	5	\$3.81	\$19.05	11/26/18	<a href="https://www.mcmaster.com">https://www.mcmaster.com</a>		
5	Roller Chain	Steel	6261k173	McMaster	4ft	\$18.16	\$18.16	11/26/18	<a href="https://www.mcmaster.com">https://www.mcmaster.com</a>		



Bill of Materials (BOM) - Auxiliaries										Total Sub-System:	Total Project:
The Incompressibles										\$505.06	\$2,516.95
Item #	Description	Material	Manufacturer PN	Manufacturer	Link	Qty.	Cost.	Price Extended	Date Received		
1	Front and Rear Brakes		BR-CX50	Shimano	<a href="https://www.amaz">https://www.amaz</a>	2	\$35.35	\$70.70			
2	Front Fork		FK0912	Surly	<a href="https://www.biker">https://www.biker</a>	1	\$125.00	\$125.00	11/26/18		
3	Headset		BAA0058K (ZS44)	Cane Creek	<a href="https://www.amaz">https://www.amaz</a>	1	\$34.81	\$34.81	11/26/18		
4	Front Handlebar Stem		17 Degree 70mm	Wake	<a href="https://www.amaz">https://www.amaz</a>	1	\$13.00	\$13.00			
5	Crankset		EFCM3000BC62X (170mm)	Shimano	<a href="https://www.amaz">https://www.amaz</a>	1	\$46.99	\$46.99	11/26/18		
6	Bottom Bracket		BB-UN26 (73X113mm)	Shimano	<a href="https://www.amaz">https://www.amaz</a>	1	\$12.99	\$12.99	11/26/18		
7	Regular Pedals		PD-M424	Shimano	<a href="https://www.amaz">https://www.amaz</a>	1	\$46.27	\$46.27	11/26/18		
8	Power Measuring Pedals		Assioma Duo	Favero	<a href="https://cycling.fav">https://cycling.fav</a>	0	\$747.00	\$0.00	MESFAC'd		
9	Bike Kitchen Order		Purchased handlebars, seat, seatpost, rims and stem			1	\$85.12	\$85.12	1/13/19		
10	Front and Rear Shimano V Brake		BR-T4000	Shimano	Amazon	1	\$28.20	\$28.20	Repurchase front brakes due to more clamp		
11	Shimano Universal Brake Cable Set		Y80098022	Shimano	Amazon	1	\$11.99	\$11.99			
12	DEERU Carbon Fiber Headset Spacers			DEERU	Amazon	1	\$9.99	\$9.99			
13	Shimano MTB Shift Cable Set		CABGR7BK	Shimano	Amazon	1	\$20.00	\$20.00			

Bill of Materials (BOM) - Mechatronics										Total Sub-System:	Total Project:
The Incompressibles										\$263.00	\$2,516.95
Item #	Description	Material	Source PN	Link	Qty.	Cost.	Price Extended	Date Received			
1	LCD: 240X320 Resolution 2.8"		LCD-2.8	<a href="https://www.amazon.co">https://www.amazon.co</a>	2	\$13.00	\$26.00				
2	Logic Level Converter		TE291	<a href="https://www.amazon.co">https://www.amazon.co</a>	1	\$8.00	\$8.00				
3	Magnets 100 Pieces		FINDMAG 100	<a href="https://www.amazon.co">https://www.amazon.co</a>	1	\$11.00	\$11.00				
4	Hall Effect KY-003		KY-003	<a href="https://www.amazon.co">https://www.amazon.co</a>	1	\$8.00	\$8.00				
5	Momentary Push Button		PBSM-02	<a href="https://www.amazon.co">https://www.amazon.co</a>	1	\$11.00	\$11.00				
6	Mini Hot Glue Gun		GGO20AC	<a href="https://www.amazon.co">https://www.amazon.co</a>	1	\$9.00	\$9.00				
7	Darlington Transistors		ULN2803	<a href="https://www.amazon.co">https://www.amazon.co</a>	1	\$7.00	\$7.00				
8	3D printer filament		Anet	<a href="https://www.banggood.c">https://www.banggood.c</a>	1	\$17.00	\$17.00				
9	Membrane Buttons		ADA1332	<a href="https://www.amazon.co">https://www.amazon.co</a>	1	\$7.00	\$7.00				
10	OLED Display		PI 51 Msp420	<a href="https://www.amazon.co">https://www.amazon.co</a>	1	\$9.00	\$9.00				
11	Jumper Wires		Haitronic	<a href="https://www.amazon.co">https://www.amazon.co</a>	1	\$7.00	\$7.00				
12	Pressure Transducer		2500/5v	<a href="https://www.ebay.com/it">https://www.ebay.com/it</a>	1	\$18.00	\$18.00				
13	Good Pressure Transducer		480-2541-ND	<a href="https://www.digikey.com">https://www.digikey.com</a>	1	\$125.00	\$125.00	just this needs to be bought			

Bill of Materials (BOM) - Hydraulics										Team Cost Sub-System:	Total Sub-System:	Total Project:
The Incompressibles										\$996.55	\$1,102.02	\$2,210.97
Item #	Description	Material	Source PN	Source	Qty.	Cost.	Sponsored?	Team Cost	Price Extended	Date Received	URL	
1	Coil, 12VDC DIN , J type	Other	300AA00081A	Eaton	2	\$12.22	YES	\$0.00	\$0.00			
2	Coil, 12VDC DIN , H type	Other	300AA00121A	Eaton	2	\$15.69	YES	\$0.00	\$0.00			
3	Fitting, -6 JIC male "T"	Other	2033-6-6S	Eaton	4	\$1.84	YES	\$0.00	\$0.00			
4	Fitting, -6 SAE male to -6 JIC male, straight	Other	202702-6-6S	Eaton	14	\$0.75	YES	\$0.00	\$0.00			
5	Flow Control, Needle Valve	Other	NV1-8-S-0	Eaton	1	\$11.61	YES	\$0.00	\$0.00			
6	Line Body, VC08-2, Aluminum SAE -6	Other	02-160731	Eaton	1	\$11.29	YES	\$0.00	\$0.00			
7	Line Body, VC10-2, Aluminum SAE -6	Other	878700	Eaton	4	\$11.98	YES	\$0.00	\$0.00			
8	Solenoid, 2 pos, 2 way Bi-poppet, normally Closed	Other	SBV1-10-C-0-00	Eaton	2	\$35.54	YES	\$0.00	\$0.00			
9	Solenoid, 2 pos, 2 way Bi-poppet, normally Open	Other	SBV11-10-0-0-00	Eaton	2	\$45.20	YES	\$0.00	\$0.00			
10	6061-T6 0.375" Aluminum Sheet	Aluminum	23816	Online Metals	1	\$44.10	NO	\$44.10	\$44.10	11/26/18	<a href="http://hant.cfm?pid=23816&amp;steps=4&amp;showunits=inches&amp;">hant.cfm?pid=23816&amp;steps=4&amp;showunits=inches&amp;</a>	
11	Clamping Two-Piece Shaft Collar Metric	Steel	6063K23	McMaster Carr	3	\$15.25	NO	\$15.25	\$45.75	11/26/18	<a href="http://mcmaster.com/6063k23">mcmaster.com/6063k23</a>	
12	Clamping Two-Piece Shaft Collar Imperial	Steel	6436K15	McMaster Carr	2	\$7.89	NO	\$7.89	\$15.78	11/26/18	<a href="http://mcmaster.com/6436k15">mcmaster.com/6436k15</a>	
13	Aluminum Bare Sheet 6061 T6 24" x 48"	Aluminum	1246	Online Metals	1	\$100.00	NO	\$100.00	\$100.00		<a href="https://www.onlinemetals">https://www.onlinemetals</a>	
14	Aluminum Weld Bung 1/4 NPT	Aluminum	8694T42	McMaster Carr	5	\$8.00	NO	\$8.00	\$40.00	11/26/18	<a href="https://www.mcmaster.co">https://www.mcmaster.co</a>	
15	Push-to-connect fittings 90deg, 1/4 ID/NPT	Other	5486K122	McMaster Carr	2	\$8.42	NO	\$8.42	\$10.84	11/26/18	<a href="https://www.mcmaster.co">https://www.mcmaster.co</a>	
16	Breather Fitting 1/4 NPT	Other	9833K22	McMaster Carr	1	\$1.61	NO	\$1.61	\$1.61	11/26/18	<a href="https://www.mcmaster.co">https://www.mcmaster.co</a>	
17	Barbed Fitting 1/4 NPT	Aluminum	5357K32	McMaster Carr	2	\$4.02	NO	\$4.02	\$8.04	11/26/18	<a href="https://www.mcmaster.co">https://www.mcmaster.co</a>	
18	Pump/Motor Parker	Aluminum	-	Parker	2	\$0.00	NO	\$0.00	\$0.00			
19	4L Composite Bladder Accumulator @ 3000psi	Other	AB30CN10G0N	Steelhead Comp	1	\$785.00	NO	\$785.00	\$785.00	1/10/19		
20	Accumulator Mounting Bracket	Steel	BIS6AD	Steelhead Comp	2	\$25.00	NO	\$25.00	\$50.00			
21	1/4-20 2" Bolt	Steel	-	-	2	\$0.12	NO	\$0.12	\$0.24			
22	1/4-20 1" Bolt	Steel	-	-	4	\$0.09	NO	\$0.09	\$0.36			
23	1/4-20 Nut	Steel	-	-	6	\$0.05	NO	\$0.05	\$0.30			

## Attachment 11: MATLAB Simscape Script

```
%% The Incompressibles Senior Project 2018 - Simscape Model Script
%% Usage and Description
%
% *Author* Nicholas Gholdoian & Kyle Franck
%
% Cal Poly SLO
%
% *Date Created* 5/12/2018
% *Date Modified* 4/29/2018
%
% *Description*
% This script defines the variables inside each Simscape model and
controls
% whether to run the direct drive or accumulator discharge model.
% Inspiration and details taken from Winston Wights' previous bike model.
%
%% Initializing Workspace
% Clear the workspace and windows of any figures or misc. variables.
close all
clc
clear all

%% Define Universal Parameters
% [Inputs]
gravity = 32.2; % [ft/s^2] Gravity constant
air_density = 2.29E-3; % [slug/ft^3] Density of air at 70F

%% Declare Fluid Properties
% Script below inputs the fluid properties into the Simscape model. The
current fluid used is Mobil EAL 224H.

% [Inputs]
fluid_density = 1.787; % [slug/ft^3] Fluid density
fluid_kine_viscosity = 4.28E-4; % [ft^2/s] Fluid kinematic viscosity
fluid_bulk_modulus = 2.2E5; % [lb/in^2] Fluid bulk modulus

%% Declare Tubing Parameters
% Script below inputs tubing data for a circular cross section

% [Inputs]
tube_internal_dia = 0.37; % [in] Internal tube diameter
tube_length = 120; % [in] Total tube length
tube_resistance_length = 0; % [in] Total aggregate equivalent length of
local resistances
tube_surface_roughness = 5E-6; % [ft] Internal tube surface roughness for
drawn tubing

% [Calculations]
tube_area = pi*(tube_internal_dia/2)^2; % [in^2] Tube cross sectional area

%% Road Parameters
% Script below defines the road parameters
```

```

% [Inputs]
wind_speed = 0; % [] Wind speed, positive is headwind
road_slope = 0; % [] Road slope, positive is incline

%% Declare Bike Parameters
% Script below declares the global bike parameters.

% [Weight Inputs]
bike_weight = 98; % [lbf] Bike weight excluding driver, fluid, and
accumulator weight
driver_weight = 220; % [lbf] Driver weight
fluid_weight = 1; % [lbf] Total fluid weight excluding accumulator fluid
weight
front_wheel_weight = 2.8; % [lbf] Weight of front wheel
rear_wheel_weight = 2.8; % [lbf] Weight of rear wheel

% [Weight Distribution Inputs]
CG_front_distance = 28.5; % [in] Horizontal distance from CG to front axle
CG_rear_distance = 16.5; % [in] Horizontal distance from CG to rear axle
CG_height = 33; % [in] Vertical distance of CG above ground

% [Bike Parameter Inputs]
number_of_wheels = 1; % [-] Number of wheels on each axle
front_tire_dia = 686; % [mm] Front wheel diameter
rear_tire_dia = 686; % [mm] Rear wheel diameter
front_gear_ratio = 1/10.3; % [-] Front sprocket gear ratio (input/output)
rear_gear_ratio = 3.0; % [-] Rear gear ratio (pump input/wheel output)
rolling_resistance_coef = 0.008; % [-] Rolling resistance coefficient
frontal_area = 528.3; % [in^2] Frontal area of bike for aero
drag_coef = 0.9; % [-] Drag coefficient for bike
crank_length = 6.5; % [in] Front crank arm length for pedal

% [Mass & Weight Distro. Calculations]
driver_mass = driver_weight/gravity; % [slug] Driver mass
bike_mass = bike_weight/gravity; % [slug] Bike mass excluding driver and
fluid
fluid_mass = fluid_weight/gravity; % [slug] Fluid mass excluding
accumulator fluid mass
front_wheel_mass = front_wheel_weight/gravity; % [slug] Mass of front
wheel
rear_wheel_mass = rear_wheel_weight/gravity; % [slug] Mass of rear wheel
rear_wheel_inertia = rear_wheel_mass*((rear_tire_dia/2)^2); % [slug*mm^2]
Moment of inertia of wheel (thin hoop, mr^2)

%% Declare Accumulator Parameters (Single Run Mode)
% The below script declares the accumulator parameters from the Hydac
SB330
% data sheet
% (http://www.hydac-na.com/sites/hydac-na/SiteCollectionDocuments/Accumulators.pdf)
% Accumulator Inputs
% accu_volume_range = [0.29, 0.98, 1.47, 2.45, 4.87, 9.00, 10.04, 13.87];
% [gal] Table of Hydac SB 330 bladder accumulator volumes

```

```

% accu_housing_weight = [10, 30, 33, 86, 140, 226, 270, 330]; % [lbf]
Table of Hydac SB 330 bladder accumulator housing weights (excluding fluid
weight)

% [Inputs]
accu_volume = 0.98; % [gal] Total accumulator volume
precharge_press = 900; % [psi] Accumulator nitrogen precharge pressure
accu_max_press = 3000; % [psi] Accumulator max allowable pressure
accu_housing_weight = 10.8; % [lbf] Weight of accumulator housing without
fluid
accu_exit_dia = 0.75; % [in] Diameter of accumulator exit orifice
specific_heat_ratio = 1.47; % [-] Specific heat ratio of nitrogen in an
adiabatic process

% [Accumulator Calculations]
accu_exit_area = pi*(accu_exit_dia/2)^2; % [in^2] Accumulator exit orifice
cross sectional area
accu_housing_mass = accu_housing_weight/gravity; % [slug] Mass of
accumulator housing without fluid
accu_vol_fluid_storage = accu_volume*(1-
((precharge_press/accu_max_press)^(1/specific_heat_ratio))); % [gal]
Initial fluid volume inside accumulato before discharge
accu_fluid_mass = fluid_density*accu_vol_fluid_storage/7.48; % [slug] Mass
of fluid inside accumulator before discharge

%% Total Bike Mass Calculation
total_bike_mass = bike_mass + driver_mass + fluid_mass + accu_fluid_mass +
accu_housing_mass + rear_wheel_mass + front_wheel_mass; % [slug] Total
bike mass including fluid mass and rider mass

%% Ride Power Definition
rider_power = 300; % [watts] Rider constant power input

%% Model Runtime Definition
model_runtime = 300; % [sec] Model total runtime

%% Model Selection
% [Input]
model_sel = 1;
% Defined as:
% [1] for direct drive model
% [2] for accumulator discharge model
% [3] for accumulator discharge model to maintain bike at certain speed
% [4] for accumulator recharge model

if model_sel == 1
    sim('Direct_Drive_Model.slx')
elseif model_sel == 2
    sim('Accumulator_Discharge_Model.slx')
elseif model_sel == 3
    sim('Accumulator_Discharge_Model_Maintain_Speed.slx')
elseif model_sel == 4
    sim('Accumulator_Recharge_Model.slx')
else

```

```

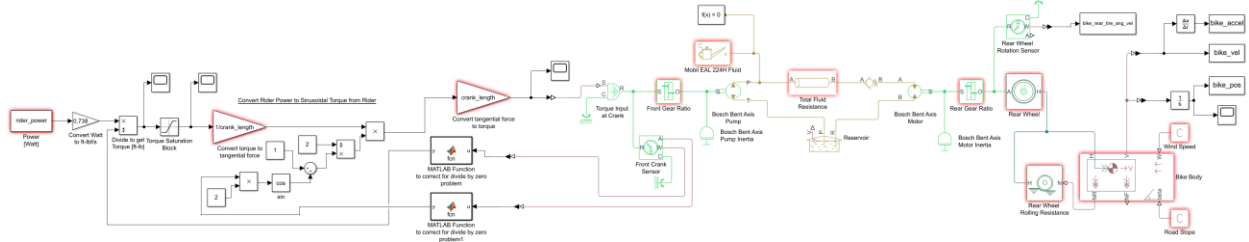
    error('Invalid model or no model selected')
end

%% Efficiency Score Calculation
% Below calculates a mock efficiency score derived from the competition
rules
% factoring in total weight, distance traveled, accu. volume and precharge
% press.
bike_distance = max(bike_pos); % [ft] Total bike distance traveled
total_bike_weight = total_bike_mass*gravity; % [lbf] Total bike weight
efficiency_score =
((bike_distance*12)*total_bike_weight)/(precharge_press*accu_volume*231);
% [-] Efficiency score calculation,  $S=(W[lbf]*L[in])/(P[psi]*V[in^3])$ 

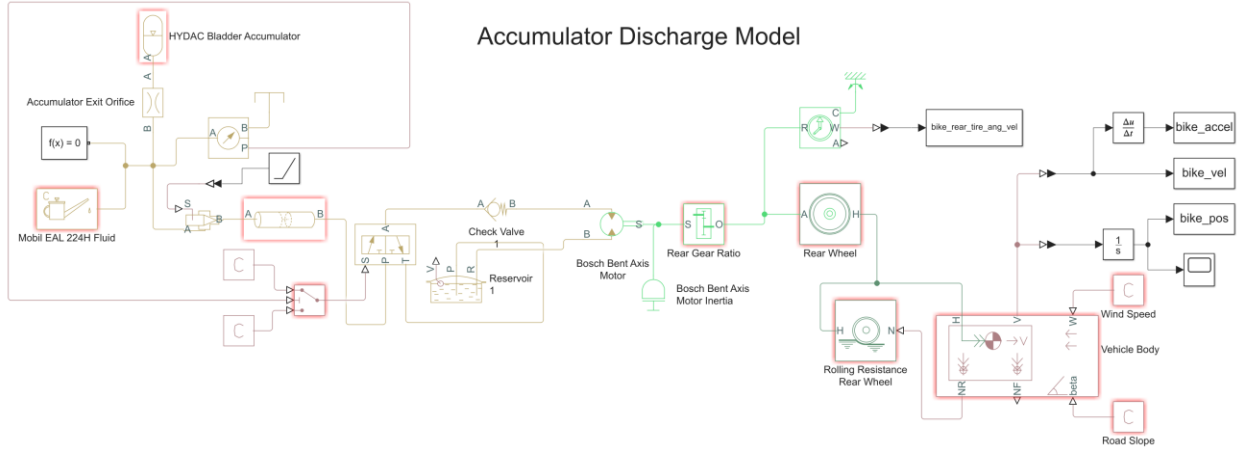
```

# Attachment 12: Simscape Models

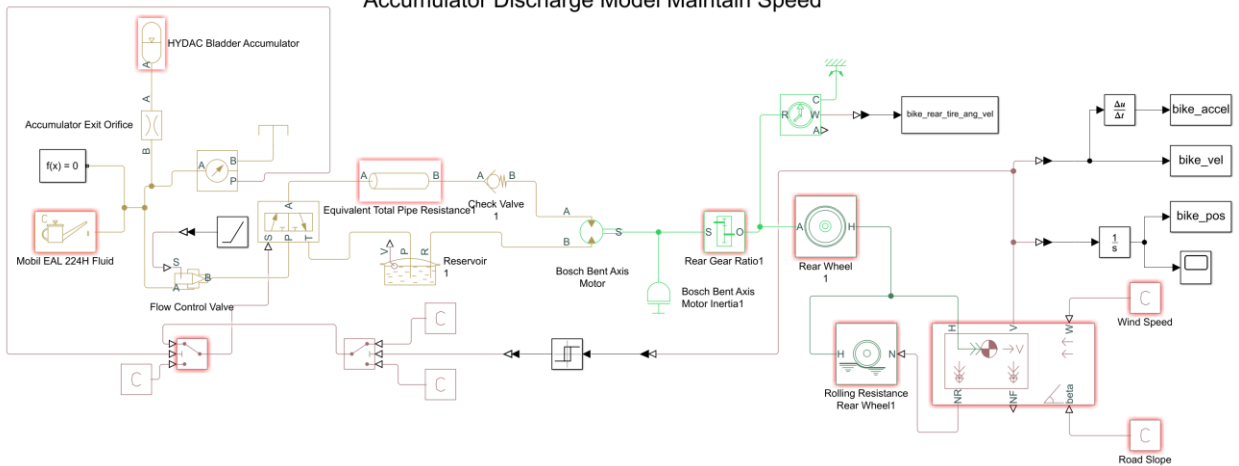
Direct Drive Model



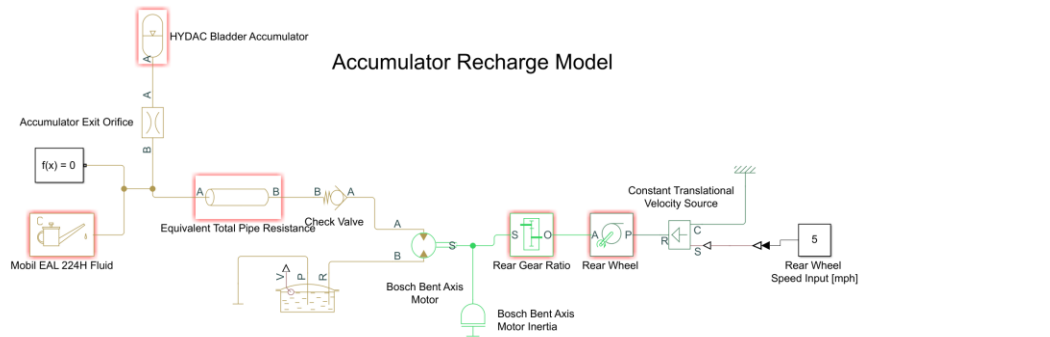
Accumulator Discharge Model



Accumulator Discharge Model Maintain Speed

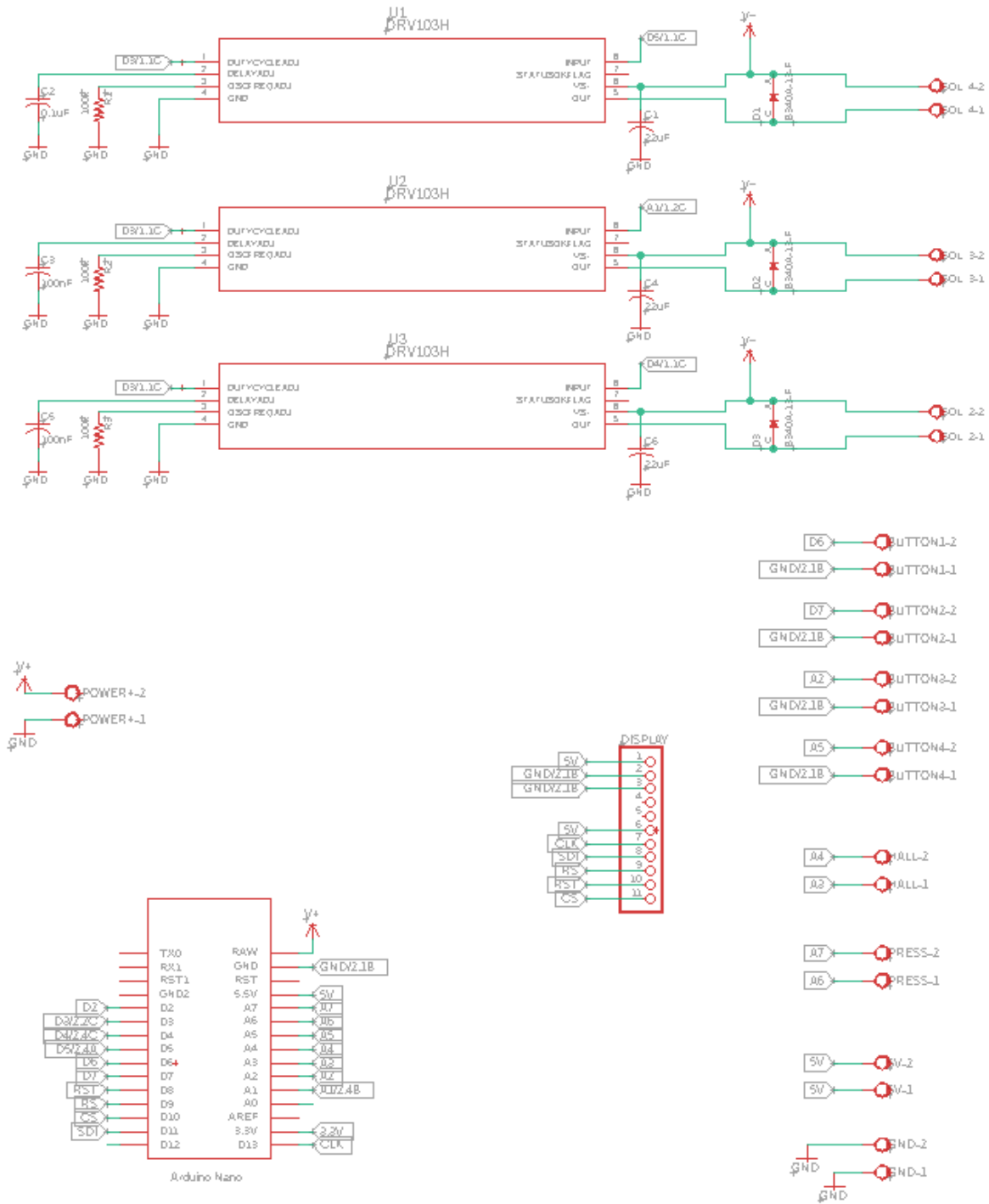


Accumulator Recharge Model

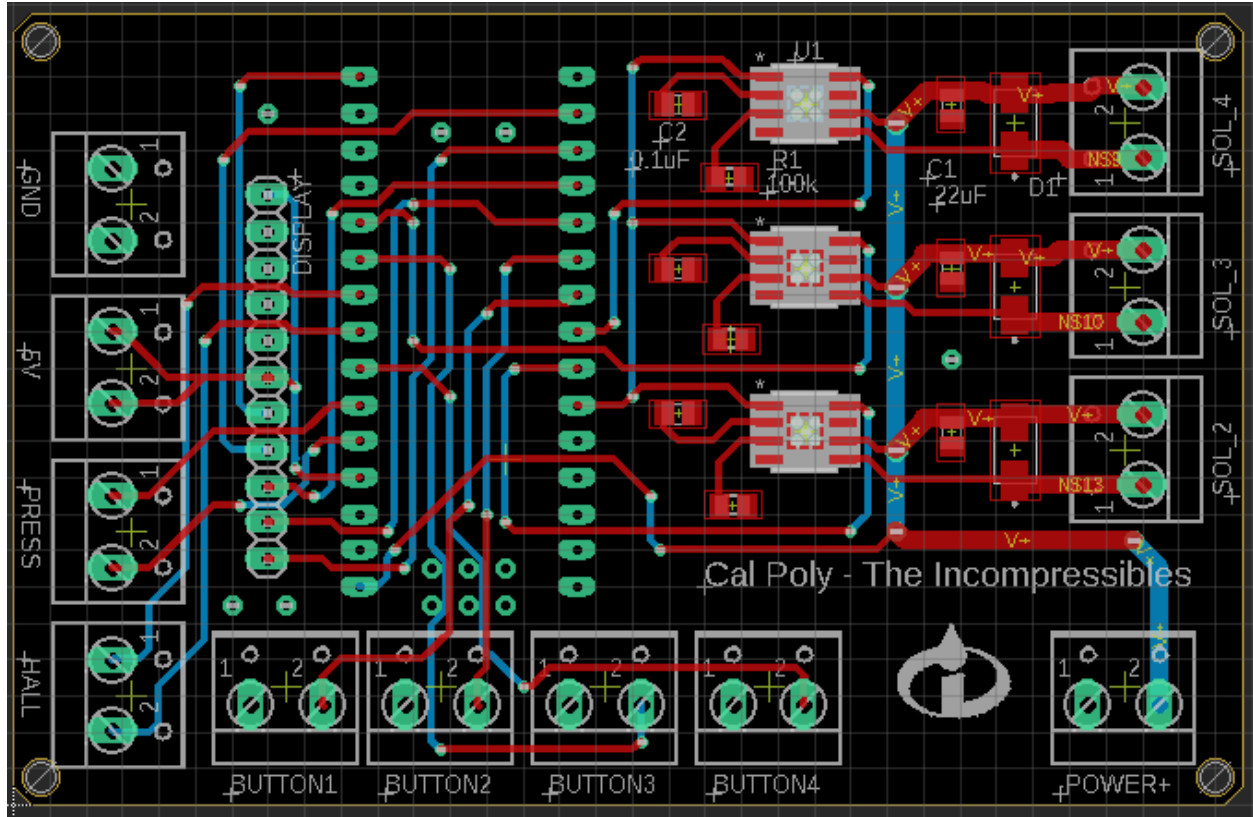


# Attachment 13: Printed Circuit Board

## Schematics



*Board Layout*





## Attachment 14: 2019 FPVC Competition Results

### NFPA Fluid Power Vehicle Challenge SCORING RUBRIC

Team: California Polytechnic State University

<b>MIDWAY REVIEW</b>
<b>Design objectives</b> are clearly stated and appropriate to the competition.
<b>Vehicle design</b> clearly supports the design objectives and is of obvious quality.
<b>Fluid power circuit design</b> is complete and reflects an understanding of fluid power components and systems.
<b>Selection of hardware</b> is complete and is appropriate to the design objectives.
<b>Analyses</b> have been performed and their results have been incorporated into vehicle and/or circuit designs.
<b>Prototype</b> vehicle assembly has begun.
<b>Presentation</b> is completed on time and demonstrates team synergy.

<b>JUDGES COMMENTS:</b>
<p>*Great analysis, good improvements from last year. *Good progress. Make sure you speak to the safety aspects of your design as well. *Covered in detail the requirements for the machine, covering in detail the races and requirements. The bike looks like a pretty good idea. May have some issues with mounting reservoir and/or accumulators. Good circuit diagrams. Make sure to add a pressure relief valve, filter, and a gauge near the accumulator. Poppet solenoids are a good idea. The bent axis pump is an acceptable decision (depending on calculations). Glad you opted for SAE fittings. Would have ranked higher if I knew what component size was based on. Studying bike stability and control sensitivity were smart for the competition. Missing power, speed and flow requirement calculations which are necessary for sizing pumps and motors. No discussion about fabrication so far. Team had good cohesion and seemed to work well together. Overall a good presentation. *Very nice presentation ad progress. *Good job with all your calculations and specifications. *Excellent and impressive presentation. I really liked how you outlined goals and then tied expected performance to it. You've shown tremendous progress on design with solid justification for design decisions and trade-offs. *Make sure there is a way to safely dissipate the accumulator pressure... maybe a needle valve to the reservoir. Is filtration a concern? Calculations should be included in the presentation... proper sizing cannot be determined without them. *liked the electronic circuit board with programming and sensors. (mechatronics) Be careful to not have too much complexity, sometimes simple is better. Good analytics and planning for the project. Would like to see calendar in a Gantt chart format.</p>

<b>OVERALL SCORE:</b>
4.03/5

NFPA Fluid Power Vehicle Challenge  
**SCORING RUBRIC**

Team: California Polytechnic State University

<b>FINAL PRESENTATION</b>
<b>Summary of midway presentation</b> is succinct and well organized.
<b>Vehicle construction</b> was completed on-time and performed mostly by the team members.
<b>Vehicle testing</b> was performed and improvements were made based on results.
<b>Final vehicle</b> brought to competition appears reliable, safe and of quality craftsmanship.
<b>Lessons learned</b> are clearly stated and appropriate to the design/build experience described.
<b>Presentation</b> is completed on time and demonstrates good team synergy.

<b>JUDGES COMMENTS:</b>
*Nice integration of all the disciplines throughout presentation. Great summary of test goals vs results. Best I saw. Great job. *The team seemed to put a lot of time and effort into the early design phase with concrete goals. This appeared to pay off by allowing for more time to test and optimize the vehicle rather than troubleshooting assembly. This was the most complex electrical system I saw, and I'm looking forward to see it perform. Well done team! *Team seemed very well prepared and had good planning and execution. Impressive PCB work and mechatronic development. Also, custom bike frame and optimized balancing dependent on bike speed. Good modeling and preparation work shows good effort by all. Lots of engineering done on this one. *Awesome presentation and presenters. I'm excited to see your bike. Super impressed about all of the custom components you created. *Very impressive teamwork and inclusion of all team members.

<b>OVERALL SCORE:</b>
4.31/5

NFPA Fluid Power Vehicle Challenge  
**SCORING RUBRIC**

Team: California Polytechnic State University

<b>VEHICLE INSPECTION</b>
Quality of vehicle design associated with <b>reliability</b> . The vehicle is robust and durable, but not too heavy.
Quality of vehicle design associated with <b>operator safety and comfort</b> . The vehicle is ergonomic and easy to use.
Quality of vehicle design associated with <b>originality and uniqueness</b> . The vehicle incorporates innovative concepts and could be marketable as a production vehicle.

<b>JUDGES COMMENTS:</b>
Lots of engineering here. *Nice quality frame build; cool application of right-angle drive*Nice use of piston pump and motor. *Right angle pump drive is unique, and custom mechatronics. *Wiring components could be loomed and covered to improve robustness. Keeping most hydraulic components away from the operator increased safety. Electronics fail safe. *Nice use of electronics. Consider using chain guards. *Consider packaging the electronics and wrapping the wires. Many failures can occur in improperly packaged wiring. *Unique gearbox design! *Clean routing. Looks top heavy. Electronics not protected. *Looks very functional and robust. Not sure about comfort but based on your presentation I expect good results in the competitions.

<b>OVERALL SCORE:</b>
3.82/5

NFPA Fluid Power Vehicle Challenge  
**SCORING RUBRIC**

Team: California Polytechnic State University

<b>FPVC Mentorship</b>
Introduction and initial discussion about vehicle design.
Discussion about component design.
Discussion about assembly and testing
Final discussion on adjustments

<b>JUDGES COMMENTS:</b>

<b>OVERALL SCORE:</b>
4/4

<b>Endurance Challenge</b>		
	<b>University Name</b>	<b>Time</b>
1st	California Polytechnic State University, San Luis Obispo	4:50:45
2nd	Cleveland State	5:40:00
3rd	Montana State University	5:45:48
4th	West Virginia University Inst. Of Tech	6:40:00
5th	Purdue Northwest	10:42:00
6th	University of Akron	10:57:25
7th	University of Denver	13:41:00
8th	University Of Utah	13:52:00
9th	Colorado State University	16:42:00
	Purdue University	-
	University of Cincinnati	-
	Kennesaw State University	-
	Murray State University	-
	Iowa State University	-
	Western Michigan University	-

<b>Efficiency Challenge</b>		
	<b>University Name</b>	<b>Score</b>
1st	Western Michigan University	31.63
2nd	Cleveland State	10.46
3rd	Cal Polytechnic State University	7.54
4th	Montana State University	4.16
5th	Purdue University	3.32
6th	Iowa State University	3.30
7th	West Virginia University Inst. Of Tech	2.79
8th	Murray State University	2.76
9th	University of Akron	2.72
10th	Colorado State University	2.55
11th	Purdue Northwest	2.46
12th	University of Denver	2.15
13th	University of Cincinnati	1.71
14th	Kennesaw State University	1.28
15th	University Of Utah	1.04
	<b>Team</b>	<b>Max Distance</b>
	University of Akron	404
	Murray State University	384
	University Of Utah	412
	Kennesaw State University	287
	University of Denver	377
	California Polytechnic State University, San Luis Obispo	515
	Purdue Northwest	557
	University of Cincinnati	1044
	Purdue University	4809
	Montana State University	605
	Cleveland State	466
	Colorado State University	579
	West Virginia University Inst. Of Tech	418
	Western Michigan University	1943
	Iowa State University	556

<b>Sprint Challenge</b>		
	<b>University Name</b>	<b>Best Time (sec)</b>
1st	Cleveland State	14.71
2nd	Murray State University	14.94
3rd	Western Michigan University	21.75
4th	Purdue University	22.24
5th	California Polytechnic State University, San Luis Obispo	23.09
6th	West Virginia University Inst. Of Tech	32.16
7th	University of Akron	32.23
8th	Montana State University	35.7
9th	University of Cincinnati	36.91
10th	Colorado State University	39.06
11th	Iowa State University	41.54
12th	University of Denver	46.88
13th	Purdue Northwest	48.13
14th	University Of Utah	50.02
15th	Kennesaw State University	95.29